



Durham E-Theses

Fruit dehiscence in Brassicas

Spence, Jacqueline

How to cite:

Spence, Jacqueline (1996) *Fruit dehiscence in Brassicas*, Durham theses, Durham University. Available at Durham E-Theses Online: <http://etheses.dur.ac.uk/5439/>

Use policy

The full-text may be used and/or reproduced, and given to third parties in any format or medium, without prior permission or charge, for personal research or study, educational, or not-for-profit purposes provided that:

- a full bibliographic reference is made to the original source
- a [link](#) is made to the metadata record in Durham E-Theses
- the full-text is not changed in any way

The full-text must not be sold in any format or medium without the formal permission of the copyright holders.

Please consult the [full Durham E-Theses policy](#) for further details.

FRUIT DEHISCENCE IN BRASSICAS

Student Jacqueline Spence

Supervisor Dr. N. Harris

The copyright of this thesis rests with the author.
No quotation from it should be published without
his prior written consent and information derived
from it should be acknowledged.

Submitted for the degree of Doctor of Philosophy
Department of Biological Sciences
University of Durham



- 4 JUN 1996

ABSTRACT

Dehiscence is a means by which some wild plants release their seeds. In Brassicas the mature fruit or 'pod', strictly a silique, releases seed by a sometimes explosive mechanism triggered by mechanical pressure and referred to as 'shatter'. This mechanism is a problem in Brassica crop plants and results in loss of seed, and hence loss of revenue, during harvesting. This problem is further compounded by the distribution of volunteers which contaminate future crops and the environment.

The post-fertilisation development of the carpel wall of a number of Brassica species has been examined including, a range of *Arabidopsis* ecotypes and mutants, and fruits from two other Brassicas, *Brassica napus* and *Brassica juncea*, which exhibit differences in the dehiscence characteristic. These have been studied by a combination of cytological, cytochemical and molecular techniques.

Following fertilisation, dehiscence zones form at the carpel margins, separating the carpel walls from the replum and forming two valves. Cells within the dehiscence zone exhibit reduced cellular cohesion due to breakdown of the middle lamella. Differentiation of the carpel wall layers results in a thickened exocarp, a senescing mesocarp, and modification of the endocarp layers in which the inner layer *Enb* lignifies whilst *Ena* collapses. It is proposed that the patterns of differentiation result in the development of the dehiscence mechanism. The dehiscence mechanism and pod 'shatter' is a result of; 1) weakening of valve attachment due to reduced cell cohesion in the dehiscence zone, and, 2) tensions which develop within the carpel walls due to desiccation and shrinkage of the mesocarp which is attached to a thickened, non-shrinking endocarp.

The fruits from all of the *Arabidopsis* ecotypes examined exhibited a similar pattern of carpel wall development and similar dehiscence characteristics. Light microscopical examination of the fruits of *Brassica napus* and *Brassica juncea* which do not shatter as easily as those of *Arabidopsis* showed a different pattern of endocarp development in the post fertilised fruit. *Ena* tangential walls thickened considerably in the post-fertilised *Brassica napus* and *Brassica juncea* fruit, prior to the collapse of this cell layer. In Indian mustard, the *Brassica juncea* variety which had a non-shattering phenotype, the lignified walls of *Enb* were surrounded by a highly pectinised layer. This deposition of pectins confers more elasticity to the carpel walls, hence reducing the tensions which normally result in dehiscence and cause pod shatter.

The model of the shattering and non-shattering phenotypes described in this study suggest a number of strategies which may be used to reduce the problems of pod shatter. These include modification of the separation layer to increase cellular cohesion, and modifications to the patterns of differentiation in the carpel wall to reduce the tensions which normally develop during fruit ripening.

CONTENTS

ACKNOWLEDGEMENTS	1
MEMORANDUM	2
LIST OF FIGURES	3
LIST OF TABLES	6
1. INTRODUCTION	7
1.1. OILSEED RAPE CROPS AND THE PROBLEM OF POD SHATTER	8
1.1.1. The Oilseed Rape Crop	8
1.1.2. Pod Shatter	8
1.1.3. Methods to Overcome Pod Shatter	9
1.1.4. The <i>Brassica napus</i> Silique	9
1.2. THE DEVELOPMENT OF <i>ARABIDOPSIS THALIANA</i>	10
1.2.1. <i>Arabidopsis thaliana</i>	10
1.2.2. Genetic Variability in <i>Arabidopsis</i>	12
1.2.3. The Meristem	12
1.2.3.1. The Vegetative Meristem	14
1.2.3.2. The Inflorescence Meristem	14
1.2.3.3. Control Factors in the Inflorescence Meristem	16
1.2.3.4. The Floral Meristem	17
1.2.3.5. Patterns in Flower Development	18
1.3. EARLY FRUIT DEVELOPMENT	20
1.3.1. Fruit Structure	20
1.3.2. The Gynoecial Meristem	21
1.4. FRUIT RIPENING AND THE DEHISCENCE MECHANISM	24
1.4.1. Fruit Ripening in <i>Arabidopsis</i>	24
1.4.2. Senescence	26
1.4.3. Abscission	27
1.5. THE PLANT CELL WALL	28
1.5.1. Structure of the Plant Cell Wall	29
1.5.2. Plant Cell Wall Proteins	30
1.5.3. Hydrolytic Enzymes	31
1.5.3.1. Polygalacturonase	32
1.5.3.2. Pectinesterase	32
1.5.3.3. Cellulase (β -(1-4) glucanase)	33

1.6. LIGNIFICATION	34
1.6.1. Lignin Synthesis	35
1.6.2. Phenylalanine Ammonia Lyase (PAL)	35
1.6.3. Cinnamyl Alcohol Dehydroginase (CAD)	36
1.6.4. Peroxidases	37
1.6.5. Phenoloxidases	37
1.7. HORMONES	38
1.7.1. Auxins	39
1.7.2. Gibberellins	40
1.7.3. Cytokinins	41
1.7.4. Abscisic Acid	41
1.7.5. Ethylene	42
1.7.6. Polyamines	43
1.8. HYPOTHESIS	44
1.9. PROJECT AIMS	44
2. MATERIALS AND METHODS	45
2.1. STANDARD SOLUTIONS	46
2.2. PLANT MATERIAL	47
2.2.1. Sterilising seeds	47
2.2.2. Standard growth conditions for <i>Arabidopsis thaliana</i>	47
2.2.3. Standard growth conditions for <i>Arabidopsis</i> mutants	47
2.2.4. Standard growth conditions for <i>Brassica juncea</i>	47
2.3. SATURATED SOLUTIONS	47
2.3.1. Preparation of Saturated Solutions	48
2.3.2. Humid chambers	48
2.4. TISSUE PREPARATION FOR MICROSCOPY	48
2.4.1. Fixation	48
2.4.2. Dehydration	48
2.4.3. Embedding in Paraplast Wax	49
2.4.4. Embedding in LR White Acrylic Resin	49
2.4.5. TESPA (aminopropyltriethoxysilane) coating of microscope slides	49
2.4.6. Formvar coating grids	50
2.4.7. Sectioning wax embedded material	50
2.4.8. Sectioning resin embedded material	50
2.5. HISTOCHEMISTRY	51
2.5.1. Acridine orange	51

2.5.2. Calcofluor	51
2.5.3. Ruthenium red	51
2.5.4. Toluidine blue	51
2.6. IMMUNOCYTOCHEMISTRY	51
2.6.1. Immunocytochemistry for light microscopy	52
2.6.2. Immunogold/Silver Detection	52
2.6.3. Immunocytochemistry for electron microscopy	52
2.6.4. Sodium metaperiodate treatment	53
2.7. MOLECULAR HISTOCHEMISTRY	53
2.7.1. Preparation of digoxigenin labelled Riboprobes	53
2.7.2. Restriction digest of plasmid DNA	53
2.7.3. Cleaning cut plasmid DNA	53
2.7.4. <i>In Vitro</i> transcription	53
2.7.5. <i>In-Situ</i> hybridisation	54
2.7.5.1. Pre-treatment	54
2.7.5.2. Pre-hybridisation	54
2.7.5.3. Hybridisation	54
2.7.5.4. Post-hybridisation washes	55
2.7.5.5. Immunological detection	55
2.8. LIGNIN ANALYSIS	55
2.8.1. Tissue extraction for Alkaline oxidation procedures	55
2.8.2. Copper oxidation	56
2.8.3. Nitrobenzine oxidation	56
2.8.4. Tissue extraction for Microwave digestion	56
2.8.5. Microwave digestion	56
2.8.6. Ethyl acetate extraction	56
2.8.7. HPLC analysis	57
2.8.8. Standard solutions	57
2.9. CELL WALL CARBOHYDRATE ANALYSIS	57
2.9.1. Acid hydrolysis	57
2.9.2. Standard solutions	58
2.9.3. Paper chromatography	58
2.9.4. Staining	58
2.10. LIST OF SUPPLIERS	58

3. RESULTS	59
3.1. A STUDY ON THE DEHISCENCE CHARACTERISTICS OF SOME ECOTYPES OF <i>ARABIDOPSIS THALIANA</i>	61
3.1.1. Selection of the ecotypes	61
3.1.2. Some phenotypic differences between <i>Arabidopsis</i> ecotypes	61
3.1.3. 'Pod shatter' in <i>Arabidopsis</i> ecotypes	65
3.1.4. Histology of the siliques of <i>Arabidopsis</i> ecotypes	65
3.1.5. Variations in silique structure	68
3.1.6. The phenotype of ecotype Ag-0 (N901)	70
3.2. THE EFFECTS OF HUMIDITY ON DEHISCENCE IN <i>ARABIDOPSIS</i>	72
3.2.1. Ripening and dehiscence in ambient conditions	72
3.2.2. Ripening and dehiscence in a humidity of 7%	74
3.2.3. Ripening and dehiscence in a humidity of 12%	74
3.2.4. Ripening and dehiscence in a humidity of 29.5%	76
3.2.5. Ripening and dehiscence in a humidity of 50%	76
3.2.6. Ripening and dehiscence in a humidity of 75.5%	76
3.2.7. Ripening and dehiscence in a humidity of 96%	76
3.3. DEVELOPMENT OF THE <i>BRASSICA NAPUS</i> SILIQUE	79
3.3.1. Development of the dehiscence zones in the post-fertilised silique	79
3.3.2. Development of the carpel walls in the post-fertilised silique	81
3.4. DEVELOPMENT OF THE <i>BRASSICA JUNCEA</i> SILIQUE	84
3.4.1. Phenotypic variations in the varieties	84
3.4.2. Structure of the mature pre-fertilised fruit	84
3.4.3. Development of the post-fertilised silique	86
3.4.4. Carpel wall development in mature Indian mustard siliques	91
3.5. DEVELOPMENT OF <i>ARABIDOPSIS</i> ETHYLENE MUTANT SILIQUES	96
3.5.1. The phenotype of the <i>Ein</i> 1-1 and <i>Ein</i> 2-1 plants	96
3.5.2. Development of the dehiscence zones and carpel walls in the post fertilised siliques	96
3.5.3. The phenotype of the <i>Etr</i> mutant plant	97
3.5.4. Development of the dehiscence zones in the post-fertilised silique	97
3.5.5. Development of the carpel wall in the post-fertilised silique	99
3.6. IMMUNOCYTOCHEMISTRY OF THE SILIQUE	101
3.6.1. Localisation of JIM13 binding	101

3.6.1.1. JIM13 binding in <i>Arabidopsis</i> and <i>Brassica juncea</i>	105
3.6.1.2. JIM13 binding in Indian mustard	105
3.6.1.3. Localisation of JIM13 binding in endocarp <i>b</i> cells of <i>Arabidopsis</i>	105
3.6.2. Localisation of JIM5 binding	107
3.6.2.1. Localisation of JIM5 binding in young <i>Brassica</i> fruits	107
3.6.2.2. Localisation of JIM5 binding in mature <i>Brassica</i> fruits	109
3.6.2.3. Localisation of JIM5 binding in the cell walls of mature <i>Arabidopsis</i> carpel tissues	112
3.6.3. Localisation of JIM7 binding	115
3.7. MOLECULAR HISTOCHEMISTRY OF THE SILIQUE	116
3.7.1. Localisation of SAC25 mRNA	116
3.7.2. Localisation of SAC51 mRNA	116
3.7.2.1. Localisation of SAC51 mRNA in young <i>Brassica</i> fruits	119
3.7.2.2. Localisation of SAC51 mRNA in mature <i>Brassica</i> fruits	119
3.7.3. Localisation of Oilseed rape extensin (EXTA)	123
3.7.3.1. Localisation of EXTA mRNA in young <i>Brassica</i> fruits	123
3.7.3.2. Localisation of EXTA mRNA in mature <i>Brassica</i> fruits	126
3.7.4. Pea Lignin Probe (pLP18)	126
3.8. ANALYSIS OF SILIQUE LIGNIN	129
3.8.1. Oxidation procedures	129
3.8.2. <i>Arabidopsis</i> ecotypes	129
3.8.3. Leaf tissues	131
3.8.4. Stem tissues	131
3.8.5. Carpel wall tissues	132
3.9. DEVELOPMENT OF THE <i>ARABIDOPSIS Sin 1-1</i> MUTANT SILIQUE	135
3.9.1. The phenotype of the <i>Sin 1-1</i> plant	135
3.9.2. Development of the dehiscence zones in the post-fertilised silique	137
3.9.3. Development of the carpel wall in the post-fertilised silique	137
3.10. ANALYSIS OF SILIQUE CELL WALL POLYSACCHARIDES	139
3.10.1. Analysis of monosaccharides from <i>Brassica napus</i> tissues	139
3.10.1.1. Pod wall tissues	139
3.10.1.2. The septum	141
3.10.1.3. The endocarp	141
3.10.1.4. The exocarp	141

3.10.2. Analysis of monosaccharides from <i>Arabidopsis</i> tissues	141
3.10.2.1. Pod wall tissues	143
3.10.2.2. The septum	143
3.10.2.3. The endocarp	143
3.10.2.4. The exocarp	143
4. DISCUSSION	145
4.1. The Dehiscence Mechanism	146
4.2. Pod Shatter	147
4.3. Dehiscence and Pod Shatter in <i>Arabidopsis</i>	148
4.4. Dehiscence and Pod Shatter in <i>Brassica napus</i> and <i>Brassica juncea</i>	150
4.5. The Non-Shattering Phenotype	151
4.6. The Tissues of the Dehiscence Zone	152
4.7. The Tissues of the Carpel Wall	153
4.7.1. The Exocarp	154
4.7.2. The Mesocarp	155
4.7.3. The Endocarp	157
4.7.3.1. Endocarp <i>A</i>	158
4.7.3.2. Endocarp <i>B</i>	159
4.8. A Strategy to Reduce 'Pod Shatter'	160
4.9. Conclusion	161
5. REFERENCES	162

ABBREVIATIONS

ABA	abscisic acid
ACC	1-aminocyclopropane-1-carboxylic acid
AG	AGAMOUS
AGP	arabinogalactan protein
AP	APETALA
BAW	butan-1-ol/acetic acid/water
BSA	bovine serum albumin
°C	degrees Centigrade
CA	p-coumaric acid
CAD	cinnamyl alcohol dehydrogenase
CCR	hydroxycinnamyl CoA reductase
cDNA	complimentary deoxyribonucleic acid
CJ	cell wall junction
4CL	p-coumarate CoA ligase
CLV	CLAVATA
cm	centimetre
COPS	controller of phase switching
CW	cell wall
CWB	carpel wall vascular bundle
C3H	p-coumarate 3 hydroxylase
C4H	cinnamate 4 hydroxylase
DAA	days after anthesis
DEPC	diethylpyrocarbonate
DIC	differential interference contrast
DNA	deoxyribonucleic acid
DTT	dithiothrietol
Eco	<i>Escherichia coli</i>
EDTA	ethylenediamine tetracetic acid
<i>Ein</i>	ethylene insensitive
En	endocarp
<i>Ena</i>	endocarp <i>a</i>
<i>Enb</i>	endocarp <i>b</i>
EPW	ethyl acetate/pyridine/water
<i>Etr</i>	ethylene resistant
Ex	exocarp
EXT	EXTENSIN
FA	ferulic acid
Fig.	figure
FLIP	floral initiation process
FLO	FLORICAULA
F5H	ferulate 5 hydroxylase
µg	microgram

(G)	guaiacyl
GA	gibberellic acid
GLO	GLOBOSA
GRP	glycine rich protein
(H)	hydroxyphenyl
HCl	hydrochloric acid
Hind	<i>Haemophilus influenzae</i>
HPLC	high pressure liquid chromatography
L	lignified cell wall
LC	lignified dehiscence zone cell
LFY	LEAFY
µm	micrometre
M	molar
Me	mesocarp
mg	milligram
ml	millilitre
mm	millimetre
mRNA	messenger ribonucleic acid
NaCl	sodium chloride
NaOH	sodium hydroxide
ng	nanogram
nm	nanometre
OMT	caffeic acid O methyltransferase
p	plasmid
PA	polyamine
PAL	phenylalanine ammonia lyase
PBS	phosphate buffered saline
PBST	phosphate buffered saline Tween 20
PI	PISTILLATA
PM	plasma membrane
PRP	proline rich protein
PVP	polyvinyl pyrrolidone
PX	peroxidase
RNA	ribonucleic acid
r.p.m.	reolutions per minute
R.T.	room temperature
S (legends)	septum
S	syringaldehyde
(S)	syringyl
SA	syringic acid
SAM	S-adenosyl-L-methionone
SDS	sodium dodecyl sulphate
SL	separation layer
SSC	standard saline citrate buffer
TBS	Tris buffered saline

TE	Tris/EDTA buffer
TESPA	aminopropyltriethoxysilane
TFL	TERMINAL FLOWER
Tris	2-amino-2-(hydroxymethyl)-1,3-propanediol
UV	ultra-violet
V (legends)	vacuole
V	vanillin
VA	vanillic acid
VB	vascular bundle
v/v	volume:volume ratio
W	watt
w/v	weight:volume ratio
Xho	<i>Xanthomonas holcicola</i>

Symbols

α	alpha
β	beta
$^{\circ}$	degree
μ	micro

ACKNOWLEDGEMENTS

This thesis would not have been possible without the support of the following people. My sincere and heartfelt thanks go to all of them.

Special thanks to my supervisor Dr. Nick Harris for his confidence, patience, expertise and guidance throughout this project.

Special thanks also to Dr. Robert Edwards for his expert help and guidance with the biochemistry that was performed during this project.

Dr. S. Coupe and Dr. J Roberts for providing the SAC25 and SAC51 probes, Dr. A. Shirsat for providing the EXT A probe and Dr. J. Drew and Dr. J. Gatehouse for providing the pLP probe.

Mr. P. Sidney and Mr. D. Hutchinson for outstanding photographic services.

Finally thanks to my family and friends for their encouragement and support and my most sincere thanks to my son Kieren who, as Dr Stephen Hawking so eloquently said as being typical of children, 'didn't quite know enough not to ask the important questions'.

MEMORANDUM

The work in this thesis was carried out by myself in the Department of Biological Sciences at the University of Durham. I declare that this work has not been submitted previously for a degree at this or any other University. This thesis is a report of my own work, except where acknowledged by reference. The copyright of this thesis rests with the author. No quotation should be published without her written consent, and information derived from it should be acknowledged.

LIST OF FIGURES

Figure 1.	Structure of the <i>Brassica napus</i> silique	10
Figure 2.	Metameric structure of <i>Arabidopsis</i> (after Shultz & Haughn 1991)	11
Figure 3.	Diagrammatic representation of meristem structure	13
Figure 4.	Diagrammatic representation of the three functions in the floral meristem	19
Figure 5.	Diagrammatic illustration of the possible arrangements of the carpels in <i>Arabidopsis</i>	20
Figure 6.	Diagrammatic illustration of the carpel wall layers in the <i>Arabidopsis</i> gynoecium	23
Figure 7.	Transverse section showing the tissues of the dehiscence zones of <i>Arabidopsis</i>	25
Figure 8.	Scheme of monolignol biosynthesis and some of the enzymes involved	34
Figure 9.	Scheme of ethylene synthesis	42
Figure 10.	Plants of <i>Arabidopsis</i> ecotypes Landsberg <i>erecta</i> and Columbia	60
Figure 11.	<i>Arabidopsis</i> siliques from the Landsberg <i>erecta</i> ecotype	62
Figure 12.	<i>Arabidopsis</i> siliques from the Columbia ecotype	62
Figure 13.	Plants of <i>Arabidopsis</i> ecotypes Dijon G and Hodja-Obi-Garm	64
Figure 14.	Structure of young and mature siliques from ecotype Columbia	66
Figure 15.	Structure of mature siliques from ecotypes Estland and Da(1)-12	67
Figure 16.	Structure of mature siliques from ecotypes Enkheim-D and Sn(5)-1	69
Figure 17.	Plant from ecotype Ag-0 (N901)	71
Figure 18.	Senescing leafy structures and lateral shoots of ecotype Ag-0 (N901)	71
Figure 19.	<i>Arabidopsis</i> siliques after 3 days incubation at a humidity of 7%	73
Figure 20.	<i>Arabidopsis</i> siliques after 3 days incubation at a humidity of 12%	73
Figure 21.	<i>Arabidopsis</i> siliques after 3 days incubation at a humidity of 29.5%	75
Figure 22.	<i>Arabidopsis</i> siliques after 3 days incubation at a humidity of 50%	75
Figure 23.	<i>Arabidopsis</i> siliques after 3 days incubation at a humidity of 75.5%	77
Figure 24.	<i>Arabidopsis</i> siliques after 3 days incubation at a humidity of 96%	77
Figure 25.	Structure of the dehiscence zones in the post-fertilised <i>Brassica napus</i> fruit	80
Figure 26.	Structure of the carpel walls in the post-fertilised <i>Brassica napus</i> fruit	82

Figure 27.	Four varieties of <i>Brassica juncea</i>	83
Figure 28.	Structure of the pre-fertilised <i>Brassica juncea</i> fruit	85
Figure 29.	Structure of the young post-fertilised <i>Brassica juncea</i> fruit	87
Figure 30.	Cellular structure of the dehiscence zones in <i>Brassica juncea</i> fruit (indian mustard variety)	88
Figure 31.	Structure of the carpel walls in the maturing fruits of four varieties of <i>Brassica juncea</i>	90
Figure 32.	Structure of the dehiscence zones in the mature senescing siliques of four varieties of <i>Brassica juncea</i>	92
Figure 33.	Structure of the endocarp in the mature senescing siliques of four varieties of <i>Brassica juncea</i>	93
Figure 34.	Structure of the dehiscence zone and endocarp in senescing siliques of the indian mustard variety of <i>Brassica juncea</i>	95
Figure 35.	<i>Etr</i> mutant siliques showing attached senescing floral organs	98
Figure 36.	Structure of the young post-fertilised fruit	98
Figure 37.	Structure of the mature post-fertilised fruit	100
Figure 38.	Localisation of JIM13 binding in <i>Arabidopsis</i> siliques	102
Figure 39.	Localisation of JIM13 binding in <i>Brassica juncea</i> siliques	102
Figure 40.	Localisation of JIM13 binding in indian mustard	103
Figure 41.	Control sections incubated in pre-immune rat serum	104
Figure 42.	Transmission electron micrograph showing the localisation of JIM13 in the endocarp cells of the mature <i>Arabidopsis</i> silique	106
Figure 43.	Control sections incubated in pre-immune rat serum	106
Figure 44.	Localisation of JIM5 binding in young Brassica fruits	108
Figure 45.	Localisation of JIM5 binding in the carpel walls of young Brassica fruits	110
Figure 46.	Localisation of JIM5 binding in the carpel walls of mature Brassica fruits	110
Figure 47.	Control sections incubated in pre-immune rat serum	111
Figure 48.	Transmission electron micrograph showing the localisation of JIM5 in the exocarp cell wall of mature <i>Arabidopsis</i> fruits	113
Figure 49.	Transmission electron micrograph showing the localisation of JIM5 in the mesocarp cell walls of young <i>Arabidopsis</i> fruits	113
Figure 50.	Transmission electron micrograph showing the localisation of JIM5 in the locule wall of endocarp <i>a</i> cells in young <i>Arabidopsis</i> fruits	114

Figure 51.	Transmission electron micrograph showing the localisation of JIM5 in the cell wall junctions of endocarp <i>a</i> and endocarp <i>b</i> cells in mature <i>Arabidopsis</i> fruits	114
Figure 52	Control section incubated in pre-immune rat serum	115
Figure 53.	<i>In-situ</i> localisation of SAC51 mRNA in the carpel walls of young <i>Brassica</i> fruits	117
Figure 54.	<i>In-situ</i> localisation of SAC51 mRNA in the dehiscence zones of young <i>Brassica</i> fruits	118
Figure 55.	<i>In-situ</i> localisation of SAC51 mRNA in the carpel walls of mature <i>Brassica</i> fruits	120
Figure 56.	<i>In-situ</i> localisation of SAC51 mRNA in the dehiscence zones of mature <i>Brassica</i> fruits	121
Figure 57.	Control sections incubated with SAC51 sense riboprobe	122
Figure 58.	<i>In-situ</i> localisation of AS58 mRNA in young <i>Brassica</i> fruits	124
Figure 59.	<i>In-situ</i> localisation of AS58 mRNA in the carpel walls of mature <i>Brassica</i> fruits	125
Figure 60.	<i>In-situ</i> localisation of AS58 mRNA in the dehiscence zones of mature <i>Brassica</i> fruits	127
Figure 61.	Control sections incubated with AS58 sense riboprobe	128
Figure 62.	HPLC analysis of lignin oxidation products	130
Figure 63.	Graphical view of the relative percentages of lignin oxidation products from the first digestion	133
Figure 64.	Graphical view of the relative percentages of lignin oxidation products from the second digestion	134
Figure 65.	The <i>Arabidopsis Sin 1-1</i> mutant plant	135
Figure 66.	Structure of the dehiscence zones in the post-fertilised <i>Sin 1-1</i> fruit	136
Figure 67.	Structure of the carpel walls in the post-fertilised <i>Sin 1-1</i> fruit	138
Figure 68.	Scanned images of paper chromatograms showing the separation of cell wall saccharides from tissues of <i>Brassica napus</i> and <i>Arabidopsis</i>	140
Figure 69.	Graphical representation of cell wall saccharides from tissues of <i>Brassica napus</i>	142
Figure 70.	The dehiscence mechanism in <i>Arabidopsis</i>	147

LIST OF TABLES

Table 1.	Mutants of <i>Arabidopsis</i> and <i>Antirrhinum</i> and the areas in the flower which they influence	18
Table 2.	Brief summary of <i>Arabidopsis</i> silique development	22
Table 3.	Characteristics of <i>Arabidopsis</i> ecotypes	63
Table 4.	Salt solutions and relative humidities	72

1. INTRODUCTION

1.1. OILSEED RAPE CROPS AND THE PROBLEM OF POD SHATTER

1.1.1. The Oilseed Rape Crop

Over recent years oilseed rape (*Brassica napus*) has become an important crop plant (Wrathall 1978, Labuda 1981, Wrathall & Moore 1986); the fields of bright yellow aromatic flowers can be easily identified in Spring. Although it was introduced as a break crop in barley production (Bunting 1984), it is now an important source of vegetable oil for human consumption and protein meal for animal foodstuffs. Oilseed rape belongs to the Brassicaceae family which also includes other important crop plants such as cauliflower, turnip and mustard. Oilseed rape is an amphidiploid species and is believed to originate from interspecific hybridisation between the diploid species *Brassica oleracea* and *Brassica rapa* (U 1935, Song & Osborn 1992). The oilseed rape plant grows to a height of 0.5-2m and possesses a main stem with axillary branches which all terminate in a raceme bearing many flowers. The flowers develop sequentially along the stem as it elongates.

1.1.2 Pod Shatter

The more recent introduction of oilseed rape as a crop plant means that selection and breeding programmes have been limited, in comparison to those applied to cereals and pulses, for example. Much present research is directed at seed oil modification using genetic engineering (Knauf 1987, Murphy 1992). 'Pod shatter', a means by which seed may be released, is of benefit to wild species but is an economically significant problem with *Brassica* crops and has still to be overcome. The fruits of the oilseed rape plant do not mature synchronously, but sequentially, and some pods 'shatter' before harvesting. The first formed pods are of highest yield but also mature first so are more susceptible to shatter. This can cause a loss of up to 50% of the potential yield if harvesting is delayed by adverse conditions (MacLoed 1981) and volunteers, which grow from the seeds of 'shattered' pods, may remain in the soil to contaminate future crops. The seeds from 'shattered' pods are frequently scattered outside the boundary of the field and contaminate the environment. Oilseed rape plants are now often seen in hedgerows and road verges for example.

1.1.3. Methods to Overcome Pod Shatter

There are a number of ways to approach the problem of 'pod shatter'. The developmental pattern of the whole plant may be altered to synchronise the development of the pods, or pod tissue development may be modified to reduce the shattering characteristic. Modifying the pattern of development of the plant may prove difficult due to the indeterminate nature of the inflorescence meristem. Using the pool of genetic material, available from the various ecotypes of the plant, breeding programmes may be utilised to alter the phenotype of the plant for example, reducing the number and length of the racemes, opening up the canopy and allowing more synchronous pod development (R. D. Child pers. comm.). However, shatter losses may still be considerable. Interspecific hybridisation of *Brassica napus* with a non-dehiscing variety of the related species *Brassica juncea* has been performed (Prakash & Chopra 1988, 1990). Although the resulting hybrids had a high resistance to shattering, the seed yield was very low.

A more favourable option may be to modify tissues within the pods themselves and reduce the 'shattering' characteristic by genetic modification. Genetic modification of the pods will probably have to be via molecular biology as the pool of available plant material does not appear to show enough variation in 'shattering' characteristics. Before any approach can be made at the molecular level however, a detailed knowledge of the developmental patterns of the tissues involved in 'pod shatter' is first required.

1.1.4. The *Brassica napus* Silique

The structure of the *Brassica napus* pod, or silique, which is diagrammatically illustrated in transverse section in Fig 1, has been described (Picart & Morgan 1984) and consists of two carpels separated by a false septum. The dehiscence zones develop at the carpel margins adjacent to the septum and run the length of the silique. The cells of the dehiscence zone eventually begin to degrade and this weakens the contact between the carpel walls, or valves, and the septum. The loss of cellular cohesion is confined to the cells of the dehiscence zone and results from middle lamella breakdown (Meakin & Roberts 1990a). The development of the tissues of the carpel wall, and the tensions that result from the patterns of differentiation, as the silique wall lignifies and desiccates are less well studied. Rather than work on rape itself, which is large, slow to mature and

rather aromatic, the following study on 'pod shatter' has been carried out using *Arabidopsis thaliana* which is described in more detail below.

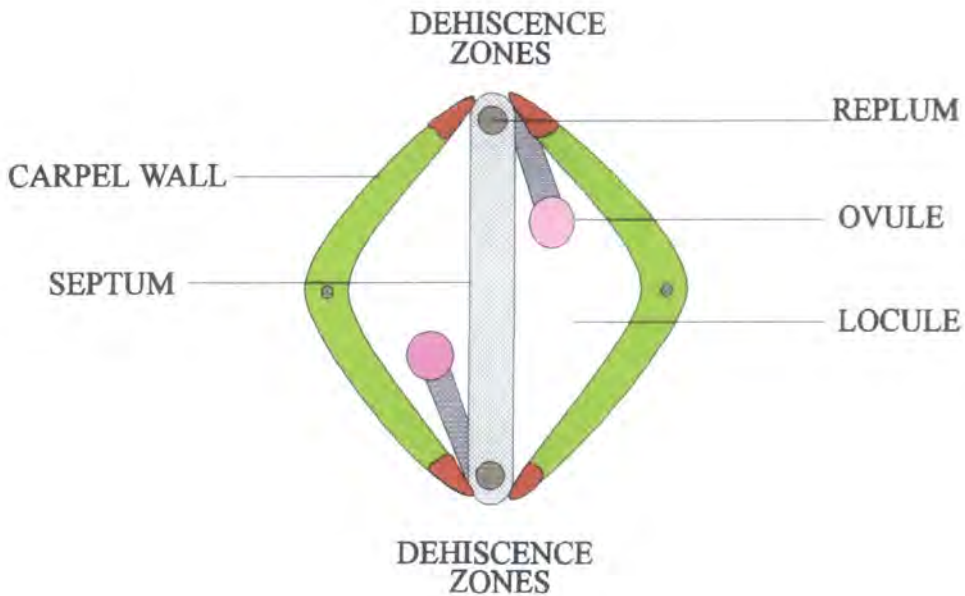


Figure 1. Structure of the *Brassica napus* silique

1.2. THE DEVELOPMENT OF *ARABIDOPSIS THALIANA*

1.2.1. *Arabidopsis thaliana*

Arabidopsis is a small plant which belongs to the Brassicacea family and is found scattered throughout the northern hemisphere. Although this small insignificant weed has negligible nutritional, aesthetic or commercial value it may be referred to as a *Drosophila* of the plant world, and has become a source of inspiration to many scientists. *Arabidopsis* has many characteristics amenable to experimentation (Redei 1975, Meyerowitz & Pruitt 1985, Estelle & Sommerville 1986, Haughn & Sommerville 1988, Meyerowitz 1989, and references therein), and many of its genes have been isolated and cloned. The diploid chromosome number is 5 pairs, and the small genome (7×10^7 base pairs per haploid genome), about one hundredth of the size of most higher plants, contains few repetitive

sequences. This allows easy screening of genomic libraries and makes chromosome walking an attractive option. The small size of the plant, its short generation time (about 5 weeks), and its requirements for only moist simple soil mixtures and fluorescent light, means that it can easily be propagated in a small space. *Arabidopsis* seeds are easily mutagenised by either soaking in chemical mutagens such as ethyl methanesulphonate (EMS) or irradiating imbibed seeds. As the plant typically self fertilises (*Arabidopsis* spontaneously outcrosses at a low frequency of about 10^{-4}) homozygous mutations are easily obtained. Cross pollination can also be easily effected to obtain multiple mutants and male sterile lines are available as an alternative to hand emasculation.

The mature *Arabidopsis* plant grows to a height of 20-30 cm and possesses a rosette of leaves at the base and a raceme of siliques, at different stages of development, along the length of the stem. The inflorescence at the tip of the stem consists of a number of small flowers at different stages of development, with the youngest buds in the centre. The flowers comprise four concentric whorls of organs. The calyx comprises four free sepals and the corolla four alternate white petals. Interior to these are six stamens, four medial long stamens and two lateral short stamens, the superior gynoecium in the centre of the flower comprises two carpels separated by a false septum. The fruits are dry dehiscent siliques with a general structure similar to that seen in *Brassica napus* (see Fig. 1).

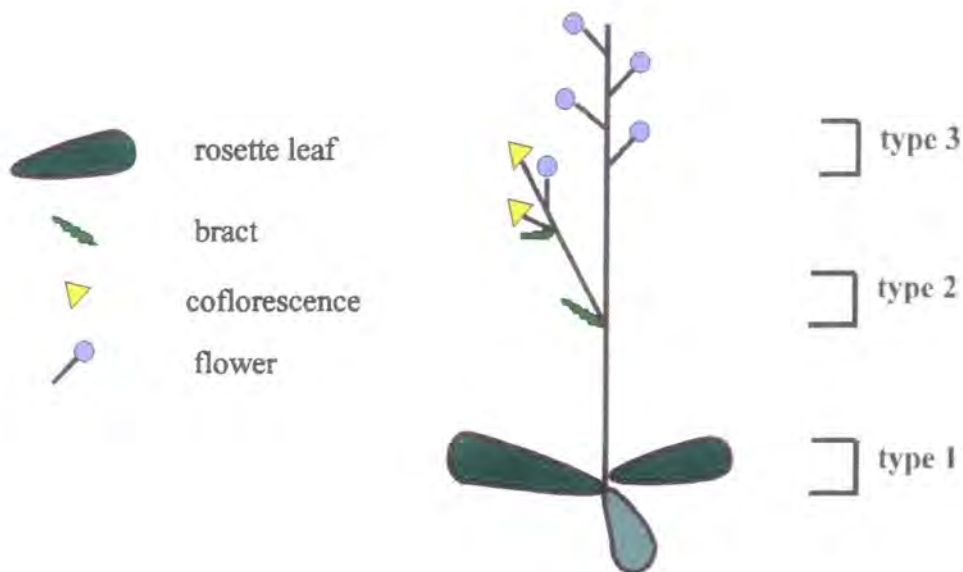


Figure 2. Metameric structure of *Arabidopsis* (after Schultz & Haughn 1991)

The shoots of angiosperms are sometimes described as consisting of a number of units or metamers. *Arabidopsis* produces three types of metamer (Schultz & Haughn 1991); type one metamers consist of a node with a leaf and a short internode and these form the rosette, type two comprise a node with a bract, an elongated internode and coflorescence, and type three consist of a bractless node, an elongated internode and a flower (Fig. 2).

1.2.2. Genetic Variability in *Arabidopsis*

There are many ecotypes of *Arabidopsis* which are found in different geographical locations and these ecotypes have natural variations in their phenotypes. The variations found among wild type plants include responses to vernalisation (Karlsson *et al.* 1993), variations in leaf morphology and number, variations in flowering time and fruit set, to name just a few. There is however, little information available concerning the extent of these natural phenotypic variations which are present in the various ecotypes.

Most experimental work has been carried out using the Columbia or Landsberg *erecta* phenotypes and many of the documented mutants are derived from one of these two races. The *erecta* mutation causes a short erect phenotype. Columbia has been used by Meyerowitz's laboratory in the United States in the research programme on the genetic control of flower development. These two phenotypes have also been crossed to generate recombinant inbred lines which can be used for mapping phenotypic and restriction fragment length polymorphism markers (Lister & Dean 1993). In the laboratory at Durham University the Landsberg *erecta* race has been used in the research programme on fruit ripening and the dehiscence mechanism. Landsberg *erecta* plants grow successfully on most general compost mixtures and seeds germinate within a week at 25°C. The plants can also be grown under continuous illumination.

1.2.3. The Meristem

The upper parts of the plant are produced from groups of undifferentiated initial cells within the tip of the shoot called the apical meristem (Steeves & Sussex 1989, Lyndon 1990, Medford 1992). As the identity of a particular meristem can change, it is usually named according to the organs it will eventually produce. The vegetative meristem produces stem, leaves and lateral branches, the inflorescence meristem produces floral meristems and the floral meristems produce flowers. The apical meristem, which is

illustrated in Figure 3, is usually dome shaped, and is composed of three generative cell layers designated L1, L2 and L3, with L1 being the outermost layer. These three distinct cell layers arise from different patterns of cell division within the meristem. L1 comprises a single layer of cells which divide only in an anticlinal plane; L2 cells divide anticlinally at the apex and also divide periclinally at the base, while those within L3 divide in any plane (Szymkowiak & Sussex 1992). Whilst all three cell layers contribute to organ primordia formation, different layers give rise to different structures; L1 produces the epidermal tissues and L2 produces mesodermal tissues while those in L3 produce the central tissues of the plant such as the cortex and vascular tissues. Because of occasional erroneous cell division, cells derived from one layer may be incorporated into a neighbouring layer. Here they behave in a way appropriate to their new layer which suggests that cell fate depends on position and not lineage.

The meristem is also divided into three zones, the rib zone, the central zone and the surrounding peripheral zone. Cells within the peripheral zone are small, divide rapidly and differentiate to produce the organ primordia. The central zone consists of larger, non-permanent initials which divide more slowly and replenish the peripheral zone (Steeves & Sussex 1989). It has been suggested that cells within the meristem of *Arabidopsis* are committed to a certain fate as they enter the peripheral zone of the meristem (Irish & Sussex 1992). Although the meristem can at present be divided into different layers and zones, it is likely that levels of gene expression will identify further levels of organisation (Meeks-Wagner 1993).

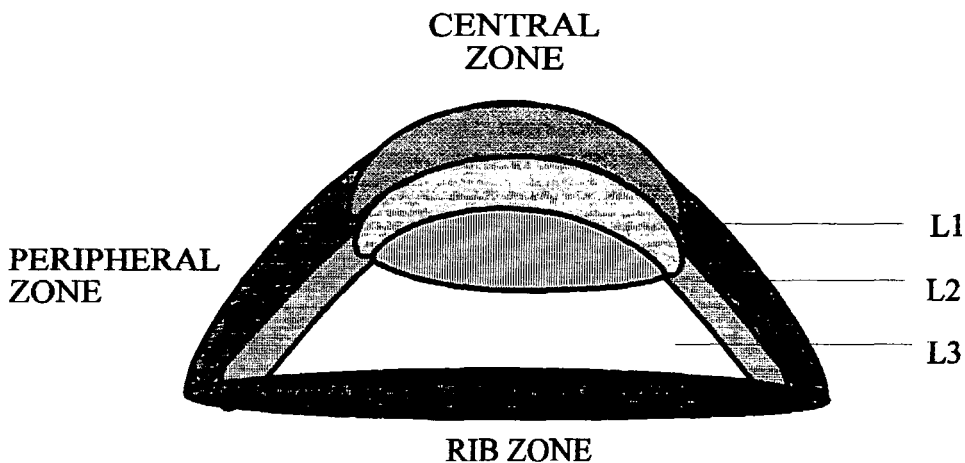


Figure 3. Diagrammatic representation of meristem structure

1.2.3.1. The Vegetative Meristem

Leaves are produced from the vegetative meristem in a specific pattern or phyllotaxy. Studies by Medford *et al.* (1992) have shown that following post embryonic development the shape of the *Arabidopsis* vegetative meristem changes, and these changes are concurrent with a change in the phyllotaxy of the organs produced from the meristem. The first pair of leaf primordia are produced in an opposing phyllotaxy from a rectangular meristem. The meristem then assumes a trapezoid shape and the second pair of leaf primordia are initiated at about 180° to the first pair. The first four leaves are small and have a rounded shape. The meristem shape then changes to a radially symmetrical dome, and further leaf primordia are initiated in a spiral phyllotaxy. Individual plants can show either clockwise or anticlockwise spirals (Smyth *et al.* 1990). These true leaves have a more complex shape being spatulate and serrated, and a new leaf is initiated at an average angle of 138° from its predecessor (Leyser & Furner 1992). About eight true leaves with unextended internodes are produced and form the rosette. The number of leaves within the rosette depends on the genotype and growth conditions. The development of the first true leaves of *Arabidopsis* has been studied in detail (Pyke *et al.* 1991).

1.2.3.2. The Inflorescence Meristem

Changes in the metabolism and gene expression within the shoot apical meristem mark the transition from vegetative to reproductive growth, and the vegetative meristem is transformed into an inflorescence meristem (Steeves & Sussex 1989). The inflorescence meristem produces stem and floral meristems and may show a determinate or an indeterminate pattern of growth depending on the species (Weberling 1989). Determinate inflorescences produce a terminal floral meristem and are short lived, as is seen in tobacco. The inflorescence meristem in *Arabidopsis* shows an indeterminate pattern of growth and does not produce a terminal flower, but does terminate eventually with senescence of the shoot apical meristem after production of a few aborted flowers.

Following the development of the rosette, the *Arabidopsis* stem bolts and the dome shaped vegetative meristem becomes more convex (Miksche & Brown 1965). The early inflorescence meristem produces several cauline leaves, or bracts, with axillary buds. The cauline leaves are smaller than those of the rosette and have a poorly defined petiole. The lateral branches which develop from the axillary buds reiterate the growth pattern of the

main stem and may themselves produce tertiary and quaternary branches. Further inflorescence meristems may also be produced basipetally from the axils of the upper rosette leaves. In the late inflorescence stage an indefinite number of floral meristems are produced on the flanks of the inflorescence meristem. These develop in the same spiral phyllotaxy as exhibited by the true leaves and the cauline leaves and each new floral meristem is initiated at an average angle of 137.5° from its predecessor (Alvarez *et al.* 1992).

Genetic studies using plants which show variations in inflorescence development have identified two major genes which affect the inflorescence of *Arabidopsis*. The gene LEAFY (LFY) has been identified as one of the factors controlling the transition from an inflorescence to a floral meristem (Okamoto *et al.* 1993). In *leafy* mutant plants the inflorescence meristem produces cauline leaves with axillary buds in the positions where floral meristems would normally develop. These axillary buds reiterate the abnormal growth pattern of the main inflorescence resulting in a highly branched vegetative plant (Schultz & Haughn 1991, Huala & Sussex 1992, Weigel *et al.* 1992, Shannon & Meeks-Wagner 1993). The mutant is defective in producing type three metamers and *in-situ* hybridisation studies show LFY RNA is expressed strongly in young floral primordia (Weigel *et al.* 1992).

Similar phenotypic mutations where shoots are produced in positions normally occupied by flowers are observed in the unrelated species *Antirrhinum majus* and are caused by two different mutations, *squamosa* (Huijser *et al.* 1992) and *floricaula* (Coen *et al.* 1990). The FLORICAULA (FLO) gene was identified using transposon mutagenesis, however if the inserted transposon is excised from the gene FLO is then expressed in the cell. Studies on these excision events occurring in the three different layers of the meristem L1, L2 and L3, has shown that expression of FLO each of these layers effects floral development (Carpenter & Coen 1995, Hantke *et al.* 1995). Expression of FLO in only L1 produced normal flowers, expression in only L2 produced slightly abnormal but fertile flowers, but expression in only L3 produced extremely abnormal flowers. This suggests that FLO acts independently between the cell layers, however it is more effective when expressed in L1. Expression of FLO also resulted in the expression of the floral genes DEFICIENS and PLENA and therefore FLO must control the activation of these downstream genes.

Another gene which affects the inflorescence meristem in *Arabidopsis*, although in an entirely different way, is TERMINAL FLOWER (TFL). In *tfl* mutants, the normally

undifferentiated central zone of the inflorescence meristem produces floral meristems. This in effect changes the pattern of growth of the inflorescence meristem from indeterminate to determinate (Shannon & Meeks-Wagner 1991, 1993, Alvarez *et al.* 1992). Again there are phenotypic similarities to the mutant *centroradialis* of *Antirrhinum* which also produces a terminal flower (Coen 1991). Both LFY and TFL act antagonistically in both the inflorescence and floral meristems to maintain meristem identity (Okamoto *et al.* 1993). Another recently identified gene which affects the inflorescence meristem of *Arabidopsis* is ACAULIS (Tsukaya *et al.* 1993). *Acaulis* plants produce only a few floral primordia from a small apical meristem and show a decrease in the elongation of internode cells, resulting in a short phenotype. The *acaulis* mutant is in effect defective in the elongation of type two and type three metamers. The correlation between the various phenotypic effects caused by *acaulis* is not yet known.

1.2.3.3. Control Factors in the Inflorescence Meristem

The major change within the inflorescence meristem is the switch from the early to the late inflorescence stage. This switch causes nodes to develop into flowers instead of coflorescence shoots. A model has recently been proposed (Schultz & Haughn 1993), to explain the interactions of various genes in this switching process.

The model proposes that the activity of a factor(s) called COPS (controller of phase switching) influences the developmental switch from early to late phase and that a decrease in COPS stimulates floral production. COPS must be influenced by developmental factors such as age and environmental factors such as temperature and daylength. The TFL mutant is proposed to reduce COPS activity in the central zone of the inflorescence meristem causing it to become a floral meristem. COPS co-ordinately activates the floral initiation process, or FLIP, which involves the interaction of three genes, LFY, APETALA1 (AP1), and APETALA2 (AP2). The latter two genes are also designated as floral homeotic genes however, *Ap1* mutants result in the floral meristem having an indeterminate pattern of growth as is seen in the inflorescence meristem (Bowman *et al.* 1993). These FLIP genes are then required for the correct expression of other downstream floral homeotic genes (see later in this chapter).

1.2.3.4. The Floral Meristem

The floral meristem produces the various floral organs, and these differ considerably among species. In *Arabidopsis* the four types of floral organs are produced in a whorled phyllotaxy, with each organ type occupying a discrete whorl. The four sepals, which develop first, occupy the outer first whorl, petals whorl two, and stamens whorl three. The gynoecium, which develops into the fruit, occupies the inner fourth whorl and is the last organ to develop. The floral meristem is therefore by its nature determinate. The early development of the *Arabidopsis* flower has been described in detail (Hill & Lord 1989, Smyth *et al.* 1990), and is similar to that described for other crucifers including *Brassica napus* (Polowick & Sawhney 1986). The TOUSLED gene has been proposed to be involved in the initiation of floral organ primordia and may be involved in organ phyllotaxy (Roe *et al.* 1993).

There are numerous documented floral mutants of *Arabidopsis* and analysis of these has led to the identification of homeotic genes, active within the floral meristem, that affect floral organ development. Research has focused mainly on five of these genes AGAMOUS (AG), APETALA1 (AP1), APETALA2 (AP2), APETALA3 (AP3) and PISTILLATA (PI). *Ap1* flowers show transformations in the first and second whorls of sepals to bracts with the formation of a new floral bud in the axil of each bract, petals are totally absent. *Ap2* flowers also show transformations in the first and second whorls of sepals to leaves and petals to mosaic petaloid stamens, although a wide range of phenotypes are observed some of which are temperature sensitive. In *Ap3* flowers the second and third whorls are affected with transformations of petals to sepals and stamens to carpelloid stamens. *Pi* flowers show transformations in three whorls; petals are mosaic organs of sepaloid petals and the stamens are incompletely formed and fused to the gynoecium, which as a result, is also abnormal. In *Ag* flowers there are no stamens or carpels so again two whorls are affected. Comparative studies on *Antirrhinum* have shown the floral homeotic genes of these two species control floral organ morphogenesis by similar mechanisms, and has led to proposed models of how these genes act alone, and in combination, within the floral meristem to specify floral organ identity.

The genetic control of flower development is an extensive topic which will not be discussed in great detail, for reviews see Schwartz-Sommer *et al.* (1990), Coen (1991), Coen & Meyerowitz (1991), Weigel & Meyerowitz (1994), Carpenter & Coen (1995).

The homeotic gene AGAMOUS is expressed in whorl three and exclusively in whorl four and is required for the temporal and spatial initiation of the anther and gynoecial primordia; *Agamous* mutant flowers produce only sepals and petals in repetitive concentric whorls (Bowman *et al.* 1989). AG is therefore also responsible for the determinate nature of the floral meristem. The AG gene has been isolated and sequenced (Yanofsky *et al.* 1990, Ma *et al.* 1991) and this has allowed the temporal and spatial actions of the gene to be determined by transgenic and tissue *in-situ* hybridisation methods (Bowman *et al.* 1991, Drews *et al.* 1991, Mizukami & Ma 1992).

1.2.3.5. Patterns in Flower Development

The phenotype of the floral homeotic mutants of both *Arabidopsis* and *Antirrhinum* are very similar and affect the identity of adjacent whorls of organs. Analysis of the phenotypes of these mutants has led to models of how floral homeotic genes specify organ position and identity. The model proposes that there are three overlapping domains in the floral meristem in which genes may be active, each domain consisting of two adjacent whorls (Table 1).

Floral whorls affected	<i>Arabidopsis</i> mutant	<i>Antirrhinum</i> mutant	Domain where gene is active
whorls 1 and 2	<i>apetela 1</i> , <i>apetela 2</i>	<i>ovulata</i> , <i>macho</i>	A
whorls 2 and 3	<i>pi</i> , <i>apetela 3</i>	<i>deficiens</i> , <i>globosa</i> , <i>sepaloidia</i>	B
whorls 3 and 4	<i>agamous</i>	<i>plena</i> , <i>pleniflora</i> , <i>petaloidea</i>	C

Table 1. Mutants of *Arabidopsis* and *Antirrhinum* and the areas that they influence in the flower.

This suggests that there are three regulatory functions A, B and C, respectively which specify organ type as follows; if A alone is present petals are formed, if A and B are

present petals are formed, if B and C are present stamens are formed and if C alone is present carpels are formed. Figure 4 illustrates the interactions of the A, B and C functions and can be used to predict the phenotype of double and triple floral mutants (Coen & Meyerowitz 1991) however the model will have to be updated as more data is collected.

The homeotic genes each affect one of these functions however, they also work in combination to regulate each others' activity (Irish & Sussex 1990, Bowman *et al.* 1991, Drews *et al.* 1991, Trobner *et al.* 1992, Yanofsky *et al.* 1994). Some of the floral homeotic genes in both *Arabidopsis* and *Antirrhinum* have been cloned and characterised and there are striking sequence similarities (Sommer *et al.* 1990, Yanofsky *et al.* 1990, Jack *et al.* 1992, Schwartz-Sommer *et al.* 1992, Trobner *et al.* 1992). A DNA binding region called the MADS box (Shiraishi *et al.* 1993) is present in the floral homeotic genes from both species which suggests that floral development has been highly conserved throughout evolution. The MADS box is named after MCM1, a transcription regulator of mating type specific genes in yeast, AG, the floral homeotic gene in *Arabidopsis*, DEFA, a homeotic floral gene in *Antirrhinum majus* and SRF, serum response factor in humans, which all show similar DNA binding domains.

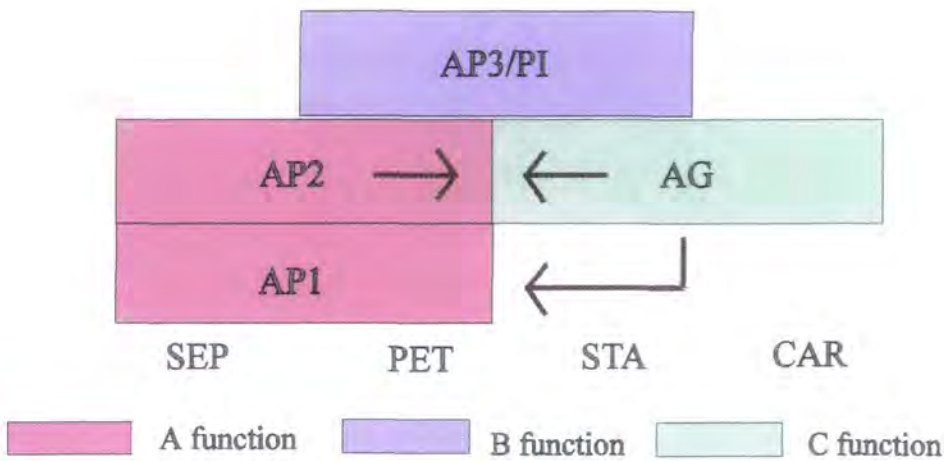


Figure 4. Diagrammatic representation of the three functions in the floral meristem (after Yanofsky *et al.* 1994)

sep sepal; pet petal; sta stamens; car carpels; arrows indicate the proposed antagonism between some of the genes.

1.3. EARLY FRUIT DEVELOPMENT

1.3.1. Fruit Structure

The female part of the flower, the gynoecium, which develops into the fruit varies in morphology between different species and although the origin and structure of the fruit is still a subject of controversy, the classical view is that the fruit developed from modified leaves or leaf-like structures (Gillaspy *et al.* 1993). The fruit is composed of either a single or a number of units called carpels. The carpel comprises a stigma to which the pollen adheres and germinates, a style through which the pollen tubes grow, and an ovary which contains the ovules. The ovules are attached to the placental tissue, which lines part of the ovary wall, by a stalk called the funicle. The cavity into which the ovules protrude is called the locule and the structure which separates two or more locules is the septum. Most gynoecia comprise two or more carpels and the carpels may be free, in which case the gynoecium is called apocarpous, or they may be fused, in which case the gynoecium is termed syncarpous. The fruit wall is usually termed the pericarp and generally develops from the carpel walls. The pericarp is usually differentiated into three distinct tissue layers. The outer exocarp, the middle mesocarp and the inner endocarp.

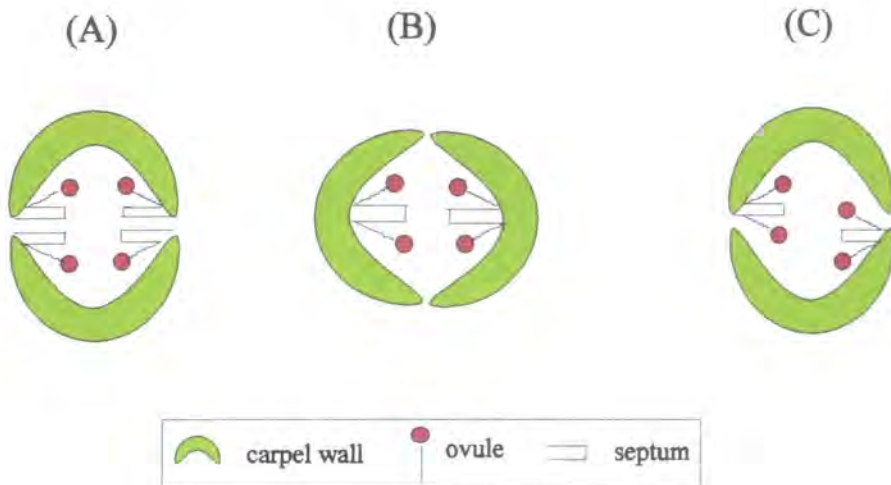


Figure 5. Diagrammatic illustration of the possible arrangements of the carpels in *Arabidopsis*

The position of the ovary with respect to other floral parts is another method to classify and describe carpel structure. An ovary which is above the point of attachment of the other floral organs is described as superior, and one below the attachment of other floral organs is described as inferior. The *Arabidopsis* fruit develops from a superior, syncarpous gynoecium.

There are conflicting hypotheses concerning the number of carpels which constitute the fruit (Saunders 1929, Eames 1931, Gasser & Robinson-Beers 1993). Okada *et al.* (1989) proposed a "carpel-forming unit" to explain the structure of various floral mutants of *Arabidopsis* which show variations in fruit structure. This unit consists of a carpel wall with marginal ovular placentae and one central and two marginal vascular bundles. The margins of the two carpels are fused and the marginal bundles are shared. This arrangement is illustrated in Figure 5 as diagram (A). Although this successfully explains the vasculature and position of the ovules in the fruit, it does not attempt to describe the presence of the septal tissue.

Development of the septum can be more easily explained if each carpel possesses a central placenta from which a septum possessing a row of ovules on each side develops. If the margins of each carpel are fused, growth of the septa towards each other would result in a false partition. This arrangement is illustrated in Figure 5 as diagram (B). It is also possible for each carpel to possess a placenta along one margin, from which the septum and two rows of ovules develop. The two carpels would in this instance be fused in a laterally opposed orientation. This arrangement is illustrated in Figure 5 as diagram (C). However, as this controversy is not a main concern of this thesis, for simplicity and in keeping with others (Hill & Lord 1989, Kunst *et al.* 1989, Okada *et al.* 1989) the gynoecium is considered to consist simply of two carpels each possessing two rows of ovules.

1.3.2. The Gynoecial Meristem

The central portion of the *Arabidopsis* flower first gives rise to a dome-shaped gynoecial primordia which consists entirely of meristematic cells. These cells differentiate to form an elliptical, open-ended cylinder with a central fissure, which is lined with meristematic cells, (Hill & Lord 1989, Okada *et al.* 1989, Smyth *et al.* 1990), and has two opposing, rudimentary vascular bundles. The histological development of the *Arabidopsis* silique has been studied (Spence 1992), and development divided into ten different stages based on

distinct histological events (Table 2). The first five stages are concerned with the development of the gynoecium, from inception until fertilisation, and are briefly described below.

At stage one, the gynoecium is first visible as an elliptical, open-ended cylinder comprising several layers of cells. The two inner layers, lining a narrow fissure, stain very darkly and resemble meristematic tissue and appear to extend around the tip of the cylinder. The differentiation of the replar bundles in the centre of each of the longer sides of the ellipse occurs during the first stage of gynoecial development. The number of cell layers present during the first stage of development does not appear to change during gynoecial growth, and development, instead the gynoecium increases in diameter by anticlinal divisions within the cell layers, and increases in length by periclinal divisions at the meristematic tip and cell elongation.

Stage	Key events
1.	gynoecium differentiates into open ended cylinder, vascular bundles develop
2.	placentae develop
3.	ovules develop, carpel walls differentiate
4.	placentae fuse, endocarp differentiates
5.	transmitting tissue and stigmatic papillae develop
6.	carpel margins constrict
7.	separation layer forms
8.	dehiscence zone cells and endocarp <i>b</i> lignify
9.	endocarp <i>a</i> disintegrates, mesocarp desiccates
10.	valves separate

Table 2. Brief summary of *Arabidopsis* silique development

The central fissure of the cylindrical gynoecium gradually widens and two opposing placentae develop from the meristematic layer at stage two and are seen as two bulges protruding from the meristematic layers into the centre of the fissure. The placentae develop adjacent to the vascular bundles and are always parallel to the axis of the inflorescence. A row of ovules develop at each side of the placentae at stage three and the carpel walls differentiate to form three distinct cell types. The outer exocarp layer

comprises a single layer of cells, with thickened outer walls, which are interspersed with guard cells and stomata. The mesocarp layer comprises several layers of chlorenchymatous cells between which there are small intercellular spaces. The endocarp layer, lining the inside of the fissure, comprises a single layer of thin walled cells.

The placentae fuse to form a false septum at stage four, creating a bilocular ovary, and the gynoecium eventually closes at the top. There is also further differentiation within the carpel walls the tissue types of the carpel walls are shown in Figure 6. A second endocarp layer (**Enb**) differentiates between the innermost endocarp (**Ena**) and the mesocarp. The cells of **Enb** are comparatively narrow and this distinct cell layer appears to arise from continual anticlinal cell divisions. During the last stage of gynoecial development the stigmatic papillae and the transmitting tissue develop prior to fertilisation.

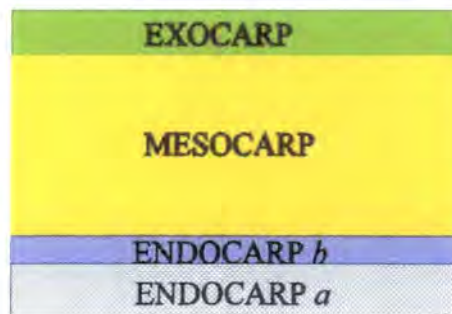


Figure 6. Diagrammatic illustration of the carpel wall layers in the *Arabidopsis* gynoecium

Mutations which affect the gynoecium may be used to study its ontogeny and development and a histological study of the development of the *clavata1* (*clv1*) mutant silique has been performed (Spence 1992). *clv1* siliques are club shaped and possess from two to five locules, although four locules is the most common (Haughn & Sommerville 1988, Okada *et al* 1989, Leyser & Furner 1992), and some flowers have extra organs in the other floral whorls. The increase in the number of carpels in the *clv1* silique seems to arise from an enlarged floral meristem which, at the first stage of development, initiates four vascular bundles. An increased number of placentae develop adjacent to the vascular bundles.

Most *clv1* siliques were also found to contain an extraneous degenerate organ which frequently possessed stigmatic papillae tissues (Spence 1992, Clark *et al.* 1993, Crone and Lord 1993). This 'vestigial' gynoecium develops from a clump of meristematic cells in the centre of the gynoecium and may develop in the enlarged meristem if the CLV gene plays a role in the maintenance of the floral meristem, or cell division patterns within the meristem (Clark *et al.* 1993). It has also been suggested by Crone and Lord 1993 that the *clv* mutant phenotype may be a result of heterochronic changes within the floral meristem. Mutations which affect the gynoecium and produce similar phenotypes to *clv* have been isolated. The *flo82* mutant (Komaki *et al.* 1988) produces flowers in which the number of carpels is increased to three or more and extra organs are frequently produced in the other floral whorls. The carpels in this mutant, which is not allelic to *clv*, are often unfused resulting in a sterile gynoecium. Intraspecific, periclinal chimeras, in which the meristematic layers are genetically marked, have been generated between tomato plants that differ in the number of carpels per flower. This has demonstrated that, although all three meristematic layers participate in floral organ formation, it is the genotype of cells within L3 that determine floral meristem size and carpel number in tomato plants (Szymkowiak & Sussex 1992, Huala & Sussex 1993).

1.4. FRUIT RIPENING AND THE DEHISCENCE MECHANISM

1.4.1. Fruit Ripening in *Arabidopsis*

Two of the major processes involved in fruit ripening are post-fertilisation development of the seeds, which is not a main concern of this thesis, and development of the fruit wall (Brady 1987, Fisher & Bennett 1991). Maturation of the fruit wall in *Arabidopsis* involves the development of the dehiscence zones and differentiation of the carpel walls. The general cellular structure of the *Arabidopsis* dehiscence zone is illustrated in Figure 7. Previous work in this laboratory, involving histological studies on *Arabidopsis* fruit development, identified five stages of development which are concerned with the differentiation of tissues within the fruit wall (see Table 2.)

Following fertilisation at stage six, cell division in the carpel wall gradually ceases, and the cells of all of the carpel wall layers begin to differentiate and expand. Cells in the exocarp thicken along the outer walls and begin to expand predominantly along the long axis of the silique. The mesocarp cells expand in all planes and there is an increase in the number of

intercellular spaces between the cells. Cells comprising **Enb**, which are adjacent to the mesocarp, continue to divide and expand predominantly along the long axis of the silique forming long thin tapered cells. **Ena** cells which line the locule of the silique thicken slightly along the outer walls and begin to expand predominantly along the long axis of the silique.

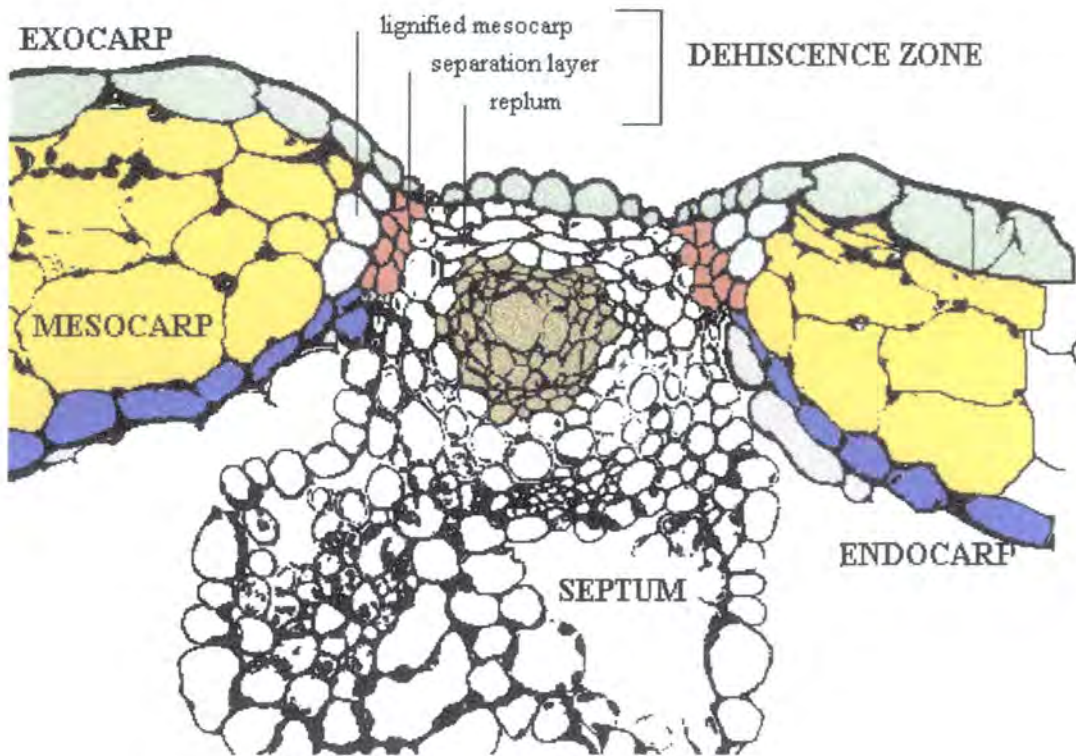


Figure 7. Transverse section showing the tissues of the dehiscence zones of *Arabidopsis*

About four rows of cells at the extreme carpel wall margins do not increase in size at the same rate as those in the other layers of the carpel wall. These smaller marginal wall cells will form the dehiscence zones. At stage seven about two rows of dehiscence zone cells on the extreme carpel wall margins begin to degrade, these cells will form the separation layer. The separation layer extends through all of the carpel wall layers. The degradation

observed in these cells is indicative of middle lamella breakdown as the cells have a rounded appearance and are always observed intact in sections from dehiscing siliques.

At stage eight the remaining two or three rows of smaller dehiscence zone cells adjacent to the mesocarp begin to lignify. This isolates the carpel walls from the rest of the fruit, forming two valves. The exocarp outer cell walls continue to thicken and form a waxy cuticular coat on the outside surface of silique. The cells of *Enb* show no further cell division and this cell layer lignifies at stage nine. The mesocarp begins to desiccate sequentially, starting from the mesocarp cells which are adjacent to the exocarp and proceeding gradually through to the endocarp. This is seen as a visible yellowing of the silique. The fruit usually turns yellow from the tip of the silique to the base.

The endocarp layer *Ena*, which lines the inside of the locule collapses following lignification of *Enb* and the cell wall remnants can be observed in tissue sections from mature siliques. At stage ten the valves detach from the mature fruit at the separation layer, leaving the seeds exposed. The dehiscence mechanism, and "pod shattering", is therefore facilitated by; 1) weakening of valve attachment, due to lack of cell cohesion in the separation layer, and 2) tensions, which develop within the carpel walls due to the desiccation and shrinkage of the mesocarp, which is attached to a thickened, non-shrinking endocarp.

1.4.2. Senescence

Fruit ripening has many features in common with both senescence, the ageing and death of organs or whole plants, and abscission, the shedding of leaves and other organs, and many plant enzymes and hormones are common to all of these processes. During leaf senescence in annual plants, nitrogen, carbon and minerals are mobilised from the leaf into the developing fruits. This process involves the degradation of chloroplasts and loss of chlorophyll, and the breakdown of cell proteins (Thimann 1980).

Arabidopsis plants exhibit a monocarpic growth habit in which the entire plant senesces following reproductive growth. The rosette leaves are the first structures to exhibit senescence, and this occurs before the fruits are mature. The stem, cauline leaves and siliques become senescent after apical arrest which occurs when the terminal floral buds on the inflorescence meristem degenerate. The senescing rosette leaves show progressive

yellowing, typically caused by degeneration of the chloroplasts and consequent loss of chlorophyll, followed by complete desiccation. This pattern of development is similar to that seen in the carpel wall in the ripening siliques.

The common biochemical marker associated with photosynthesis is Rubisco (ribulose biphosphate carboxylase) which can be detected in whole organs using extraction techniques or on tissue sections using antibodies raised to the protein. Previous work conducted by the author utilised antibodies raised against pea Rubisco (kindly donated by Dr. M. Cercos) to detect the protein in the *Arabidopsis* silique. Rubisco was localised to the mesocarp layer in the maturing fruit and was present prior to and after fertilisation. Binding was strongest during stages five to eight and decreased during stage nine as the silique begins to desiccate.

The timing of leaf senescence is thought to involve the partitioning of resources between vegetative and reproductive development which involve control signals between the leaf and developing fruit. Hensel *et al.* (1993) found that in *Arabidopsis* the timing of leaf senescence was the same in both Landsberg *erecta* and a late flowering mutant (*Co-2*), suggesting that leaf senescence is not controlled by reproductive development but probably by an age related process.

1.4.3. Abscission

Abscission is a very precisely controlled process, both temporally and spatially, which results in cell wall separation (Osborn 1989). Bean (*Phaseolus vulgaris*) leaves have been used as one of several model systems to study abscission. The abscission zone in bean generally comprises a number of rows of isodiametric cells which form a layer across the organ to be shed. A separation layer, one to five rows thick, develops and the cells have a rounded, swollen appearance, indicative of middle lamellar breakdown (Sexton & Roberts 1982). Distal to the abscission zone adjacent cells thicken and begin to lignify. The leaves detach from the plant at the separation layer due to lack of cell cohesion, although the separation layer cells remain intact.

Recent work by Robert's group in Nottingham has employed elder (*Sambucus nigra*) leaves to study abscission. The elder leaf has three large abscission zones comprising about 20 rows of cells making it ideal for biochemical and molecular studies (Coupe *et al.*

1995). Differential screening of mRNA from ethylene-treated, abscission-zone tissues, against ethylene-treated non-zone tissues, has identified several cDNA clones which are up-regulated in abscission zone tissues of elder leaves; these include a number of pathogenesis related proteins, a polyphenoloxidase and a metallothioneine-like protein.

The functional and cytological similarities between leaf abscission zones and the dehiscence zones in both *Brassica napus* siliques (Meakin 1988), and *Arabidopsis* siliques, suggests that their development may be controlled by the same or similar processes. The fruit undergoes many biochemical as well as structural and textural changes during ripening such as loss of chlorophyll, a change in the respiration rate, an increase in ethylene synthesis and changes in the molecular size of cell wall polymers. This involves complex reactions between a number of plant enzymes and hormones. Investigations into fruit ripening have mainly been concerned with the ripening of fleshy fruits such as tomato, and hydrolytic enzymes, which are also associated with abscission, have been identified as playing a major role in fruit softening.

1.5. THE PLANT CELL WALL

Cellular differentiation within the carpel tissues that accompanies fruit ripening is seen as a change in the shape of cells, or thickening of cell walls. The plant cell wall forms part of the cell surface and it interacts with the plasmalemma, a sheet-like membrane composed of a lipid bi-layer with associated protein molecules, and hence it also interacts with the filaments and microtubules of the cytoskeleton. Microfilaments are composed of the protein actin and are usually located in the cytoplasm beneath the plasmalemma. The actin cytoskeleton is involved in processes such as cytoplasmic streaming and cytokinesis (Eamons *et al.* 1995). Microtubules are composed of subunits of the protein tubulin and are found in abundance in the cell cytoplasm, they are very dynamic and can reorientate from transverse to parallel to the cells long axis and *vice-versa*.

Microtubules are involved in the maintenance of cell shape, cell elongation, intracellular transport and also in cell division, where they form the mitotic spindle and part of the phragmoplast, which assembles the cell plate. Microtubules can be stained by the introduction of fluorescent labelled tubulin into the cell which is incorporated into the cytoskeleton, and using the relatively recent technique of Confocal Laser Scanning Microscopy, the three dimensional microtubule arrays within the cell can now be

visualised (Hush 1995, Lloyd *et al.* 1995). In elongating cells it has been shown that the orientation of the microtubules associated with radial cell walls is longitudinal or oblique, but those associated with the outer cell walls change from the longitudinal to the transverse. The orientation of the microtubules may therefore be involved in the restructuring of the cell wall during cell elongation and differentiation.

Although there are structural and compositional differences between different plant cell walls, the general composition of the primary cell wall is approximately 30% cellulose, a linear β -(1-4) glucan; 30% hemicelluloses, of which the principle one is usually xyloglucan; 35% pectins of which the principal ones are galacturonic acid and rhamnogalacturonans I and II, and their methyl esters; and 5% protein (Fisher & Bennett 1991, Carpita & Gibeau 1993).

1.5.1. Structure of the Plant Cell Wall

Carpita & Gibeau (1993) have proposed a model of cell wall structure which contains three domains. The first domain comprises a network of precisely orientated cellulose microfibrils which are wrapped around the cell and are interlocked by chains of xyloglucan. The xyloglucan chains are bound to the microfibrils and span the spaces in-between. The cellulose and xyloglucan framework is embedded in the second domain, a matrix or gel of cross linked pectic polysaccharides. The pectin matrix is not a random mixture but also comprises precisely orientated polymers which appear to be at right angles to the orientation of the cellulose microfibrils. Esterified and non-esterified pectins show different spatial distributions, with esterified pectins usually found evenly distributed throughout the wall, and non-esterified pectins in the middle lamella and adjacent to the plasma membrane (Knox *et al.* 1990, Roberts 1990). The cell wall is locked into shape by the structural proteins which comprise the third domain.

Adjacent plant cell walls are cemented together by a pectic matrix called the middle lamella, but there are also intercellular spaces, in between areas of cell wall contact. In transverse section these intercellular spaces are usually found at three way junctions. These intercellular spaces comprise another domain which is formed by precise, enzymic dissolution of the walls (Roberts 1990). Intercellular spaces may be large and "empty" or small and filled with various matrix materials. This apoplastic domain may be important in pathogen and ethylene response mechanisms.

1.5.2. Plant Cell Wall Proteins

The most abundant and well studied proteins in the cell wall fall into five main classes and include; extensins, glycine-rich proteins (GRPs), proline-rich proteins (PRPs), arabinogalactan proteins (AGPs), and solanaceous lectins (Cassab & Verner 1988, Marcus *et al.* 1991, Keller 1993, Showalter 1993). The distinction between these classes of proteins is becoming less distinct as more novel proteins are identified.

Extensins are a family of hydroxyproline-rich glycoproteins and are usually associated with the cambial cells and phloem tissues. They are structural proteins that also have a role in development, wound healing and defence, and may interact with the acidic pectins within the cell wall and play a part in wall strengthening during stress, by oxidative crosslinking. The primary structure of extensins varies between different plants and different tissue types and the structure of the protein may be related to its role in the cell. The EXTA extensin gene isolated from *Brassica napus* (Evans *et al.* 1990), is expressed in high amounts in roots and is only induced in green tissues after wounding. Using glucuronidase (GUS) fusion techniques, the tissue expression pattern of the EXTA gene has been determined in rape roots, and was found to be localised to the phloem tissues (Shirsat *et al.* 1991). The EXTA gene has been isolated and used to isolate an *Arabidopsis* homologue ArabD (Barnett & Shirsat 1995, Elliott & Shirsat 1995). The expression pattern of these two genes appears to differ in that the *Arabidopsis* gene is expressed in leaf and petiole tissues as well as the root.

GRPs are usually associated with lignifying tissues and are commonly localised to the xylem elements. The structure of the GRP proteins (β pleated sheet), also suggests that they provide some elasticity and tensile strength to the cell wall. PRPs frequently show a similar localisation pattern to the GRPs and they may also be involved in lignification and interact with acidic pectins within the cell wall. The AGP proteins are mainly made up of carbohydrate and are also found associated with the cell plasmalemma. Although no function has yet been established for these diverse glycoproteins, it has been proposed that they are involved in cell-cell recognition (Cassab & Verner 1988, Showalter 1993). Solanaceous lectins, as their name implies, are only found in solanaceous plants. They mainly consist of hydroxyproline and arabinose and bind n-acetylglucosamine.

Recent work on plant proteins has employed immunocytochemical methods to localise specific polysaccharide epitopes within the cell. Roberts has utilised antibodies raised against specific carbohydrate epitopes of AGPs (Knox *et al.* 1989, 1992, Pennell *et al.* 1989, 1991, Pennell & Roberts 1990, Stacey *et al.* 1990, Baldwin *et al.* 1993) to localise these glycoproteins within the cell. Although the precise function of these proteins is still not known they appear to play a variety of roles in the cell. Localisation studies suggest they may be specific to a cells position during development (Knox *et al.* 1989, 1992, Pennell & Roberts 1990, Pennell *et al.* 1991) and may also aid in binding the cell wall to the plasma membrane (Pennell *et al.* 1989, Baldwin *et al.* 1993).

Previous work by the author has employed immunocytochemical methods to localise an AGP using the antibody JIM13 (kindly supplied by the John Innes Institute) to specific tissues in the *Arabidopsis* fruit. The JIM13 epitope was localised to the vascular tissues of the carpel walls and the vascular tissues of the replum, and to the lignifying cells of the dehiscence zone and endocarp layer in the carpel walls of the maturing silique. The JIM13 epitope was only detected in these tissues in the later stages of lignification and although its function is unknown its localisation pattern suggests that it is involved in the later stages of wall thickening.

1.5.3. Hydrolytic Enzymes

The three main hydrolytic enzymes which have been associated with fruit ripening and abscission are polygalacturonase, pectinesterase and cellulase (β -(1-4) glucanase) (Sexton & Roberts 1982, Cassab & Varner 1988, Fischer & Bennett 1991). Tomato fruit ripening has been used as a model system to study plant gene expression and many of the genes for ripening-related enzymes have been identified (Fray & Grierson 1993). Using antisense technology, genetically engineered tomato plants with a much-reduced polygalacturonase level in the fruit have been produced. These fruit are more resistant to mechanical damage so may be harvested at a later stage, and the fruit extracts have a higher viscosity making them ideal for the processing industry (Grierson & Schuch 1993, Gray *et al.* 1994). Genetically engineered commercial varieties are expected to be available on the US market in 1995 (Grierson & Schuch 1993).

1.5.3.1. Polygalacturonase

Polygalacturonase degrades demethylated pectin by catalysing the hydrolysis of α -(1-4) galacturonan linkages and is believed to be a major factor in wall softening in tomatoes due to the increase in soluble pectins (Smith *et al.* 1990). Polygalacturonase transcription has been reported to be controlled by both positive and negative regulatory elements throughout the thick fruit pericarp (Montgomery *et al.* 1993). However, genetic studies have shown that in tomato the polygalacturonase in leaf abscission zones is different from that in the ripening fruit, and that these isoenzymes are probably controlled by different genes (Taylor *et al.* 1990).

Polygalacturonase has also been studied in the abscission zones of elder, (Roberts *et al.* 1989, Taylor *et al.* 1990, Taylor *et al.* 1993a) where it was found to show the characteristics of an endo-acting enzyme, resulting in an increase in the solubility of the cell wall, a process associated with fruit ripening. Two polygalacturonase cDNAs JET37 and JET39 have been isolated from elder (Coupe *et al.* 1995, Bell *et al.* 1995); one of them, JET37, codes for a protein which shows homology to other polygalacturonases isolated during fruit ripening. Although Meakin & Roberts (1990b) found no correlation between polygalacturonase activity and rape dehiscence, Coupe (1993) found there was a rise in polygalacturonase activity in dehiscence zone cells of two rape varieties.

1.5.3.2. Pectinesterase

Pectinesterases catalyse the demethylation of the C6 carboxyl group of galacturonosyl residues, and are present in most plant cells where they probably have a role in many cell wall modifications. Unesterified and methylesterified pectins have been localised to different positions within the cell wall (Knox *et al.* 1990). The level of pectinesterase increases in ripening fruit, and as it is present in quite large amounts in tomato it has been studied extensively in this fruit (Markovic & Jornvall 1986, Ray *et al.* 1988, Tieman *et al.* 1992, Hall *et al.* 1993).

The primary structure of the enzyme has been determined and a cDNA clone sequenced which has allowed the use of antisense technology to study enzyme action. Gaffe *et al.* (1994) have demonstrated that there are two major groups of isoforms of pectin

methylesterase in tomato tissues, those synthesised during fruit development, and those present throughout the growth and development of vegetative and fruit tissues. Three isoforms of the enzyme are present in high amounts during tomato fruit ripening and expression of an antisense gene decreases the amount of the three isoenzymes in the fruit, but does not affect the expression of the enzyme during plant development. The proposed role of pectinesterase in tomato fruit ripening is to make pectin more susceptible to degradation by polygalacturonase. There is still no direct evidence to link pectinesterase activity with abscission or fruit dehiscence.

1.5.3.3. Cellulase (β -(1-4) glucanase)

Cellulases degrade carboxymethylcellulose although the precise substrate on which they act in the cell wall is unknown (Fischer & Bennett 1991). There are two types of cellulase present in bean leaf abscission zones and these can be separated by their different isoelectric points into 4.5 cellulase and 9.5 cellulase (del Campillo *et al.* 1988). Immunocytological and *in-situ* hybridisation techniques have been used to localise 9.5 cellulase to specific tissues in the bean abscission zone (Tucker *et al.* 1988, 1991, del Campillo *et al.* 1990). In bean the enzyme first appears in the vascular tissues of the pulvinus and abscission zone, before it is detected in the cortical cells of the separation layer.

The abscission zones of the leaf, flower and pod of *Glycine max* also have high levels of a 9.5 cellulase which is immunologically similar to that of bean and which is not present in the root or apical buds (Kemmerer & Tucker 1994). The non-abscising roots and apical buds of *Glycine max* contain a different type of cellulase, probably associated with cell growth and expansion. Cellulase activity during elder leaflet abscission has also been studied (Taylor *et al.* 1993b, Webb *et al.* 1993, Coupe *et al.* 1995) and it shows a similar expression pattern to that observed in bean leaf. Cellulase from the elder leaf abscission zone shows homology to cellulase from bean leaf abscission zones and cellulase from avocado fruit during ripening (Coupe *et al.* 1995).

Recent work by Thompson and Osborne (1994) on the abscission zone of bean leaf, has demonstrated that the vascular tissues may affect the activity of cellulase during the process of abscission. Removal of the vascular tissues of the pulvinus and abscission zone, at a critical time, prevents cellulase activity in the abscission zone tissues and cell

separation. Although the reason for this is not yet known they suggest that the vascular tissues may release signalling molecules, perhaps cell wall fragments from hydrolytic enzyme activity, which influence cellulase activity in the abscission zone or induce new gene expression. An increase in cellulase activity has been reported in the dehiscence zone cells of rape pods prior to dehiscence (Coupe 1993) where it is preceded by an increase in production of the plant hormone ethylene (Meakin & Roberts 1990b). This suggests that ethylene induces, or may play a regulatory role in, cellulase activity.

1.6. LIGNIFICATION

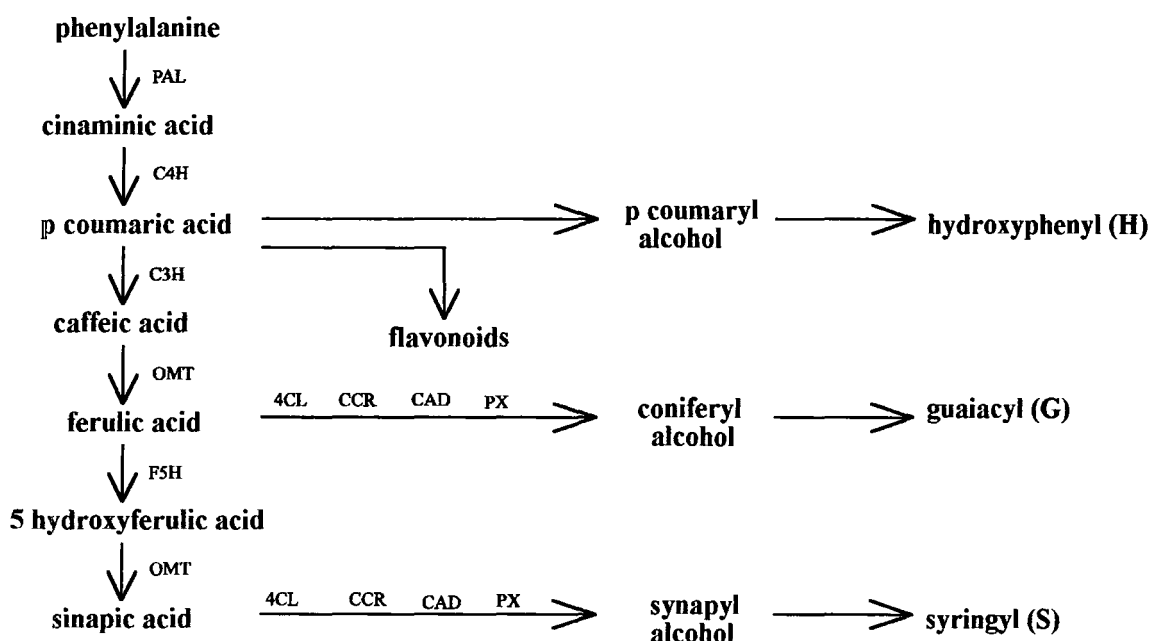


Figure 8. Scheme of monolignol biosynthesis and some of the enzymes involved

PAL phenylalanine ammonium lyase; **C4H** cinnamate 4 hydroxylase; **C3H** p coumarate 3 hydroxylase; **OMT** caffeic acid O methyltransferase; **F5H** ferulate 5 hydroxylase; **4CL** p coumarate CoA ligase; **CCR** hydroxycinnamyl CoA reductase; **CAD** hydroxycinnamyl alcohol dehydrogenase; **PX** peroxidase.

Lignin is one of nature's most abundant compounds and although it is industrially important as one of the major determinants in paper quality, little is known about the temporal and spatial factors controlling lignification (Lewis & Yamamoto 1990). One of

the major roles of lignin is to strengthen the cell wall however, its deposition can be influenced by many things such as infection, wounding, inhibitors, hormones and metal ions (Grand *et al.* 1982).

The structure of lignin varies throughout the plant and the plant cell wall, however the polymers are derived from only three precursor monolignols, p-coumaryl, coniferyl and sinapyl alcohols, and are classified as consisting of various proportions of hydroxyphenyl (H), guaiacyl (G) and syringyl (S) moieties respectively (Fig. 6). These are transported from the cytoplasm to the cell wall where they are polymerised. In *Arabidopsis* lignin has been reported to consist of G and S units only, typical of the angiosperms, and these have been found in the ratio 77:23 in bolting seedlings (Dharmawardhana *et al.* 1992), and 2:1 in rachis tissue (Chapple *et al.* 1992). In both cases there was a predominance of guaiacyl units.

1.6.1. Lignin Synthesis

Monolignol synthesis forms part of the general phenylpropanoid pathway (Fig. 8) and many of the enzymes involved have been characterised (Hahlbrock & Scheel 1989). Little data however, is available concerning the synthesis of lignins from their monolignol precursors. Mutants defective in the phenylpropanoid pathway have been identified. In *Arabidopsis* the *sin 1* mutation (Chapple *et al.* 1992) has an effect on lignin composition, and probably affects the conversion of ferulic acid to sinapic acid, producing a plant whose lignin has a much reduced S content. Lignin deposition has been shown to be associated with the activities of enzymes such as phenylalanine ammonia lyase (PAL), cinnamyl alcohol dehydrogenase (CAD) and peroxidase.

1.6.2. Phenylalanine Ammonia Lyase (PAL)

PAL has been identified in the xylem tissues of *Arabidopsis* (Ohl *et al.* 1990), tobacco and potato (Beven *et al.* 1989), and pea (Wilkinson & Butt 1992), where it is likely involved in the very early stages of lignin synthesis (Fig. 8). It catalyses the first step in phenylpropanoid synthesis and is probably the key regulator of the lignin pathway. Immunocytochemical studies by Smith *et al.* (1994) localised antibodies to bean PAL, and cinnamate 4 hydroxylase (C4H) subunits, to the lignifying xylem of bean hypocotyls. Both enzymes were also found in adjacent cells, which probably supply lignin precursors to the

vascular tissues. The two enzymes were located in different parts of the cell, PAL was found in the cytosol and C4H was found to be associated with the endoplasmic reticulum and Golgi bodies.

Both of these enzymes are central to the phenylpropanoid pathway, and so they are also involved in the production of compounds such as flavonoids and phenolics which are both involved in other responses in addition to lignification. PAL belongs to a small gene family and has been well characterised in several species including *Arabidopsis*, bean, parsley and rice (Ohl *et al.* 1990).

1.6.3. Cinnamyl Alcohol Dehydrogenase (CAD)

CAD has also been isolated from various plant species (Wyrambik & Grisbach 1975, Halpin *et al.* 1991, Goffner *et al.* 1992, Hibino *et al.* 1993, Holt *et al.* 1995), and usually occurs in two isoforms, CAD1 and CAD2, which have different substrate affinities. CAD2 is usually associated with the final step of lignin precursor synthesis due to its high affinity for the monolignol precursors, however it is also required for the synthesis of lignans and phenolics and may also serve a variety of functions in addition to structural lignin synthesis.

Several natural maize mutants have been identified in which the plants lignin is affected; they are known as brown midrib mutants because of the red-brown colouration of the leaf midrib and stem sclerenchyma. These mutants have improved digestibility compared to normal plants. One of these mutants, *bml*, has reduced CAD levels and the lignin in *bml* maize plants has reduced G and S units (Holt *et al.* 1995). Although the levels of both G and S units is reduced in this mutant, the ratio of the units is not affected. The more recent introduction of antisense technology has allowed the study of CAD activity in genetically altered tobacco plants (Halpin *et al.* 1995). Tobacco plants expressing the CAD antisense gene also have red-brown lignin and have reduced levels of cinnamyl alcohols but increased levels of cinnamyl aldehydes and therefore an altered lignin structure. This technology has wide implications for the paper making and forage crop industries.

1.6.4. Peroxidases

Peroxidases are present as multiple isoenzymes (van Hutstee 1987, Lewis and Yamamoto 1990) and are widely distributed throughout the plant, animal and microbial kingdoms. Their role in lignification is thought to be in catalysing the polymerisation of monolignols in the cell wall, and both anionic peroxidases (Mader *et al.* 1980), and cationic peroxidases (Sato *et al.* 1993), have been implicated in the lignification process. It has been shown that calcium is required for the release of cationic peroxidases in plant cells (Sticher *et al.* 1981, Xu & van Huystee 1993) and that the anionic isozyme is under the control of calmodulin (Xu & van Huystee 1993). Peroxidase from horseradish (*Armoracia rusticana*), another member of the Brassicacea family, has been well studied and, using the gene for horseradish peroxidase as a probe, *Arabidopsis* peroxidase genes have been screened from a genomic library and sequenced (Intapruk *et al.* 1991).

Lewis & Yamamoto (1990) have proposed four criteria that must be fulfilled for a peroxidase enzyme to be associated with lignification; it must have the appropriate substrate specificity, primary structure, and its temporal and spatial expression should correlate with lignification. Peroxidases can be isolated from cell culture media and tissue extracts and purified. Both anionic and cationic isoenzymes have been found in extracts of bean leaf from the abscission zone, pulvinus, and petiole (McManus 1994). However, whilst the cationic isoenzymes were predominantly found in the pulvinus and anionic isoenzymes in the petiole, both types of isoenzyme were found in the abscission zone where cell separation occurs. Immunocytochemical techniques using antibodies raised to purified peroxidase proteins, have frequently been used to determine the spatial patterns of particular isoenzymes in the cell (Kim *et al.* 1988 Smith *et al.* 1994).

1.6.5. Phenoloxidases

Over the past few years phenoloxidases such as laccase and laccase-like oxidases have been implicated in lignification (O'Malley *et al.* 1993). Laccase is a blue copper-containing metalloprotein which can polymerise monolignols *in vitro* and is found in lignifying cell walls (Sterjiades *et al.* 1992, 1993, Bao *et al.* 1993, McDougall *et al.* 1994). Laccases, in common with peroxidases, may be either basic or acidic and the two types of enzyme appear to carry out similar functions although laccases are active in the absence of hydrogen peroxide. Both peroxidase and laccase enzymes are coded by diverse families of

related genes (O'Malley *et al.* 1993). Peroxidases are present in great excess compared to oxidases and McDougall *et al.* (1994) suggest that oxidase enzymes are strongly attached or covalently bound to the cell wall, which makes their isolation and purification more difficult. Sterjiades *et al.* (1993) have reported that laccases are less active on substrates with multiple aromatic rings, and therefore may be active before peroxidase during lignification.

Histochemical techniques have been employed to identify phenoloxidase activity in the lignifying tissues of the *Arabidopsis* silique (Spence 1992). Oxidase activity was first detected in the vascular tissues of the young fruit and the highest oxidase activity was detected in the vascular tissues of the mature fruit. Activity was also detected in the lignifying endocarp of the mature fruit. The implication that oxidase enzyme activity may be one of the initial steps during lignin deposition (Sterjiades *et al.* 1993, McDougall *et al.* 1994) makes these enzymes ideal candidates for genetic manipulation using antisense technology.

1.7. HORMONES

Plant hormones are small molecules which have effects on physiological processes within the plant. These hormones mainly influence growth and differentiation and are active at very low concentrations. There have so far been six chemical substances, or groups of substances, identified as plant hormones; auxins, gibberellins, cytokinins, abscisic acid, ethylene and polyamines. These hormones may affect the tissues in which they are produced, or may be transported, either cell-cell or via the vascular system, and affect tissues in another part of the plant. Because of their low concentrations, it is often difficult to determine the site of hormonal synthesis and, as many of these hormones act synergistically, it is also difficult to ascertain their precise independent mode of action. Hormonal activity has therefore often been studied indirectly using specific inhibitors or, more recently, by analysis of mutant and transgenic plants. The analysis of mutant plants seems to indicate that hormonal defects are either caused by a fault in the synthesis of one of the precursors or the hormone itself or by a fault in the hormonal receptors.

1.7.1. Auxins

The most common plant auxin is indole-3 acetic acid (IAA); it is synthesised from tryptophan and is most abundant in the leaf primordia, young leaves, roots and developing seeds. Auxin is the only hormone to exhibit polar transport, its movement being basipetal in the shoot and acropetal in the root, although the mechanisms of polar transport are still not well known. Auxins have been located in the cytosol and chloroplasts within the cell (Sitbon *et al.* 1993), and have been identified with processes such as cell elongation, vascular differentiation (Aloni 1987), abscission (Sexton & Roberts 1982), fruit ripening and bilateral symmetry (Lui *et al.* 1993). Dehiscence in *Brassica napus* has been shown to be affected by the application of a synthetic auxin (Picart & Morgan 1986) which delayed the autolysis of dehiscence zone parenchyma cells and caused a reduction in water loss from the pod walls. The number of auxin receptors on the surface of a plant cell is probably associated with its sensitivity to the hormone (Barbier-Brygoo *et al.* 1991), and molecular techniques have been used to isolate and characterise the gene for an auxin binding protein, ABP1, from *Arabidopsis* (Palme *et al.* 1992, Shimomura *et al.* 1993).

Various *Arabidopsis* mutants have been identified which show impaired responses to auxin. The *axr1* mutants which are dwarfed show a reduced sensitivity to auxin (Lincoln *et al.* 1993, Leyser *et al.* 1995), which may be caused by a mutation in the protein required for auxin perception. The AXR1 gene has been cloned (Leyser *et al.* 1995) and encodes a protein with homology to ubiquitin activating enzyme, however the role of this protein in auxin response is not yet understood. The dominant *axr2* mutants are also resistant to ethylene and abscisic acid and therefore probably show a defect in general signal transduction in some manner (Wilson *et al.* 1990, Timpte *et al.* 1992). The *axr3* mutant is also resistant to auxin, but the effect of this gene is seen only in the root where it affects cell elongation (Leyser *et al.* 1995).

The *pin* mutant (Okada *et al.* 1991) and *gnom* mutant (Mayer *et al.* 1993) affect polar transport in specific parts of the plant and have shown the requirement for auxin in diverse processes such as bilateral symmetry and floral bud formation. Auxin stimulates ethylene synthesis (Yang & Hoffman 1984) therefore the action of auxin alone is often difficult to determine. Romano *et al.* 1993 have used transgenic plants to try to uncouple the effects of these two hormones and showed that the effects due to auxin included cell elongation and apical dominance.

1.7.2. Gibberellins

Gibberellins are synthesised from mevalonic acid in shoots and developing seeds and are transported via the vascular system. Gibberellins affect cell growth, seed germination and fruit setting. Several gibberellin (GA) mutants have been identified in various plant species including *Arabidopsis*. GA-sensitive mutants in *Arabidopsis* are dwarfed, have reduced apical dominance and are darker green than wild type. GA-sensitive mutations have been identified at 5 loci and all mutant plants are sensitive to exogenously applied GA (Talon *et al.* 1990). *ga1* mutants are defective in gibberellin synthesis and do not flower under short day conditions, indicating a role for gibberellin in floral initiation in *Arabidopsis* (Wilson *et al.* 1992). The *ga4* and *ga5* mutations affect enzymic steps in GA synthesis (Talon *et al.* 1990). Another gibberellin mutant in *Arabidopsis*, *gai*, is not sensitive to exogenous GA and this mutation is proposed to affect the response of the plant cells to GA (Peng & Harbard 1993).

Pea (*Pisum sativum*) has been used to study the effects of gibberellic acid on fruit set and development. Garcia & Carbonell (1980, 1985) found that unpollinated pea ovaries treated with gibberellic acid (GA₃) developed into mature fruits, while unpollinated untreated ovaries senesced. The cells of the pea carpel walls enlarge and differentiate as the fruit matures following pollination. One of the cell layers in the pea endocarp shows a similar pattern of differentiation to the lignified endocarp *b* cell layer in the *Arabidopsis* carpel wall, producing a single layer of elongated thick walled cells (Vercher *et al.* 1984). The application of GA₃ to unpollinated ovaries stimulated the enlargement of the mesocarp cells and induced the processes necessary for the elongation and cell wall thickening of the endocarp (Vercher *et al.* 1987). Unpollinated *Arabidopsis* ovaries also respond to GA₃ treatment and show enlargement of the exocarp and mesocarp cells and differentiation of the endocarp cells as seen in wild type fruits (Y. Vercher pers. comm.).

Recent work by Lloyd *et al.* (1995), involving the three dimensional visualisation of the cortical microtubule array in pea epidermal cells, has shown that application of gibberellin causes reorientation of these microtubules from the longitudinal to the transverse. This suggests that gibberellin may stimulate cell elongation by its effects on microtubule dynamics.

1.7.3. Cytokinins

Cytokinins are synthesised from adenine and are found mainly in developing seeds and the roots, from where they are transported via the vascular system, to other parts of the plant. Cytokinins affect cell division, protein synthesis, and sink activity but little is known about their mode of action. The role of cytokinins in fruit development is not well documented, however recent reports have indicated that they may play a major role in controlling flower development (Estruch *et al.* 1993). Increased cytokinin levels in floral tissues of tobacco plants reduce the expression of the tobacco floral homeotic genes which are homologous to DEFA, GLO and PLENA of *Antirrhinum majus*. The phenotypic abnormalities due to increased cytokinin levels resemble those seen in floral homeotic mutations.

1.7.4. Abscisic Acid

Abscisic acid (ABA) is also synthesised from mevalonic acid in mature leaves and seeds, however there may be two different metabolic pathways in plants to produce ABA (Zeevaart & Creelman 1988). ABA is a weak acid which dissociates to varying degrees in different cellular compartments, depending on the pH of the compartment. The main action of ABA is in response to water stress where its action is on guard cells, causing the stomata to close. Loss of cell turgor pressure is proposed to initiate ABA synthesis. ABA is also found in the seeds where it prevents precocious germination and induces seed storage protein synthesis.

ABA activity has been implicated in the process of leaf abscission (Sexton & Roberts 1982). Rinne *et al.* (1992) have proposed that the non abscising phenotype of a species of birch may be a result of low ABA levels. The hydration of the cells of the leaves is essential for active abscission to occur; low ABA levels affect the cells hydration and may cause leaves to wilt before abscission occurs.

Some ABA mutants of *Arabidopsis* have been documented. The *aba* mutant is defective in ABA synthesis and does not accumulate ABA in response to stress (Zeevaart & Creelman 1988). Mutations which are insensitive to ABA have been identified at three different loci and are designated *abi1*, *abi2* and *abi3*. *abi1* and *abi2* mutant plants wilt under water stress, but *abi3* is seed specific (Ooms *et al.* 1993).

1.7.5. Ethylene

Ethylene is the only gaseous hormone and is synthesised from methionine (Fig. 9) in most plant tissues via S-adenosyl-L-methionone (SAM) and 1-aminocyclopropane-1-carboxylic acid (ACC); these reactions being catalysed by the enzymes AdoMet synthase, ACC synthase and ACC oxidase respectively (Yang & Hoffman 1984, Kende 1993). The SAM-1 gene of *Arabidopsis* has been sequenced and cloned and shows high expression in the vascular and sclerenchyma tissues of the stem and root but appears to be correlated with the extent of tissue lignification rather than to ethylene biosynthesis (Peleman *et al.* 1989). Although ethylene is involved in many developmental processes and in defence responses, its main role is as a key regulator of senescence and fruit ripening. The biochemical pathway of ethylene synthesis has been well studied but there is still little information on how ethylene is perceived or how physiological responses are initiated, although calcium has been implicated in some ethylene-dependent processes (Raz & Fluhr 1992).

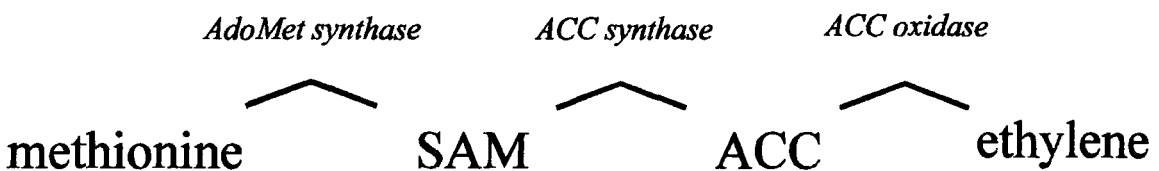


Figure 9. Scheme of ethylene synthesis

Climacteric fruits exhibit a rise in ethylene production at the onset of ripening and a similar rise in ethylene has been reported to occur in leaves before abscission (Sexton & Roberts 1982, Morgan *et al.* 1992). Responses to ethylene during abscission, ripening and senescence include a rise in the respiration rate, degradation of chlorophyll, synthesis of carotenoids, and an increase in the activity of hydrolytic enzymes. A rise in ethylene synthesis in oilseed rape is correlated with a rise in the activity of the hydrolytic enzyme cellulase (Meakin & Roberts 1990b). The control of ethylene biosynthesis is therefore of commercial importance to the agricultural industry (Theologis 1992).

Two different strategies have been utilised to reduce ethylene biosynthesis in tomato fruit (Kende 1993). Ethylene biosynthetic enzymes such as ACC synthase can be inhibited, or

the cellular level of ACC can be reduced by the introduction of an ACC deaminase gene (Klee 1993). ACC synthase is encoded by a multigene family and genes are differentially expressed in different tissues and in response to different stimuli. Antisense technology using an ACC synthase gene specifically expressed in the fruit has enabled the production of a non-ripening tomato fruit whose phenotype can be reversed by the application of exogenous ethylene (Theologis 1992, Gray *et al.* 1994). Although there are a number of ethylene mutants which have been identified in *Arabidopsis* such as the *etr* and *ein* mutations (Bleeker *et al.* 1988, Guzman & Ecker 1993) the effects of these mutations on *Arabidopsis* fruit ripening have not yet been reported.

1.7.6. Polyamines

Polyamines (PAs) are positively charged alkamines and are also found in animal and microbial systems, where they have been more extensively studied. In plants the three major polyamines are putrescine, spermidine and spermine and these are found either in their free forms or bound forms where they are conjugated to phenolic compounds such as p-coumaric, ferulic and caffeic acids, which are involved in the phenylpropanoid pathway (Evans & Malmberg 1989). PAs are present in all plant cells and are found at much higher levels than other plant hormones so are most likely synthesised *in-situ*. They are essential for growth and normal morphology but their precise effects are still unknown and their definition as hormones is still a subject of controversy.

PAs bind to nucleic acids and stabilise helical and loop structures by binding strands together, and they also bind to negatively charged phospholipids on cell membranes where they alter membrane permeability. It is also suggested that PAs affect ethylene synthesis by metabolic competition for the ethylene precursor SAM or inhibition of ACC synthase (Evans & Malmberg 1989, Tiburcio *et al.* 1993). PAs have been implicated in the control of senescence, flower development and fruit ripening and exogenous application of PAs has been reported to delay plant senescence by preventing chlorophyll loss, stabilising membranes, and reducing the activity of proteolytic enzymes and ethylene (Tiburcio *et al.* 1993). A reduction in PA levels may therefore be an early step in triggering senescence.

Exogenously applied PAs affect floral development in some plants by increasing floral initiation and a decline in PA activity can alter floral morphology (Kakkar & Rai 1993). PAs are therefore involved in some way in flower development. Basic hydroxycinnamic

amides are more abundant in female flowers, suggesting a relationship between the levels of certain polyamines and the sexuality of the plant. In some fruits PA levels are high early in development but decrease as the fruit matures indicating a relationship between PA levels and fruit ripening, where they may act antagonistically with ethylene (Evans & Malmberg 1989, Tiburcio *et al.* 1993). Exogenously applied PAs delay fruit ripening and therefore improve the shelf life of certain fruits, and their mode of action is therefore of commercial importance.

1.8. HYPOTHESIS

Previous work by the author has identified the patterns of tissue differentiation in the carpel walls and dehiscence zones of the Brassica *Arabidopsis thaliana* during fruit ripening. This thesis proposes that the differentiation of the endocarp layer in the carpel wall plays a key role in the pod 'shatter' characteristic of Brassica fruits. To test the hypothesis this study has the following practical aims.

1.9. PROJECT AIMS

This study aims to use a variety of approaches to further understand the phenotype responsible for the 'shattering' characteristic seen in some Brassicas. The study also aims to identify some of the physiological processes and control factors which are involved in the process of fruit ripening and dehiscence. This may aid in the identification of genes which can be manipulated to alter the pattern of silique development and hence reduce pod 'shattering'. A number of approaches will be used in this study and these are outlined below.

A study of the siliques of some ecotypes of *Arabidopsis thaliana* will be performed with the aim to identify any some phenotypic variations within the wild type populations. The 'shattering' characteristics of the siliques will be assessed and histological studies will be performed on fixed material using microscopical techniques. The patterns of development of the *Arabidopsis* ecotypes will be compared to that of the Landsberg *erecta* ecotype, which has been studied previously by the author.

Using microscopical techniques on fixed material, a histological and cytological study of the siliques of two other Brassica species, *Brassica napus* and *Brassica juncea*, will be performed. These two species exhibit different 'shattering' characteristics to *Arabidopsis*.

The patterns of development and the morphology of these siliques will be assessed, and compared to *Arabidopsis* with the aim to identify those tissues responsible for the different patterns of 'shattering'.

Specific components within the cell walls of the carpel wall and dehiscence zone will be examined in the different species by a combination of histochemical, immunocytochemical and biochemical techniques. The major carbohydrate components of the cell walls, such as pectins, can be isolated and compared by biochemical analysis as can the cell wall lignins. Specific proteins can be localised to tissue types within the silique by immunocytochemical methods using light microscopy, and these proteins can then be localised within the cell wall using electron microscopy.

5) *in-situ* hybridisation methods will be used to identify specific mRNAs in tissues from fixed material. The probes used for the *in-situ* hybridisations will hopefully identify some novel genes which are expressed in specific tissues within the siliques and this may aid in the further characterisation of the genes function.

A study of the siliques of some mutants of *Arabidopsis thaliana* will be performed. Variations in the 'shattering' characteristics will be assessed and histological studies will be performed on fixed material using light microscopical techniques. The phenotype of the siliques from mutant plants will be compared to the wild type.

2. MATERIALS AND METHODS

2.1. STANDARD SOLUTIONS

DEPC (diethyl pyrocarbonate) Treated Solutions

The solutions to be treated were prepared then DEPC was added to a concentration of 0.1% (v/v). The solutions were shaken and the pressure released then the solutions were stirred overnight. The solutions were then autoclaved at 120°C for 20 minutes.

50X Denhardts Solution

1% (w/v) bovine serum albumen (BSA)

1% (w/v) ficoll

1% (w/v) polyvinyl pyrrolidone (PVP)

20X Standard Saline Citrate Buffer (SSC)

3.0M sodium chloride

0.3M sodium citrate

10X Tris Buffered Saline (TBS)

1.0M 2-amino-2-(hydroxymethyl)-1,3-propanediol (Tris)

1.5M sodium chloride

pH to 8 with hydrochloric acid

TE Buffer

10mM TBS pH 8

1.0mMethylenediamine tetracetic acid (EDTA)

2.2. PLANT MATERIAL

2.2.1. Sterilising seeds

Seeds were soaked in 70% (v/v) ethanol for 15 minutes then rinsed in sterile water. Seeds were then soaked for a further 15 minutes in 20% (v/v) chlorox and thoroughly rinsed in sterile water.

2.2.2. Standard growth conditions for *Arabidopsis* ecotypes

Seeds from *Arabidopsis* were sprinkled evenly over the surface of moist Levingtons F2 Standard pH Compost in small plant pots. Four plant pots were placed in a cat tray and the compost was kept moist by watering from below every 2-3 days. Plants were grown in 24h daylight conditions (using fluorescent tube lighting) at 25°C.

2.2.3. Standard growth conditions for *Arabidopsis* mutants

Seeds from the *Arabidopsis* mutants were sprinkled evenly over the surface of moist Levingtons F2 Standard pH Compost in small plant pots. Four plant pots were placed in a cat tray and the compost was kept moist by watering from below every 2-3 days. Plants were grown in 8 hour daylight (using fluorescent tube lighting) at 19°C.

2.2.4. Standard growth conditions for *Brassica juncea*

Seeds from *Brassica juncea* were sprinkled evenly over the surface of moist Levingtons F2 Standard pH Compost in medium plant pots. Two plant pots were placed in a cat tray and the compost was kept moist by watering from below every 2-3 days. Plants were grown in the window of the laboratory during the Summer months.

2.3. SATURATED SOLUTIONS

Six different saturated solutions were prepared to create a range of constant humidities. sodium hydroxide was used to create a relative humidity of 7%, lithium chloride to create

12% humidity, calcium chloride to create 29.5% humidity, calcium nitrate to create 50% humidity, sodium chloride to create 75.5% humidity, and potassium hydrogen phosphate to create 96% humidity.

2.3.1. Preparation of Saturated Solutions (Winston & Bates 1960)

All saturated solutions were prepared by gradually adding the salt to 200ml of boiling distilled water until the solution was saturated. The mixture was allowed to cool to 50°C then a small amount of salt was added. When the mixture had cooled to R.T. more salt was added to cover the bottom of the flask then the flasks were sealed with Parafilm. The solutions were allowed to stand at 25°C for 4 weeks before using.

2.3.2. Humidity chambers

Five filter papers were placed in the bottom of a petri dish and 20ml of saturated salt solution was poured in. Mature but not yet desiccating siliques were excised from plants at the base of the pedicle and placed in polypropylene lids. These were then sealed into the petri dishes with parafilm and incubated under standard growth conditions.

2.4. TISSUE PREPARATION FOR MICROSCOPY

2.4.1. Fixation

Excised tissues were immediately placed in a solution containing freshly prepared 3% (w/v) paraformaldehyde, 1.25% (w/v) glutaraldehyde, 50mM phosphate buffer pH 7. Tissues were fixed for 12 hours at R.T..

2.4.2. Dehydration

Fixed tissues were dehydrated in a graded series of alcohols 12.5%, 25%, 50%, 75%, 95% (v/v) and twice in 100%, allowing 1 hour for each step.

2.4.3. Embedding in Paraplast Wax

An equal volume of HistoClear was added to the dehydrated samples and the solutions thoroughly mixed. Tissues were infiltrated for 2 hours then the solution was replaced with 100% HistoClear. Tissues were infiltrated in several changes of HistoClear for at least 15 hours then an equal volume of molten wax was added. Tissues were infiltrated for 12 hours at 60°C then the solution was replaced with 100% wax. Tissues were infiltrated in several changes of wax for 36 hours. Tissues were embedded in wax using suitably sized plastic moulds.

2.4.4. Embedding in LR White Acrylic Resin

LR White medium grade resin was used. The resin was stored at 4°C and allowed to equilibrate at R.T. before opening to prevent the absorption of atmospheric water. All manipulations involving the resin were carried out in a fume hood and protective clothing was used.

An equal volume of resin was added to the dehydrated samples and the solutions thoroughly mixed. Tissues were infiltrated for 12 hours at R.T., then the solution was replaced with 100% resin. Tissues were infiltrated in several changes of resin for 36 hours. Tissues were embedded in polypropylene capsules and the resin polymerised for 12 hours at 65°C.

2.4.5. TESPA (aminopropyltriethoxysilane) coating of microscope slides

Microscope slides were washed in detergent then rinsed thoroughly in distilled water. The slides were immersed in a 2% solution of TESPA in acetone for 10 seconds, then rinsed in two changes of acetone and finally in distilled water. The slides were air dried at R.T. in a dust free environment.

2.4.6. Formvar coating grids

A thin film of 0.3% (w/v) Formvar in chloroform was floated onto distilled water and the grids carefully placed on the formvar film. The film and grids were picked up using a strip of parafilm and allowed to air dry at R.T. in a dust free environment.

2.4.7. Sectioning wax embedded material

Ten μm sections were cut on a Leitz 1512 microtome. The sections were floated onto a drop of distilled water on the microscope slides and allowed to dry overnight on a 40°C hotplate. Sections were dewaxed by incubating the slides for 5 minutes in HistoClear, then rinsing twice in 100% ethanol, once in 50% ethanol and finally in distilled water.

2.4.8. Sectioning resin embedded material

LR White embedded material was sectioned using glass knives on a Sorvall MT2-B ultra microtome. The sections were floated onto a reservoir of water, which was created on the glass knives using insulating tape sealed with dental wax.

Semi-thin 1 μm sections, for light microscopy, were removed from the reservoir with fine tweezers and placed on a drop of water on TESPA coated slides. Sections were dried down on a hotplate for a few minutes until the sections had adhered to the slides.

Ultra thin 150nm sections were collected onto grids from the reservoir. Sections for morphological studies were collected onto 300 mesh copper grids and sections for immunocytochemical studies were collected onto the palladium side of 300 mesh copper/palladium grids.

2.5. HISTOCHEMISTRY

2.5.1. Acridine orange

Sections were stained for 1 minute in a 0.01% (w/v) aqueous solution of acridine orange. Sections were rinsed in distilled water and mounted in Citifluor. Sections were viewed with epi-fluorescent illumination using a Nikon blue filter block (wavelength 495nm).

2.5.2. Calcofluor

Sections were stained for 5 minutes in a 0.01% (w/v) aqueous solution of Calcofluor. Sections were rinsed in distilled water, mounted in citifluor and viewed with epi-fluorescent illumination using a Nikon ultra-violet filter block (wavelength 405nm).

2.5.3. Ruthenium red

Sections were stained for 5 minutes in a 0.02% (w/v) aqueous solution of ruthenium red. Sections were then rinsed in distilled water, mounted in Citifluor and viewed under bright field illumination.

2.5.4. Toluidine blue

Sections were stained for 1-3 minutes in a solution of freshly filtered 0.01% (w/v) toluidine blue in 1% boric acid. Sections were rinsed in distilled water, air dried and mounted in DPX.

2.6. IMMUNOCYTOCHEMISTRY

Primary antibody dilutions and incubation times were first optimised for both light and electron microscopical studies. Immunocytochemical studies on resin-embedded tissues were always carried out on sections from LR White embedded material.

2.6.1. Immunocytochemistry for light microscopy

Sections were first rinsed in TBS (100mM Tris, 150mM NaCl) pH 8, then incubated in a blocking solution containing 1% pre-immune serum, 0.01% Tween 20 in TBS for 30 minutes at R.T.. Excess blocking solution was removed from the slides and then the sections were incubated in primary antibody diluted with blocking solution. Optimised incubations for different antisera ranged from 4-24 hours at 4-20°C. Sections were then washed in several changes of TBS for 15 minutes, then incubated with conjugated secondary antibody (diluted as manufacturers instructions).

2.6.2. Immunogold/Silver Detection

Sections were incubated in 5nm gold-labelled secondary antibody (diluted as manufacturers instructions) for 2 hours at R.T. in darkness. Sections were sequentially rinsed in several changes of TBS, distilled water, Milli-Q (heavy metal-free) water. Sections were then silver enhanced for 1-3 minutes in darkness using Amersham IntenSE M following manufacturers instructions (the reaction was monitored). The sections were rinsed in Milli-Q water, air dried and mounted in DPX. Sections were viewed under epifluorescence illumination using a Nikon IGGS filter block.

2.6.3. Immunocytochemistry for electron microscopy

Immediately after sections had been collected, grids were incubated in PBST (100mM phosphate buffer, pH 7.5, 0.05% Tween 20) for 10 minutes. Grids were incubated in a blocking solution containing 1% pre-immune serum in PBST for 1 hour at R.T.. Sections were then incubated in primary antibody diluted with blocking solution at 4°C overnight. Grids were sequentially washed in several changes of PBST over a period of 1 hour. Grids were then incubated with 20nm gold conjugated secondary antibody (diluted as manufacturers instructions) for 1 hour at R.T. in darkness. Grids were washed in several changes of PBST and finally rinsed in distilled water. Sections were stained with 1% aqueous uranyl acetate for 30 minutes, washed in distilled water, and allowed to air dry in a dust free environment.

2.6.4. Sodium metaperiodate treatment

Control sections were incubated in a 1:10 dilution of saturated aqueous sodium metaperiodate for 30 minutes, then washed in distilled water prior to incubation in the primary antibody.

2.7. MOLECULAR HISTOCHEMISTRY

2.7.1. Preparation of digoxigenin labelled Riboprobes

2.7.2. Restriction digest of plasmid DNA

Two separate digests were performed for each plasmid using the appropriate restriction enzymes to linearise the plasmid DNA. 10 μ l of solution containing the plasmid DNA was digested overnight at 37°C in a total volume of 60 μ l containing 6 μ l 10X restriction buffer 2 μ l restriction enzyme and 42 μ l DEPC treated water.

2.7.3. Cleaning cut plasmid DNA

Restricted plasmid DNA was cleaned using the GeneClean DNA extraction kit as described in the manufacturers instructions. The cleaned DNA was precipitated by adding 1/10th volume 3M sodium acetate and 2.5 volumes of cold (-20°C) ethanol, vortexing and incubating the solution at -80°C for 1 hour. The solution was microcentrifuged for 5 minutes at 13,000 r.p.m. and the supernatant discarded. The pellet was washed with cold (-20°C) 80% ethanol, air dried and resuspended in TE buffer. The concentration of DNA in the sample was measured at an optical density of 260nm on a Beckman DU 7500 spectrophotometer.

2.7.4. *In Vitro* transcription

1 μ g of DNA in a volume of 10 μ l was used for each transcription reaction using either T3 or T7 RNA polymerase. Digoxigenin labelled Riboprobes were transcribed in a total

volume of 20µl containing 10µl DNA solution, 4µl 5X transcription buffer, 2µl DTT, 2µl labelling mix and 2µl of T3 or T7 enzyme. The solution was centrifuged briefly and incubated at 37°C for 2 hours.

The reaction was stopped by the addition of 2µl 0.2M EDTA and the Riboprobes precipitated overnight at -20°C by the addition of 2.5µl 4M lithium chloride and 75µl ethanol. The solution was microcentrifuged for 10 minutes at 13,000 r.p.m. and the supernatant discarded. The pellet was washed with -20°C 80% ethanol, air dried and resuspended in 50µl of TE buffer. The concentration of probe was estimated by gel electrophoresis by comparing a known quantity of RNA

2.7.5. *In-Situ* hybridisation

2.7.5.1. Pre-treatment

Ten µm sections from wax embedded tissues were dewaxed in HistoClear for 10 minutes and rehydrated through 100% and 50% alcohol, for 5 minutes each, to DEPC water. Sections were then rinsed in PBS and incubated in 10µg/ml proteinase K in buffer (10mM Tris/HCl pH 8, 5mM EDTA, 0.5% SDS) for 10 minutes at 37°C. Sections were then submerged in 0.2% glycine in PBS for 10 minutes at RT, then rinsed twice in PBS for 5 minutes each.

2.7.5.2. Pre-hybridisation

Sections were incubated in pre-hybridisation buffer (containing 50% deionised formamide, 4X SSC, 1X Denhards solution, 125µg/ml tRNA, 100µg/ml denatured salmon sperm DNA) for 1 hour at 42°C in a humidified chamber moistened with 50% formamide 4X SSC.

2.7.5.3. Hybridisation

The probe was heated at 60°C for 5 minutes and pre-hybridisation buffer was chilled on ice. The hot probe was added to cold buffer to a concentration of 2µg/µl. 50µl of

hybridisation buffer was pipetted onto each slide and sections covered with a parafilm coverslip. Sections were incubated overnight at 42°C in a humidified chamber.

2.7.5.4. Post-hybridisation washes

Parafilm coverslips were removed and sections briefly rinsed in 2X SSC. Sections were first washed in a solution containing 2X SSC, 50% formamide at 42°C for 30 minutes, then in 1X SSC 50% formamide at 42°C for 30 minutes, and finally in 0.5X SSC 50% formamide at 42°C for 30 minutes.

2.7.5.5. Immunological detection

Sections were rinsed in buffer 1 (100mM Tris pH 8, 150mM NaCl, pH 7.5) then incubated in 2% sheep serum in buffer 1, 0.05% (v/v) Tween 20, for 30 minutes. Sections were incubated in a 1:500 dilution of alkaline phosphatase-conjugated polyclonal sheep anti-digoxigenin antibody in buffer1, 0.05% (v/v) Tween 20 for 2 hours at RT then rinsed in twice in buffer 1 for 30 mins. Sections were then incubated in darkness at RT in freshly-prepared substrate solution containing 0.5mM naphthol AS-MX phosphate, 2.0mM Fast Red TR in Tris buffer pH 8.0. Colour development was monitored. Sections were given a final rinse with distilled water, air dried, and mounted in Bondaglass adhesive.

2.8. LIGNIN ANALYSIS

2.8.1. Tissue extraction for Alkaline oxidation procedures

Freshly excised tissues were extracted for 48 hours in several changes of methanol to remove alcohol soluble cellular components such as chlorophyll, then the tissues were air dried. Tissues were then extracted for 16 hours in 0.5M NaOH to remove alkali soluble components such as hemicelluloses. The alkaline solution was then neutralised with HCl, and tissues incubated for a further 3 hours. Tissues were then washed in several changes of distilled water, dehydrated in methanol, then air dried. Extracted, dried tissues were then frozen using liquid nitrogen and ground as finely as possible using a pestle and mortar.

2.8.2. Copper oxidation

(Hammerschmidt 1984)

50mg of ground tissue was mixed with 340mg of copper sulphate and 2.5ml. of 3M NaOH in a teflon PFA Digestion Vessel. The digestion vessel was sealed and the tissues oxidised for 2 1/2 hours at 180°C.

2.8.3. Nitrobenzine oxidation

(Galletti *et al.* 1989)

50mg of ground tissue was mixed with 50µl of nitrobenzine and 2.5ml. 2M NaOH in a teflon PFA Digestion Vessel. The digestion vessel was sealed and tissues oxidised for 2 1/2 hours at 180°C.

2.8.4. Tissue extraction for Microwave digestion

(Provan *et al.* 1994)

Freshly-excised tissues were freeze dried for 24 hours then extracted with several changes of methanol for 48 hours. Tissues were air dried then pulverised using liquid nitrogen.

2.8.5. Microwave digestion

50mg of ground tissue was mixed with 5ml. of 4M NaOH in a teflon PFA Digestion Vessel. The digestion vessel was sealed then microwaved at 650W for 150 seconds.

2.8.6. Ethyl acetate extraction

Following oxidation the contents of the digestion vessel was mixed with 5ml. of water and transferred to a test tube. The solution was centrifuged at 4,000 r.p.m. for 5 minutes and the supernatant transferred to a clean tube. The pH was then adjusted to 1 with 6M HCl. 5mls of ethyl acetate was added to the sample and mixed by vortexing. The sample was then centrifuged for 5 minutes at 4,000 r.p.m. and the organic phase pipetted into a fresh

tube. The ethyl acetate extraction was repeated twice and the extracts combined. The sample was then dried on a rotary evaporator and the residue redissolved in 5mls of methanol. Samples were stored in sealed glass vials at 4°C prior to HPLC analysis.

2.8.7. HPLC analysis

HPLC was performed on a Gilson system (Anachem Ltd.), employing a 231-401 auto-sampling injector and a 116 dual wavelength UV detector, under the control of Gilson 715 software. The phenolics were fractionated on a Spherisorb ODS-3 (5 μ) column (250mm long 4.5mm i.d., Alltech UK), and eluted with a linear gradient from 5-30% acetonitrile in 1% phosphoric acid over 45 minutes at 0.8ml/min. UV absorbances were measured at 280nm.

2.8.8. Standard solutions

Six phenolic standard solutions (p-coumaric acid, ferulic acid, vanillic acid, vanillin, syringic acid, syringaldehyde) were used to generate calibration curves. The phenolics were dissolved in methanol and 360ng of the standard phenolics were injected into the HPLC.

2.9. CELL WALL CARBOHYDRATE ANALYSIS

(S. C. Fry Chemical Analysis of Components of the Primary cell wall in Plant cell Biology A Practical Approach Chapter 9 pp 199-220 1994)

2.9.1. Acid hydrolysis

10mg of tissue was suspended in 1ml of 2M trifluoroacetic acid and sealed in a glass tube. The tube was heated in an oven at 120°C for one hour then the tube was allowed to cool. The suspension was then centrifuged at 13,000r.p.m. for ten minutes and the supernatant removed to a fresh tube.

2.9.2. Standard solutions

12 carbohydrate standard solutions (arabinose, fructose, galactose, galacturonic acid, β -D (+) glucose, D (+) glucose, maltose, mannose, α -L rhamnose, ribose, sucrose, xylose) were prepared at a concentration of 10mg/ml.

2.9.3. Paper chromatography

50 μ l of hydrolysate and 5 μ l of each standard were applied to Whatman no. 1 paper as 1cm spots. The paper was developed by the descending method using butan-1-ol/acetic acid/water (BAW) in the ratio 12:3:5 for 16 hours as the first solvent. The chromatogram was dried then developed using ethyl acetate/pyridine/water (EPW) in the ratio 8:2:1 for 16 hours as the second solvent.

2.9.4. Staining

16g of phthalic acid was dissolved in 490ml of acetone and 20ml of water then 490ml of diethyl ether was added. Immediately before use 5mls of aniline was added to 100 ml of solution and the paper dipped in the stain. The paper was dried for 10 minutes then heated in an oven at 105°C for 10 minutes.

2.10. LIST OF SUPPLIERS

AGAR SCIENTIFIC LTD. 66A Cambridge Road, Stansted, Essex. CM24 8DA:-
microscopy supplies

BDH LABORATORY SUPPLIES MERCK LTD. Hunter Boulevard, Lutterworth,
Leicester. LE17 4XN:- microscopy supplies and general chemicals

BOEHRINGER MANNHEIM UK (Diagnostics and Biocemicals) LTD. Bell Lane,
Lewes, East Sussex. BN7 1LG:- digoxigenin RNA labelling kit

PROMEGA CORPORATION Delta House, Enterprise Road, Chilworth Research Centre,
Southampton. SO16 7NS:- restriction enzymes

SIGMA-ALDRICH COMPANY LTD. Fancy Road, Poole, Dorset. BH17 7NH:- general
chemicals

STRATECH SCIENTIFIC LTD. 61-63 Dudley Street, Luton, Bedfordshire. LU2 0NP:-
GeneClean DNA extraction kit

TAAB LABORATORIES EQUIPMENT LTD. 3 Minerva House, Calleva Industrial Park,
Aldermaston, Berkshire. RG7 4QW:- microscopy supplies

3. RESULTS

NW20
Landsberg erecta



Columbia
N908



Figure 10. Plants of *Arabidopsis* ecotypes *Landsberg erecta* and Columbia

3.1. A STUDY ON THE DEHISCENCE CHARACTERISTICS OF SOME ECOTYPES OF *ARABIDOPSIS THALIANA*

Arabidopsis thaliana is found growing in various geographical locations throughout the Northern hemisphere. These different ecotypes exhibit natural variations in form such as plant height, leaf size and leaf colour, and they also respond differently to physiological processes such as vernalisation, for example. Plants from all of the ecotypes examined in this study produce bilocular fruit which gradually turn yellow on ripening then split along the carpel or valve margins in the process of dehiscence. The siliques from a selection of different ecotypes were examined to assess any natural variations in 'pod shattering' between these wild type plants.

3.1.1. Selection of the ecotypes

Seeds of 30 ecotypes of *Arabidopsis thaliana* were kindly supplied by The Nottingham *Arabidopsis* Stock Centre. Each ecotype has a common name and an assigned Stock Centre accession number. In the following descriptions the common name of the plant has been used, and when initially mentioned the common name is followed by the assigned Stock Centre accession number in brackets. The seeds from all ecotypes were sown at the same time and grown under the same conditions, but not all of the ecotypes reached maturity and produced siliques. Ecotypes Ag-0 (N901), Kas-1 (N903) and Ms-0 (N905) produced rosettes which appeared to be normal, but they failed to bolt and flower under our growth conditions, and ecotypes Condara (N916), Petergof (N926) and Rubezhoe-2 (N928) produced only sterile fruit. Ecotypes S96 (N914), H55 (N923) and Shahdara (N929) failed to germinate, which suggests that the seeds from these three ecotypes may have needed further vernalisation. The phenotype of Ag-0 is described in more detail below. Those ecotypes which produced healthy plants, and set seed were selected for further study, and phenotypic differences between the siliques and growth characteristics were noted from second generation plants.

3.1.2. Some phenotypic differences between *Arabidopsis* ecotypes

Landsberg *erecta* (NW20) plants showed obvious phenotypic differences to plants from the other ecotypes, which are represented by the Columbia (N908) ecotype in this study. Landsberg *erecta* plants have shorter, thicker, more erect stems as can be seen in Figure



Figure 11. *Arabidopsis* siliques from the Landsberg *erecta* ecotype showing the flattened shape at the tip of the fruits (indicated by arrows).

Figure 12. *Arabidopsis* siliques from the Columbia ecotype showing the pointed shape at the tip of the fruits (indicated by arrows).



10, while plants from the other ecotypes were similar in appearance to Columbia also seen in Figure 10. The siliques from Landsberg *erecta* were generally shorter, and much more blunt-ended than those from all of the other ecotypes. The blunt-ended shape of the Landsberg *erecta* silique is shown in Figure 11 (indicated by arrows), and can be compared with the pointed shape of siliques from Columbia (Fig. 12).

Stock centre number	Name	Average mature pod length (mm)	Average time from sowing to bolting (days)	Average time from bolting to senescence (days)
NW20	Landsberg <i>erecta</i>	10.2	20	39
N900	Aa-O	12.1	32	29
N902	Cvi-O	12.5	31	24
N904	Mh-O	12.1	34	38
N906	C24	12.5	41	36
N907	Col (0)	10.6	30	28
N908	Columbia	12.9	25	33
N910	Dijon G	17.3	25	24
N911	Estland	11.5	22	27
N913	RLD1	15.6	21	28
N915	Wassilewskija	12.5	21	28
N917	Da(1)-12	11.2	20	34
N919	Dijon-M	10.6	22	39
N920	Enkheim-D	14.2	22	37
N921	Enkheim-T	10.9	20	34
N922	Hodja-Obi-Garm	10.2	30	25
N924	Je54	11.5	31	30
N925	Litva	12.4	27	30
N927	Rubezhnoe-1	11.5	28	32
N930	Sn(5)-1	10.9	27	18
N931	Sorbo	12.9	20	31

Table 3. Characteristics of *Arabidopsis* ecotypes

Dijon G
N910



Hodja-Obi-Garm
N922



Figure 13. Plants of *Arabidopsis* ecotypes Dijon G and Hodja-Obi-Garm

There was very little difference in the time taken for all of the ecotypes to germinate, however, there was quite a wide variation in the time taken to reach the bolting stage. Results (Table 3) show a range from an average of 20 days in four of the ecotypes Landsberg *erecta* (NW20), Da(1)-12 (N917), Enkheim-T (N921), and Sorbo (N931), up to an average of 41 days in ecotype C24 (N906). There was also a marked variation in the times taken for plants to go from the bolting stage to plant senescence. Results (Table 3) show a range from an average of 18 days in ecotype Sn(5)-1 (N930) up to 39 days in ecotypes Landsberg *erecta* and Dijon-M (N919). Ten mature siliques were taken at random from different plants of each ecotype and an average silique length calculated. Ecotypes Landsberg *erecta* (Fig. 10) and Hodja-Obi-Garm (N922) shown in Figure 13 had the shortest siliques (10.2mm), and ecotype Dijon-D (N910) shown in Figure 13, had the longest 17.3mm (Table 3).

3.1.3. 'Pod shatter' in *Arabidopsis* ecotypes

The shattering characteristic proved very difficult to measure. Mature siliques from all ecotypes gradually turned yellow from the tip to the base and appeared to show a generally-uniform pattern of dehiscence. The valve walls usually started to split away from the fruit at the tip and this was most noticeable in the Landsberg *erecta* phenotype. The valves from Landsberg siliques were frequently observed to be splitting away from the yellowing tip whilst the remainder of the silique was still green. Shattered siliques were, however, observed on plants from all the ecotypes examined in this study. The valve walls of desiccated fruit were easily detached from the siliques of all the ecotypes by mechanical stimulation simply by touching the siliques, or even by slight air currents moving the plant.

3.1.4. Histology of the siliques of *Arabidopsis* ecotypes

Five young (stage 6-7), post-fertilised siliques and five mature (stage 8-10) siliques were taken at random from plants of each ecotype, the tissues were embedded in LR White resin, and histological analyses of toluidine blue stained sections was performed. Previous work has described in detail the development of the silique of the Landsberg *erecta* ecotype (Spence 1992). This developmental pattern has been used as a standard, and the development of the siliques of the other ecotypes has been compared with that described for Landsberg *erecta*.

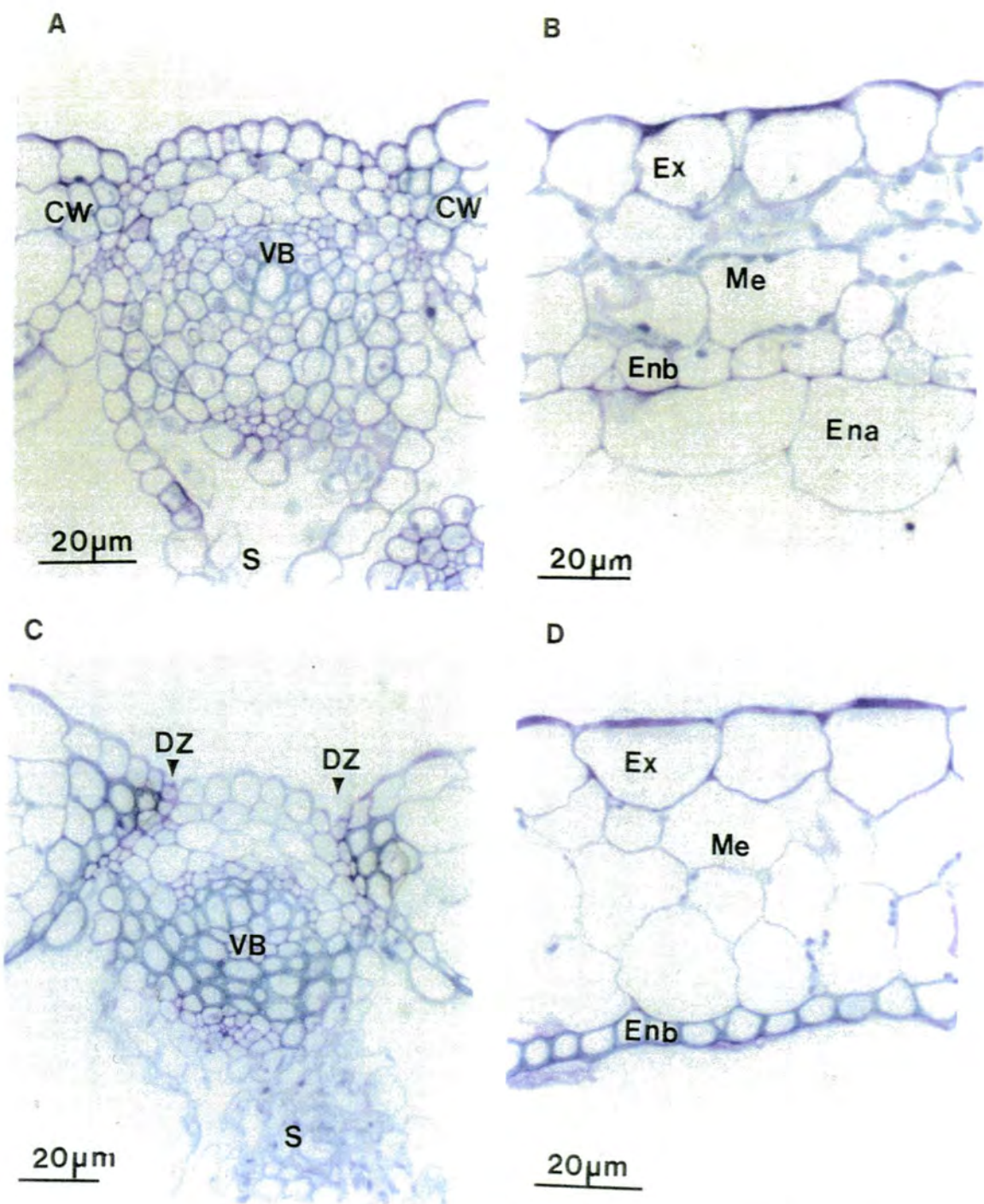


Figure 14. Structure of young and mature siliques from ecotype Columbia

- A) Carpel margins of young silique
- B) Carpel wall of young silique
- C) Dehiscence zone of mature silique
- D) Carpel wall of mature silique

CW = carpel wall, DZ = dehiscence zone, Ena = endocarp *a*, Enb = endocarp *b*, Ex = exocarp, Me = mesocarp, S = septum, VB = vascular bundle

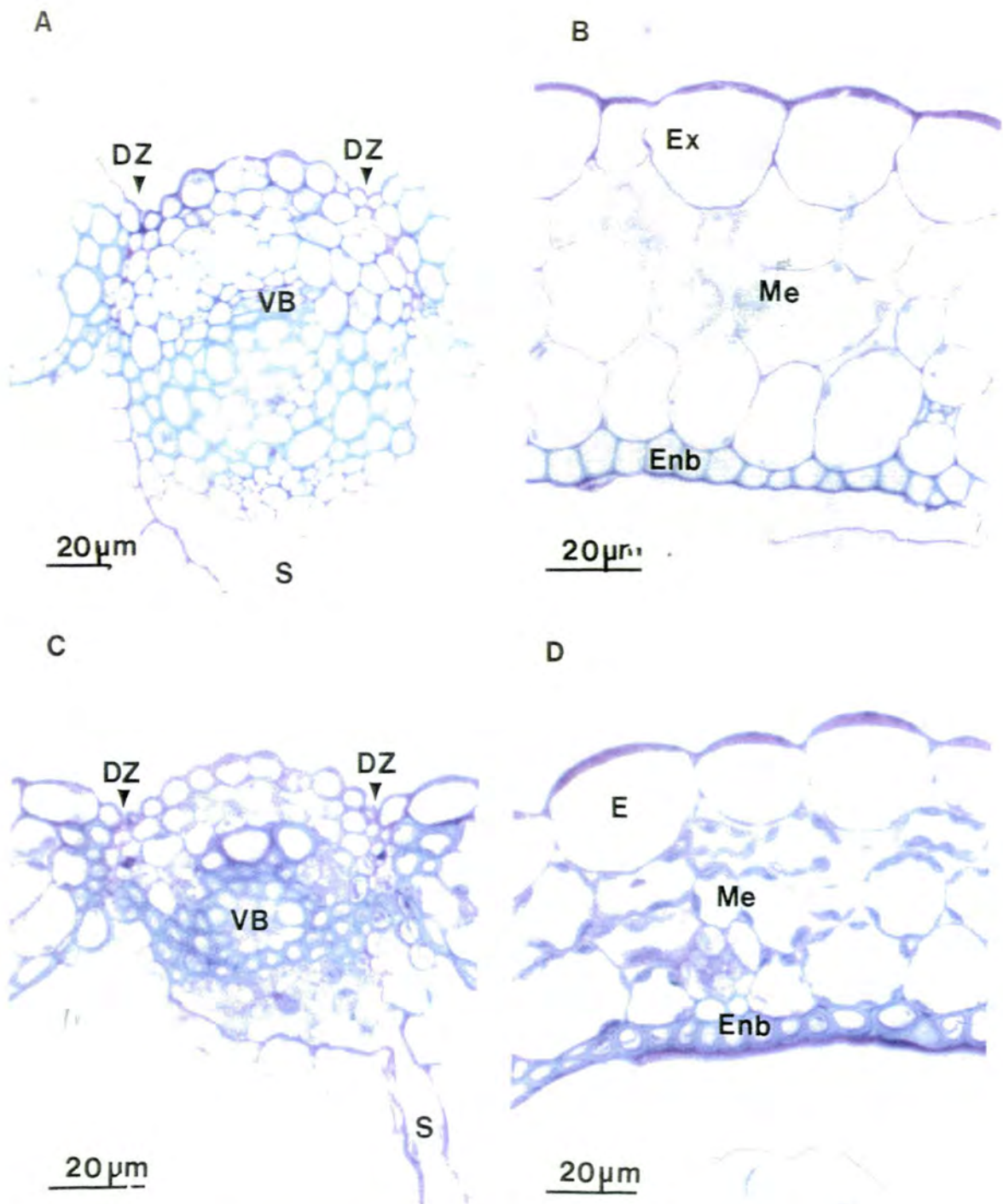


Figure 15. Structure of mature siliques from ecotypes Estland and Da(1)-12

- A) Dehiscence zone of mature Estland silique**
- B) Carpel wall of mature Estland silique**
- C) Dehiscence zone of mature Da(1)-12 silique**
- D) Carpel wall of mature Da(1)-12 silique**

DZ = dehiscence zone, Enb = endocarp *b*, Ex = exocarp, Me = mesocarp, S = septum, VB = vascular bundle

Analysis of toluidine blue stained sections from the other 21 selected ecotypes showed no obvious variations in tissue patterns within putative dehiscence zones, or the carpel walls at the earliest stage (Stage 6) of post-fertilisation development. Sections from Columbia are shown in Figure 14 and are representative of those from the other ecotypes in this study. Sections through the carpel margins of young siliques (Fig. 14a) showed that there is a constriction occurring at each margin, the same pattern of development as described in Landsberg *erecta* siliques. Sections from young siliques show that the carpel walls of all of the ecotypes contain three distinct layers (Fig. 14b); an outer exocarp, a central mesocarp and a double-layer endocarp (*Ena* the outer layer, and *Enb* the inner layer). This pattern of development is similar to that identified in Landsberg *erecta*.

Sections from mature siliques (Stage 8-9) show that the dehiscence zones of all of the ecotypes also have the same histological structure as that described for Landsberg *erecta*. The dehiscence zones comprise a few outer rows of lignified cells, adjacent to the mesocarp, and a separation layer which is formed from a few rows of small cells which show evidence of cellular degradation (indicated by arrows in Fig. 14c). The carpel wall tissues also show the same patterns of differentiation as that of Landsberg *erecta*. The exocarp is thickened along the outer edge to form a protective, cuticular layer and the mesocarp was observed to dry out from the outer through to the inner tissue layers. The second endocarp layer (*Enb*) has lignified, and the first endocarp layer (*Ena*) has degenerated, or shows signs of degeneration, as can be seen in Figure 14d.

3.1.5. Variations in silique structure

Although the patterns of tissue differentiation are generally similar in all of the ecotypes examined, slight differences were observed between the mature siliques within each individual ecotype (Fig. 15). This is illustrated by comparing the thickened *enb* layer in the section from the carpel wall of ecotype Da(1)-12 (Fig. 15b) with *enb* in the carpel walls of ecotype Estland (N911) (Fig. 15d). This cell layer is much thicker in Da(1)-12, which suggests that these cells have lignified to a further extent than the equivalent cell layers in Estland. The lignified cells of the dehiscence zone and vascular bundles in Da(1)-12 (Fig. 15c) are also thicker than those of Estland (Fig. 15a).

There is also a marked difference in size of the cells comprising the whole of the carpel wall when comparing, for example, the siliques from ecotypes Enkheim-D (N920) and

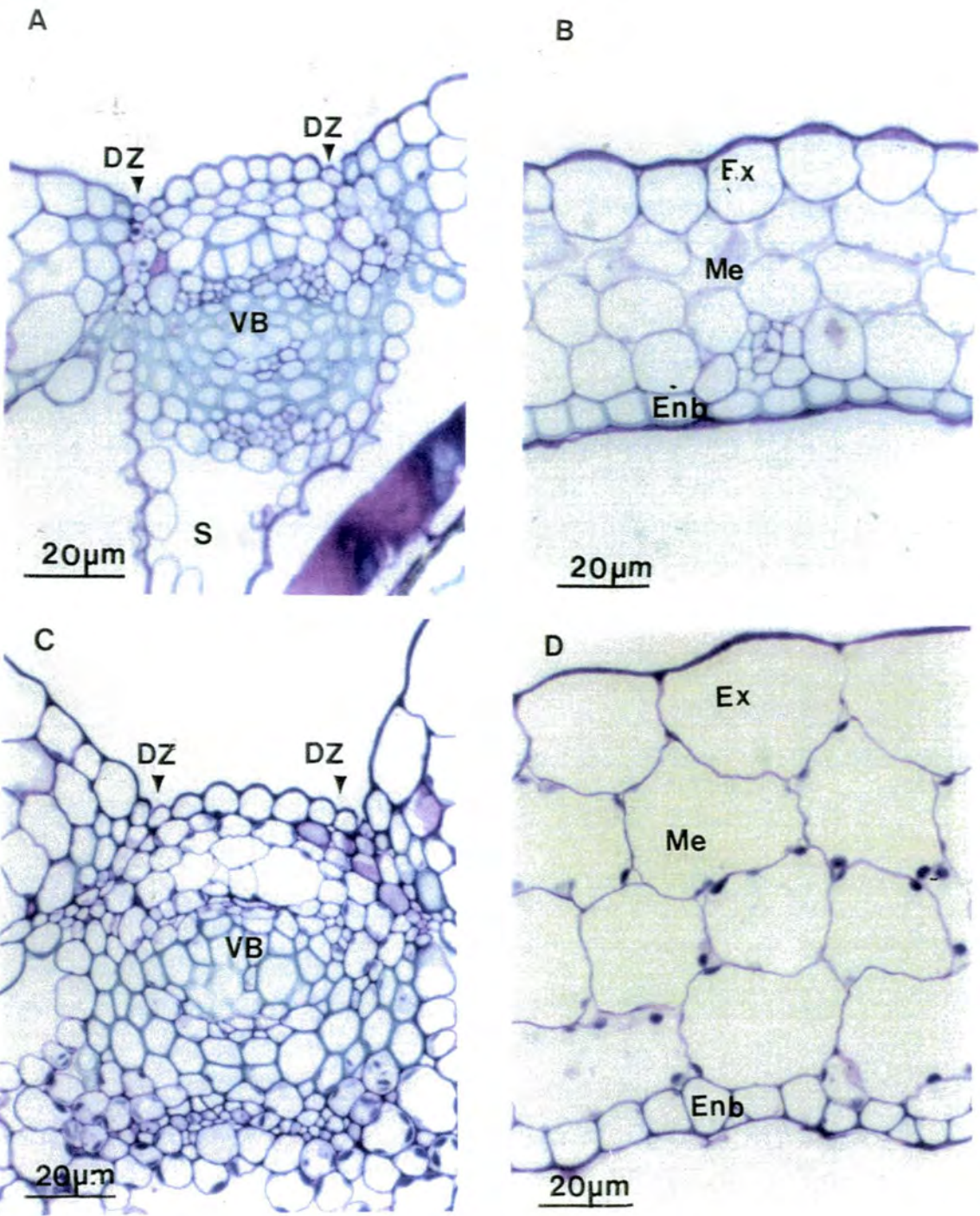


Figure 16. Structure of mature siliques from ecotypes Enkheim-D and Sn(5)-1

- A) Dehiscence zone of mature Enkheim-D silique**
- B) Carpel wall of mature Enkheim-D silique**
- C) Dehiscence zone of mature Sn(5)-1 silique**
- D) Carpel wall of mature Sn(5)-1 silique**

DZ = dehiscence zone, Enb = endocarp *b*, Ex = exocarp, Me = mesocarp, S = septum, VB = vascular bundle

Sn(5)-1 (Fig. 16). Cells within the exocarp, mesocarp and endocarp layers of Enkheim-D (Figs. 16a and 16b) are much smaller than those from Sn(5)-1 (Figs. 16c and 16d). These results suggest that all of the ecotypes of *Arabidopsis* exhibit the characteristic of dehiscence and pod 'shatter'. There are only minor histological variations in the siliques of the ecotypes of *Arabidopsis*, and the patterns of tissue differentiation, resulting in the development of the dehiscence zones and the carpel walls, are common to all of the ecotypes examined in this study.

3.1.6. The phenotype of ecotype Ag-0 (N901)

The phenotype exhibited by Ag-0 suggests that flowering in this ecotype is temperature sensitive and, although not a main concern of this thesis, the phenotype of Ag-0 is described briefly. Very few seeds from Ag-0 germinated under normal growth conditions at 25°C, and those seeds which did germinate, produced very slow-growing plants which did not mature. Ag-0 plants first produced a very small, slow-growing, but apparently normal rosette of leaves (Fig. 17) then, after a period of approximately thirty days, one of the plants bolted. This plant did not produce flowers however. Instead, small leaf like structures developed in a whorled phyllotaxy in place of flowers and several of these leafy structures developed along the length of the stem (Fig. 18).

The temperature of the growth cabinet was lowered to 20°C and the Ag-0 plant was induced to flower. The main stem bolted from the centre of the most recently formed leafy structure and normal flowers were then produced along the length of the stem. Fruits produced from these flowers developed normally and set seed. Lateral shoots also began to develop from the centre some of the leaf like structures further down the stem (Fig. 18). These lateral shoots did not produce flowers as the plant began to senesce. Senescing leaves in the rosette, and in the leafy structures, can be seen in both Figure 17 and Figure 18.

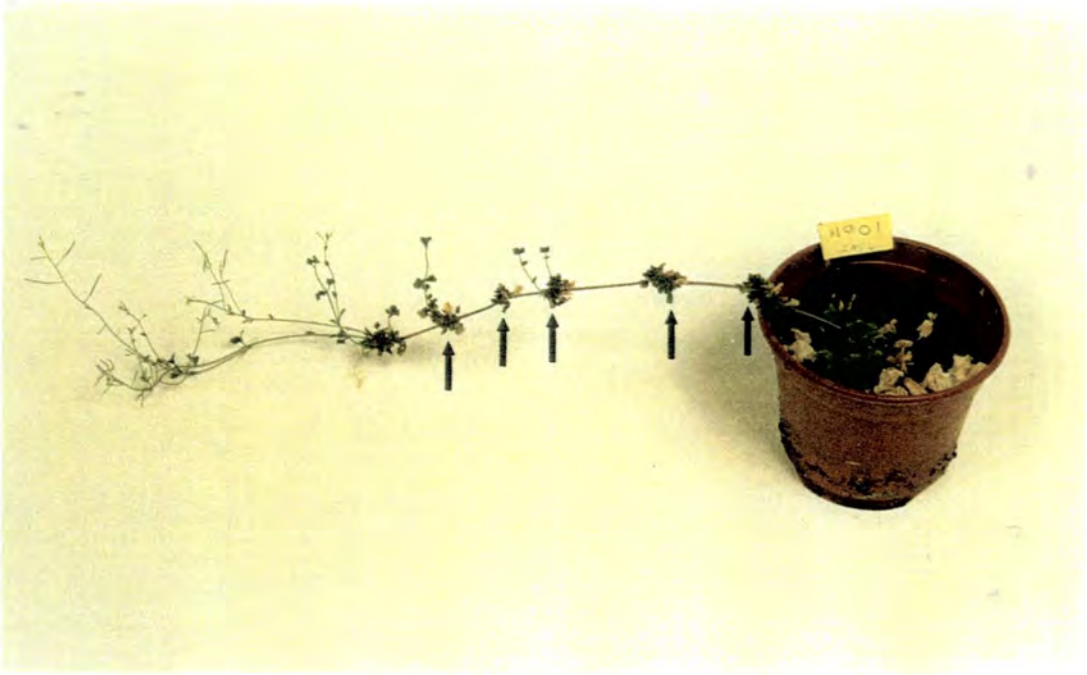


Figure 17. Plant from ecotype Ag-0 (N901) showing the main stem with mature fruits and leafy structures, indicated by arrows.

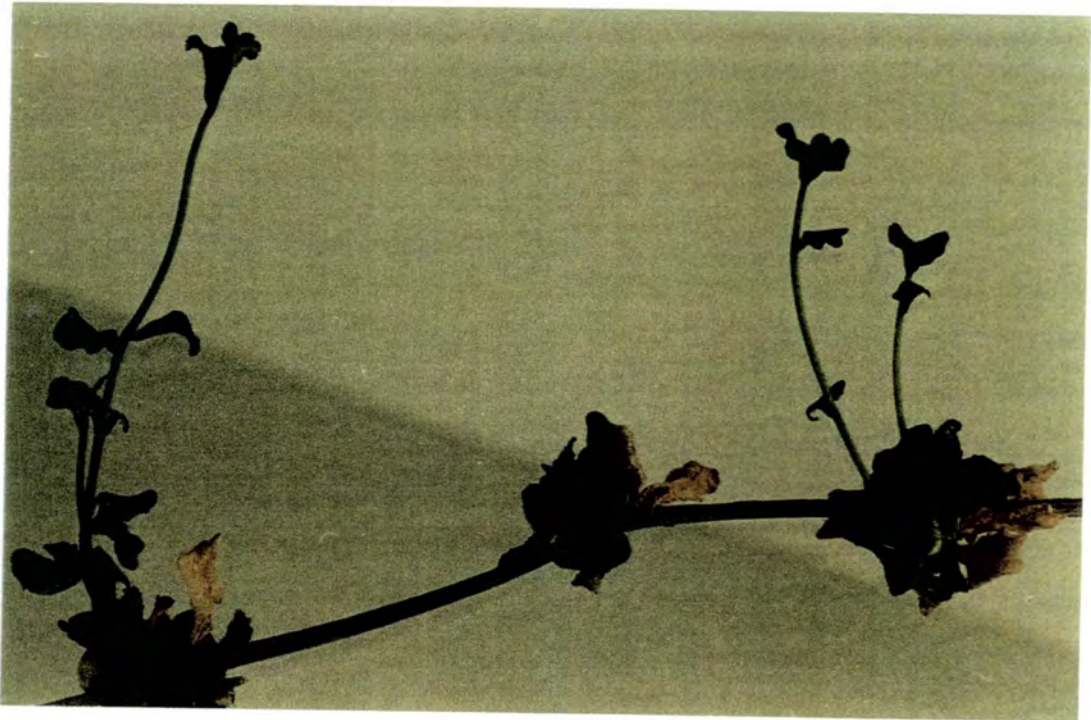


Figure 18. Senescing leafy structures and lateral shoots of ecotype Ag-0 (N901)

3.2. THE EFFECTS OF HUMIDITY ON DEHISCENCE IN *ARABIDOPSIS*

Humidity is an expression of the moisture content of the atmosphere, and therefore it is important in many ecological and physiological processes. Six different saturated salt solutions, in sealed petri dishes, were used to create a range of constant relative humidities from 7% to 96%; the various saturated salt solutions and the relative humidities produced are shown in Table 4. Five siliques, excised from different plants of both the Landsberg and Columbia ecotypes of *Arabidopsis*, were used for each experiment. Siliques that were mature, but still green (stage 8-9) and which were adjacent to other fruits that had started to senesce and turn yellow, were selected. The effects of the different humidities on the senescence and dehiscence of the siliques was recorded over a period of three days, after which time the siliques were removed from the chambers and examined. The results show that humidity does have an effect on the dehiscence of *Arabidopsis* siliques, and that the effects are similar for both the Landsberg and Columbia ecotypes.

SATURATED SALT SOLUTION	RELATIVE HUMIDITY
sodium hydroxide	7%
lithium chloride	12%
calcium chloride	29.5%
calcium nitrate	50%
sodium chloride	75.5%
potassium hydrogen phosphate	96%

Table 4. Salt solutions and relative humidities

3.2.1. Ripening and dehiscence in ambient conditions

The relative humidity of the growth cabinet was measured using a Dimplex Precision-Hygrometer and was found to average 64%. Excised siliques, which were placed in an open petri dish, showed a generally similar pattern of ripening and dehiscence to those fruit attached to the plant (results not shown). The first visual sign of ripening in the



Figure 19. *Arabidopsis* siliques after 3 days incubation at a humidity of 7%

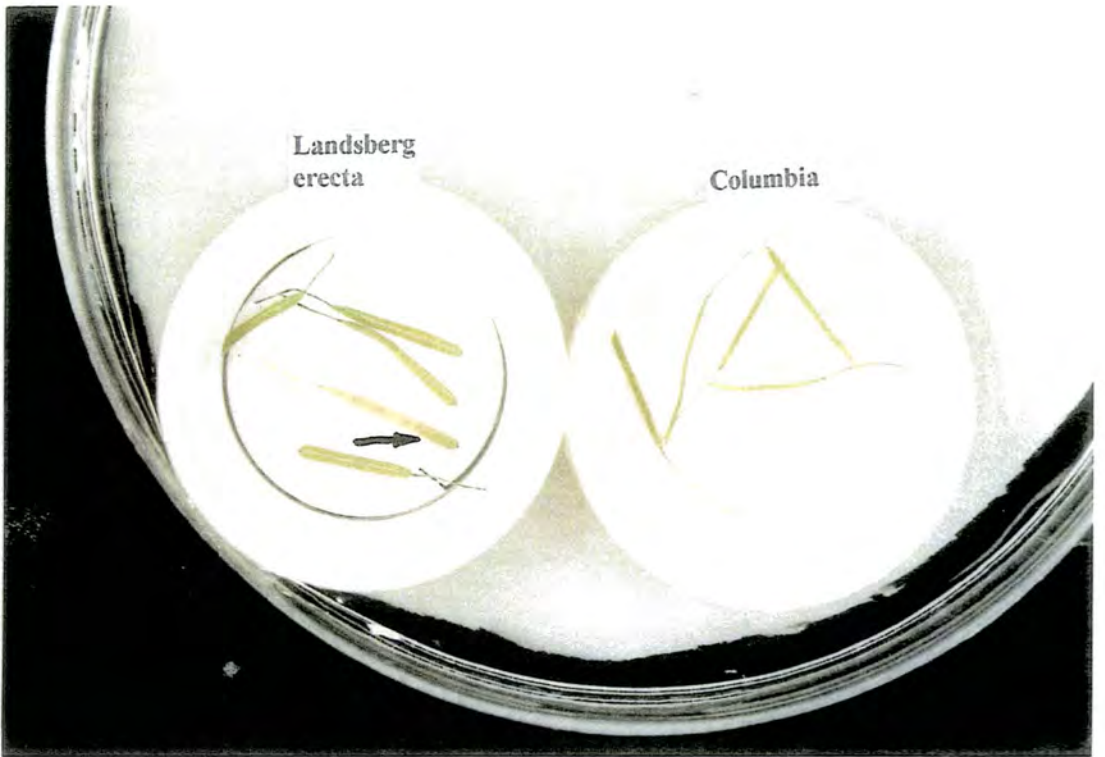


Figure 20. *Arabidopsis* siliques after 3 days incubation at a humidity of 12%
Arrow indicates the yellowing of the silique from the base to the tip

mature, attached *Arabidopsis* fruit is a gradual yellowing of the silique, which is usually first observed at the tip and gradually proceeds to the base of the fruit. In excised fruits the yellowing was first observed at the base and gradually proceeds along the entire length of the silique to the tip. This can be best seen in one of the siliques of the Landsberg ecotype in Figure 20 and is indicated by the arrow. As the siliques senesce, they gradually dry out and eventually become quite desiccated, when they become a much duller colour, and finally the valves begin to split away from the fruit. The valves first begin to split from the tip of the fruit in both attached and detached fruit. When mechanical pressure is applied to mature desiccated fruits the valves detach very easily from the fruit, even before there is evidence of natural splitting.

3.2.2. Ripening and dehiscence in a humidity of 7%

After one day incubation in the lowest of the tested humidities the siliques had begun to show a slight yellow discolouration; this appeared in small patches along the entire length of the siliques. When incubated for two days, the siliques entirely discoloured to light brown and appeared to have desiccated totally. Despite their appearance as normal, very mature, fruits there was no signs of dehiscence in any of the siliques. After three days incubation at a humidity of 7% the siliques from both the ecotypes had begun to shrivel up (Fig. 19) but despite this, none of the siliques dehisced. When removed from the chamber, the siliques were very desiccated and brittle, but the valves did not detach easily from the fruit even when mechanical pressure was applied with the fingertips.

3.2.3. Ripening and dehiscence in a humidity of 12%

There was an uneven, patchy discolouration along the length of the siliques after the siliques had been incubated for one day at a humidity of 12%, as was observed above. After two days the colour of the fruits had changed and the siliques had a mottled yellow, dull green appearance. The colour of the siliques did not substantially change after three days incubation, however most of the siliques had begun to show signs of shrivelling (Fig. 20). When removed from the chamber, the siliques were desiccated and the whole silique was brittle despite still being greenish in colour, but the valves did not detach easily from the fruit under mechanical pressure.

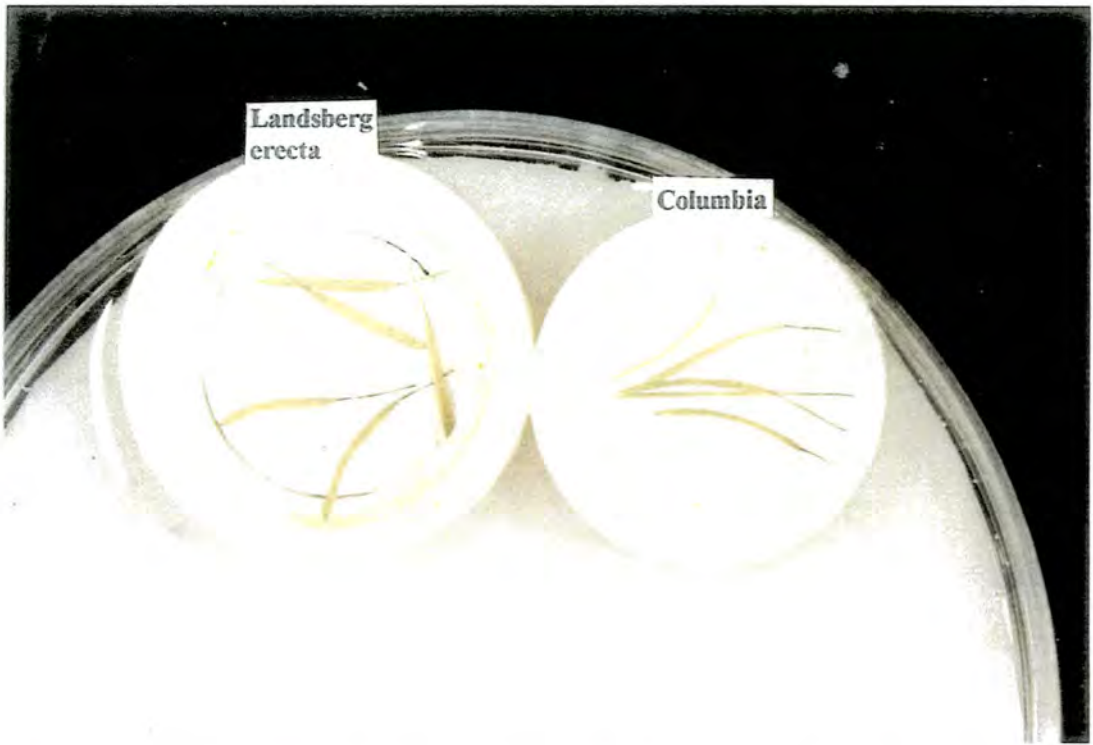


Figure 21. *Arabidopsis* siliques after 3 days incubation at a humidity of 29.5%

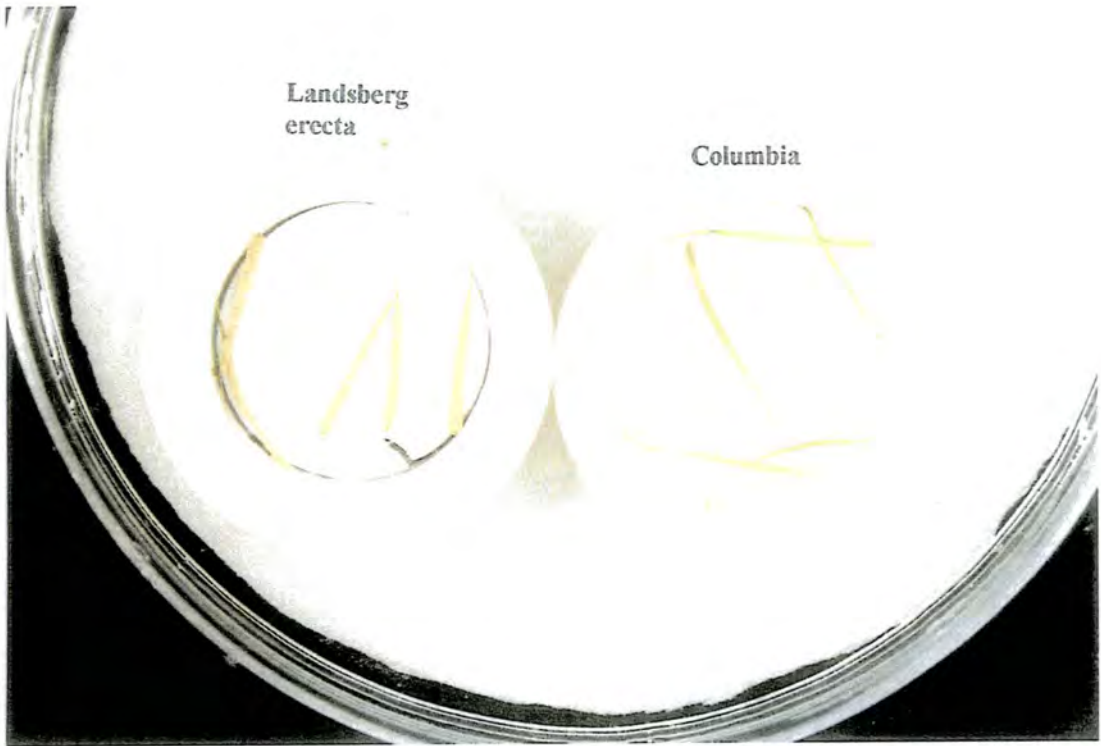


Figure 22. *Arabidopsis* siliques after 3 days incubation at a humidity of 50%

3.2.4. Ripening and dehiscence in a humidity of 29.5%

After one day incubation at a humidity of 29.5%, slight yellowing was observed at the bases of the siliques. This discolouration had preceded further along the length of the siliques after two days incubation. After three days most of the fruits still had a slight residual greenish colour as can be seen in Figure 21, and none of the siliques showed any evidence of dehiscence. When removed from the chamber however, the siliques were dry and quite brittle, and when mechanical pressure was applied with the fingertips the valves did detach from the fruit.

3.2.5. Ripening and dehiscence in a humidity of 50%

After one day incubation at a humidity of 50%, slight yellowing was observed at the base of the siliques. After two days, the yellowing had progressed along the entire length of most of the siliques. No green colour was observed on any of the siliques after three days incubation (Fig. 22) and, although the majority of the fruits showed no evidence of dehiscence, the valves from two of the Landsberg siliques were starting to split away from the tip of the fruits. When removed from the chamber, the siliques were dry and quite brittle and the valves detached from the fruit very easily

3.2.6. Ripening and dehiscence in a humidity of 75.5%

The fruits incubated for one day at a humidity of 75.5% had begun to yellow at their base. After two days the yellowing had progressed along the entire length of the majority of siliques. When the siliques had been incubated for three days most of the fruits had totally senesced, and in the Landsberg ecotype the valves were detaching from the fruit in the majority of the siliques, as can be seen in Fig. 23. When removed from the chamber, the siliques were dry and quite brittle and any remaining attached valves detached from the fruit very easily.

3.2.7. Ripening and dehiscence in a humidity of 96%

After one day incubation at the highest of the tested humidities the siliques showed discolouration at the base of the fruits. This yellowing progressed along the length of the

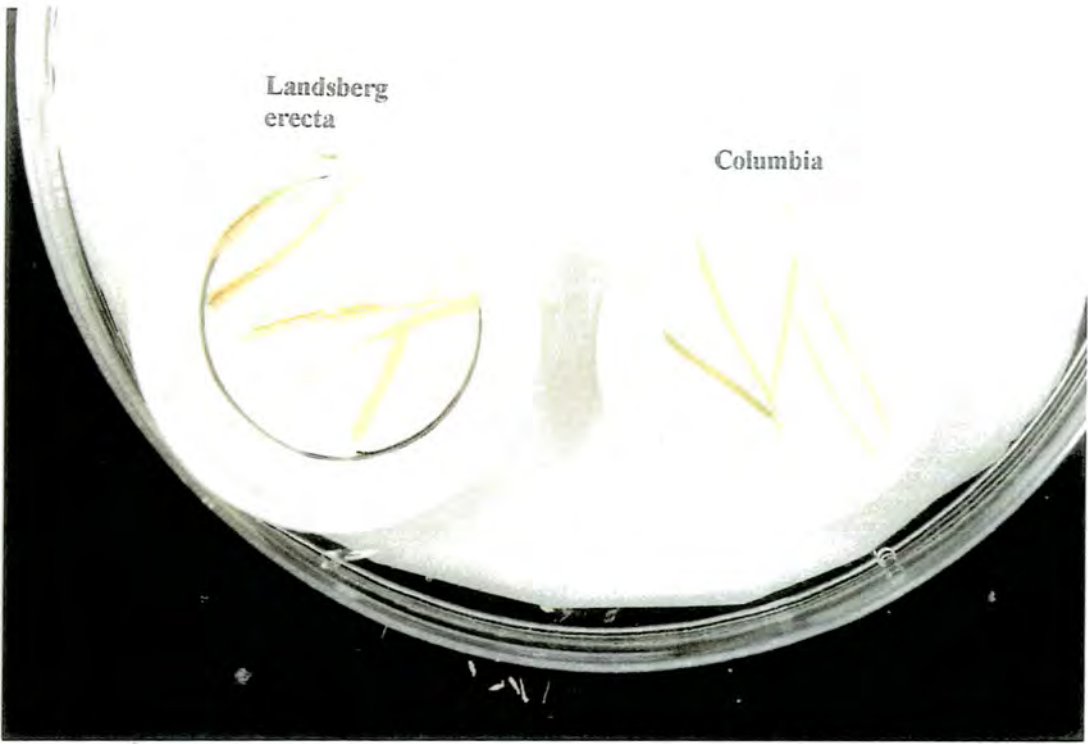


Figure 23. *Arabidopsis* siliques after 3 days incubation at a humidity of 75.5%



Figure 24. *Arabidopsis* siliques after 3 days incubation at a humidity of 96%

fruit and after two days all of the fruits were yellow. The siliques remained a bright yellow after three days incubation, and the valves from two of the siliques of the Landsberg ecotype were beginning to split away from the fruit (Fig. 24). When removed from the chamber, the siliques were soft and flaccid but the valves still detached easily from the fruit when mechanical pressure was applied.

3.3. DEVELOPMENT OF THE *BRASSICA NAPUS* SILIQUE

The fruits of *Brassica napus* have a similar gross anatomy and mode of dehiscence to the fruits of two other Brassicas, *Arabidopsis* and *Brassica juncea*. The fruits of *Brassica napus* are bilocular siliques, however they are much larger than those of *Arabidopsis*, measuring up to 10cm in length. The structure of the *Brassica napus* silique has been described (Picart & Morgan 1984, Meakin 1988, Meakin & Roberts 1990a). Maturing siliques from plants of the Westar Spring variety of *Brassica napus* were kindly donated by Mr. R. Swinhoe and light microscopical studies were performed on 1µm sections from LR White embedded tissues which were stained with toluidine blue. The structure of the carpel wall tissues and dehiscence zones of post-fertilised, maturing *Brassica napus* silique is described only briefly in this report for comparative purposes.

3.3.1. Development of the dehiscence zones in the post-fertilised silique

The young post-fertilised *Brassica napus* fruit is similar in structure to that of *Arabidopsis* and *Brassica juncea*. The carpel margins are narrower than the rest of the carpel walls, this results from a reduction in the extent of cell expansion in several rows of non-chlorenchymatous cells at the extreme carpel margins. This pattern of development is similar to that identified in the *Arabidopsis* silique and described as developmental stage six (Table 2). A few rows of these marginal cells adjacent to the replar bundle eventually degrade and form the separation layer (Figure 25a), as occurs at stage seven in *Arabidopsis* silique development. The mode of degeneration of the separation layer cells in *Brassica napus* has been described by Meakin and Roberts (1990a) and identified as being due to middle lamella breakdown within the cell walls.

As the silique increases in size there is extensive lignification of the replar bundle and the smaller cells at the carpel margins adjacent to the separation layer also lignify during the next stage in the development of the dehiscence zone. Figure 25a shows the structure of the lignifying dehiscence zone which begins to lignify from the exocarp around the separation layer to join up with the lignifying endocarp. The arrows indicate those cells which have not yet lignified. Development of the lignified zone and separation layer isolates the carpel walls from the replar bundles resulting in the formation of two valves. This stage of development in *Brassica napus* is also similar to that seen in the *Arabidopsis* silique at stage eight of development.

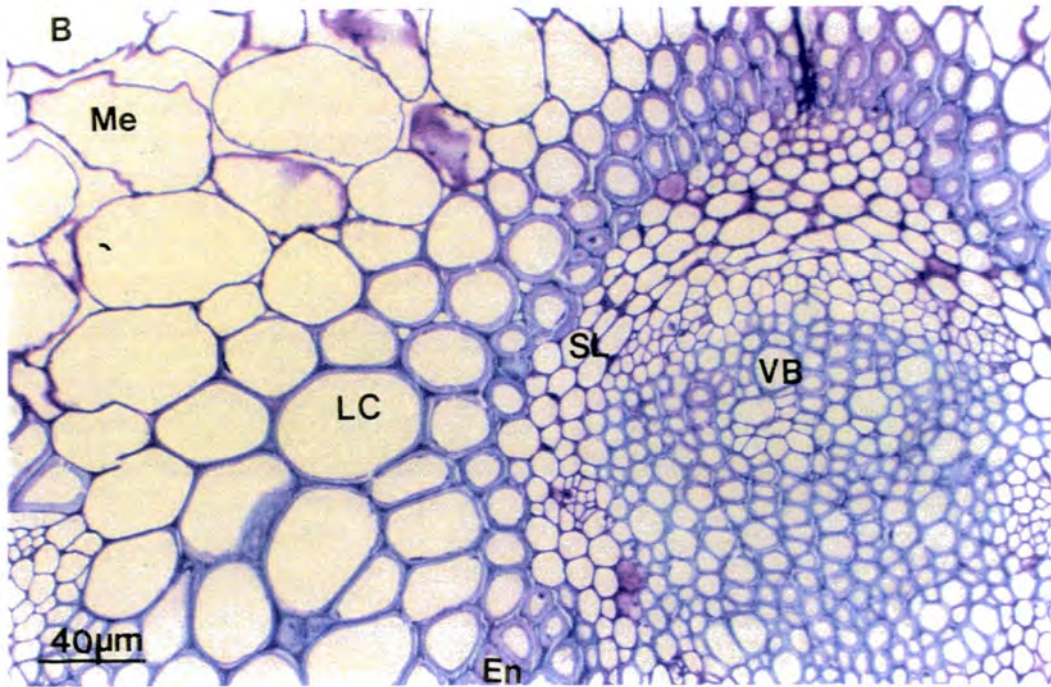
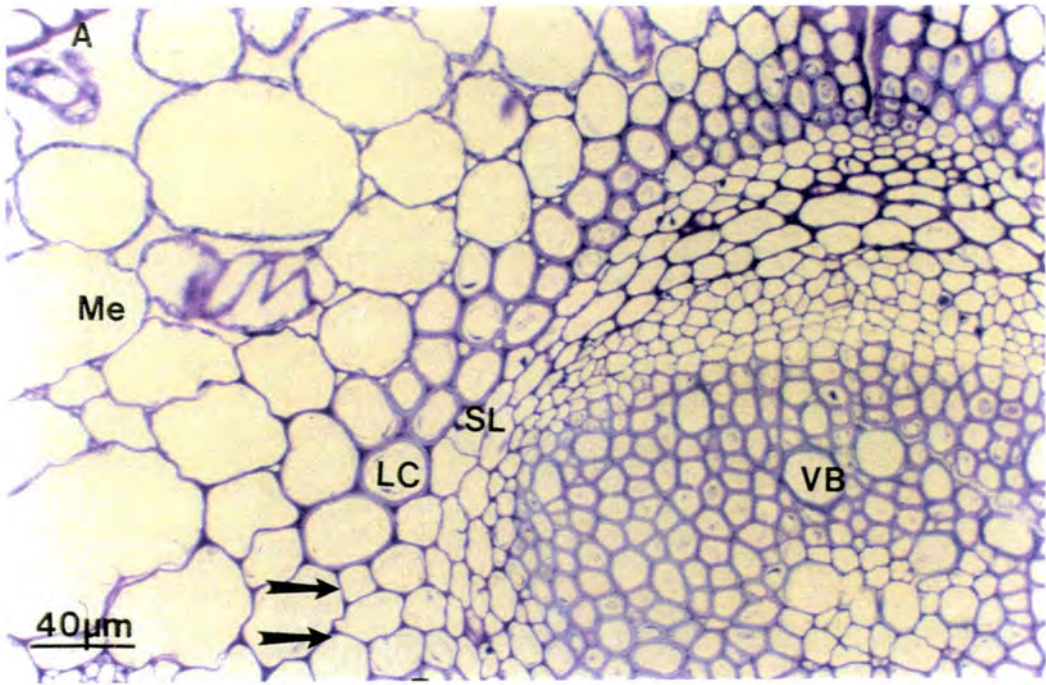


Figure 25. Structure of the dehiscence zones in the post-fertilised *Brassica napus* fruit

A) Structure of the dehiscence zones of the young post-fertilised fruit

B) Structure of the dehiscence zones in the mature post fertilised fruit

En = endocarp, LC = lignified dehiscence zone cell, Me = mesocarp SL = separation layer cell, VB = vascular bundle. Arrows indicate non-lignified cells in the dehiscence zone

The mature *Brassica napus* silique (Fig. 25b) shows much more lignification around the carpel margins prior to dehiscence, than is seen in the *Arabidopsis* silique. In the mature silique the lignified dehiscence zone cells not only join up with the lignified endocarp but extend into the mesocarp layer. In *Brassica napus* this lignified area of the dehiscence zone can extend to include eight or nine rows of mesocarp cells.

3.3.2. Development of the carpel walls in the post-fertilised silique

The carpel walls of the young, post-fertilised silique have a similar structure to those of *Arabidopsis* during the sixth stage of development, and show differentiation of four distinct cell layers (Fig. 26a), which have been named in accordance with those of *Arabidopsis*. The outer exocarp forms a single layer of thick-walled cells which are interspersed with guard cells and stomata. The mesocarp comprises several rows of thin-walled, chlorenchymous cells and the endocarp contains two distinct layers, endocarp A (*Ena*), which forms a single layer of thin-walled cells which line the inside of the locule and endocarp B (*Enb*), a single layer of long, fibrous cells adjacent to the mesocarp.

As the silique extends and matures there is considerable cell expansion in all of the cell layers of the carpel wall and the cell walls in the exocarp and *Ena* continue to thicken along the tangential walls. The uneven wall thickening in *Ena* can be clearly seen in Figure 26b. The cells of *Enb* differentiate during the next stage of carpel wall development and begin to lignify (Figs. 26b and 26c). A similar pattern of development is seen in *Arabidopsis* siliques at stage eight of development. The mesocarp eventually begins to desiccate from the outer layer adjacent to the mesocarp; this is associated with yellowing of the silique. The inner endocarp layer, *Ena*, degrades and the remnants of this cell layer are indicated by arrows in Figure 26c. This pattern of development is also seen in *Arabidopsis* siliques at stage nine of development. Eventually the valves detached from the fruit at the separation layers.

Tissue differentiation during ripening in the post-fertilised silique of *Brassica napus*, appears to show the same pattern of dehiscence zone and carpel wall development as that previously described for *Arabidopsis* and which is summarised in Table 2.

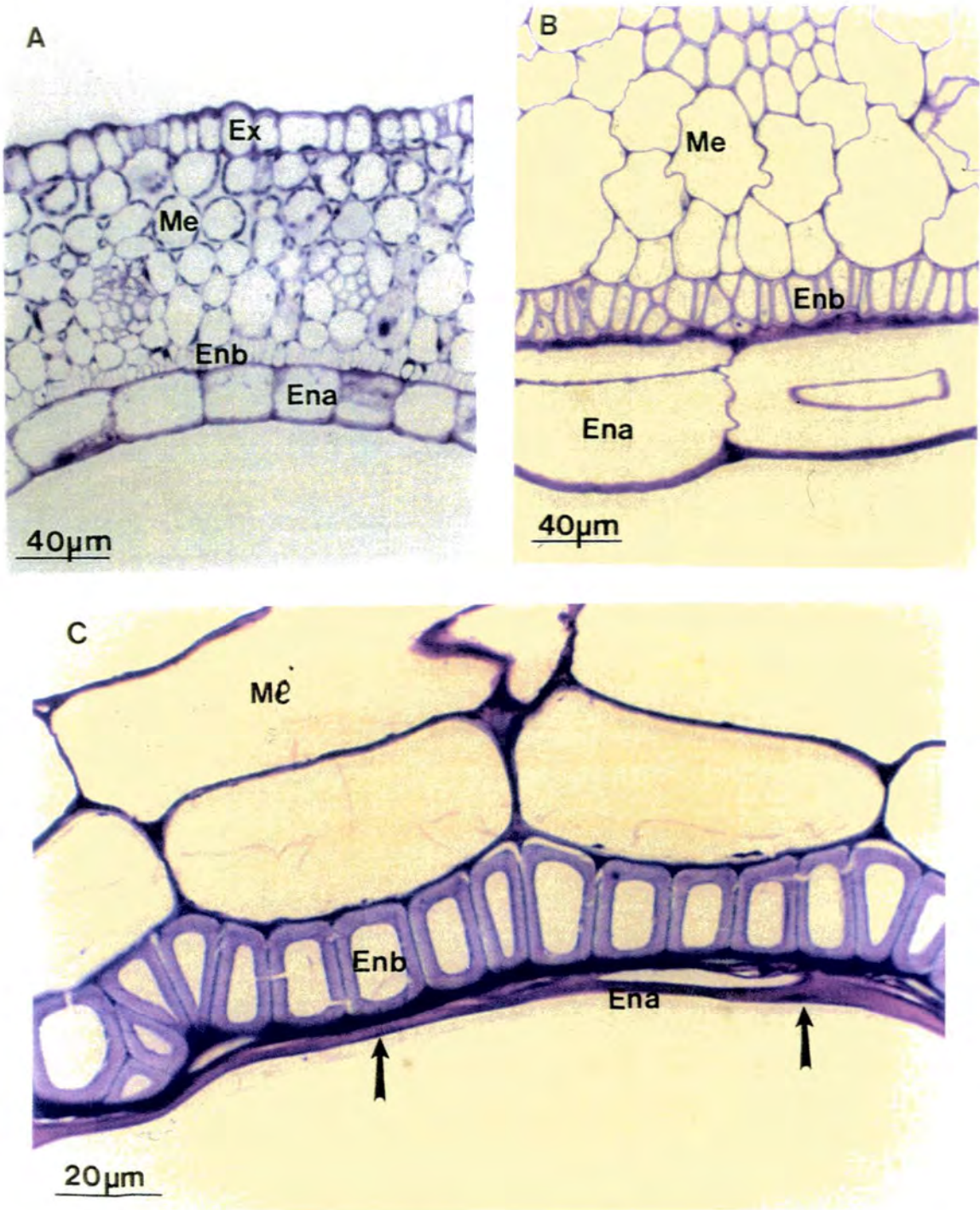


Figure 26. Structure of the carpel walls in the post-fertilised *Brassica napus* fruit

- A) Structure of carpel wall in the young post fertilised fruit**
- B) Structure of carpel wall in the mature post fertilised fruit**
- C) Structure of carpel wall in the senescing post fertilised fruit**

Ena = endocarp a, Enb = endocarp b, Ex = exocarp, Me = mesocarp. Arrows indicate the collapsed cells of Ena.

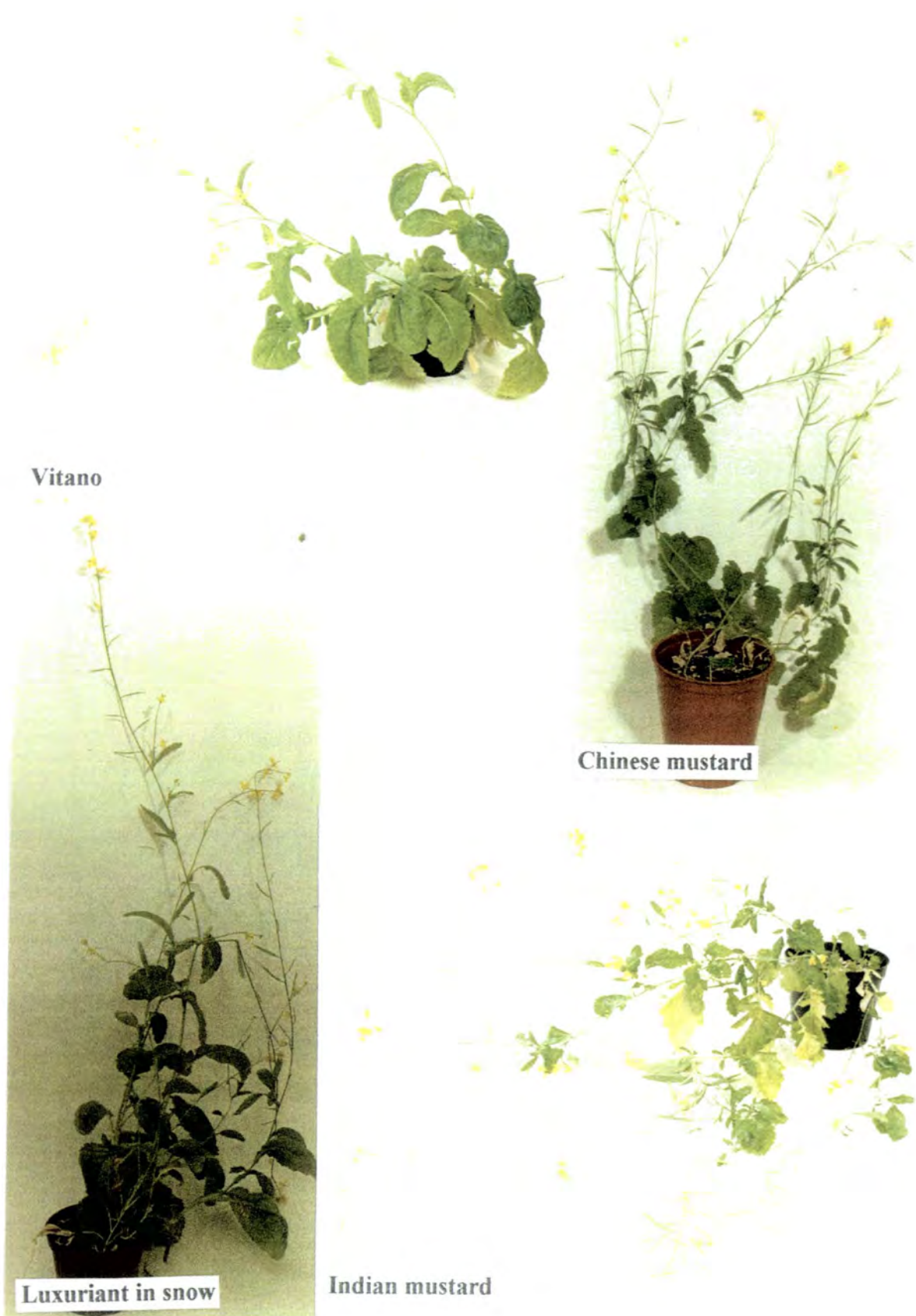


Figure 27. Plants of four varieties of *Brassica juncea*

3.4. DEVELOPMENT OF THE *BRASSICA JUNCEA* SILIQUE

Brassica juncea, or mustard, is another member of the Brassicaceae family which is an important crop plant. The siliques from four varieties of *Brassica juncea*, which are known to show variations in the 'pod shatter' characteristic, have been microscopically examined in this study. Seeds from three of the varieties Vitano, Chinese mustard and Luxuriant in snow were kindly supplied by Nickerson Bioc hem Limited and originate from New Zealand. Vitano is an oilseed crop. Seeds from the fourth variety, Line 74-3, were kindly supplied by Dr. S. P. Singh, and were obtained from the Agricultural University, Hissar, Haryana India. Line 74-3 is referred to as Indian mustard in the following text.

3.4.1. Phenotypic variations in the varieties

The maturing plants, seen in Figure 27, exhibit a number of phenotypic variations although all of the varieties reached an average height of 1m and produced four-petalled, yellow flowers. Although not a concern of this thesis, it was noted that the plants from the four varieties showed variations in germination time, growth rate, flowering time and leaf structure (results not shown). The phenotypic differences between the leaves of the four varieties for example, can be clearly seen in Figure 27.

The siliques of *Brassica juncea* have the same gross anatomy as those of *Brassica napus* and *Arabidopsis*, being bilocular siliques. The varieties examined in this study, however exhibited considerable variation in the length of their mature siliques, ranging from 2cm to 6cm, in our growth conditions. The number of seeds per silique therefore also varied and ranged from 1 to 12. There were a number of un-fertilised fruits observed on all the plants examined and these were generally found near the base of the stem.

3.4.2. Structure of the mature pre-fertilised fruit

Light microscopical studies were performed on 1µm thick sections, from LR White embedded tissues, which were stained with toluidine blue. Figure 28 shows that the mature pre-fertilised fruit has a similar cellular structure to that of *Arabidopsis*. The main vascular bundles are adjacent to the septum, which is aerenchymous and contains the transmitting tissue. As can be seen in Figure 28a, the vascular bundles exhibit very little

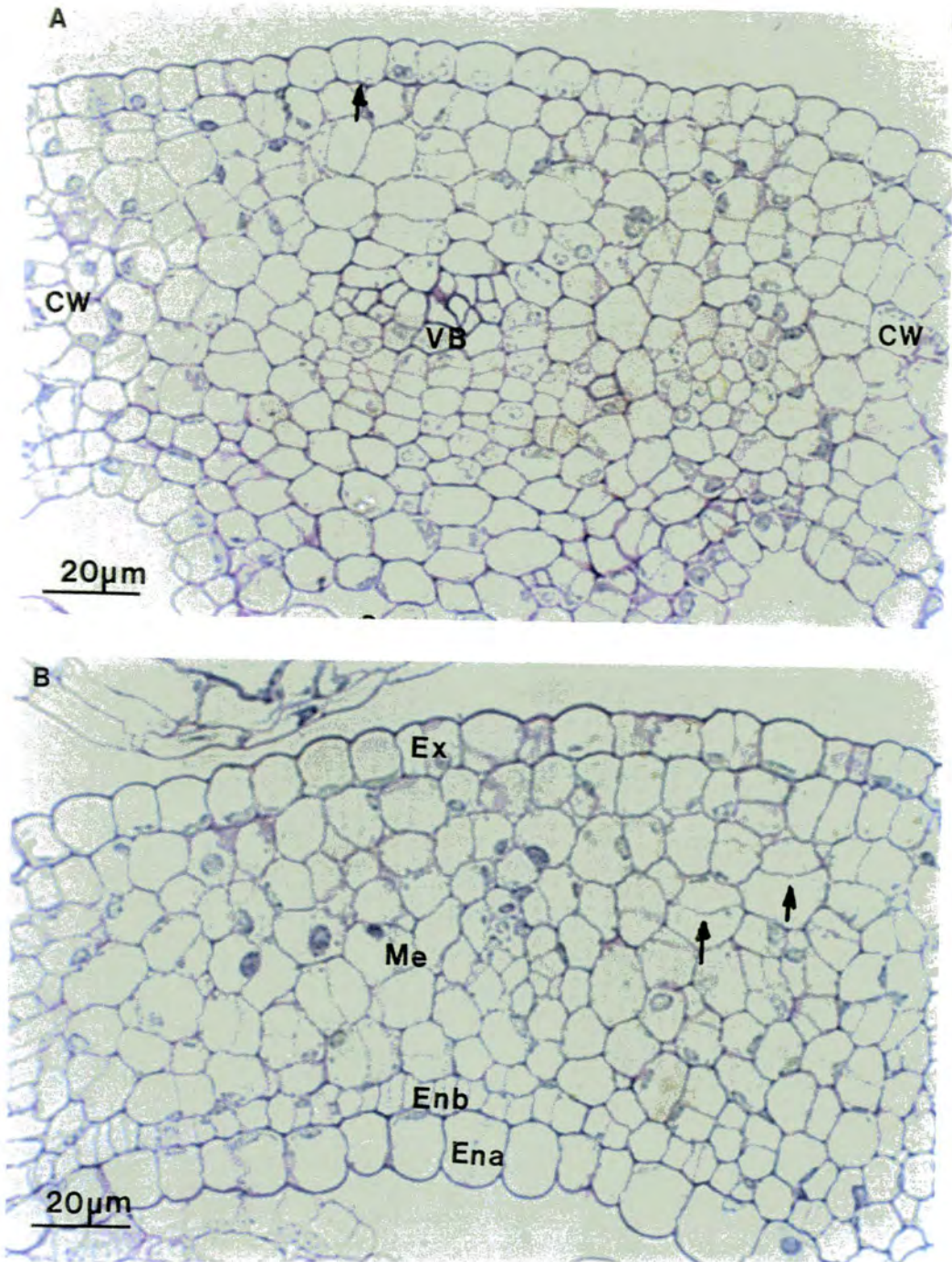


Figure 28. Structure of the pre-fertilised *Brassica juncea* fruit

A) Structure of the carpel margins (Indian mustard variety)

B) Structure of the carpel walls (Indian mustard variety)

CW = carpel wall, Ena = endocarp *a*, Enb = endocarp *b*, Ex = exocarp, Me = mesocarp S = septum, VB = vascular bundle. Arrows indicate some sites of cell division.

lignification prior to fertilisation. The carpel walls (Fig. 28b) comprise four different cell layers which have been named in accordance with those of *Arabidopsis*. The outer exocarp layer comprises a single layer of thick-walled cells interspersed with guard cells and stomata, and the mesocarp comprises six or seven layers of thin-walled, chlorenchymatous cells.

The endocarp, as in *Arabidopsis* and *Brassica napus*, has differentiated to form two distinct cell layers. Endocarp *a* (*Ena*) lines the inside of the locule and comprises a single layer of thin-walled, parenchymatous cells and endocarp *b* (*Enb*), which comprises a single layer of long, narrow cells, adjacent to the mesocarp. As can be seen in both Figure 28a and Figure 28b, prior to fertilisation all cell layers contain actively dividing cells, indicated by arrows, which are most prominent in the mesocarp layer. The structure of the pre-fertilised *Brassica juncea* fruit is similar to that of *Arabidopsis* fruits at stage five of development (Table 2), and the tissue types of the carpel wall are determined before fertilisation.

3.4.3. Development of the post-fertilised silique

Following fertilisation, the siliques from all of the *Brassica juncea* varieties showed a similar pattern of development to those of both *Arabidopsis* and *Brassica napus* (Fig. 29). There is considerable cell expansion in all planes in the exocarp, mesocarp and *Ena* layers and much less cell division is evident (Figs. 29b and 29d). *Enb* cells remain narrow in transverse section, but continue to divide anticlinally and expand along the long axis of the silique. Chloroplasts can be identified around the margins of the mesocarp cells (Figs. 29b and 29d), indicating that this chlorenchymatous layer is probably actively photosynthesising. The carpel wall cells continue to differentiate as the silique expands, and there is a general increase in cell size in all the carpel wall layers. The exocarp and *Ena* (Figs. 29b and 29d), thicken considerably along both the inner and outer walls, while the tangential walls show only slight thickening.

Development of the dehiscence zones begins post fertilisation, as a few rows of carpel margin cells and parenchymatous cells around the primary vascular bundles fail to increase in size at the same rate as those in the rest of the carpel wall. This causes a constriction at each carpel margin (Figs. 29a and 29c) which runs the length of the silique. This pattern of

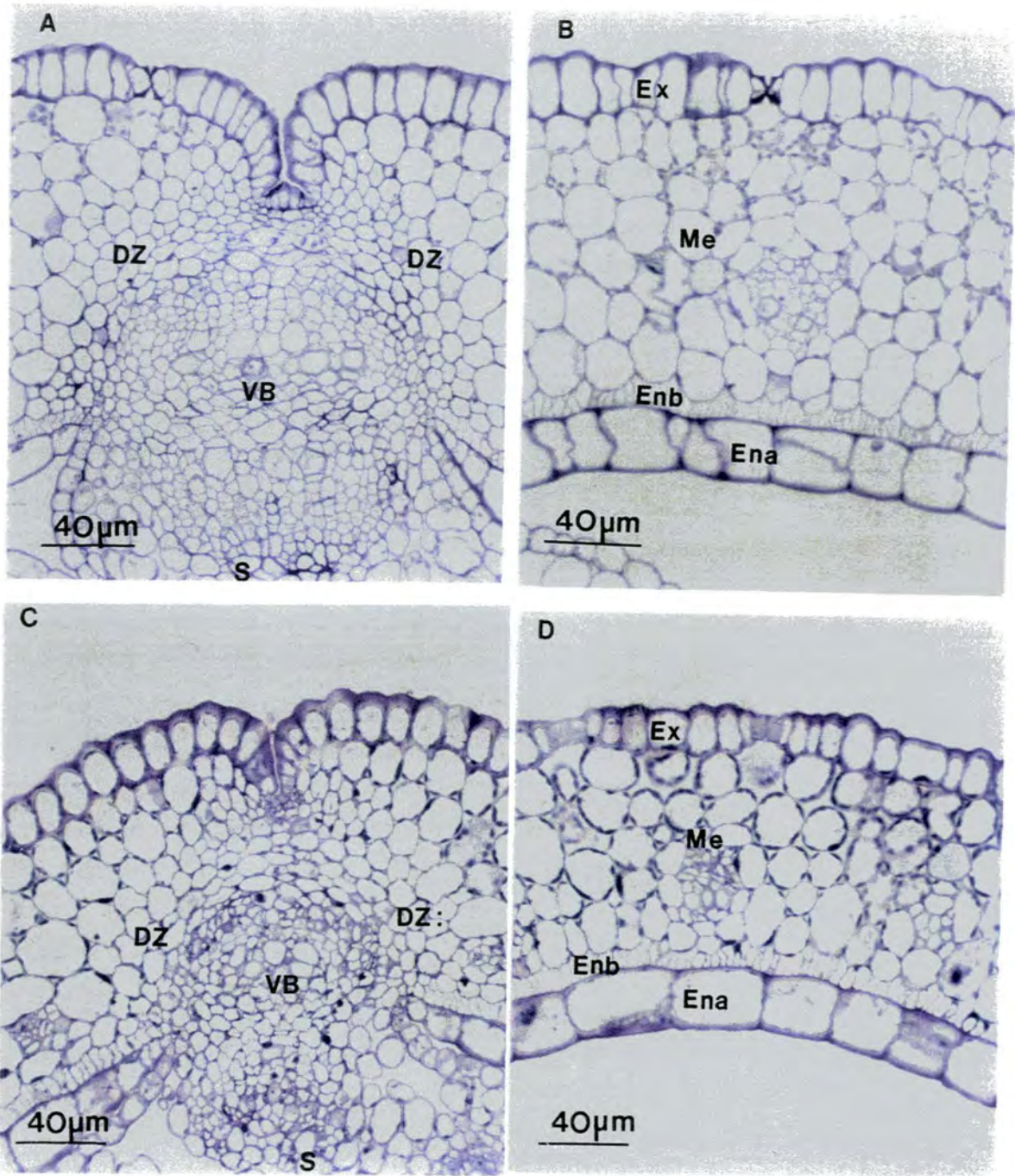


Figure 29. Structure of the young post-fertilised *Brassica juncea* fruit

- A) Structure of the carpel margins (Vitano variety)
- B) Structure of the carpel wall (Vitano variety)
- C) Structure of the carpel margins (Chinese mustard variety)
- D) Structure of the carpel wall (Chinese mustard variety)

DZ = dehiscence zone, Ena = endocarp a, Enb = endocarp b, Ex = exocarp, Me = mesocarp, S = septum, VB = vascular bundle

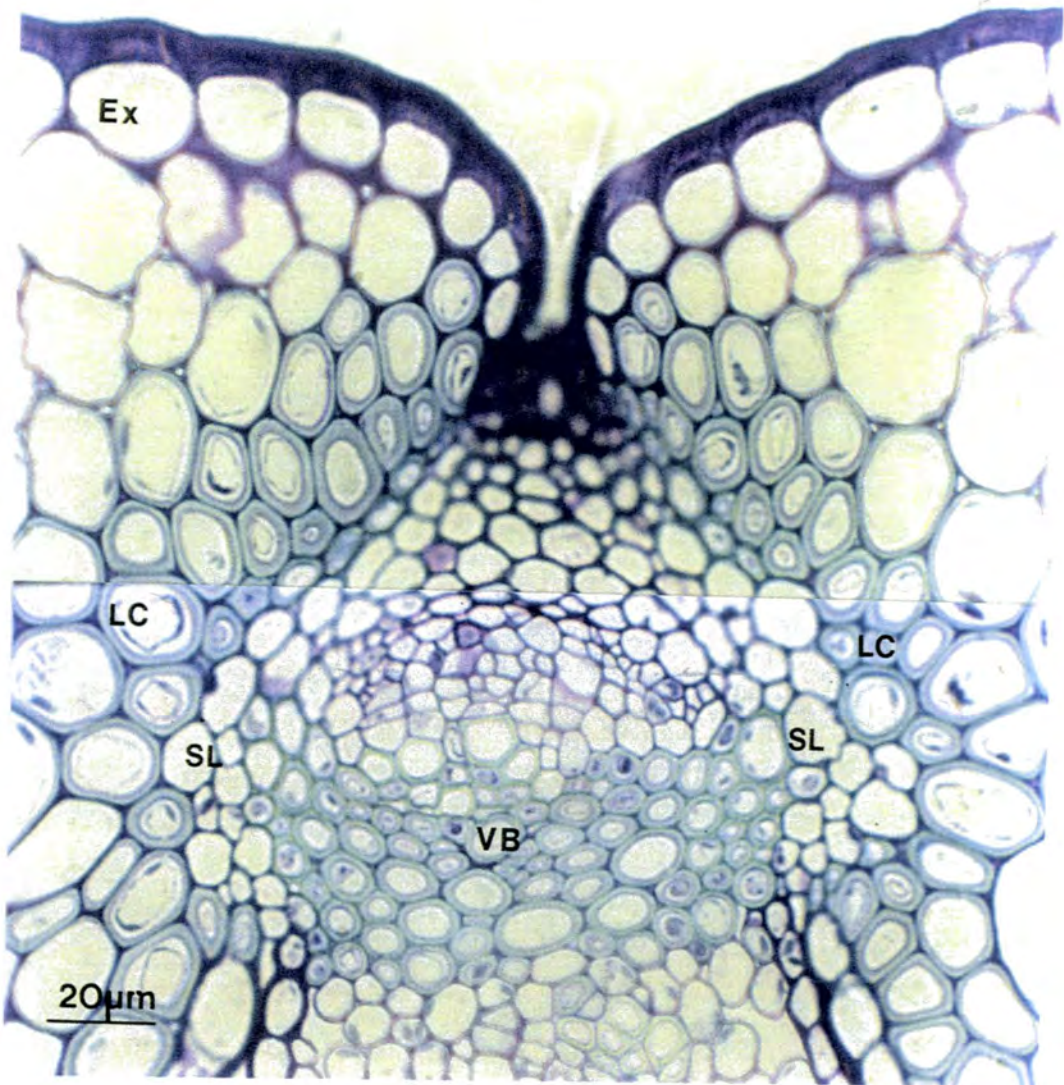


Figure 30. Cellular structure of the dehiscence zones in *Brassica juncea* fruit (Indian mustard variety)

Ex = exocarp, LC = lignified dehiscence zone cell, SL = separation layer cell, VB = vascular bundle

development is seen in stage six *Arabidopsis* siliques (Table 2) and is also seen in *Brassica napus* siliques (Figs. 25 and 26). The dehiscence zones become increasingly more prominent as the silique lengthens and widens. Although the carpel margin cells are much smaller than those of the carpel walls, there appears to be no evidence of any cellular degradation or formation of a distinct separation layer at this stage of development (Figs. 29a and 29c).

As cell expansion continues the dehiscence zones further differentiate during the next stage of development. Two or three rows of cells along the marginal carpel walls lignify, and separate the carpel walls from the primary vascular bundles, forming two valves (Fig. 30). There is a marked difference in size between the carpel wall cells and those of the now clearly-defined separation layer. The separation layer cells in Figure 30 show evidence of cellular degradation, as can be seen in both the *Brassica napus* (Meakin & Roberts 1990A) and *Arabidopsis* siliques at this stage of development, following lignification of the valve edge cells.

The carpel wall cells also show extensive thickening (Figs. 31a, 31b, 31c and 31d), similar to that seen in *Arabidopsis* and *Brassica napus*. The exocarp layer further thickens along the outer walls, producing a very thick cuticular layer on the outer surface of the silique. The cells within the mesocarp layer also develop slightly thicker walls. *Ena* also shows extensive thickening along the inner and outer walls, producing another cuticular layer and forming a smooth lining on the inner surface of the silique. *Ena* cells generally showed much more thickening in the Indian mustard variety (Fig. 31d), especially along the outer walls. The inner endocarp layer, *Enb*, also begins to lignify. Lignification of the carpel margin and *Enb* cells in *Brassica juncea* fruits shows a similar pattern of development to that seen in *Arabidopsis* fruits at stage eight of development (Table 2).

Lignification continues in the dehiscence zone as the initial lignified, dehiscence zone cells further thicken and the cell lumina appear to become very small, and adjacent carpel wall cells also begin to lignify (Figs. 32a, 32b, 32c and 32d). The degree of wall thickening appears to form a gradient as it decreases with increasing distance from the dehiscence zone. The carpel wall cells also continue to differentiate and the lignified *Enb* cells continue to thicken, although there appears to be little cell expansion and the cell lumina also become very small (Figs. 32a, 32b, 32c and 32d). Lignification is also evident in some cells of the mesocarp layer which are adjacent to *Enb*.

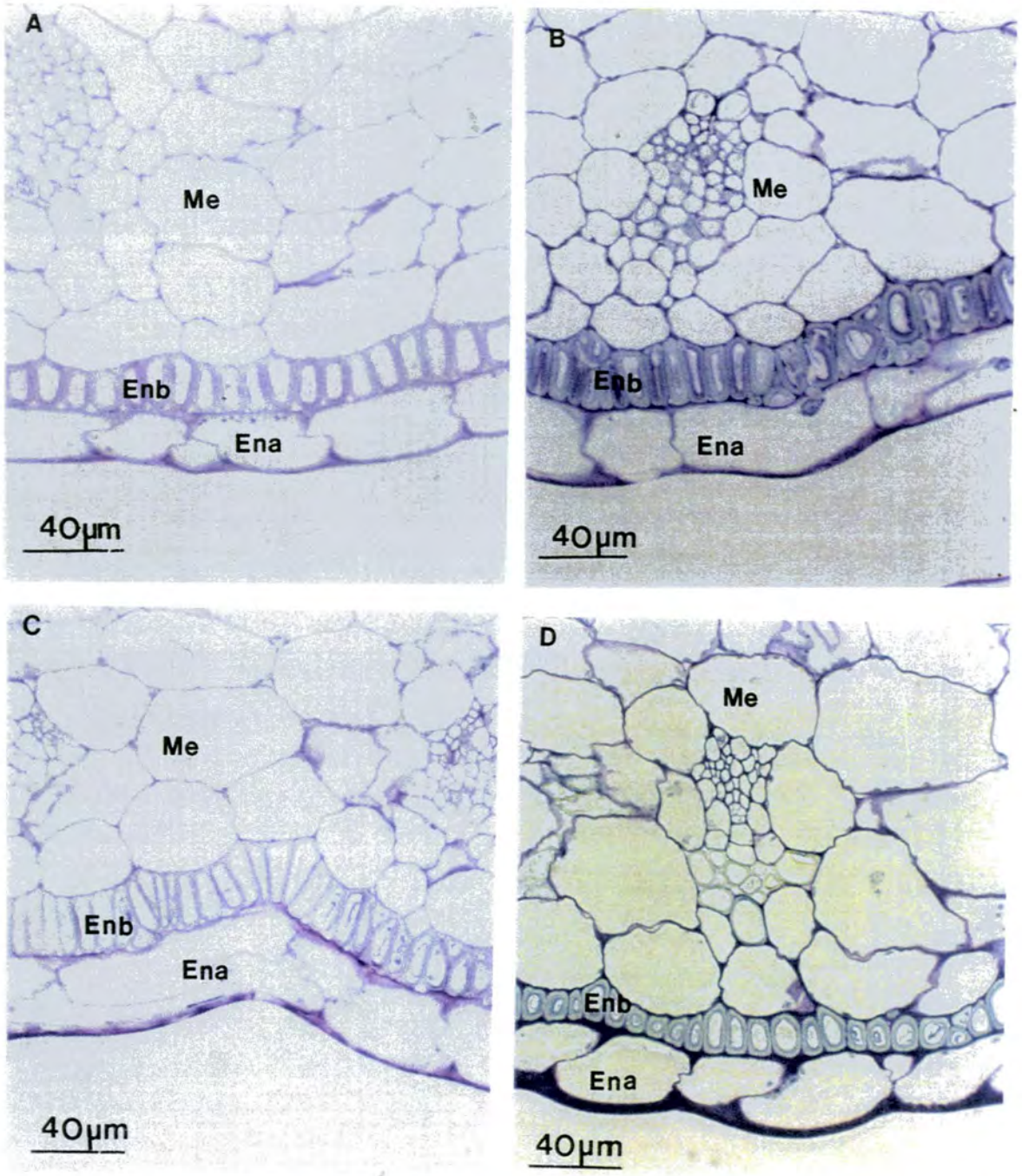


Figure 31. Structure of the carpel walls in the maturing fruits of four varieties of *Brassica juncea*

- A) Structure of the carpel wall in the Vitano variety**
- B) Structure of the carpel wall in the Chinese mustard variety**
- C) Structure of the carpel wall in the Luxuriant in snow variety**
- D) Structure of the carpel wall in the Indian mustard variety**

Ena = endocarp a, Enb = endocarp b, Ex = exocarp, Me = mesocarp

The mesocarp layer eventually begins to desiccate during the next stage of development. This initiates from the outer cell layers adjacent to the exocarp and can be seen as a gradual yellowing of the green silique. This pattern of cellular senescence is also seen in *Arabidopsis* fruits during stage nine (Table 2) and in *Brassica napus* fruits. The inner endocarp layer, *Ena*, begins to degrade in three of the varieties, Vitano, Chinese mustard and Luxuriant in snow (Figs. 33a, 33b and 33c), and most of the cells appear to collapse and form a flat "cuticular" layer. A similar pattern of development is seen in *Arabidopsis* and *Brassica napus* fruits. In the Indian mustard variety however, most of the cells in *Ena* remained intact (Fig. 33d).

The mesocarp of the siliques eventually desiccates and the valve walls in Vitano Chinese mustard and Luxuriant in snow siliques began to split away from the tip of the fruit. No more than three 'naturally shattered' siliques were observed on each plant from Vitano, Chinese mustard and Luxuriant in snow, however, the valves of desiccated siliques detached easily from the fruits of the three varieties when mechanical pressure was applied with the fingertips. In Indian mustard, no 'shattered' siliques were observed on any of the plants and considerably more mechanical pressure was required to detach the valves from the fruits. If desiccated siliques of Indian mustard plants were left attached to the plant, the seeds frequently underwent precocious germination.

3.4.4. Carpel wall development in mature Indian mustard siliques

The Indian mustard variety of *Brassica juncea* has a 'non shattering' phenotype, and shows a different pattern of carpel wall differentiation to the other three varieties examined in this study, during the last stages of silique development. The desiccation of the mesocarp layer appears to be similar to that of the other three varieties of *Brassica juncea* and similar to that of *Arabidopsis* and *Brassica napus*. There is, however, more extensive lignification in the mesocarp cells adjacent to the lignified dehiscence zone cells and mesocarp cells adjacent to the lignified, endocarp layer. Lignin is stained yellow with acridine orange and Figure 34a shows the extent of lignification in the mesocarp layer adjacent to the dehiscence zone in mature Indian mustard siliques. The cell walls of the exocarp also show more wall thickening in the Indian mustard variety, and acridine orange staining reveals lignified secondary wall deposition in some exocarp cells. This can be seen in Figure 34a as a narrow, yellow band along the inside of the the red-stained tangential outer cell wall and is indicated by arrows.

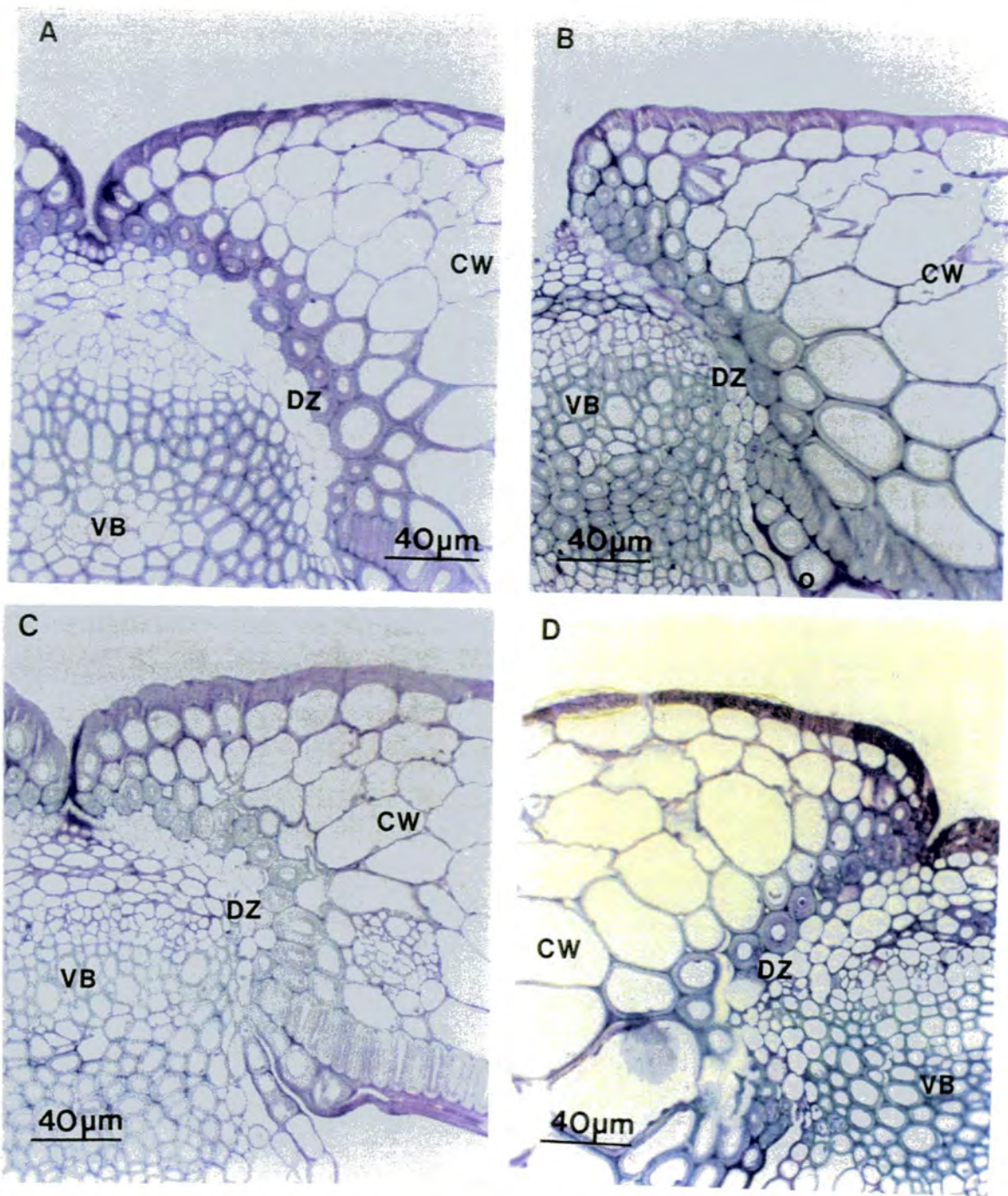


Figure 32. Structure of the dehiscence zones in the mature senescing siliques of four varieties of *Brassica juncea*

- A) Structure of the dehiscence zones in the Vitano variety
- B) Structure of the dehiscence zones in the Chinese mustard variety
- C) Structure of the dehiscence zones in the Luxuriant in snow variety
- D) Structure of the dehiscence zones in the Indian mustard variety

CW = carpel wall, DZ = dehiscence zone VB = vascular bundle

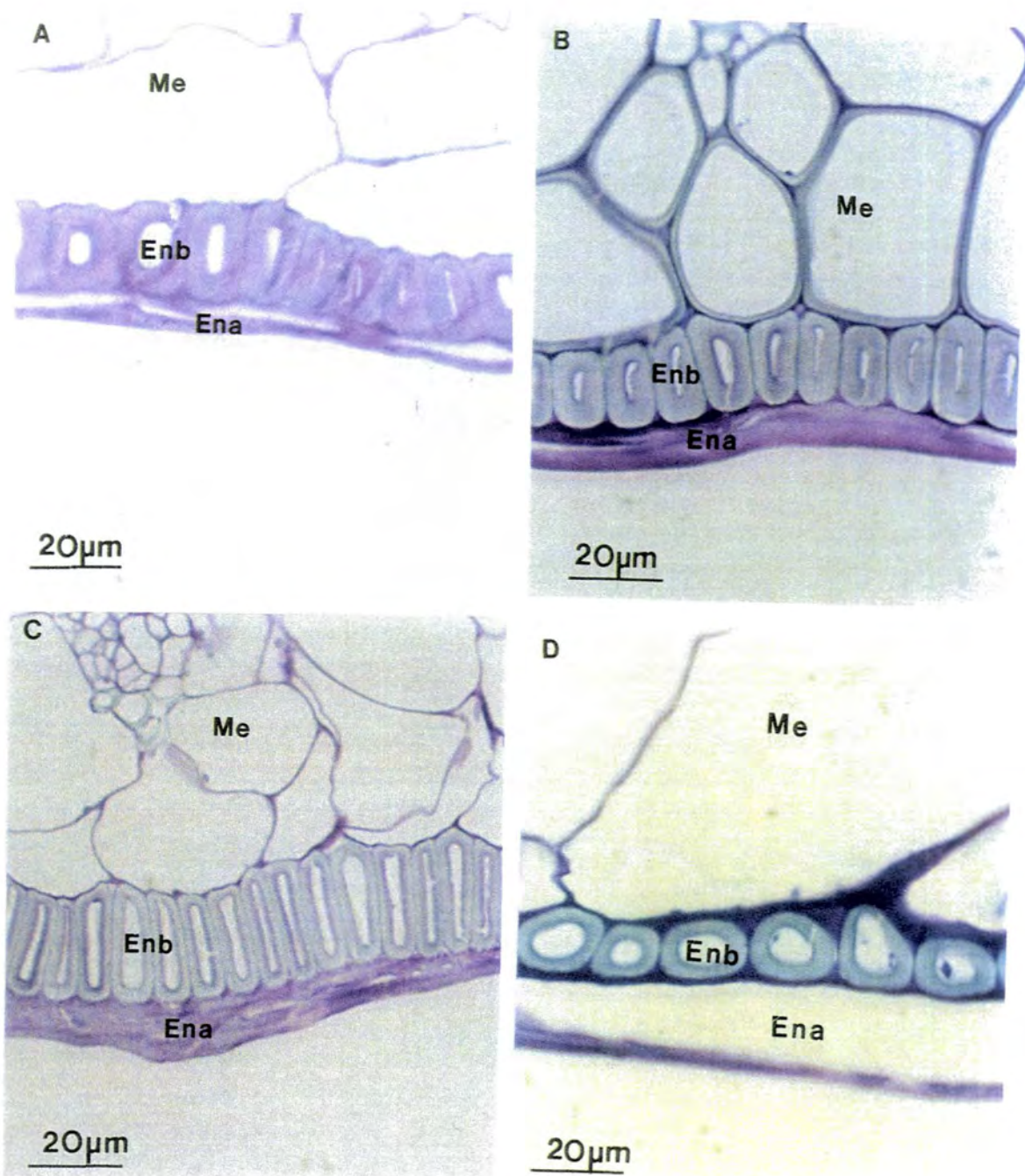


Figure 33. Structure of the endocarp in the mature senescing siliques of four varieties of *Brassica juncea*

- A) Structure of the endocarp in the Vitano variety**
- B) Structure of the endocarp in the Chinese mustard variety**
- C) Structure of the endocarp in the Luxuriant in snow variety**
- D) Structure of the endocarp in the Indian mustard variety**

Ena = endocarp *a*, Enb = endocarp *b*, Me = mesocarp

The endocarp layers in Indian mustard show much more thickening than is seen in Vitano, Chinese mustard and Luxuriant in snow. *Ena* shows much less cellular degradation and the majority of cells do not collapse, but appear to continue thickening. The thickened walls of *Ena* do not stain with calcofluor, as can be seen in Figure 34b; however, they are stained red with both ruthenium red (Fig. 34c) and acridine orange (Fig 34d). This pattern of staining suggests that the cell walls of *Ena* have a high pectin content. There also appears to be secondary wall deposition in *Ena* cells (indicated by arrows in Fig. 34d), similar to that seen in exocarp cells.

The second endocarp layer, *Enb*, also shows a different pattern of development in the siliques of Indian mustard. The lignified cells of *Enb* continue to thicken as the fruit continues to ripen and to desiccate, but they do not appear to expand, producing extensively thickened cells with a small lumen. The calcofluor-stained section shown in Figure 34b reveals a silver/blue stained area on the outer lignified edge of *Enb* cells which is not seen in the desiccated mesocarp or *Ena*. This may be components of the primary cell wall of *Enb* cells and the pattern of staining would indicate that this primary cell wall is intact and has a higher cellulose content.

The cells of *Enb* appear to be surrounded by a relatively thick 'extra-cellular matrix' (Figs 33d, 34c and 34d). This matrix can be seen adjacent to all the walls of *Enb* cells. Ruthenium red and acridine orange staining of this 'matrix' in Figure 34c and Figure 34d respectively, reveals a similar pattern of staining to that seen in *Ena* cell walls, and indicates that the 'matrix' has a high pectin content and is probably part of the secreted *Ena* cell wall.

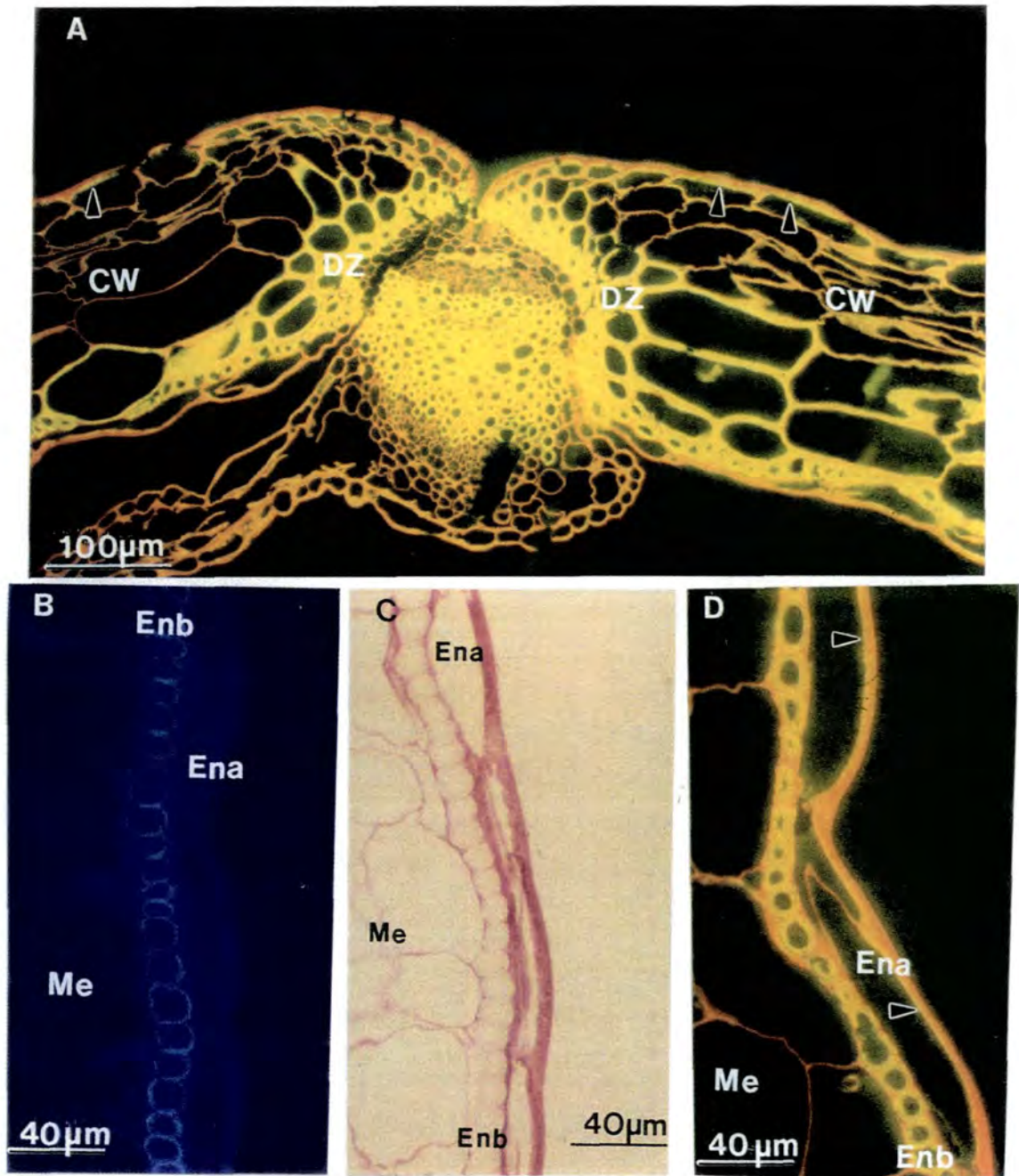
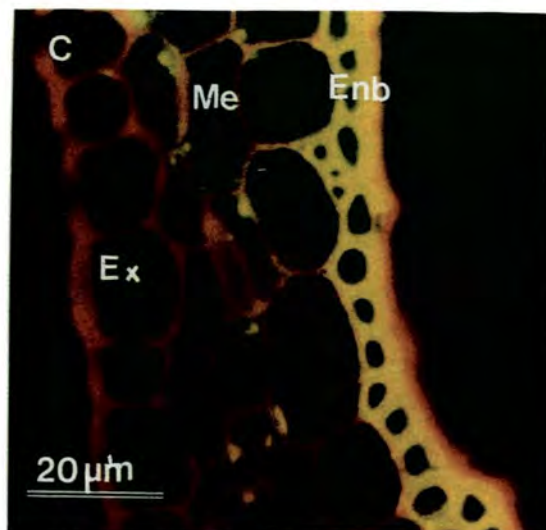
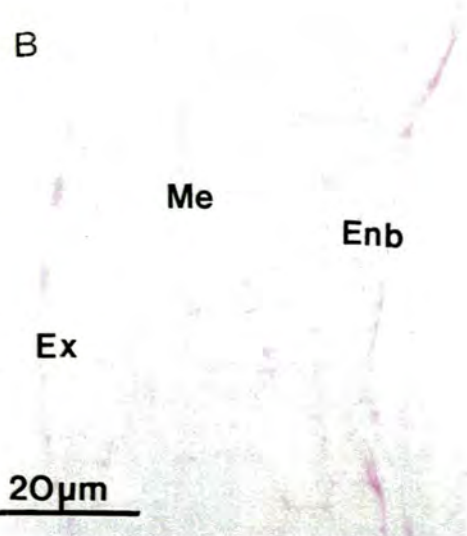
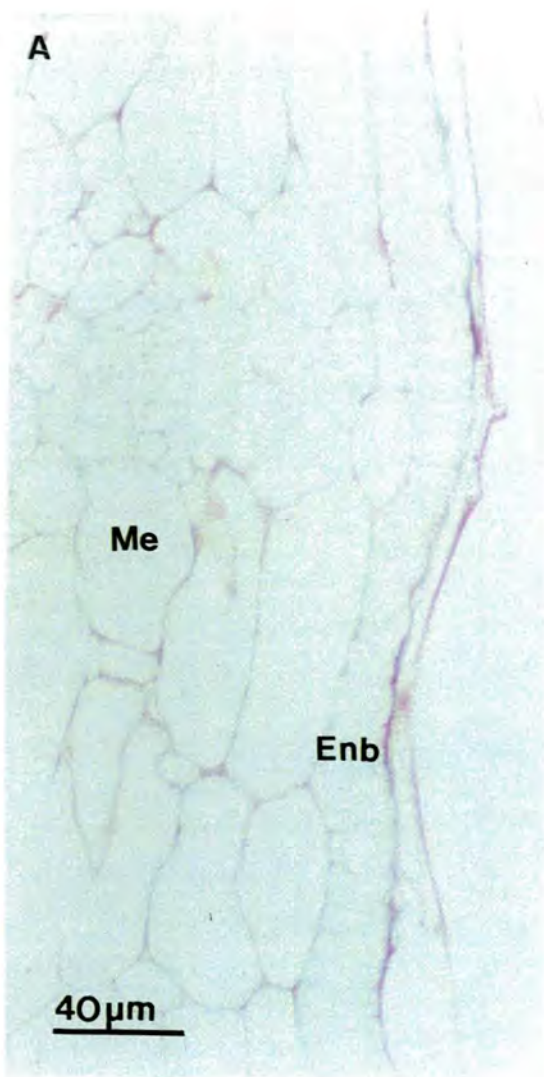


Figure 34. Structure of the dehiscence zone and endocarp in senescing siliques of the Indian mustard variety of *Brassica juncea*

- A) Structure of the dehiscence zone. Section stained with acridine orange, UV illumination - arrows indicate lignification in the exocarp cells**
B) Structure of the endocarp. Section stained with calcofluor, UV illumination
C) Structure of the endocarp. Section stained with ruthenium red, bright field illumination
D) Structure of the endocarp. Section stained with acridine orange, UV illumination - arrows indicate lignification in the endocarp cells

CW = carpel wall, DZ = dehiscence zone, Ena = endocarp a, Enb = endocarp b, Me = mesocarp



Appendix to Figure 34. Structure of the endocarp in senescing siliques of *Brassica napus* and *Arabidopsis*.

- A) Structure of the endocarp in *Brassica napus*. Section stained with ruthenium red, bright field illumination.
 B) Structure of the endocarp in *Arabidopsis*. Section stained with ruthenium red, bright field illumination.
 C) Structure of the endocarp in *Arabidopsis*. Section stained with acridine orange, UV illumination.

Enb = endocarp *b*, Ex = exocarp, Me = mesocarp

Sections from *Brassica napus* and *Arabidopsis* show that the structure of Enb in these two species is different to that of Indian mustard. The ruthenium red stained sections in Figures A and B show no red staining, indicative of pectin, surrounding the lignified Enb cells, and the acridine orange stained section in Figure C shows no red/orange staining, also indicative of pectin, surrounding Enb cells.

3.5. DEVELOPMENT OF *ARABIDOPSIS* ETHYLENE MUTANT SILIQUES

Ethylene is known to influence senescence, abscission and fruit ripening (Sexton and Roberts 1982, Theologis 1992). In this study the siliques of three *Arabidopsis* ethylene mutants have been examined to find if the mutations affect fruit ripening and carpel wall and dehiscence zone development. Seeds from *Ein* 1-1, *Ein* 2-1 and *Etr* were supplied by the Nottingham *Arabidopsis* Stock Centre. The mutants were isolated from the Columbia ecotype, *Ein* 1-1 and *Etr* are dominant mutations and *Ein* 2-1 is recessive. The *Ein* mutants are non-allelic and are insensitive to exogenous ethylene, the *Etr* mutant lacks a number of ethylene responses and so the mutation most likely affects an ethylene receptor (Bleeker *et al.* 1988, Guzman and Ecker 1993, Romano *et al.* 1993).

3.5.1. The phenotype of the *Ein* 1-1 and *Ein* 2-1 plants

Seeds from *Ein* 1-1, *Ein* 2-1 and wild type were planted at the same time and grown under the same conditions. Seeds from *Ein* 1-1 and *Ein* 2-1 germinated at the same time as wild type but grew at a slightly slower rate. The mature plants were similar in appearance to the wild type, although the mature siliques of the *Ein* 2-1 plants yellowed more gradually than those of the wild type or *Ein* 1-1. Shattered siliques were observed on both mutant plants, however there were less shattered siliques on the *Ein* 2-1 plants than observed on *Ein* 1-1 or the wild type.

3.5.2. Development of the dehiscence zones and carpel walls in the post-fertilised silique

Microscopical examination of the dehiscence zones and carpel walls of post-fertilised *Ein* 1-1 and *Ein* 2-1 mutant siliques showed a similar pattern of development to the wild type (results not shown). During stages six and seven the carpel margins constrict and the separation layer can be distinguished at stage seven. The dehiscence zone cells and the inner endocarp *Enb* begin to lignify at stage eight and isolate the carpel walls from the replum, then the inner endocarp, *Ena*, disintegrates at stage nine. Although the siliques appeared to yellow slightly slower than wild type, the desiccation of the mesocarp cells at stage nine was also histologically similar to the wild type. The mesocarp cells adjacent to the exocarp began to desiccate first and this proceeds through to the endocarp.

3.5.3. The phenotype of the *Etr* mutant plant

Seeds from *Etr* and wild type were planted at the same time and grown under the same conditions. Seeds from *Etr* germinated at the same time as wild type but grew at a slower rate. *Etr* plants bolted approximately three weeks later than the wild type and although mature *Etr* plants resembled the wild type they grew much taller and the siliques were slightly longer. The ripening siliques of *Etr* yellowed more gradually than the wild type and, as can be seen in Figure 35, the senesced petals and stamens frequently remained attached to the ripening siliques. No shattered siliques were observed on mature *Etr* plants and many desiccating yellow siliques also failed to dehisce normally. The valves from non-dehisced siliques would detach from the plant however, if mechanical stimulation was applied by pressing with the fingertips.

3.5.4. Development of the dehiscence zones in the post-fertilised silique

The putative dehiscence zones of the young post-fertilised *Etr* silique have a similar structure to that of the wild type at stages six and seven (Fig. 36a). There is a constriction at the carpel margins, indicated by arrows in Figure 36a, and little lignification of the replar vascular bundles. During the next stage of development, stage seven, the separation layer cells begin to degrade and are readily distinguished. Figure 37a shows the structure of the dehiscence zones in the mature *Etr* silique. The separation layer (indicated by small arrows) can be clearly distinguished and is similar in structure to the wild type during the later stages of development, stages nine and ten.

The lignified dehiscence zone cells begin to thicken during the next stage of development, stage eight, and lignification of the dehiscence zone begins adjacent to the exocarp and proceeds through to the mesocarp as in the wild type. However, in the *Etr* silique there is less lignification of these cells. The structure of the lignified zone in the *Etr* silique appears to differ from the wild type as it does not extend from the exocarp through the carpel wall layers to link up with the lignified endocarp. Figures 37a and 37b show that the dehiscence zone cells which are adjacent to the exocarp have lignified however, those cells adjacent to the endocarp (indicated by large arrows) have not lignified, although the replar vascular bundles and *Enb* appear to show a normal pattern of lignification.

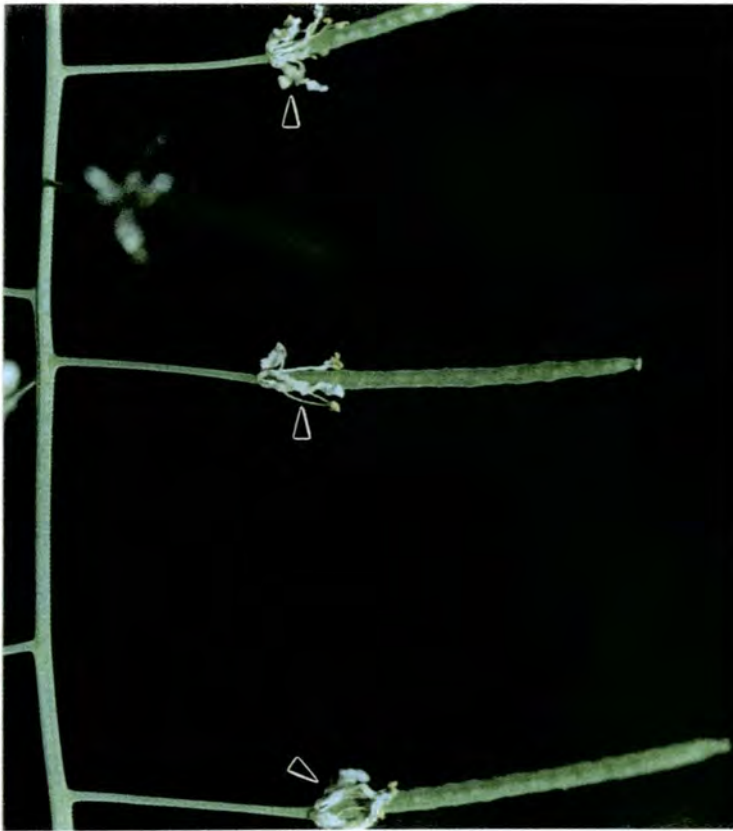


Figure 35. *Etr* mutant siliques showing attached senescing floral organs which are indicated by arrows

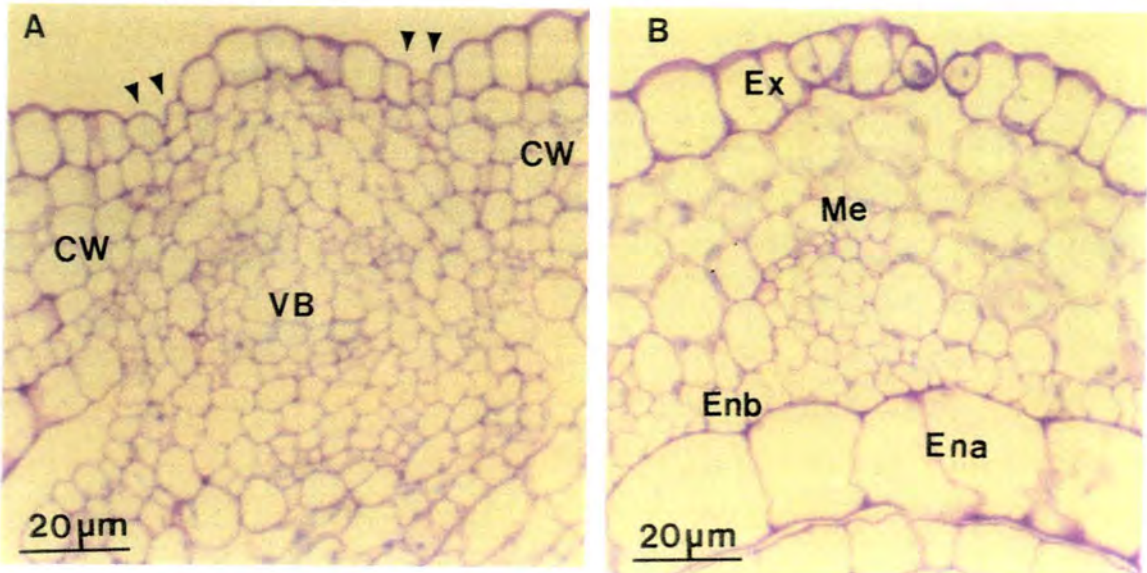


Figure 36. Structure of the young post-fertilised *Etr* fruit

- A) Structure of the dehiscence zones in the young post-fertilised fruit
- B) Structure of the carpel margins in the young post-fertilised fruit

CW = carpel wall, Ena = endocarp *a*, Enb = endocarp *b*, Ex = exocarp, Me = mesocarp, VB = vascular bundle, arrows indicate constrictions at the carpel margins

3.5.5. Development of the carpel wall in the post-fertilised silique

The carpel wall in the young *Etr* silique has a similar structure to that of the wild type during the early stages of post-fertilisation development. Figure 36b shows the carpel wall comprises the four different types of tissue identified in the wild type, the exocarp, the mesocarp *Ena* and *Enb*. The exocarp and endocarp tissues in the carpel wall appear to show the same pattern of post-fertilisation development as that identified in the wild type during stages eight and nine. The exocarp cells enlarge and thicken along the outer tangential walls and during stage eight *Enb* begins to lignify. During the next stage of development *Ena* disintegrates and as can be seen in Figure 37b, the exocarp and endocarp have a similar structure to the wild type mature post-fertilised silique. Although the mesocarp layer does begin to desiccate in the *Etr* silique following lignification of *Enb*, this process is much slower than in the wild type. Chloroplasts can often still be seen in *Etr* mesocarp cells which are adjacent to the exocarp, and which are the first to senesce in the wild type, even after *Ena* has disintegrated.

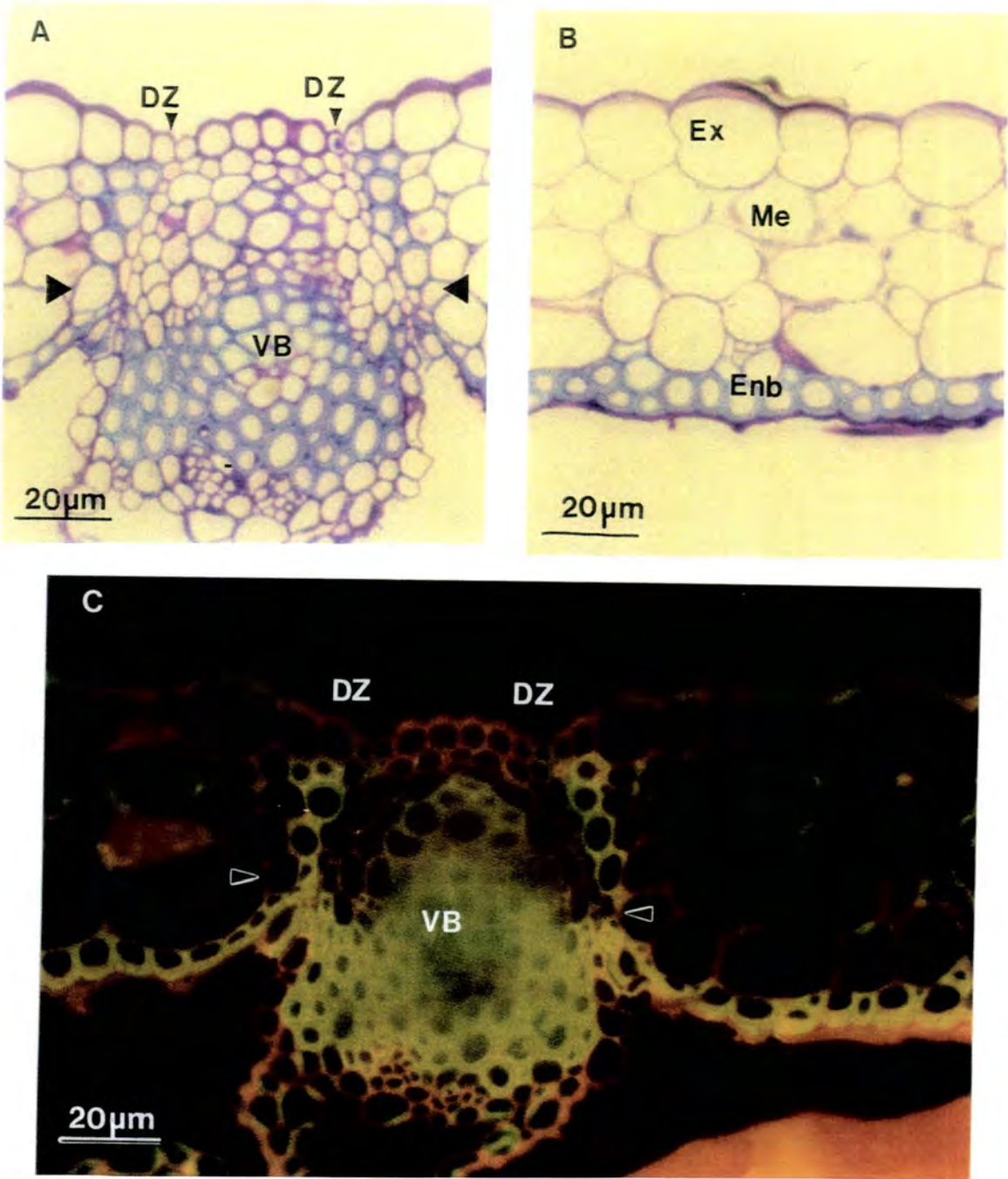


Figure 37. Structure of the mature post-fertilised *Etr* fruit

- A) Structure of the dehiscence zones in the mature post-fertilised fruit. Small arrows indicate the dehiscence zone, large arrows indicate non-lignified cells in the dehiscence zone**
- B) Structure of the carpel walls in the mature post-fertilised fruit**
- C) Structure of the dehiscence zones in the post-fertilised fruit. Section stained with acridine orange, UV illumination. Arrows indicate non-lignified cells in the dehiscence zone**

DZ = dehiscence zone, Enb = endocarp *b*, Ex = exocarp, Me = mesocarp, VB = vascular bundle

3.6. IMMUNOCYTOCHEMISTRY OF THE SILIQUE

Immunocytochemical techniques may be used to localise specific proteins and polysaccharide epitopes both temporally and spatially within a cell. Recent work done at the John Innes Institute in Norwich, has successfully utilised antibodies raised against a number of plant glycoproteins, AGPs and pectins, to localise these components to specific sites within plant cells (Knox *et al.* 1989, 1991, 1992, Pennell *et al.* 1989, 1991, Pennell & Roberts 1990, Rae *et al.* 1991, Stacey *et al.* 1990, Baldwin *et al.* 1993).

3.6.1. Localisation of JIM13 binding

JIM13 recognises a carbohydrate epitope of AGPs and the spatial and temporal distributions of the JIM13 antigen have been investigated in pea nodules (Rae *et al.* 1991) and carrot root (Knox *et al.* 1991). The antibody was specific to the thickening endodermal cells of the pea nodule where it labelled the cell wall and plasma membrane, and to the stele of the root where it labelled the endodermis and xylem. In the carrot root the JIM13 antibody labelled the epidermal cells and future xylem cells of the carrot root.

The monoclonal AGP antibody JIM13 was raised in rat from cell isolates of *Daucus carota* root (Knox *et al.* 1989, 1990, Pennell *et al.* 1989, Stacey *et al.* 1990) and kindly supplied by the John Innes Institute. The antiserum was supplied as a hybridoma culture supernatant with 0.02% sodium azide and tissue sections were incubated overnight at 4°C in a 1:10 dilution of the antiserum.

JIM13 binding was detected on LR White embedded, semi-thin tissue sections, using gold conjugated to a secondary antibody. Colloidal gold was silver enhanced and specific localisations were detected as either, black/brown deposits under bright field or differential interference contrast (DIC) illumination, or as bright silver/gold deposits on a dark background, under epi-polarising illumination. Control sections of *Arabidopsis* and the Indian mustard variety of *Brassica juncea*, which were incubated in buffered 1% pre-immune rat serum, showed no specific binding (Fig. 41) and control sections incubated in sodium periodate for 30 minutes prior to incubation in primary antibody also showed no specific binding (results not shown).



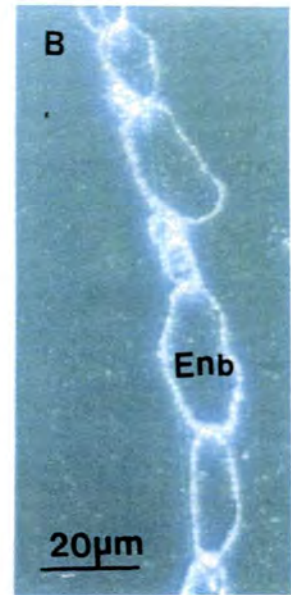
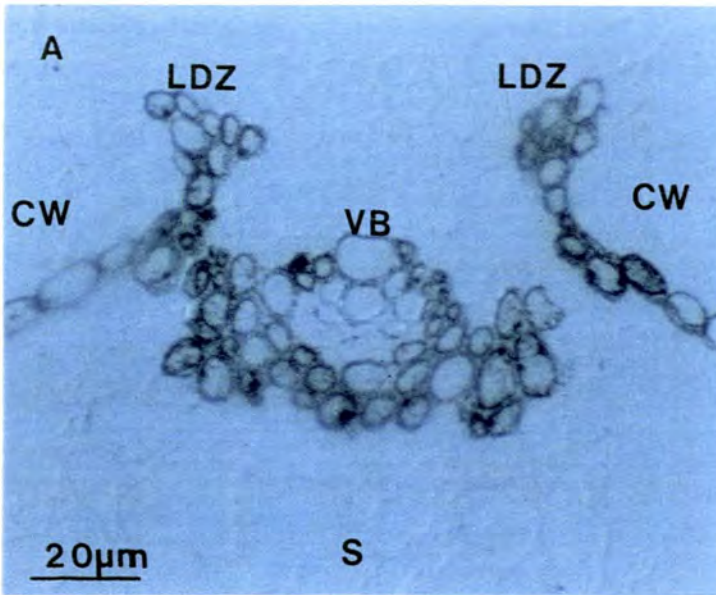


Figure 38. Localisation of JIM13 binding in *Arabidopsis* siliques

A) Immunolabelling of lignified dehiscence zone cells, DIC illumination

B) Immunolabelling of lignified endocarp cells, epi-polarising illumination

Enb = endocarp *b* CW = carpel wall LDZ = lignified dehiscence zone cells S = septum VB = vascular bundle

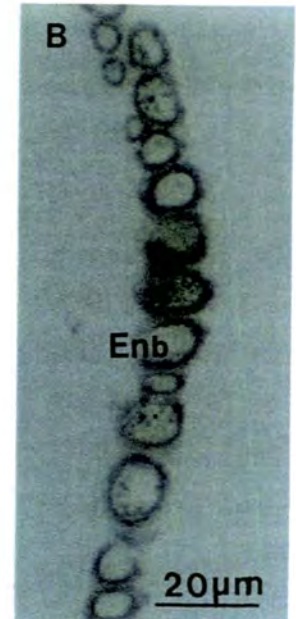
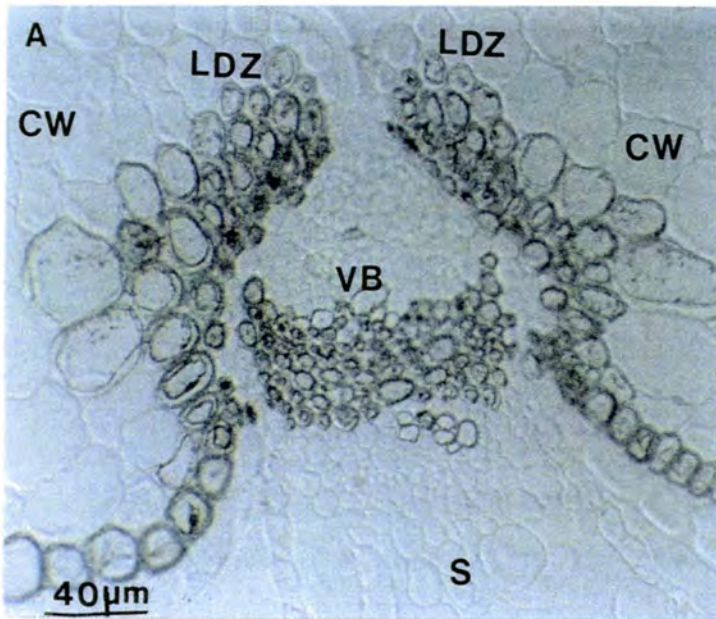


Figure 39. Localisation of JIM13 binding in *Brassica juncea* siliques

A) Immunolabelling of lignified dehiscence zone cells, DIC illumination

B) Immunolabelling of lignified endocarp cells, DIC illumination

Enb = endocarp *b* CW = carpel wall LDZ = lignified dehiscence zone cells S = septum VB = vascular bundle

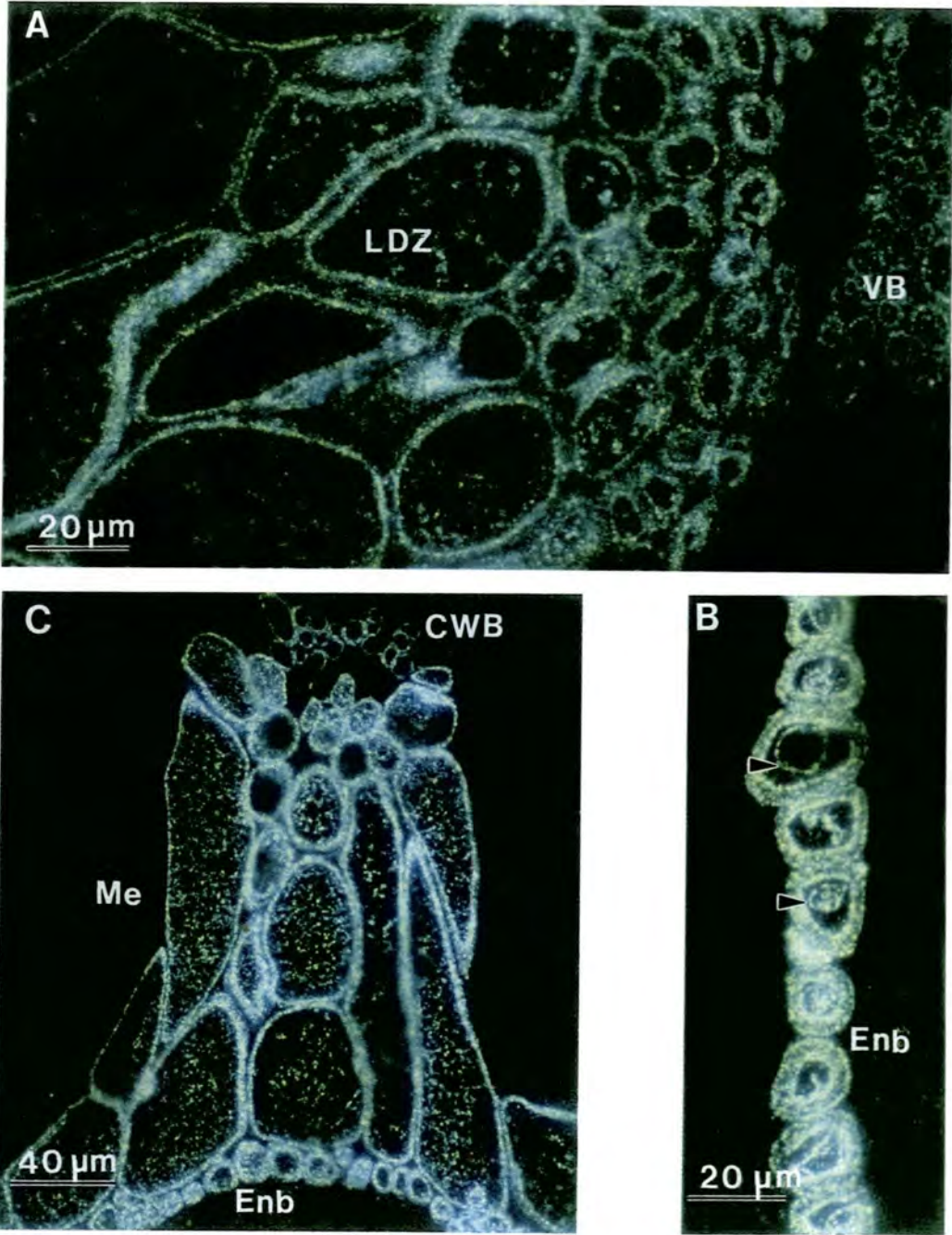


Figure 40. Localisation of JIM13 binding in Indian mustard

- A) Immunolabelling of lignified dehiscence zone cells, epi-polarising illumination**
- B) Immunolabelling of lignified endocarp cells, epi-polarising illumination. Arrows indicate the plasmalemma in *Enb* cells**
- C) Immunolabelling of lignified mesocarp cells, epi-polarising illumination**

Enb = endocarp *b* CWB = carpel wall vascular bundle LDZ = lignified dehiscence zone cells Me = mesocarp VB = vascular bundle

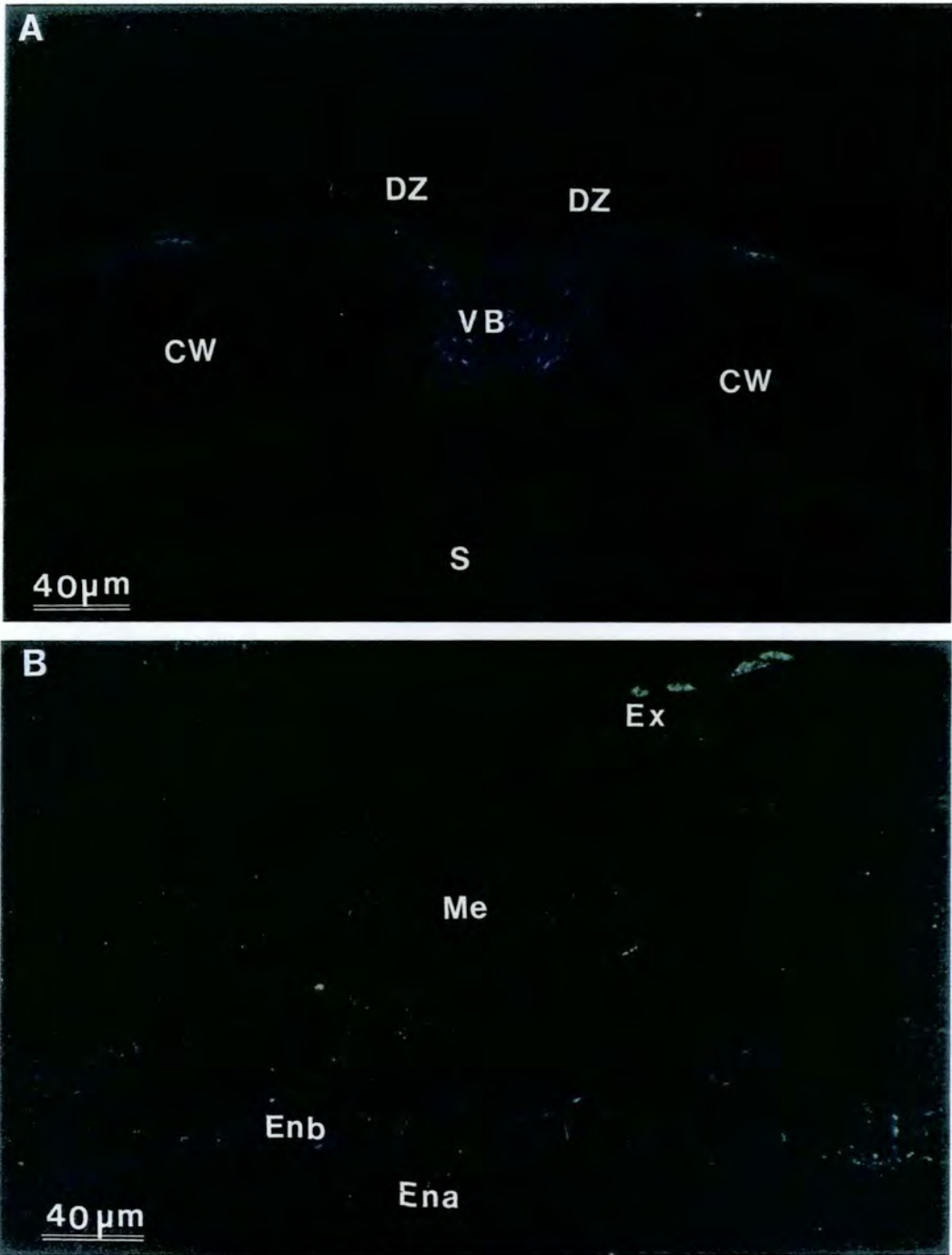


Figure 41. Control sections to JIM13 incubated in pre-immune rat serum

A) Non specific labelling in the dehiscence zones of mature *Arabidopsis* siliques

B) Non specific labelling in the carpel walls of mature *Brassica juncea* siliques

DZ = dehiscence zone, CW = carpel wall, Ena = endocarp *a*, Enb = endocarp *b*, Ex = exocarp, Me = mesocarp, S = septum, VB = vascular bundle

3.6.1.1. JIM13 binding in *Arabidopsis* and *Brassica juncea*

Previous work in this laboratory showed binding of the JIM13 antibody to the thickened, dehiscence zone cells (Fig. 38a) and thickened endocarp (*Enb*) cells (Fig 38b) of the mature *Arabidopsis* silique. Binding was detected in the last stages of silique development (stages 8-10) after the endocarp and dehiscence zone cells had thickened considerably, and just prior to and during desiccation. JIM13 binding has also been localised to the thickened dehiscence zone cells (Fig 39a), and thickened endocarp tissues of the *Brassica juncea* silique (Fig 39b). The pattern of JIM13 binding appears to be similar in both the *Arabidopsis* and *Brassica juncea* siliques and was localised to the thickening cells of the carpel wall and dehiscence zones of the fruit in both species.

3.6.1.2. JIM13 binding in Indian mustard

The pattern of JIM13 binding in the mature fruits of Indian mustard, a non-dehiscing variety of *Brassica juncea*, was different to that detected in the mature fruits of *Arabidopsis*. Figure 40a shows the extent of JIM13 binding in the lignified cells of the dehiscence zone, in a desiccating, mature Indian mustard silique. Immunolabelling extended to include at least seven or eight rows of cells. The lignified endocarp also showed strong binding, and it is obvious, from Figures 40a and 40b, that binding is to the cell plasmalemma, which is indicated by arrows, as well as to the cell walls of both these cell types. The mesocarp cells which are adjacent to the endocarp in Indian mustard siliques showed evidence of lignification in toluidine blue and acridine orange sections (Fig 33b and 34a respectively). JIM13 binding was also detected in these lignifying mesocarp cells of desiccating, mature Indian mustard siliques, and the signal was especially strong in those mesocarp cells immediately adjacent to the lignified endocarp and also those adjacent to the vascular bundles (Fig. 40c).

3.6.1.3. Localisation of JIM13 binding in endocarp *b* cells of *Arabidopsis*

Ultrastructural localisations of JIM13 was performed on LR White embedded, semi-thin tissue sections, using gold conjugated to a secondary antibody. Localisations were detected as black spots on the sections which were absent from control sections (Fig. 43). Grids were incubated overnight at 4°C in a 1:5 dilution of the antiserum. The JIM13 antigen was detected in the cell wall and in the cell plasmalemma of the thickened

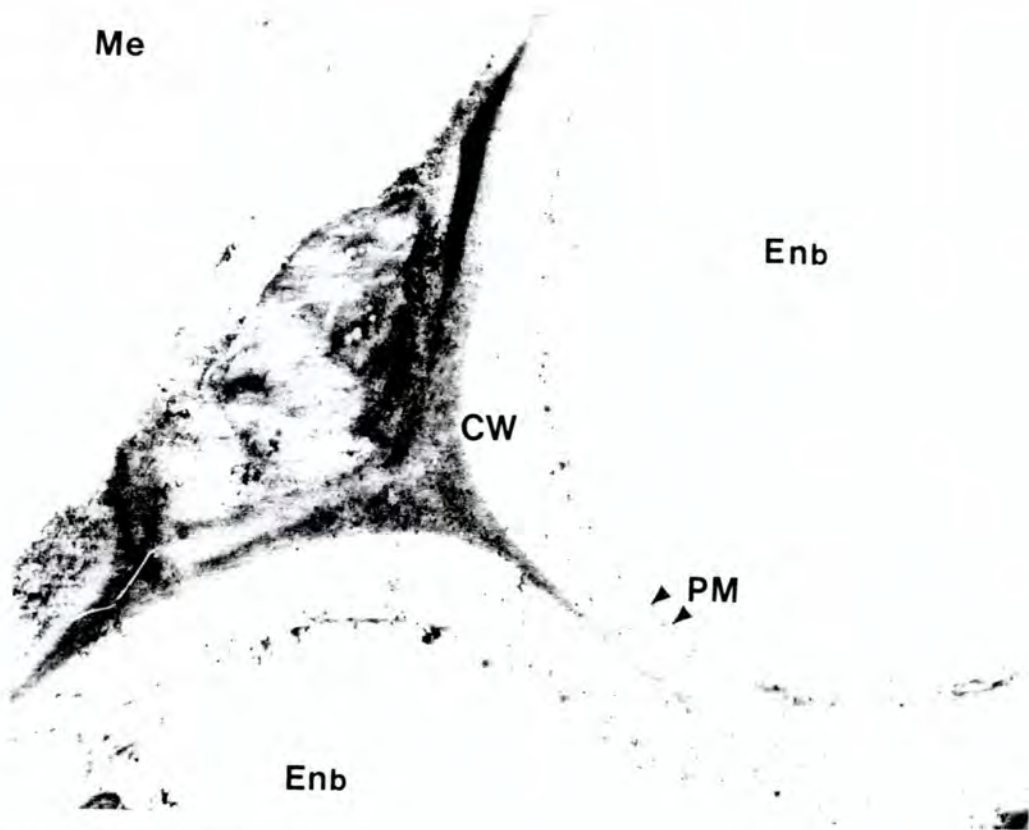


Figure 42. Transmission electron micrograph showing the localisation of JIM13 in the endocarp cells of the mature *Arabidopsis* silique (X 10,000)

CW = cell wall, Enb = endocarp *b* cell, ME = mesocarp cell, PM = plasma membrane, V = vacuole

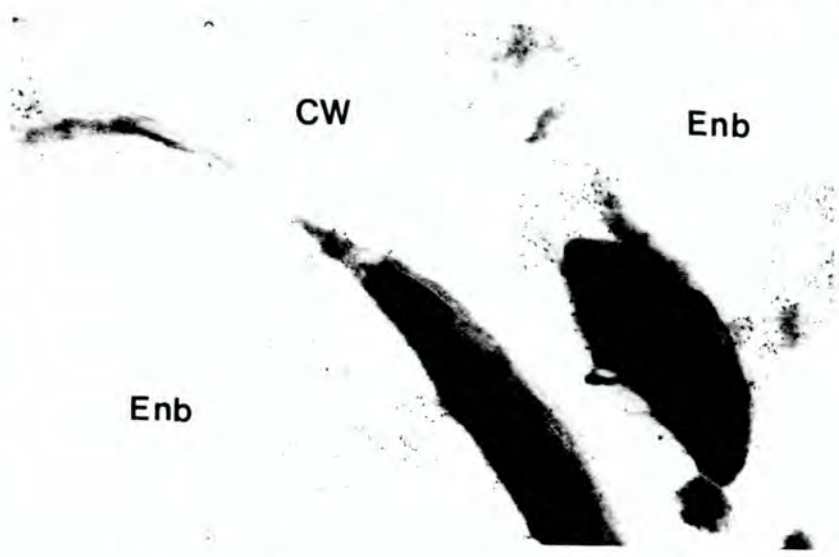


Figure 43. Control section incubated in pre-immune rat serum (X 10,000)

CW = cell wall, Enb = endocarp *b* cell

endocarp cells. As Figure 42 shows, the JIM13 antigen seems to be evenly distributed throughout the thickened layers of the cell wall. JIM13 binding was also present in quite high amounts on the inner surface of the cell wall adjacent to the plasma membrane (Fig. 42) and on the surface of the plasmalemma.

3.6.2. Localisation of JIM5 binding

The anti-polygalacturonic acid antibody JIM5, which recognises epitopes of un-esterified pectin, and the JIM7 antibody which recognises epitopes of methyl-esterified pectin, have been used to determine the spatial distribution of these two different pectins in the plant cell walls of a number of plant species. The distribution of these two types of pectin varies in the cell wall between different plant species and between different tissue types (Knox *et al.* 1990).

The monoclonal AGP antibody JIM5 was raised in rat from cell isolates of *Daucus carotta* root (Knox *et al.* 1989, 1990, Pennell *et al.* 1989, Stacey *et al.* 1990) and kindly supplied by the John Innes Institute. The antiserum was supplied as a hybridoma culture supernatant with 0.02% sodium azide and sections were incubated overnight at 4°C in a 1:10 dilution of the antiserum.

JIM5 binding was detected on LR White embedded semi-thin tissue sections, using gold conjugated to a secondary antibody. Colloidal gold was silver enhanced and specific localisations were detected as either, black/brown deposits under bright field or differential interference contrast (DIC) illumination, or as bright silver/gold deposits on a dark background, under epi-polarising illumination. Control sections of *Arabidopsis* and Indian mustard which were incubated in buffered 1% pre-immune rat serum, showed no specific binding (Fig. 47).

3.6.2.1. Localisation of JIM5 binding in young *Brassica* fruits

JIM5 binding was localised to the cell walls and cell wall junctions in all of the tissue types in the young fruits of *Arabidopsis* (developmental stage 6) and the young fruits of *Brassica juncea*. Figures 44a and 44b show JIM5 binding in the carpel margins and replar bundles of young *Arabidopsis* and *Brassica juncea* siliques respectively. Although binding is detected in the cell walls of all of the tissues of the young siliques, as can be seen in both

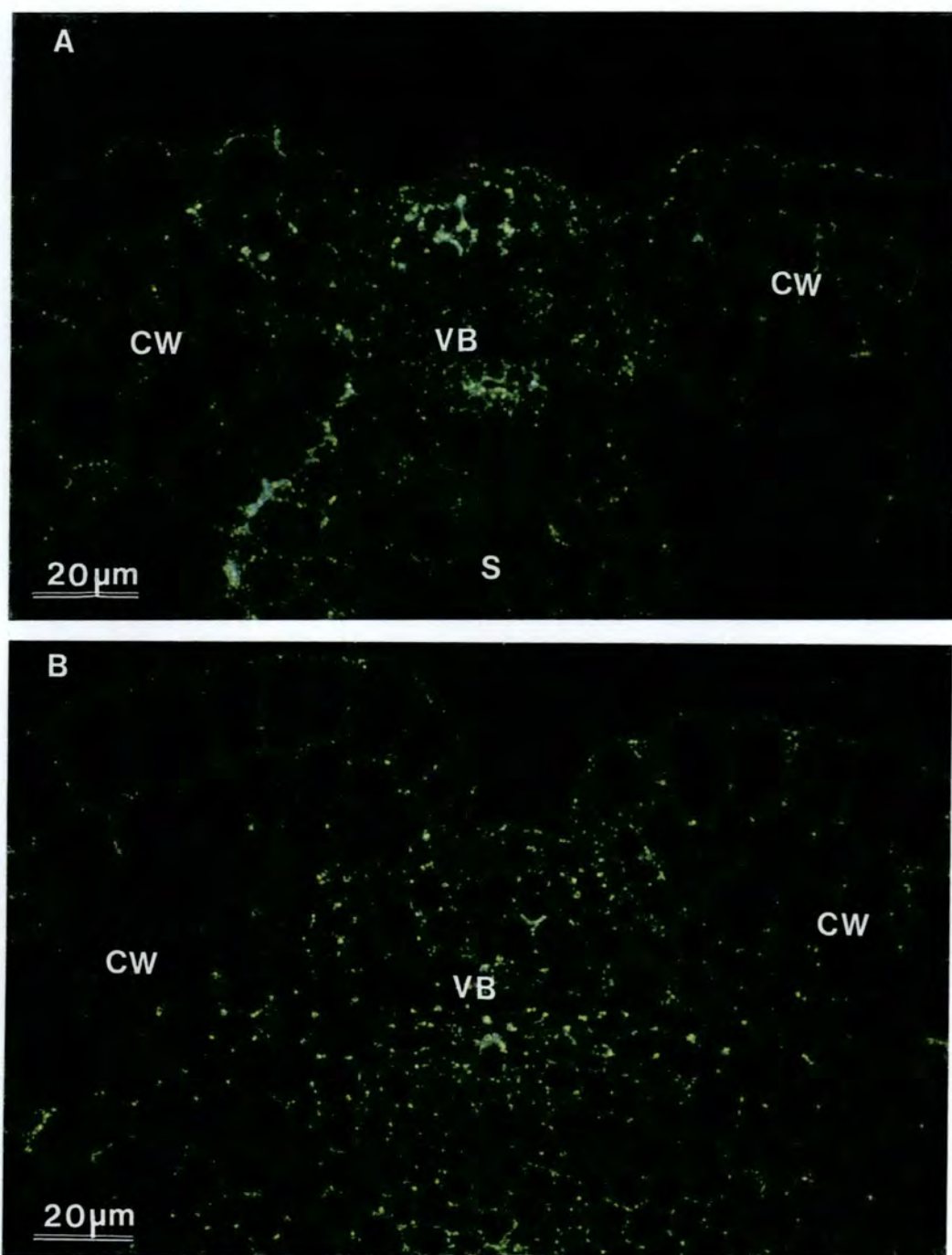


Figure 44. Localisation of JIM5 binding in young Brassica fruits

A) Immunolabelling of the carpel margins in *Arabidopsis* siliques, epipolarising illumination

B) Immunolabelling of the carpel margins in *Brassica juncea* siliques, epipolarising illumination

CW = carpel wall, S = septum, VB = vascular bundle

Figure 44a and 44b, binding is the strongest in cells above and below the replar vascular bundles, in the septum, and in a few rows of mesocarp cells at the carpel margins. Binding appears to be in the cell wall junctions in both the vascular bundle and carpel margin tissues. JIM5 binding in the septum was the strongest in the cell walls which form the inner lining of the septum and which are adjacent to the transmitting tissue (Fig. 44a).

JIM5 binding was detected in the cell walls of the exocarp, mesocarp and both endocarp layers of the carpel wall in the young siliques of *Arabidopsis* and *Brassica juncea*. As Figures 45a and 45b show, binding is the strongest in the outer tangential walls and cell junctions of the exocarp and in the cell junctions of the mesocarp cells.

3.6.2.2. Localisation of JIM5 binding in mature *Brassica* fruits

JIM5 binding was localised to the dehiscence zones and carpel walls of mature *Arabidopsis* (developmental stage 8) and mature *Brassica juncea* fruits. Binding in the dehiscence zones of both fruits was localised to the cell junctions of the lignified dehiscence zone cells (results not shown). Binding in the dehiscence zone was much reduced in the mature silique when compared to the young silique.

JIM5 binding was detected in the cell walls of the exocarp mesocarp and *Ena* layers of the carpel wall in mature *Arabidopsis* and *Brassica juncea* fruits. The pattern of JIM5 binding in the mature carpel wall tissues of *Arabidopsis* and *Brassica juncea* is different to the pattern of binding in the young carpel wall tissues. Figure 46a shows increased JIM5 binding in the outer tangential walls and cell wall junctions of the exocarp but reduced binding in the cell walls and cell wall junctions of the mesocarp. As Figures 46a and 46b show there is no binding in the lignified *Enb* layer in the mature carpel walls of either *Arabidopsis* or *Brassica juncea* fruits. Figures 46a and 46b show binding of JIM5 to the endocarp of mature *Arabidopsis* and *Brassica juncea* fruits respectively. Binding is restricted to *Ena* and stronger than that detected in the young fruits. JIM5 binding in *Ena* cells is the strongest in the tangential walls which are adjacent to *Enb*.

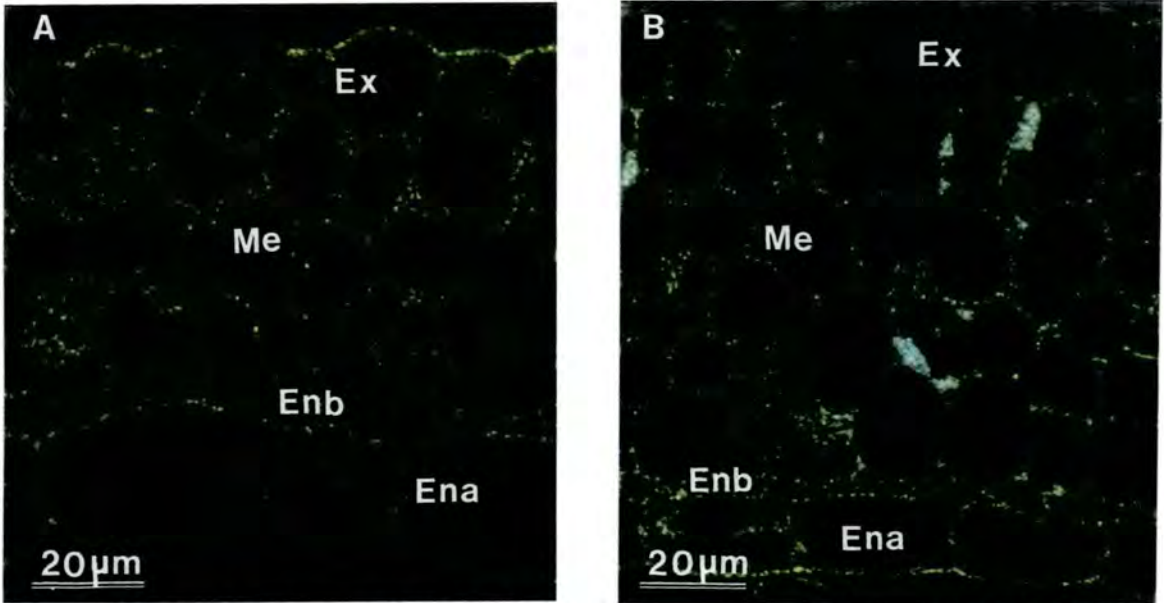


Figure 45. Localisation of JIM5 binding in the carpel walls of young Brassica fruits

- A) Immunolabelling of the carpel wall in *Arabidopsis* siliques, epi-polarising illumination
 B) Immunolabelling of the carpel wall in *Brassica juncea* siliques, epi-polarising illumination

Ena = endocarp *a*, Enb = endocarp *b*, Ex = exocarp, Me = mesocarp

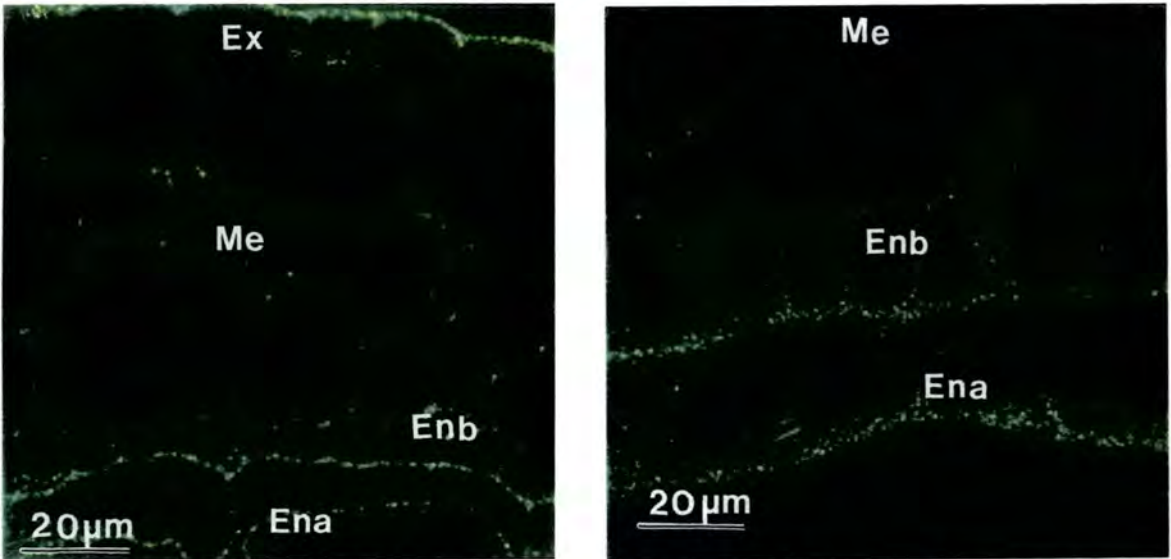


Figure 46 Localisation of JIM5 binding in the carpel walls of mature Brassica fruits

- A) Immunolabelling of the carpel wall in *Arabidopsis* siliques, epi-polarising illumination
 B) immunolabelling of the carpel walls in *Brassica juncea* siliques, epi-polarising illumination

Ena = endocarp *a*, Enb = endocarp *b*, Ex = exocarp, Me = mesocarp

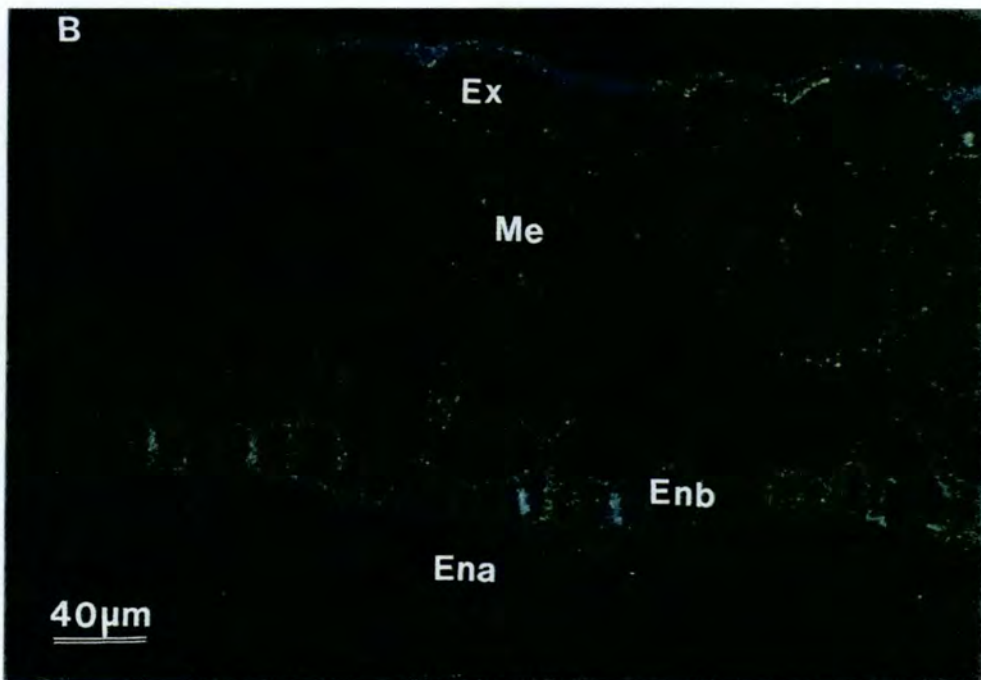
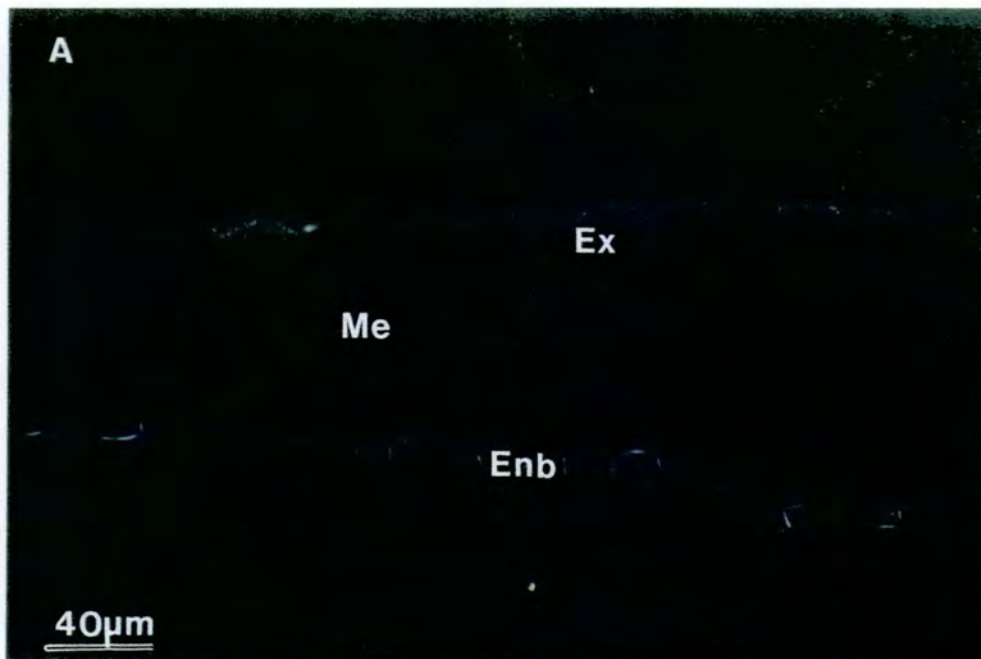


Figure 47. Control sections to JIM5 incubated in pre-immune rat serum

A) Non specific labelling in the carpel walls of mature *Arabidopsis* siliques

B) Non specific labelling in the carpel walls of mature *Brassica juncea* siliques

Ena = endocarp *a*, Enb = endocarp *b*, Ex = exocarp, Me = mesocarp

3.6.2.3. Localisation of JIM5 binding in the cell walls of mature *Arabidopsis* carpel tissues

Ultrastructural localisations of JIM5 were performed on LR White embedded, semi-thin tissue sections, using gold conjugated to a secondary antibody. Localisations were detected as black spots on the sections which were absent from control sections (Fig. 52). Grids were incubated overnight at 4°C in a 1:10 dilution of the antiserum. The JIM5 antigen showed specific localisations within the cell walls of the exocarp, mesocarp and endocarp layers of the carpel wall. In the exocarp JIM5 binding was the strongest in the mature silique and Figure 48 shows binding of JIM5 to the walls of mature exocarp cells. JIM5 was detected throughout the cell wall in the exocarp cells however, as can be seen in Figure 48 binding is stronger in the outer surface of the cell walls adjacent to the waxy cuticular layer, and in the intercellular spaces between the cells of the exocarp. In the mesocarp cell walls binding was the strongest in the young silique and Figure 49 shows JIM5 binding in the cell walls of young mesocarp cells. Binding can be detected throughout the cell wall but is strongest in the inner surface of the cell wall adjacent to the plasmalemma and also in the middle lamella.

JIM5 showed differential binding in the cell walls of the endocarp. JIM5 binding in the cell walls of *Enb* in the young silique was similar to that observed in the mesocarp (results not shown). Binding to the cell walls of *Ena* in the young silique is shown in Figure 50. Binding was detected in the inner surface of the cell wall adjacent to the plasmalemma and also in the middle lamella. As can be seen in Figure 50 binding is the strongest in the intercellular spaces between *Ena* cells and in the outer surface of the walls which line the locule.

In the mature silique JIM5 binding was weak and appeared non specific in the cell walls of *Enb*, however binding is stronger in the cell walls of *Ena* cells when compared to the young silique. Binding increases in outer surface of the walls which line the locule (results not shown) and as Figure 51 shows there is very strong binding the cell walls of *Ena* which are adjacent to *Enb*. Binding can be seen throughout the layers of this cell wall and also in the intercellular spaces between *Ena* and *Enb* cells.

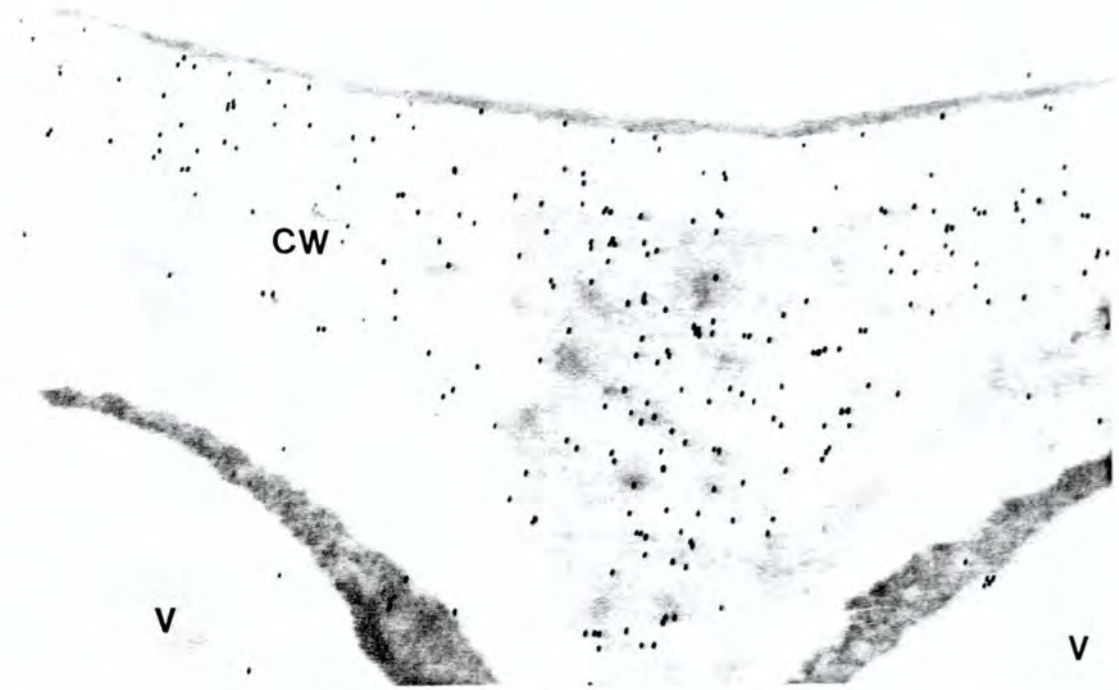


Figure 48. Transmission electron micrograph showing the localisation of JIM5 in the exocarp cell wall of mature *Arabidopsis* fruits (X 13,000)

CW = cell wall, V = vacuole

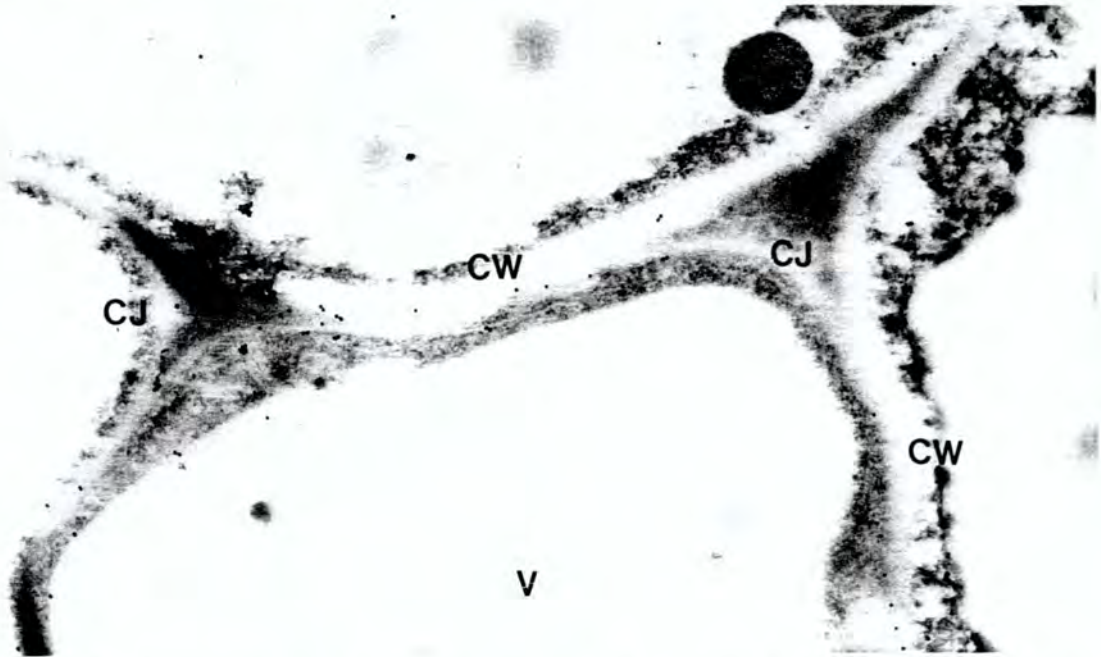


Figure 49. Transmission electron micrograph showing the localisation of JIM5 in the mesocarp cell walls of young *Arabidopsis* fruits (X 10,000)

CJ = cell wall junction, CW = cell wall, V = vacuole

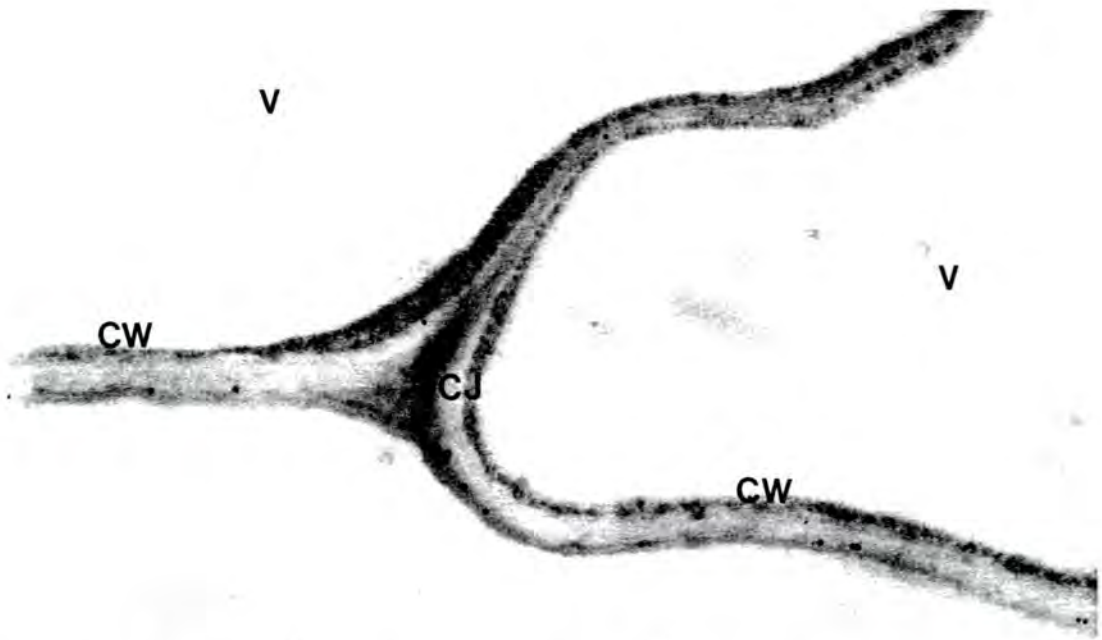


Figure 50. Transmission electron micrograph showing the localisation of JIM5 in the locule wall of endocarp *a* cells in young *Arabidopsis* fruits (X 13,000)

CJ = cell wall junction, CW = cell wall, V = vacuole

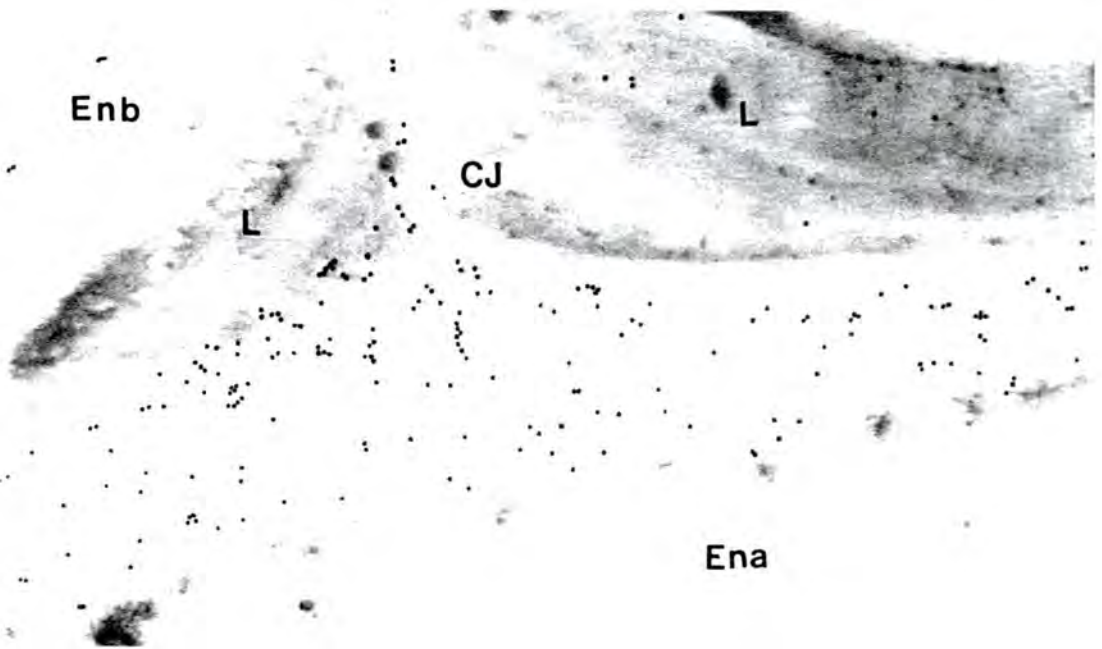


Figure 51. Transmission electron micrograph showing the localisation of JIM5 in the cell wall junctions of endocarp *a* and endocarp *b* cells in mature *Arabidopsis* fruits (X 13,000)

CJ = cell wall junction, Ena = endocarp *a* cell, Enb = endocarp *b* cell, L = lignified cell wall

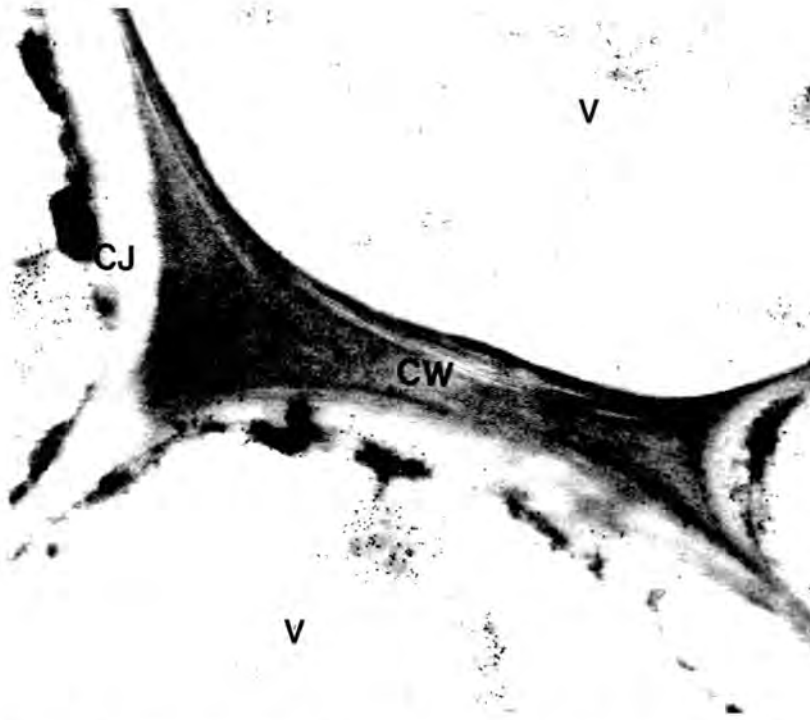


Figure 52. Control section incubated in pre-immune rat serum (X 10,000)

CW = cell wall, CJ = cell wall junction, V = vacuole

3.6.3. Localisation of JIM7 binding

JIM7 was not detected above background levels on sections from wax or LR White embedded tissues (results not shown).

3.7. MOLECULAR HISTOCHEMISTRY OF THE SILIQUE

3.7.1. Localisation of SAC25 mRNA

SAC25 was isolated from a cDNA library constructed from the dehiscence zones of developing *Brassica napus* pods (Coupe *et al.* 1994b). The clone has a transcript size of 1100 nucleotides and does not show significant homology to anything previously identified, however there is a similarity in the amino acid motifs to known dehydrogenases and it has been suggested that SAC25 may be a dehydrogenase. Northern blot analysis showed SAC25 mRNA was present in silique tissues but only at low levels 20DAA, and increased up to a maximum at 50-60DAA. pSAC25 was kindly donated by Dr. S Coupe. This consists of 1.1Kb of coding sequence cloned into the EcoR1, Xho1 sites of pBS+. pSAC25 was cut using EcoR1 and Xho1 restriction enzymes and sense and antisense Riboprobes were generated from the T3 and T7 promoters on either side of the insert.

In-situ hybridisations did not produce consistent results when performed on wax embedded tissues from *Arabidopsis*, *Brassica juncea* or *Brassica napus*, using digoxigenin-labelled Riboprobes generated from pSAC25 (Results not shown).

3.7.2. Localisation of SAC51 mRNA

SAC51 was isolated from a cDNA library constructed from the dehiscence zones of developing *Brassica napus* pods (Coupe *et al.* 1994a). The clone has a transcript size of about 700 nucleotides and the predicted polypeptide shows sequence identity to other proteins of unknown function in carrots, tomatoes, maize and soybean. Northern blot analysis showed the mRNA was present in small amounts in non-zone and dehiscence zone tissues 20 DAA, however by 60 DAA, the transcript was only detected in zone tissues and was present in larger amounts. pSAC51 was kindly donated by Dr. S Coupe. This consists of 0.8Kb of coding sequence cloned into the EcoR1, Xho1 sites of pBS+. pSAC51 was cut using EcoR1 and Xho1 restriction enzymes and sense and antisense riboprobes were generated from the T3 and T7 promoters on either side of the insert.

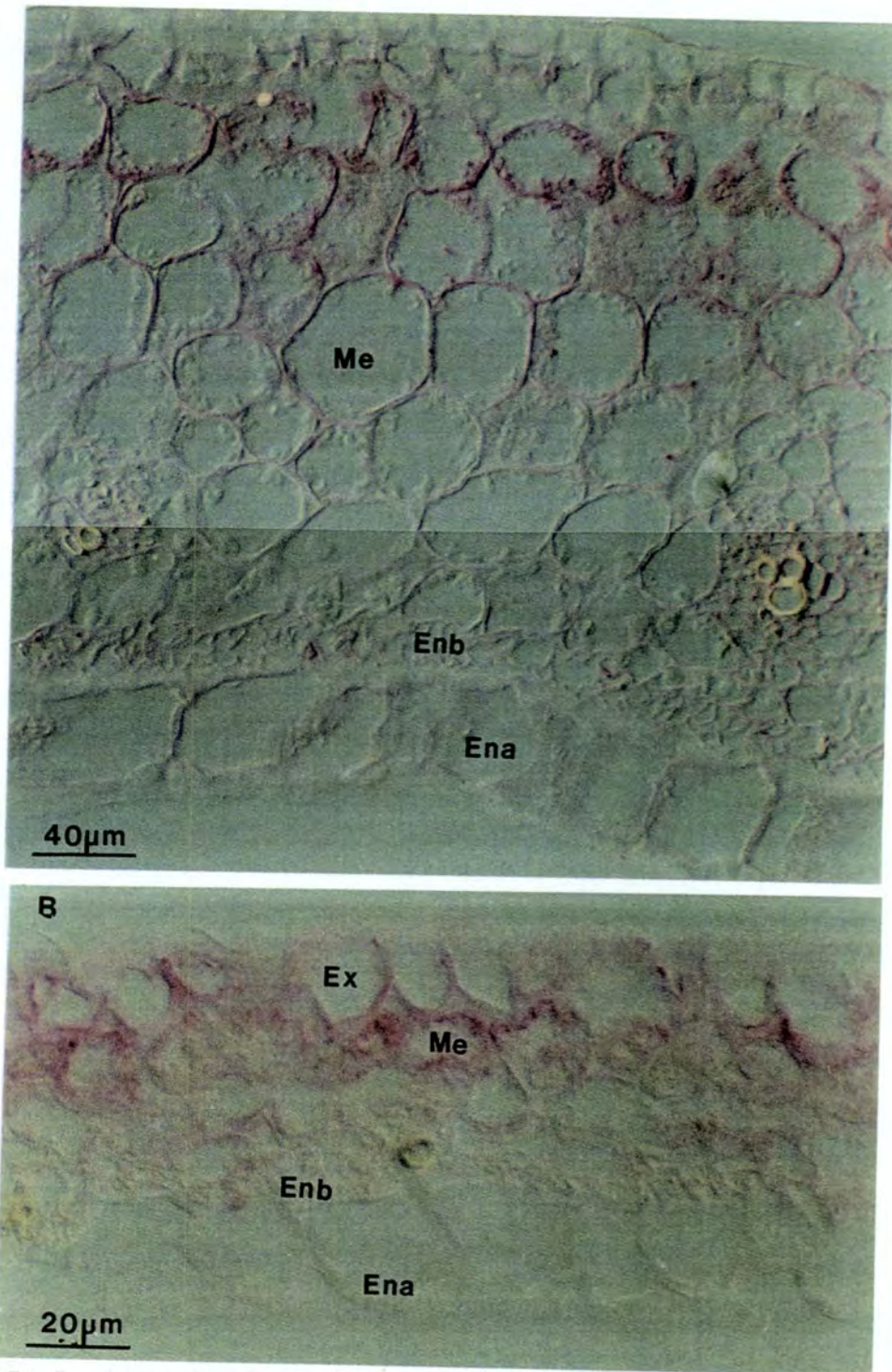


Figure 53. *In-situ* localisation of SAC51 mRNA in the carpel walls of young *Brassica* fruits

- A) Localisation of SAC51 mRNA in the carpel walls of young *Brassica napus* fruits
- B) Localisation of SAC51 mRNA in the carpel walls of young *Arabidopsis* fruits

Ena = endocarp a, Enb = endocarp b, Ex = exocarp, Me = mesocarp

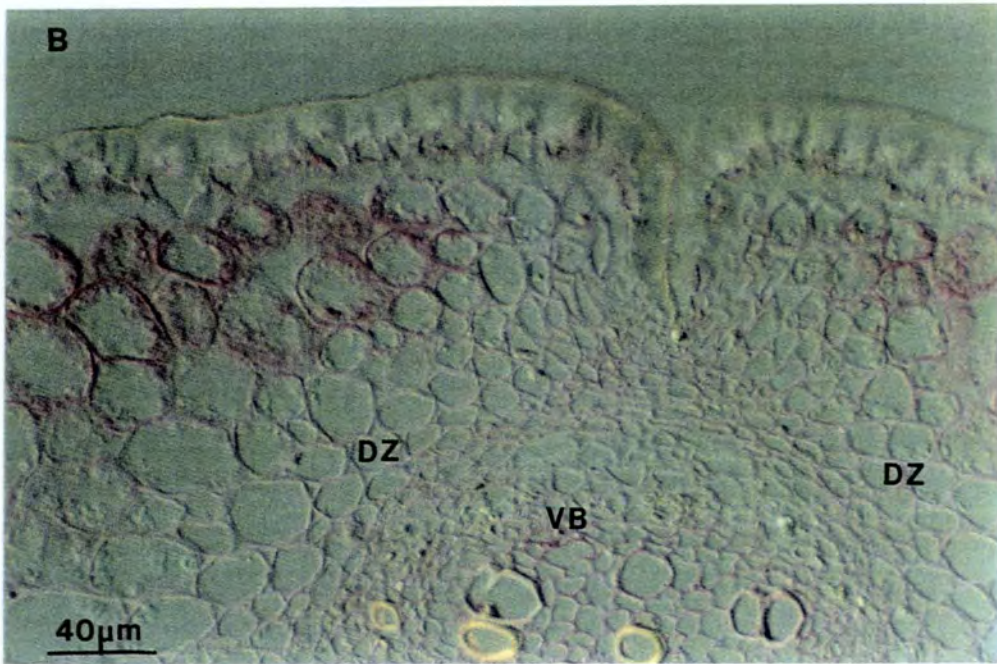
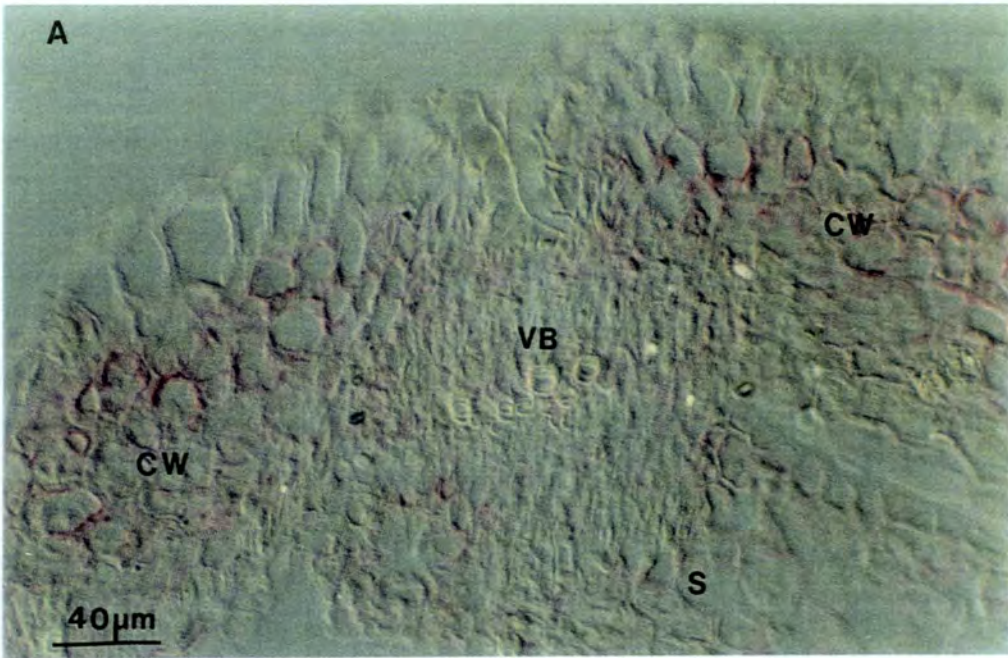


Figure 54. *In-situ* localisation of SAC51 mRNA in the dehiscence zones of young *Brassica* fruits

A) Localisation of SAC51 mRNA in the dehiscence zones of young *Brassica juncea* fruit

B) Localisation of SAC51 mRNA in the dehiscence zones of young *Brassica napus* fruit

CW = carpel wall, DZ = dehiscence zone, S = septum, VB = vascular bundle

SAC51 mRNA was detected on sections from wax embedded tissues of *Arabidopsis*, *Brassica napus* and *Brassica juncea* by hybridisation of the digoxigenin-labelled riboprobes. Bound probe was localised by an antidigoxigenin antibody conjugated to alkaline phosphatase, which was then detected histochemically as red deposits which were absent from control sections. Control sections of *Arabidopsis*, *Brassica napus* and *Brassica juncea* were incubated with the sense riboprobe. No staining was seen in control sections from all three *Brassic*as and Figure 57 shows an example of control sections from *Arabidopsis* and *Brassica juncea*.

3.7.2.1. Localisation of SAC51 mRNA in young *Brassica* fruits

SAC51 mRNA was localised to the carpel walls of young *Arabidopsis*, *Brassica juncea* and *Brassica napus* fruits during developmental stages six and seven, and a similar pattern of staining was observed in the three species examined. Staining in the carpel wall was restricted to the exocarp and mesocarp cell layers in young fruits, although staining in the exocarp was usually much less intense than that observed in the mesocarp (Figs. 53A from *Brassica napus* and 53b from *Arabidopsis*). As can be seen in Figures 53a and 53b, there is also a differential pattern of staining within the mesocarp cell layers. Much more intense staining was observed in the mesocarp cells which are adjacent to the exocarp, whilst those adjacent to the endocarp showed only very weak staining in the earliest post fertilisation stage or no staining at all.

Staining in the dehiscence zones of young fruits was only observed during stage six of development. Figure 54a shows a young *Brassica juncea* fruit in which weak staining can be seen extending through the mesocarp up to the putative separation layer. As can be seen in Figure 54b from *Brassica napus*, there is no staining in the dehiscence zone after developmental stage seven when the dehiscence zone cells have started to thicken.

3.7.2.2. Localisation of SAC51 mRNA in mature *Brassica* fruits

SAC51 mRNA was localised to the carpel walls of mature *Brassica* fruits during developmental stages eight to ten, and a similar pattern of staining was observed in the three species examined. Staining in the carpel wall was restricted to the mesocarp layers, no staining was observed in the exocarp or endocarp layers (Figs. 55a from *Arabidopsis* and 55b from *Brassica juncea*). Staining in the mesocarp of mature fruits was restricted to

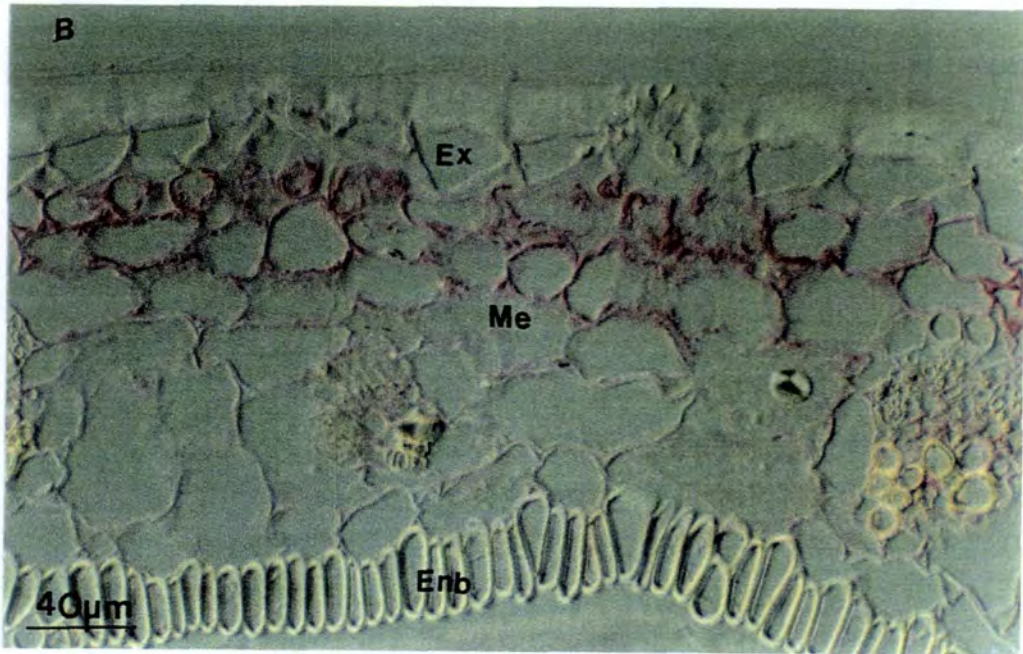
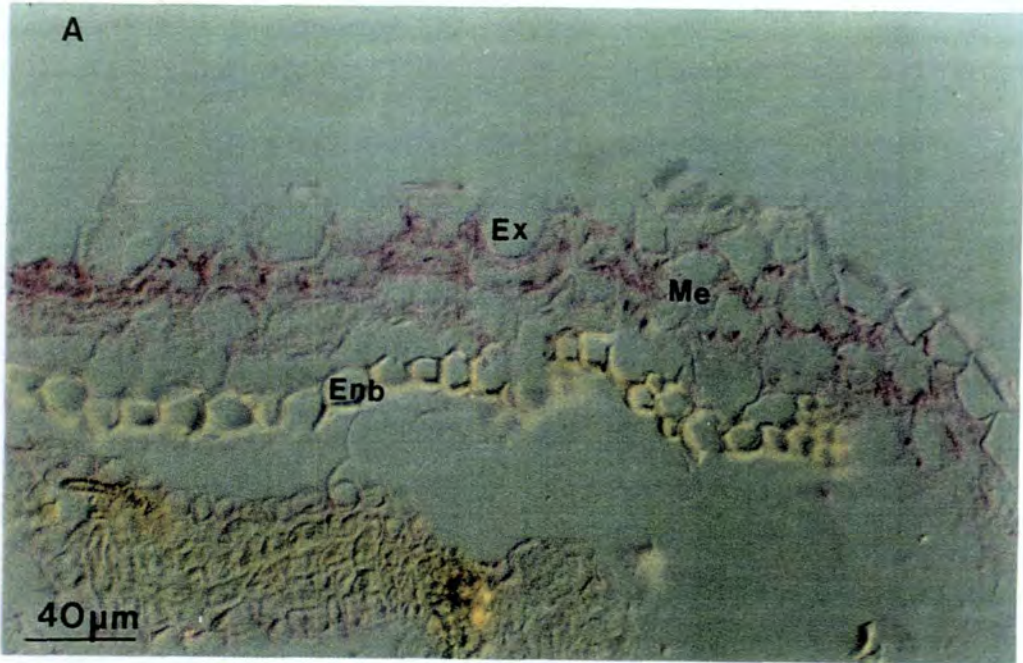


Figure 55. *In-situ* localisation of SAC51 mRNA in the carpel walls of mature *Brassica* fruits

A) Localisation of SAC51 mRNA in the carpel walls of mature *Arabidopsis* fruit

B) Localisation of SAC51 mRNA in the carpel walls of mature *Brassica juncea* fruit

Ena = endocarp a, Enb = endocarp b, Ex = exocarp, Me = mesocarp

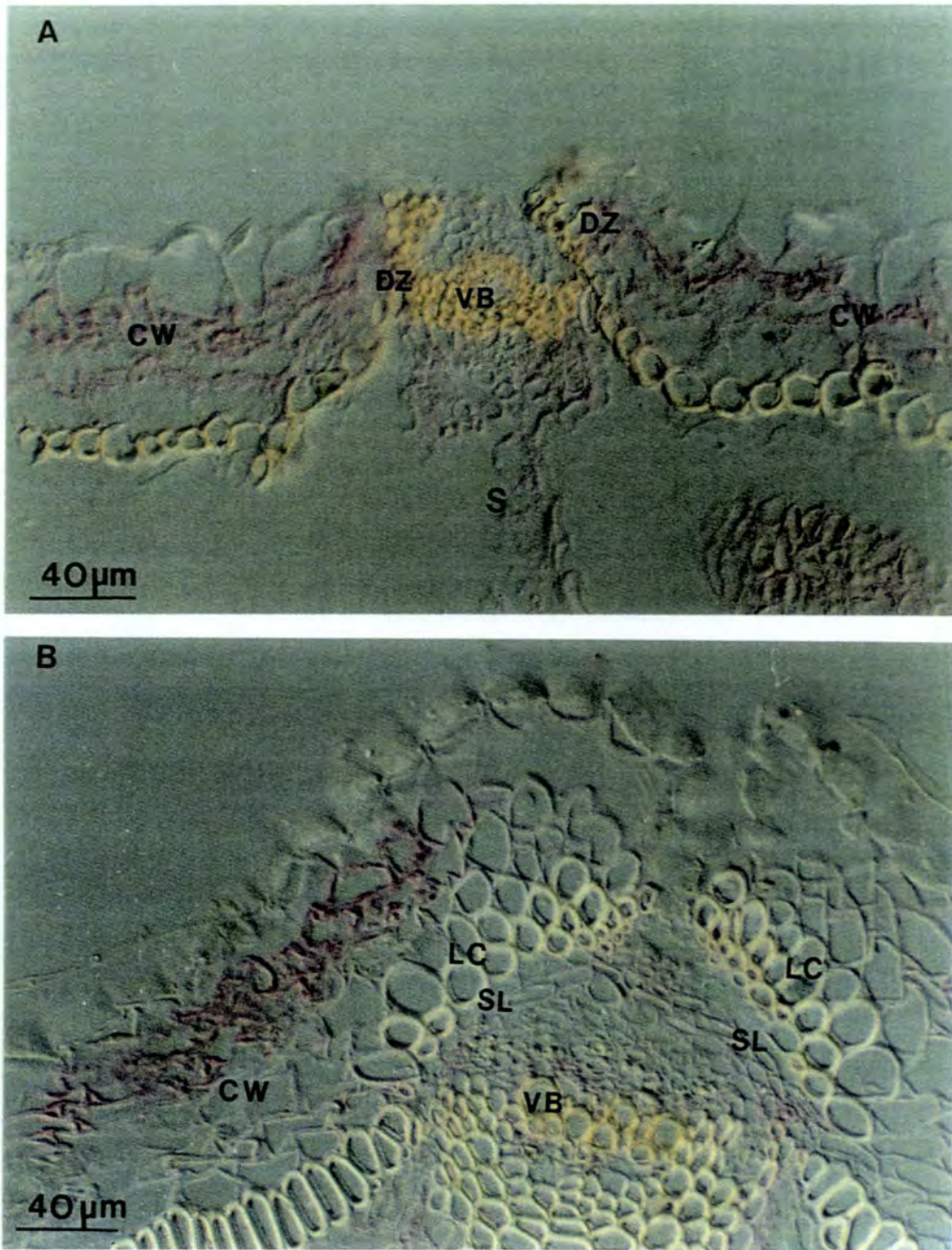


Figure 56. *In-situ* localisation of SAC51 mRNA in the dehiscence zones of mature *Brassica* fruits

A) Localisation of SAC51 mRNA in the dehiscence zones of mature *Arabidopsis* fruit

B) Localisation of SAC51 mRNA in the dehiscence zones of mature *Brassica juncea* fruit

CW = carpel wall, DZ = dehiscence zone, LC = lignified dehiscence zone cell, S = septum, SL = separation layer cell, VB = vascular bundle

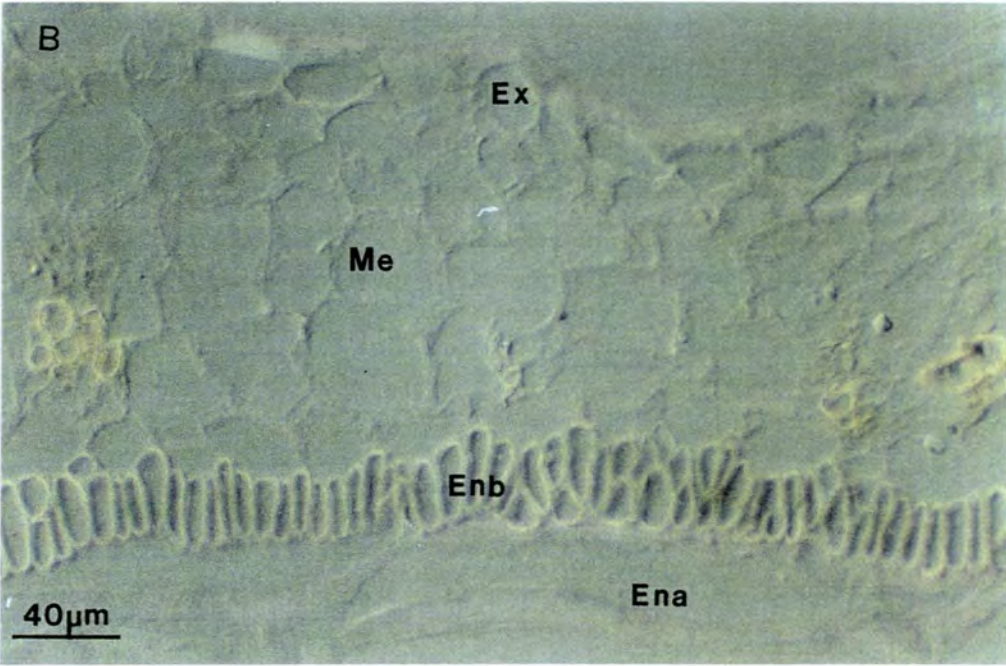
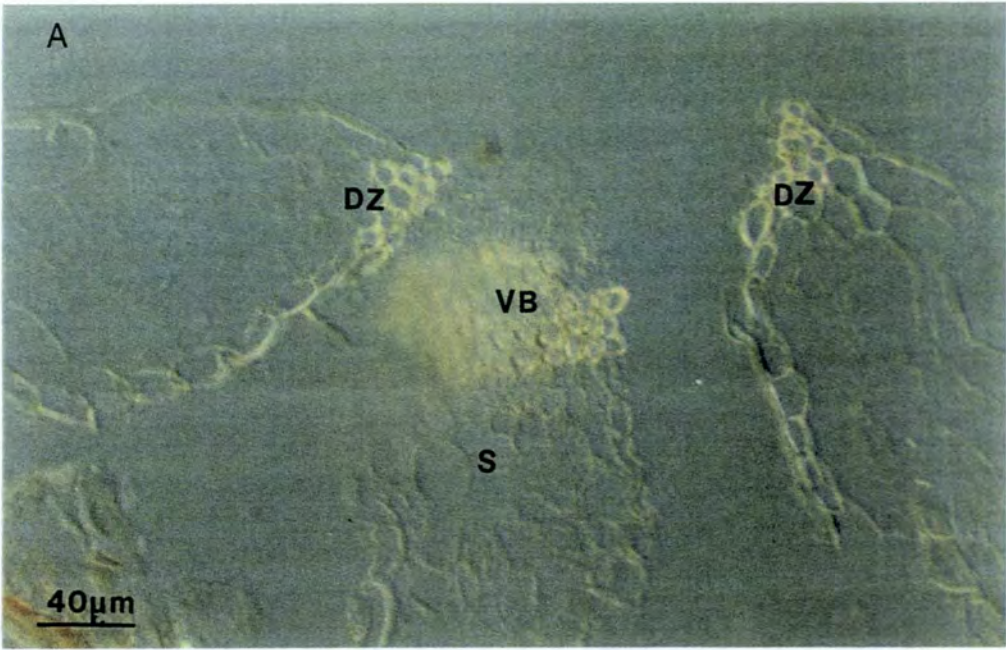


Figure 57. Control sections incubated with SAC51 sense riboprobe

- A) No specific staining in the dehiscence zones of mature *Arabidopsis* siliques**
- B) No specific staining in the carpel walls of *Brassica juncea* siliques**

DZ = dehiscence zone, Ena = endocarp a, Enb = endocarp b, Ex = exocarp, S = septum, VB = vascular bundle

the two or three layers of cells which are adjacent to the exocarp, no staining was observed in other mesocarp cells within the carpel wall. Staining in the mesocarp cells of the mature fruits was more intense than that observed in the young fruits. Although the staining in the mesocarp extends up to the lignified, dehiscence zone cells as can be seen in Figures 56a and 56b from *Arabidopsis* and *Brassica juncea* respectively; no staining was observed in any the dehiscence zone cells of mature fruits during stages eight to ten.

3.7.3. Localisation of Oilseed rape extensin (*ExtA*)

The *Brassica napus* extensin gene *ExtA* was isolated from a cDNA library constructed from mRNA from *Brassica napus* roots (Evans *et al.* 1990). The clone has a transcript size of about 1300 nucleotides and the encoded protein shows homology to a number of extensins in other species. The *ExtA* gene has been shown to be highly expressed in the phloem tissues of *Brassica napus* root. pAS58 was kindly donated by Dr. A. Shirsat. This consists of 1Kb of coding sequence cloned into the Hind III, EcoR1 sites of pSK+. pAS58 was cut using Hind III and EcoR1 restriction enzymes and sense and antisense riboprobes were generated from the T3 and T7 promoters on either side of the insert.

ExtA mRNA was detected on sections from wax-embedded tissues of *Arabidopsis*, *Brassica napus* and *Brassica juncea* by hybridisation of the digoxigenin-labelled Riboprobes. Bound probe was localised by an antidigoxigenin antibody conjugated to alkaline phosphatase, which was then detected histochemically as red deposits which were absent from control sections. Control sections of *Arabidopsis*, *Brassica napus* and *Brassica juncea* were incubated with the sense riboprobe No staining was seen in control sections from all three *Brassic*as and Figure 61 shows an example of control sections from *Arabidopsis* and *Brassica juncea*.

3.7.3.1. Localisation of *ExtA* mRNA in young *Brassica* fruits

ExtA mRNA was localised to the cells of the carpel walls and to the replar and carpel wall vascular bundles of young *Brassica* fruits during developmental stages six and seven. Staining in sections from *Brassica napus* was either extremely weak or absent (results not shown). Staining in the carpel wall layers of *Arabidopsis* (Fig. 58b) and *Brassica juncea* (Fig. 58a) was restricted to the mesocarp cells and was very weak. Weak staining was also observed in the replar bundles and septum of young fruits and can be seen here in the

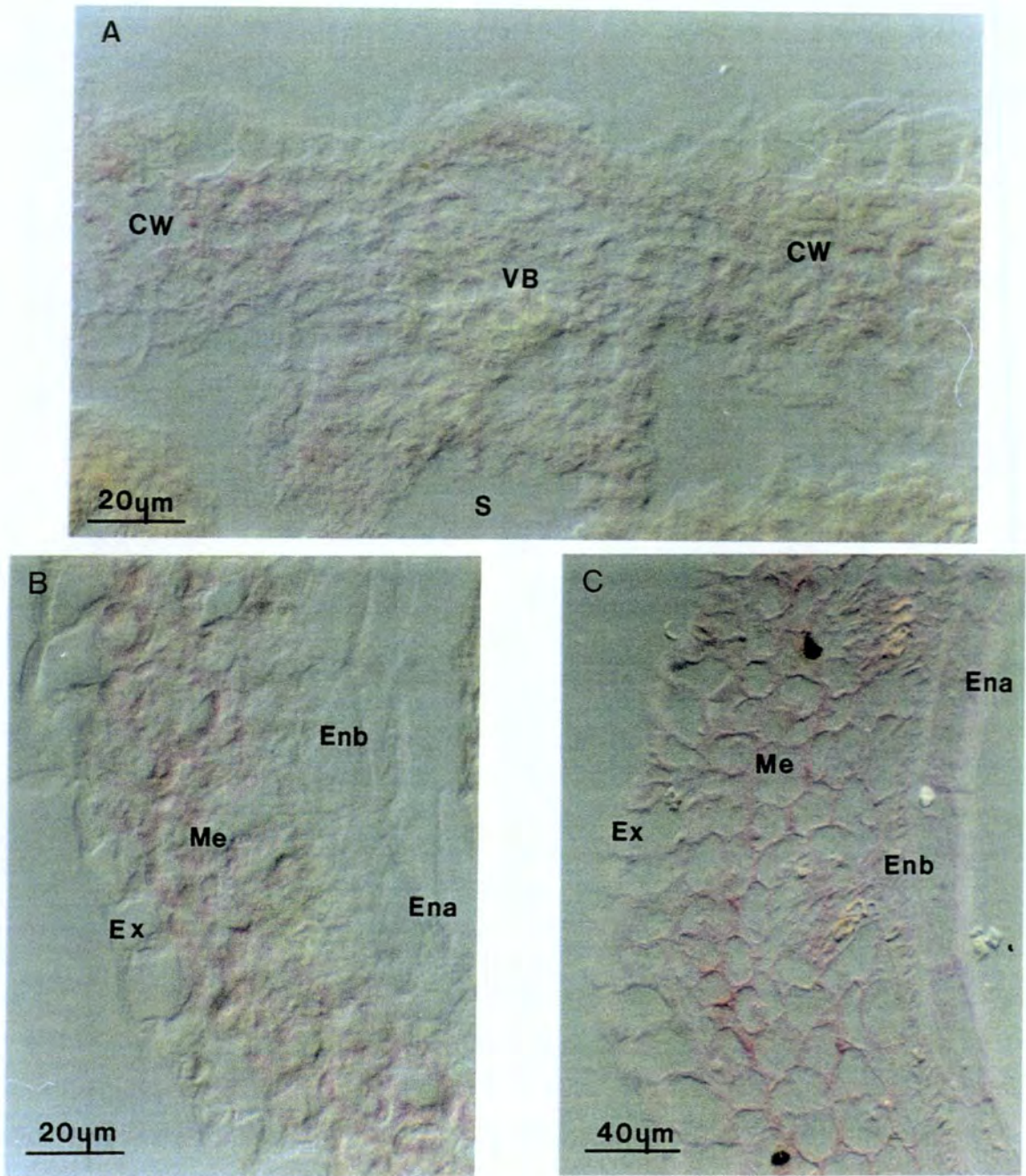


Figure 58. In-situ localisation of *ExtA* mRNA in young *Brassica* fruits

A) Localisation of *ExtA* mRNA in the dehiscence zones of young *Arabidopsis* fruit

B) Localisation of *ExtA* mRNA in the carpel wall of young *Arabidopsis* fruit

C) Localisation of *ExtA* mRNA in the carpel wall of young *Brassica juncea* fruit

CW = carpel wall, Ena = endocarp a, Enb = endocarp b, Ex = exocarp, Me = mesocarp, S = septum, VB = vascular bundle

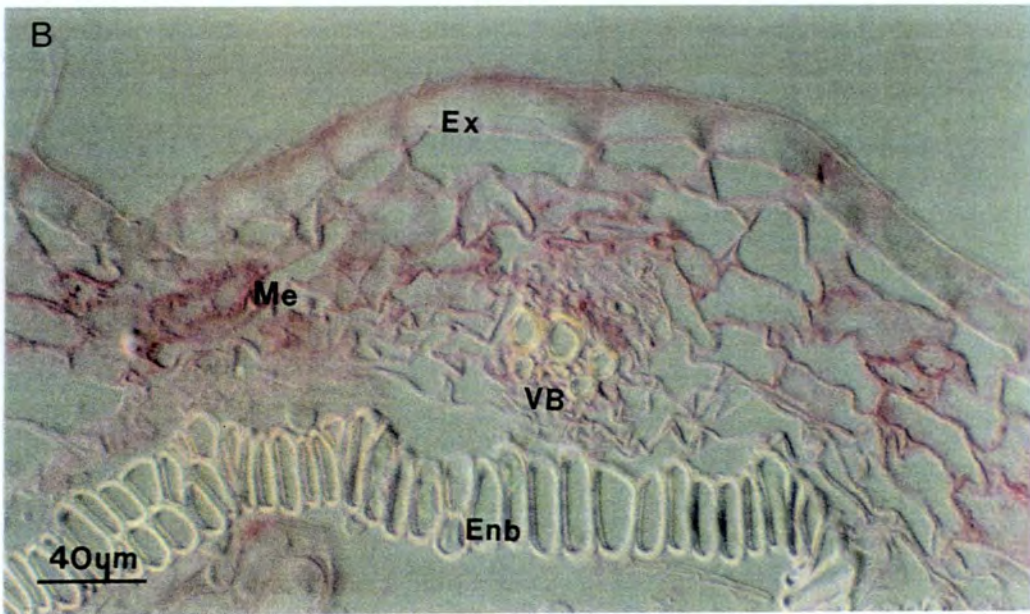
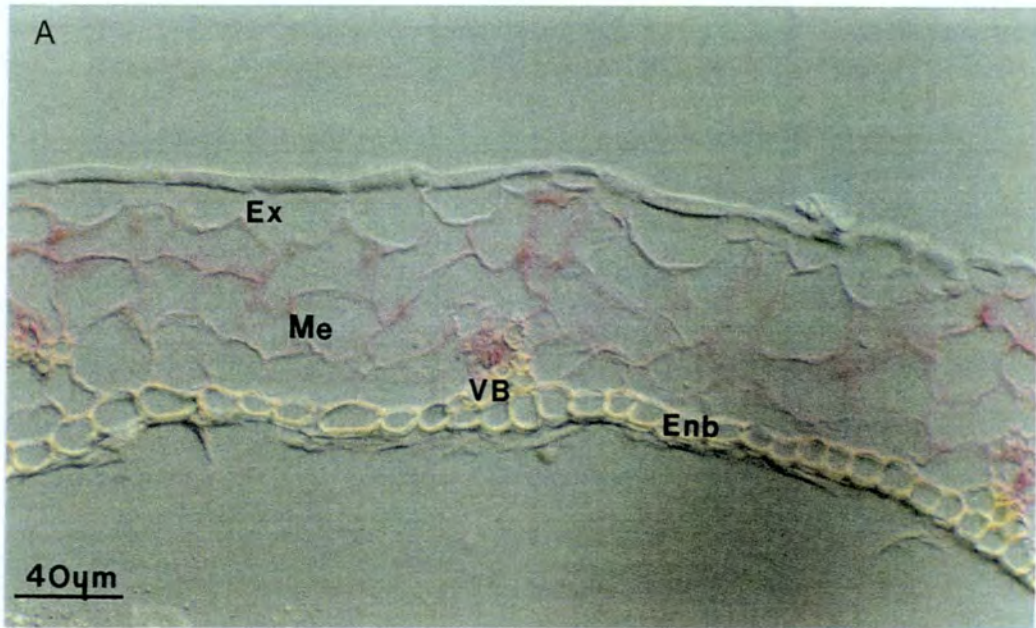


Figure 59. *In-situ* localisation of *ExtA* mRNA in the carpel walls of mature *Brassica* fruits

A) Localisation of *ExtA* mRNA in the carpel walls of mature *Arabidopsis* fruits

B) Localisation of *ExtA* mRNA in the carpel walls of mature *Brassica juncea* fruit

Enb = endocarp *b*, Ex = exocarp, Me = mesocarp, VB = vascular bundle

young *Arabidopsis* fruit in Figure 58a. Staining in the carpel wall vascular bundles in *Arabidopsis* and *Brassica juncea* was also very weak but can just be seen in Figure 58a.

3.7.3.2. Localisation of *ExtA* mRNA in mature *Brassica* fruits

ExtA mRNA was localised to the cells of the carpel walls and to the replar and carpel wall vascular bundles of mature *Brassica* fruits during developmental stages eight to ten. Staining in sections from *Brassica napus* was either extremely weak or absent (results not shown). Staining in the carpel wall cell layers was restricted to the mesocarp cells in *Arabidopsis* (Fig 59a) and *Brassica juncea* (Fig. 59b) and more intense staining was observed in the mesocarp of mature fruits than was observed in the mesocarp of young fruits. Staining intensity also increased in the carpel wall vascular bundles as can be seen in Figures 59a and 59b, and in the replar bundles (Figs. 60a and 60b), in mature *Arabidopsis* and *Brassica juncea* fruits. As can be seen in Figure 60c, staining in the mesocarp cell layer extends up to the lignified dehiscence zone cells and staining was usually quite intense in these carpel margin cells.

3.7.4. Pea Lignin Probe (pLP18)

pLP18 was isolated from a cDNA library constructed from L59 pea pods which have a lignified endocarp phenotype (Drew & Gatehouse 1994). The clone has a transcript size of about 950 nucleotides and the encoded protein shows homology to a number of blue type 1 copper proteins. The pLP18 clone was absent from cDNA prepared from L1390 pea pods which have a non-lignified endocarp which suggests that the protein is involved in lignification. pLP18 was kindly donated by Dr. J. Drew. This consists of 0.8Kb of coding sequence cloned into the EcoR1, Xho1 site of pBS+. pLP18 was cut using EcoR1 and Xho1 restriction enzymes and sense and antisense riboprobes were generated from the T3 and T7 promoters on either side of the insert.

In-situ hybridisation studies showed no binding of the pLP riboprobe to wax-embedded sections from *Arabidopsis*, *Brassica napus* or *Brassica juncea*.

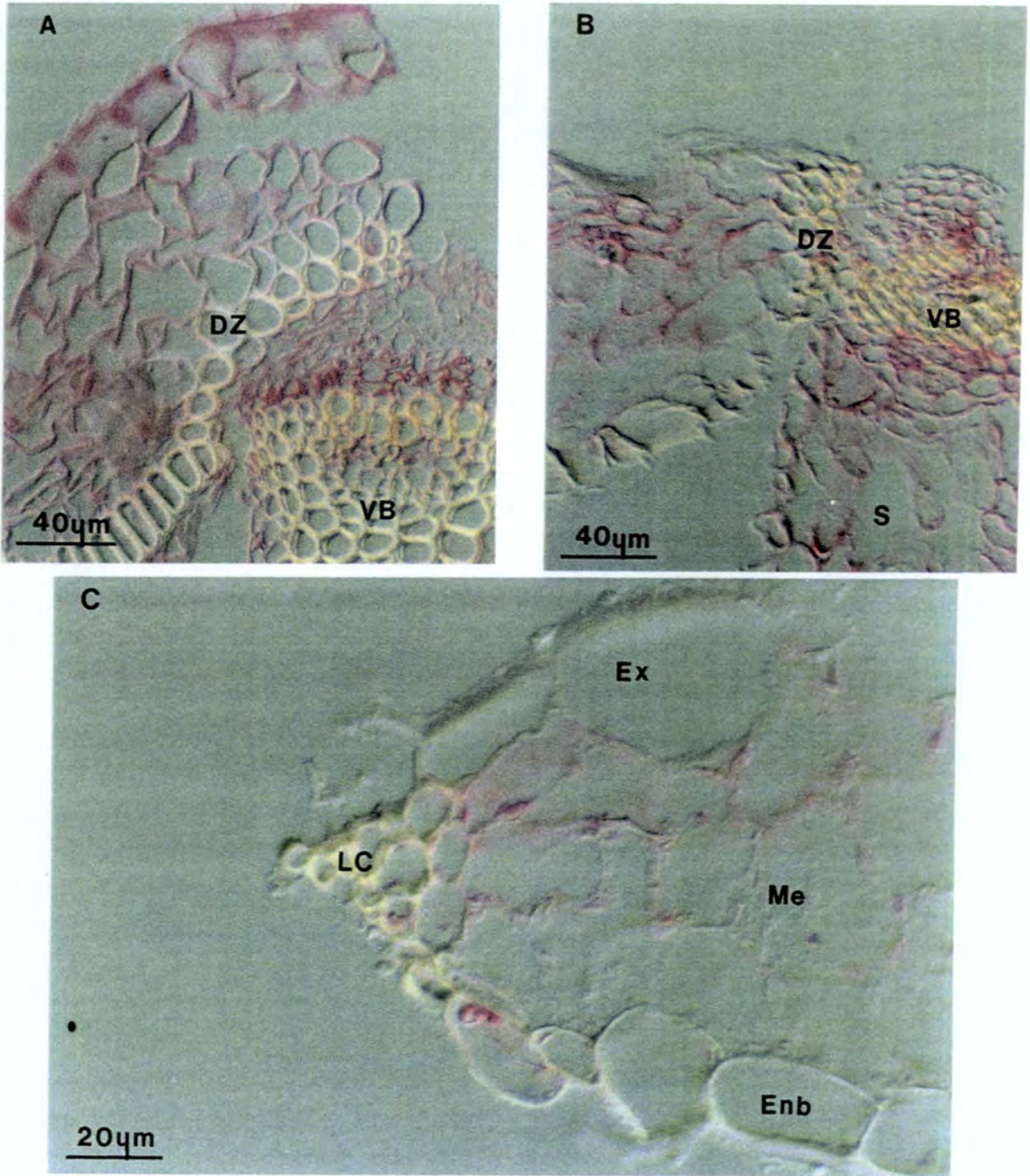


Figure 60. In-situ localisation of *ExtA* mRNA in the dehiscence zones of mature *Brassica* fruits

A) Localisation of *ExtA* mRNA in the dehiscence zone and replar bundle of mature *Brassica juncea* fruit

B) Localisation of *ExtA* mRNA in the dehiscence zone and replar bundle of mature *Arabidopsis* fruit

C) Localisation of *ExtA* mRNA in the dehiscence zone of mature *Arabidopsis* fruit

DZ = dehiscence zone, Enb = endocarp, Ex = exocarp, LC = lignified dehiscence zone cells, Me = mesocarp, S = septum, VB = vascular bundle

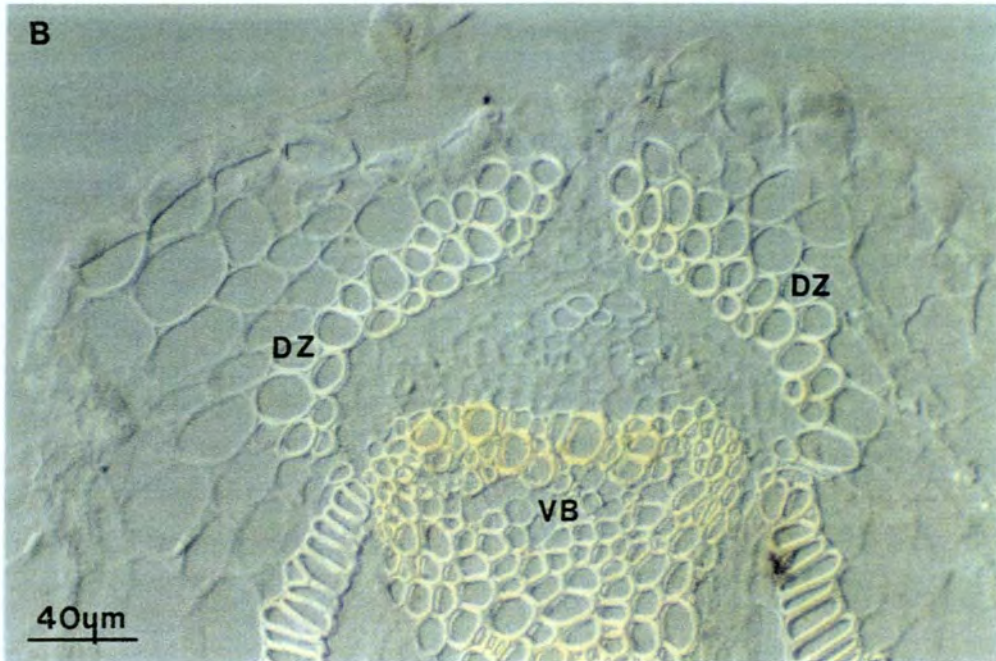
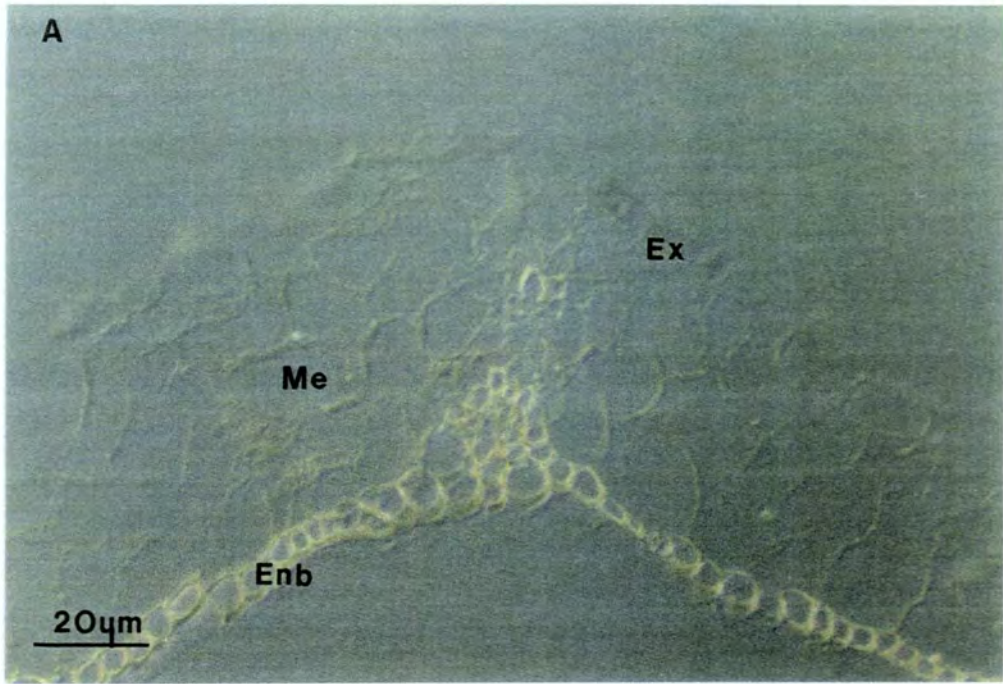


Figure 61. Control sections incubated with *ExtA* sense riboprobe

- A) No specific staining in the carpel walls of mature *Arabidopsis* siliques**
- B) No specific staining in the dehiscence zones of *Brassica juncea* siliques**

DZ = dehiscence zone, Ena = endocarp *a*, Enb = endocarp *b*, Ex = exocarp, S = septum, VB = vascular bundle

3.8. ANALYSIS OF SILIQUE LIGNIN

Lignification of the endocarp and dehiscence zone cells in the carpel walls of *Arabidopsis* during the later stages of fruit development appears to play an important part in the dehiscence mechanism of the fruit. Lignification is precisely controlled, both temporally and spatially within the carpel walls during fruit ripening. Lignin polymers can be broken down by severe oxidation procedures and their constituents analysed by HPLC for example. Using this method it should be possible to compare the units of the lignin polymers from various parts of the plant.

3.8.1. Oxidation procedures

Three different published methods were employed in analysing the phenolic constituents released by the hydrolysis of lignin polymers in *Arabidopsis* tissues. Two alkaline oxidation procedures, using either copper sulphate or nitrobenzene as the oxidising agents, and a microwave digestion procedure were used. The six major phenolics released by classical nitrobenzene oxidation; p-coumaric acid, ferulic acid, vanillic acid, vanillin, syringic acid and syringaldehyde were used as standards (Galletti *et al.* 1989). In these experiments the microwave digestion method yielded higher amounts of the six phenolics than both of the alkaline oxidation methods (results not shown).

Microwave digestion was a quicker and easier procedure which did not require the use of toxic chemicals such as nitrobenzene which, if not completely removed, can contaminate the samples and affect measurements. The microwave digestion method was therefore chosen for all further experiments. Two separate digestions were performed for each tissue type from both the Landsberg and Columbia ecotypes. The HPLC profiles of the standard solutions and the carpel walls from the second digestion are shown in Figure 62.

3.8.2. *Arabidopsis* ecotypes

The phenolics released by microwave digestion of the lignin were determined in the leaves, stems and carpel walls of both the Landsberg and Columbia ecotypes of *Arabidopsis*. Three different tissue types were analysed to see if there were any major differences in the composition of the lignin deposited in the silique walls during fruit ripening, and the lignin

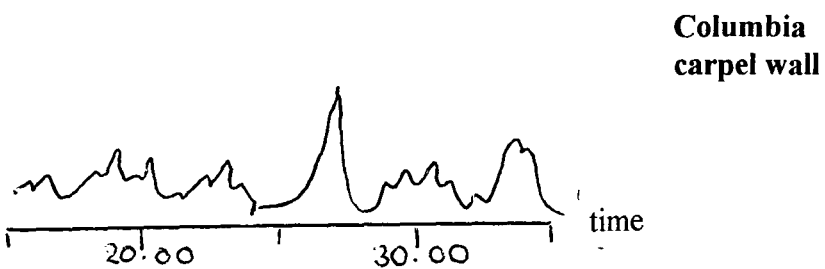
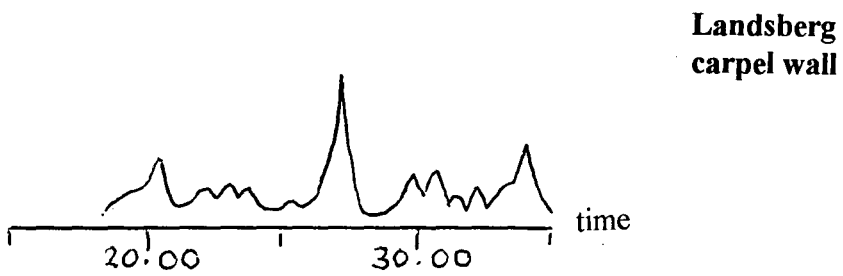
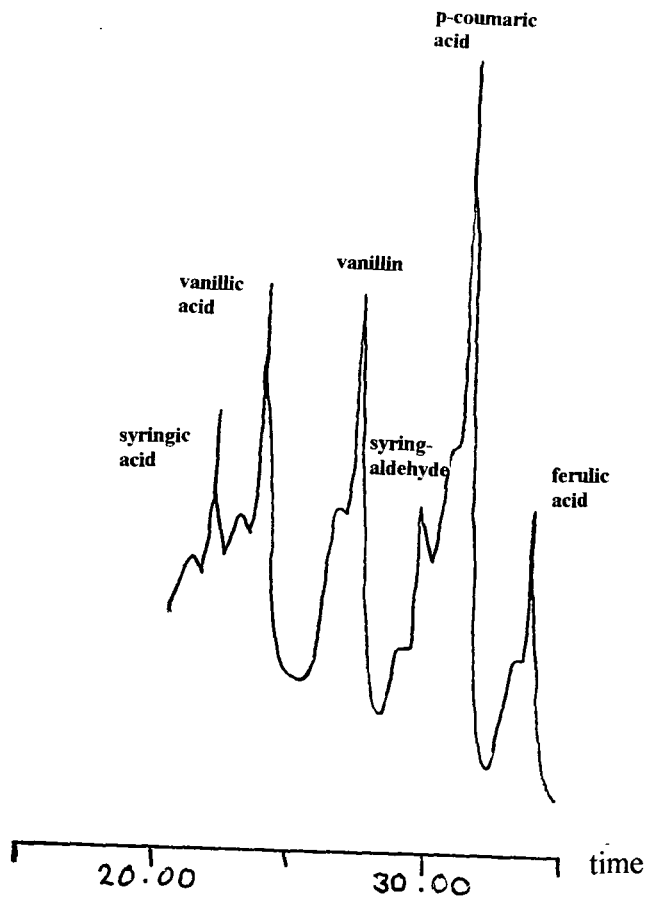


Figure 62. HPLC analysis of lignin oxidation products

deposited in the leaf and stem tissue, of which the majority is probably associated with the vascular bundles. The leaf and stem and carpel tissues were excised from many different mature plants. The carpel wall tissues were removed by hand from mature green, and yellow, siliques and samples did not include the replum, where the main vascular bundles of the fruit are located. The results show that there is no significant difference between the two ecotypes in the phenolics released from the digestion of the tissues examined, however, there are significant differences in the phenolics released from the digestions between the different tissue types.

All three tissue types yielded higher amounts of vanillin, syringic acid and syringaldehyde per mg of tissue and lower amounts of p-coumaric acid, ferulic acid and vanillic acid per mg of tissue. Although the results from the two digestions of the three different tissue types are comparable the values obtained from the experiments were in general quite low. This is most likely due to the inefficient extraction of the phenolics. The stem tissues yielded the highest amounts of total phenolics overall from all of the digestions, and the leaves yielded the lowest. The relative percentages of the extracted phenolic components from each of the tissues are represented graphically in Figures 63 and 64.

3.8.3. Leaf tissues

Syringic acid was found in the greatest quantity in the leaf tissues of both ecotypes, making up 47.7% and 45% of the total phenolics recovered in Landsberg and 35.5% and 36.6% in Columbia. Vanillin also made up an appreciable percentage of the phenolics found in the leaves, 22.6% and 28.5% in Landsberg and 28.7% and 31.7% in Columbia. The percentages of p-coumaric acid (4.3% and 1.4% in Landsberg and, 10.6% and 2.9% in Columbia) and ferulic acid (14% and 16.1% in Landsberg and 5.5% and 17.6% in Columbia) were generally much lower. Vanillic acid was not detected in the leaf tissues from either ecotype in the first digestion and accounted for less than two percent in the second digestions.

3.8.4. Stem tissues

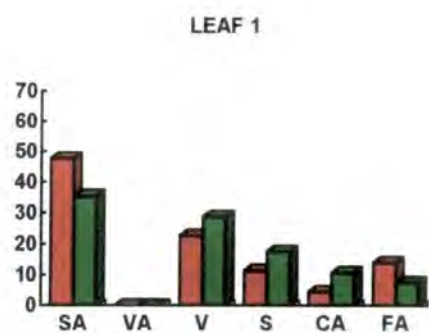
The stem tissues differed from the leaf tissues and yielded the highest percentage of vanillin, 52.2% and 68.4% in Landsberg, 46% and 65% in Columbia, and also quite a high percentage of syringaldehyde, 26.2% and 17.9% in Landsberg, 28.8% and 21% in

Columbia. p-coumaric acid, ferulic acid, vanillic acid and syringic acid were found in relatively equal amounts in the stem tissues from both ecotypes, with vanillic acid showing the overall lowest percentage of the total phenolics.

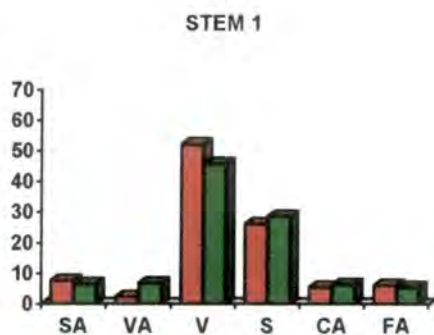
3.8.5. Carpel wall tissues

The carpel wall tissues, like those of the stem, yielded the highest percentage of vanillin, 35% and 51.6% in Landsberg and 30.1% and 55.7% in Columbia, and a relatively high proportion of syringaldehyde, 21.7% and 16.2% in Landsberg and 20% and 12.6% in Columbia. As can be seen in Figures 63 and 64, the percentages of p-coumaric and vanillic acid are also quite low in the carpel tissues as in both other tissue types, however as in the leaves, the carpel tissues yielded higher amounts of ferulic acid, 15.6% and 21.3% in Landsberg and 19.7% and 18.4% in Columbia.

The relative percentages of the phenolics released from the digestions of the carpel wall tissues show differences to those released from the stem and the leaf tissues, however the carpel wall and leaf lignin appear to show more differences than that of the carpel wall and stem. The carpel wall and stem tissues have a higher percentage of vanillin and a lower percentage of syringic acid than the leaves, and the carpel walls and the leaves have a higher percentage of ferulic acid.



█ Landsberg
█ Columbia



CA = p-coumaric acid
 FA = ferulic acid
 S = syringaldehyde
 SA = syringic acid
 V = vanillin
 VA = vanillic acid

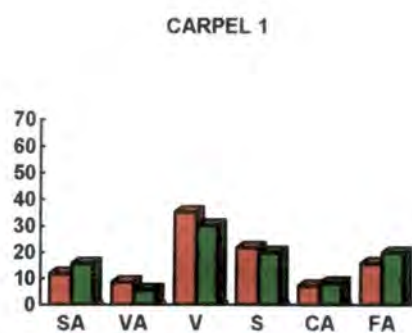


Figure 63. Graphical view of the relative percentages of lignin oxidation products from the first digestion

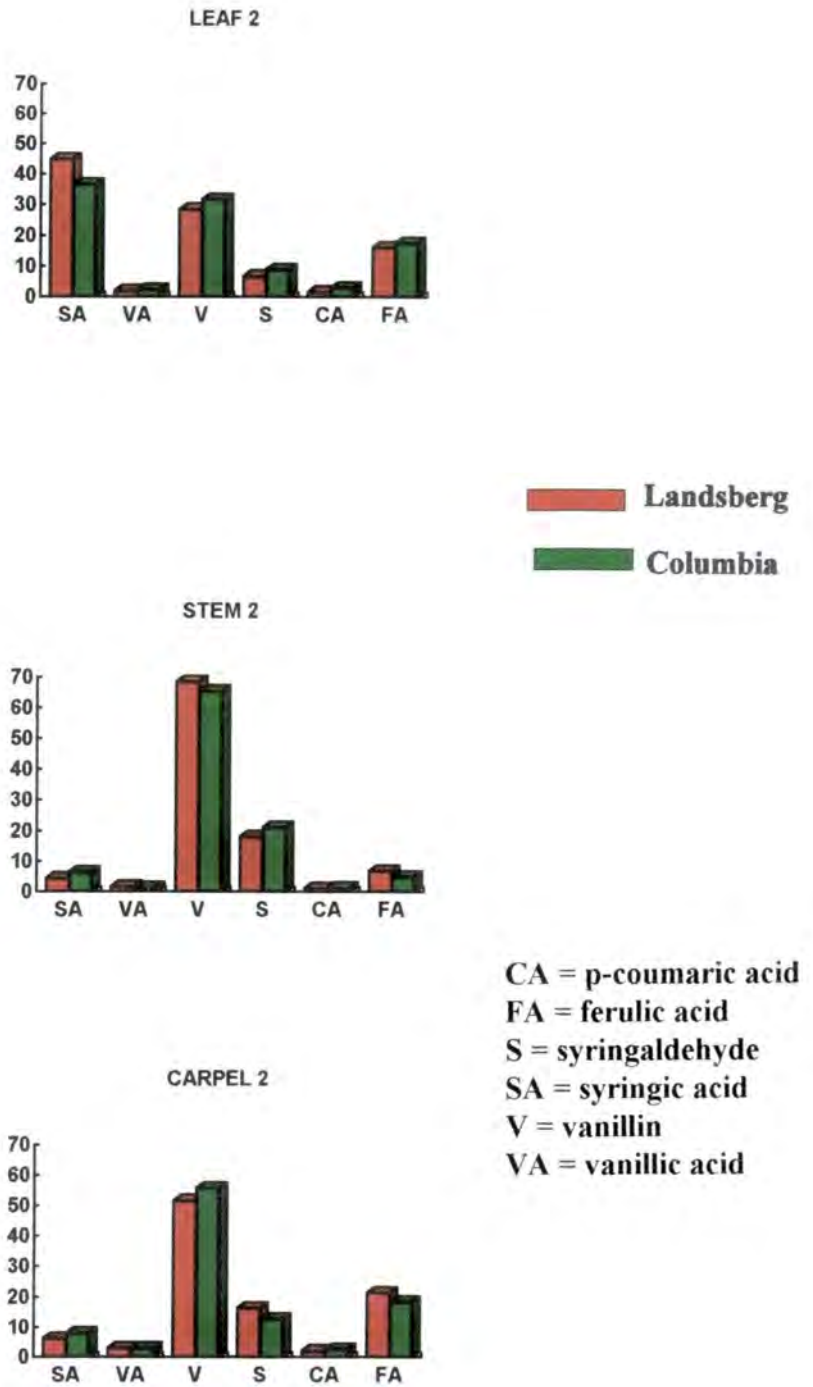


Figure 64. Graphical view of the relative percentages of lignin oxidation products from the second digestion

3.9. DEVELOPMENT OF THE *ARABIDOPSIS Sin 1-1* MUTANT SILIQUE

The *Sin 1-1* mutant was isolated from EMS mutagenised Columbia plants and the mutant phenotype exhibits a defect in the phenylpropanoid pathway. The defect results in a plant whose lignin lacks syringyl residues (Chapple *et al.* 1992). The *Sin 1-1* seeds were supplied by the Nottingham *Arabidopsis* Stock Centre. The lignin in the carpel walls of wild type *Arabidopsis* is composed of both syringyl and guaiacyl residues, however the lignin in the *Sin 1-1* siliques should be affected by the mutation and therefore be composed of only guaiacyl residues. This change in the composition of the plants lignin may have an effect on the development of the carpel wall and dehiscence zone or influence the dehiscence or 'shattering' characteristics of the siliques.

3.9.1. The phenotype of the *Sin 1-1* plant

Seeds from *Sin 1-1* and wild type were planted at the same time and grown under the same conditions. Seeds from *Sin 1-1* germinated at the same time as the wild type and grew at about the same rate however, *Sin 1-1* plants (Fig. 65) grown under the given conditions were shorter and more erect than the Columbia wild type. All of the plants reached maturity and produced seeds, the mutation did not appear to affect the development of the plant. The siliques also showed a similar pattern of ripening to the wild type and exhibited the same dehiscence characteristics. Shattered siliques were observed on all *Sin 1-1* plants.



Figure 65. The *Arabidopsis Sin 1-1* mutant plant

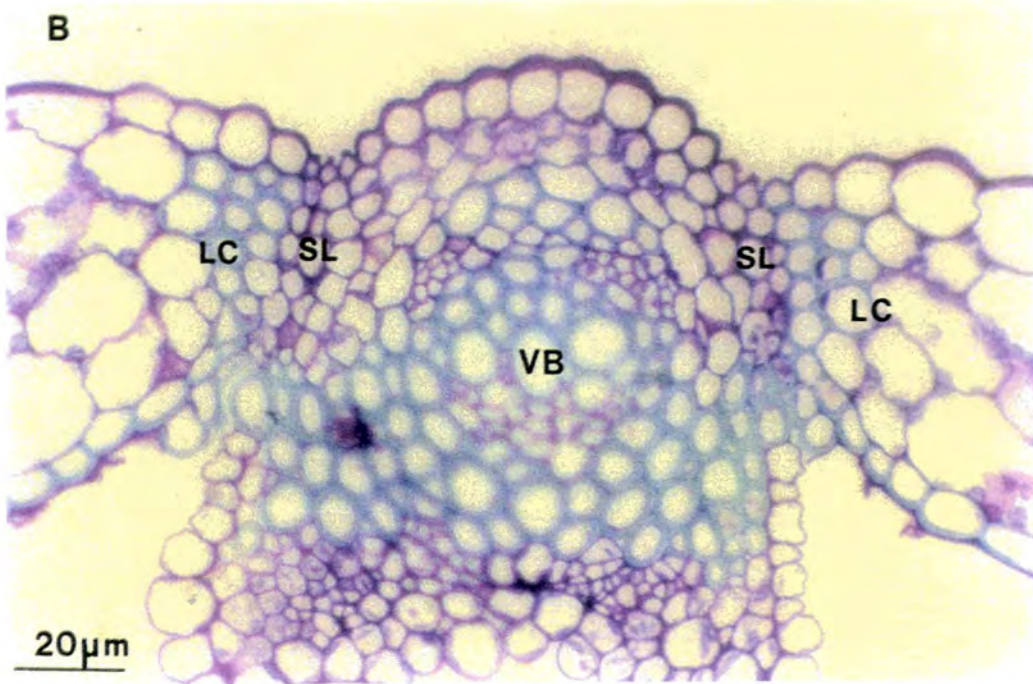
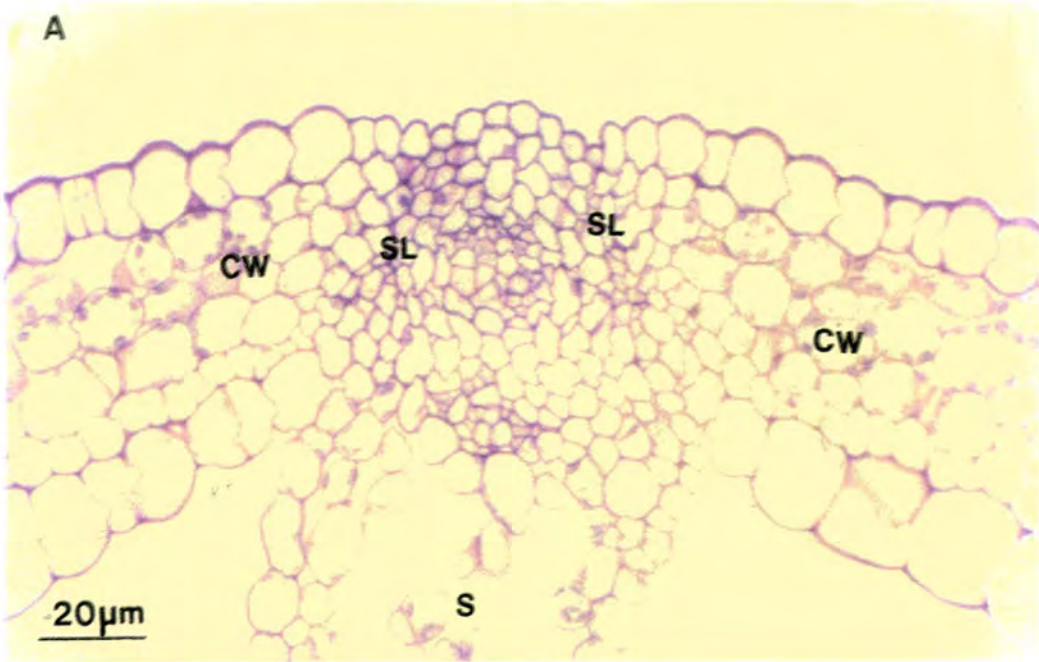


Figure 66. Structure of the dehiscence zones in the post-fertilised *Sin 1-1* fruit

A) Structure of the dehiscence zones of the young post-fertilised fruit

B) Structure of the dehiscence zones in the mature post fertilised fruit

CW = carpel wall. LC = lignified dehiscence zone cell, S = septum, SL = separation layer, VB = vascular bundle

3.9.2. Development of the dehiscence zones in the post-fertilised silique

Microscopical examination of the dehiscence zones of the *Sin 1-1* silique revealed a very similar pattern of development to that of the wild type plant. During the early stages of development (stages six and seven) the carpel margins constrict, and as can be seen in Figure 66a, the separation layer becomes distinguishable. The smaller marginal cells adjacent to the separation layer begin to lignify at stage eight and eventually the carpel wall is isolated from the replum as can be seen in wild type plants (Fig. 66b). Although the extent of the lignification in the zone cells and in the replar bundle appears to be the same as the wild type, the pattern of staining observed in toluidine blue stained sections is different. In the wild type plant the lignified cell walls in the dehiscence zone and replar bundle are stained various shades of blue with the metachromatic stain toluidine blue whilst in *Sin 1-1* the lignified walls are stained a uniform light blue. The uniform staining pattern of the *Sin 1-1* lignin results from the single residue composition of the lignin.

3.9.3. Development of the carpel wall in the post-fertilised silique

The structure of the carpel wall in the young post-fertilised silique is similar in structure to the wild type, comprising the exocarp the mesocarp and two endocarp layers (Figure 67a). Carpel wall differentiation is also similar to the wild type and *Enb* lignifies at stage eight then the mesocarp desiccates and *Ena* collapses at stage nine (Figure 67b). The lignified cells in the endocarp stain the same uniform light blue as that observed in the dehiscence zones and vascular bundles. This suggests that all of the lignin in the silique is composed of only guaiacyl residues but this does not affect the development of the silique, or alter the dehiscence characteristics.

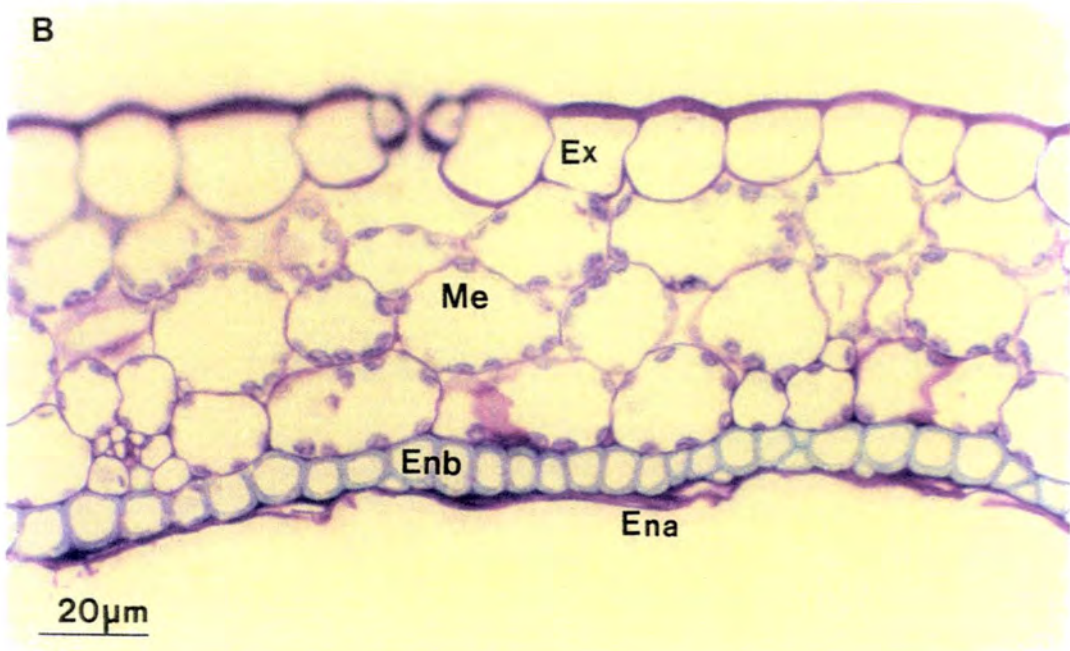
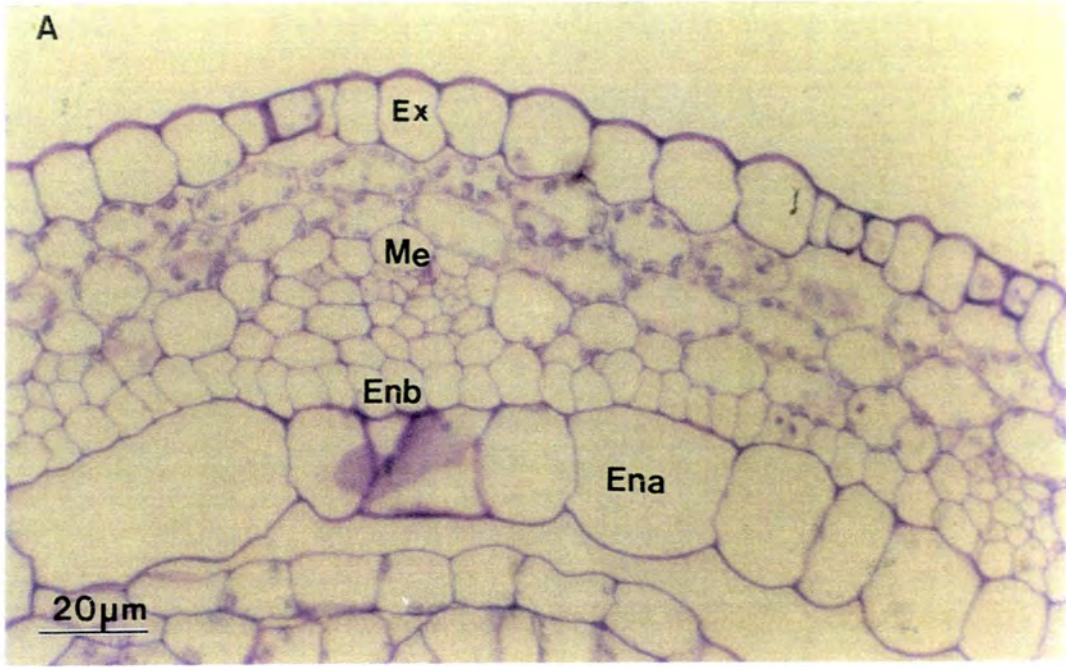


Figure 67 Structure of the carpel walls in the post-fertilised *Sin 1-1* fruit

A) Structure of carpel wall in the young post fertilised fruit

B) Structure of carpel wall in the mature post fertilised fruit

Ena = endocarp *a*, Enb = endocarp *b*, Ex = exocarp, Me = mesocarp

3.10. ANALYSIS OF SILIQUE CELL WALL POLYSACCHARIDES

Polysaccharides comprise a major component of the cell wall where they are found as homo-polysaccharides, heteropolysaccharides and glycoproteins. The type of polysaccharides, the extent to which they are cross linked within the cell wall, and their function within the wall varies between different cell types and between different species (Fisher & Bennett 1991, Carpita & Gibeau 1993). Polysaccharides can be hydrolysed by hot acid to release the constituent monosaccharides which can then be analysed by paper chromatography for example. Using this method the major monosaccharide components of the different silique tissues may be compared qualitatively.

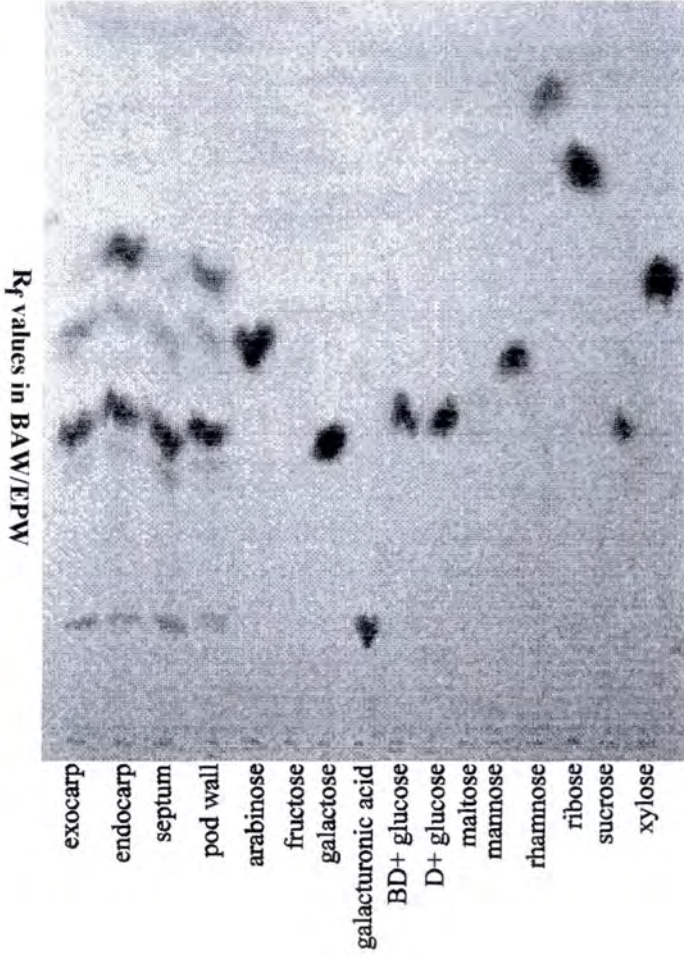
3.10.1. Analysis of monosaccharides from *Brassica napus* tissues

The exocarp layer could be peeled easily from the carpel walls of *Brassica napus* siliques however, some of the mesocarp layer always remained attached to the exocarp and therefore the samples were not 'pure'. The remaining tissue consisted of the endocarp layers and also some of the mesocarp and therefore the endocarp samples also were 'impure'. The septum tissue consisted of the septum and the replar vascular bundle tissues, and the pod wall tissues consisted of the carpel wall only. The monosaccharides released by hydrolysis were identified by spatial resolution with the twelve standards (Fig. 68). The scanned chromatogram images were then analysed using NIH Image 1.55 (Apple Macintosh version) to produce graphical representations of the released monosaccharides (Fig. 69), which are semi-quantitative. There were clear differences in the type and relative amounts of monosaccharides hydrolysed from the different types of tissue.

3.10.1.1. Pod wall tissues

Hydrolysis of the pod wall tissues released four major monosaccharides which could be identified by spatial resolution with the standards; galacturonic acid, galactose, arabinose and xylose (Fig. 68). The pod wall tissues contained higher levels of galactose and also quite a high level of xylose (Fig 69). The pod wall tissue contained lower levels of galacturonic acid as can be seen in Figure 69.

Brassica napus



Arabidopsis



Figure 68. Scanned images of paper chromatograms showing the separation of cell wall saccharides from tissues of *Brassica napus* and *Arabidopsis*

3.10.1.2. The septum

Hydrolysis of the septum tissues released three major monosaccharides which could be identified by spatial resolution with the standards; galacturonic acid, galactose and arabinose (Fig. 68). The septum tissues contained higher levels of galactose and lower levels of galacturonic acid, similar to that seen in the exocarp tissues (results not shown).

3.10.1.3. The endocarp

Hydrolysis of the endocarp tissues released four major monosaccharides which could be identified by spatial resolution with the standards; galacturonic acid, galactose, arabinose and xylose (Fig. 68). The endocarp tissues contained higher levels of xylose and appeared to show a similar level of galactose to that seen in the exocarp (Fig 69). The endocarp tissues contained lower levels of galacturonic acid as can be seen in Figure 69.

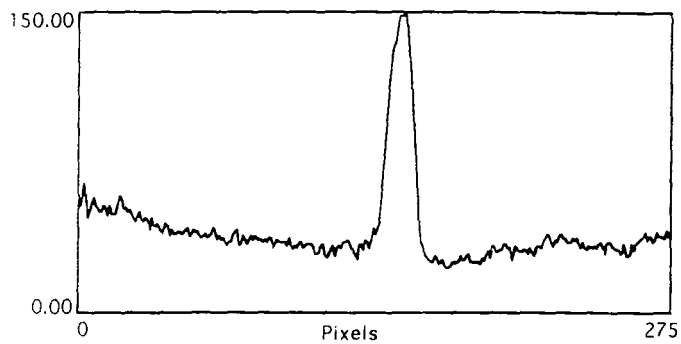
3.10.1.4. The exocarp

Hydrolysis of the exocarp tissues released three major monosaccharides which could be identified by spatial resolution with the standards; galacturonic acid, galactose and arabinose (Fig. 68). The exocarp tissues contained higher levels of galactose and lower levels of galacturonic acid as can be seen in Figure 69.

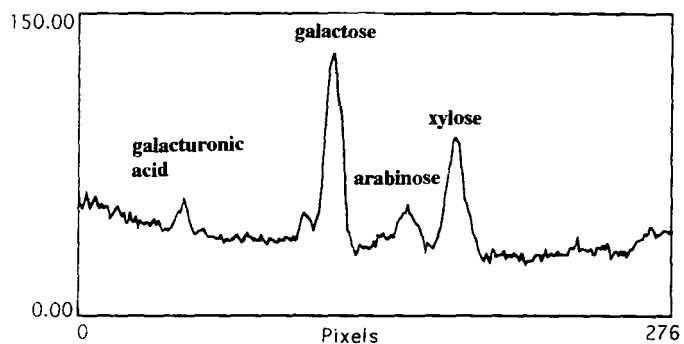
3.10.2. Analysis of monosaccharides from *Arabidopsis* tissues

The siliques from *Arabidopsis* were very small and it was difficult to separate the tissues of the *Arabidopsis* carpel wall. The exocarp did not easily peel away from the rest of the carpel wall and consequently less tissue was collected for hydrolysis. As in *Brassica napus* some of the mesocarp layer remained attached to the exocarp and endocarp tissues and therefore the samples were 'impure'. The septum tissue consisted of the septum and the replar vascular bundle tissues, and the pod wall tissues consisted of the carpel wall only. The monosaccharides released by hydrolysis were identified by spatial resolution with the twelve standards (Fig. 68). The scanned chromatogram images were then analysed using NIH Image 1.55 (Apple Macintosh version) however, the graphical representations were of poor quality due to the lighter staining of the released monosaccharides (results not

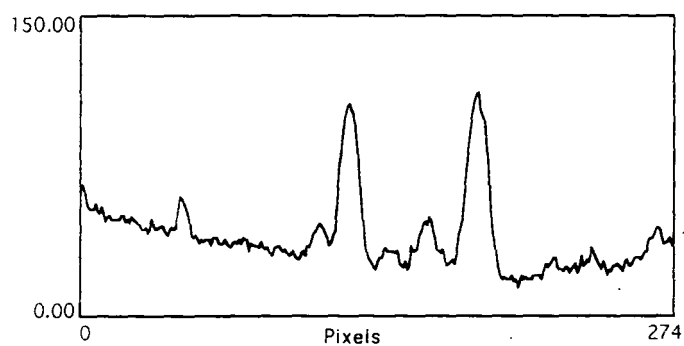
**arabinose
standard**



pod wall



endocarp



exocarp

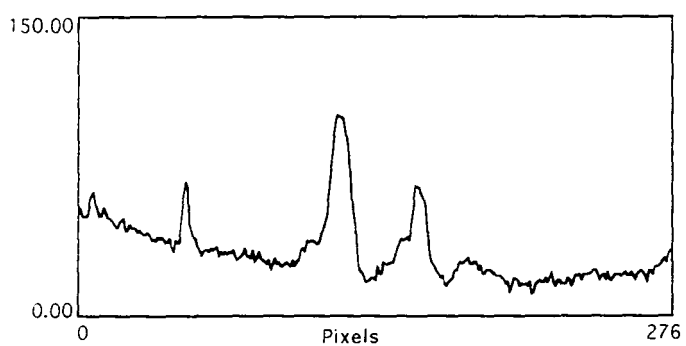


Figure 69. Graphical representation of cell wall saccharides from *Brassica napus* tissues

shown). There were clear differences in the types of monosaccharides hydrolysed from the different types of tissue and from the tissues of *Brassica napus*.

3.10.2.1. Pod wall tissues

Hydrolysis of the pod wall tissues released five major monosaccharides which could be identified by spatial resolution with the standards; galacturonic acid (not shown), galactose, glucose, arabinose and xylose (Fig. 68). The relative staining pattern of the chromatogram indicates that the pod wall tissues contained lower levels of galactose and arabinose and higher levels of galactose and xylose. Galacturonic acid was only just discernible.

3.10.2.2. The septum

Hydrolysis of the septum tissues released five major monosaccharides which could be identified by spatial resolution with the standards; galacturonic acid (not shown), galactose, glucose, arabinose and xylose (Fig. 68). The relative staining pattern of the chromatogram indicates that the septum tissues contained higher levels of glucose and arabinose and lower levels of galactose and xylose. Galacturonic acid was only just discernible.

3.10.2.3. The endocarp

Hydrolysis of the endocarp tissues released five major monosaccharides which could be identified by spatial resolution with the standards; galacturonic acid (not shown), galactose, glucose, arabinose and xylose (Fig. 68). The relative staining pattern of the chromatogram indicates that the endocarp tissues contained higher levels of xylose and glucose and lower levels of galactose and arabinose. Galacturonic acid was only just discernible.

3.10.2.4. The exocarp

Hydrolysis of the exocarp tissues released four major monosaccharides which could be identified by spatial resolution with the standards; galacturonic acid (not shown),

galactose, glucose and arabinose (Fig. 68). The relative staining pattern of the chromatogram indicates that the exocarp tissues contained higher levels of galactose and glucose and a lower level of arabinose. Galacturonic acid was only just discernible.

4. DISCUSSION

4.1. The Dehiscence Mechanism

The dehiscence mechanism is a means by which the fruits of certain plants including some Brassicas split open at maturity and release their seeds. This method of seed dispersal causes problems with crop plants such as oilseed rape where the seeds may be lost prior to harvesting. This usually occurs when harvesting is delayed by adverse weather conditions and the ripening pods split open or dehisce. The small Brassica *Arabidopsis thaliana*, which has become the focus of much plant research, has a short life cycle and develops many small dehiscent siliques, which makes this an ideal plant in which to study the dehiscence mechanism.

Using light microscopical techniques the pattern of cellular development of the dehiscent *Arabidopsis* silique has been studied (Spence 1992). The tissue types involved in the process of dehiscence, the carpel wall layers and the dehiscence zones, were identified in the Landsberg *erecta* ecotype of *Arabidopsis*. The development of the silique was divided into ten different stages five pre- and five post-fertilisation which were based on distinct histological events (Table 2). All of the major tissue types of the silique were laid down during the first five stages of development prior to fertilisation. It is the differentiation of these tissue types during the latter five post-fertilisation stages of development, which facilitates the process of dehiscence.

The differentiation of the carpel walls and dehiscence zones occurs after fertilisation and results in four cell types, the exocarp, the mesocarp and two endocarp layers which are associated with the carpel wall, and two cell types, the separation layer and the lignified dehiscence zone cells, which are associated with the dehiscence zone. Although dehiscence occurs due to precise patterns of tissue differentiation within the silique, this work indicates that development of the lignified endocarp may be a key factor in this process and, alterations to the pattern of cellular development within this layer affects dehiscence, and hence the 'shattering' characteristics of the silique.

Dehiscence occurs when tension develops within the carpel walls when the mesocarp desiccates and shrinks (Fig. 70). The mesocarp is attached to a thickened non-shrinking exocarp and to a lignified non-shrinking *Enb* layer. The inner *Ena* disintegrates prior to dehiscence. At the carpel margins the mesocarp is adjacent to the lignified non-shrinking dehiscence zone cells. The lignified endocarp and dehiscence zone cells form a continuous

rigid wall which isolates the rest of the carpel wall tissues from the separation layer cells and the replum. It is proposed that the tensions develop within the carpel walls when the mesocarp desiccates and shrinks putting stress on the inflexible lignified wall which effectively becomes 'sprung'. These tensions are strong enough to break apart the separation layer cells within the dehiscence zone, which form a weak joint between the carpel wall and replum. Cell separation occurs between the cells of the separation layer as these cells are observed still intact in dehisced siliques.

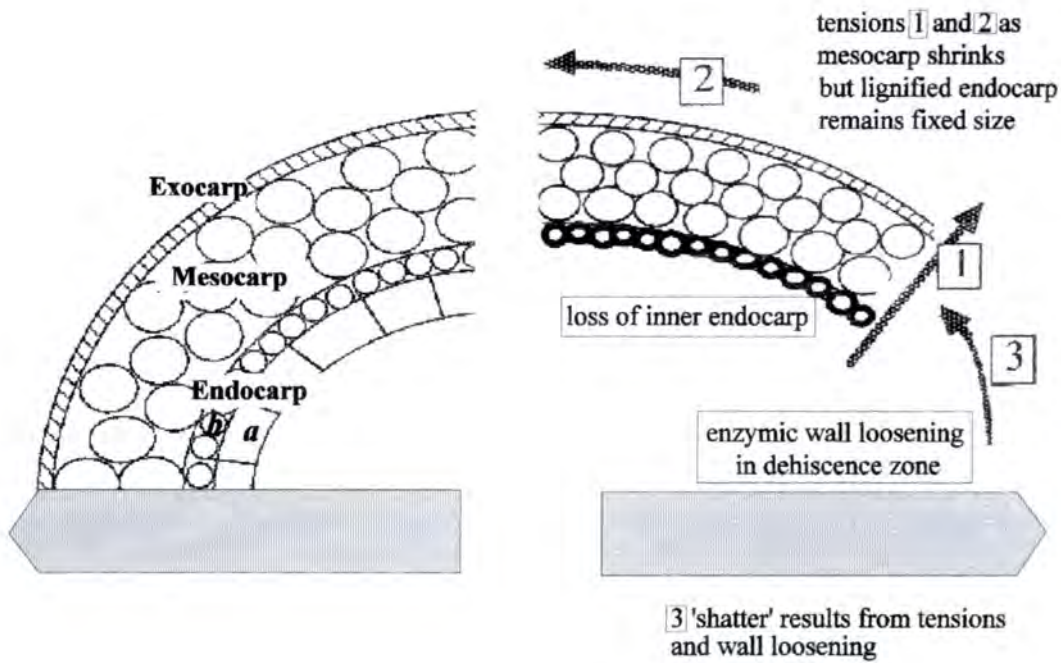


Figure 70. The dehiscence mechanism in *Arabidopsis*

4.2. Pod 'Shatter'

The dehiscence mechanism is a gradual process as the carpel walls begin to split away from the tip of the fruit and this progresses to the base. Pod 'shatter' occurs when the whole carpel wall detaches very quickly from the fruit. Pod 'shatter' can occur spontaneously but it most frequently occurs when the fruits are mechanically stimulated. It is proposed that pod 'shatter' occurs when the carpel wall tensions develop and the carpel wall effectively becomes 'sprung' along the lignified endocarp rather like a bow. The tensions are released suddenly when the weakened walls of the separation layer cells give

way, usually as a result of mechanical stimulus, resulting in the often rather explosive pod 'shattering'.

4.3. Dehiscence and Pod Shatter in *Arabidopsis*

The wild type populations of *Arabidopsis* exhibit many natural variations in form such as leaf shape and colour for example. Although the pattern of silique dehiscence appears to be very similar in wild type populations, as would be expected, the dehiscence characteristics and the post-fertilisation development of the siliques of twenty *Arabidopsis* ecotypes were studied in this report. The development of the carpel walls and dehiscence zones, during developmental stages six to ten, has been compared to that of the previously studied Landsberg *erecta* ecotype. All of the ecotypes showed similar patterns of tissue differentiation within the carpel walls and dehiscence zones during post-fertilisation development, and all of the ecotypes exhibited similar dehiscence characteristics, although more 'shattered' siliques were usually observed on Landsberg *erecta* plants.

The ecotypes used in this study originated from various geographical locations throughout the Northern hemisphere and consequently their natural growth conditions will vary. Conditions such as daylength and temperature are known to affect the growth rate and flowering of some plants, and this is evident also in *Arabidopsis*. The Ag-0 ecotype in this study exhibited a phenotype in which floral initiation is temperature dependant. Ag-0 plants only produced flowers when the temperature was lowered from 25°C to 20°C.

Nine of the original ecotypes in the study did not produce siliques or set seed when grown at 25°C under continuous illumination, and those which did exhibited a number of phenotypic variations associated with silique development such as time taken to reach the bolting stage, time taken to go from bolting to senescence, and the average length of the siliques from the ecotype. The phenotypic variations observed between these ecotypes may simply result from the growth conditions used in the study. However, the fact that twenty ecotypes did produce healthy plants which reached maturity, shows the ability of some *Arabidopsis* ecotypes to survive or adapt to non-ideal conditions.

The siliques of the Landsberg *erecta* ecotype were more blunt ended than the siliques of all the other ecotypes. This variation however, appeared to have no effect on the developmental pattern of the tissues of the siliques. The carpel walls and dehiscence zones

of all twenty ecotypes in the study, showed the same pattern of development to that previously reported for the Landsberg *erecta* silique. Although 'shattered' siliques were observed on plants from all of the ecotypes and desiccating siliques which were attached to the plants shattered very easily by slight mechanical stimulation, this was most pronounced in the Landsberg *erecta* ecotype. The carpel walls could also be removed intact at the separation layer from mature Landsberg *erecta* siliques while they were still predominantly green.

Previous work conducted by the author (Spence 1992) identified a mutant grown from EMS treated Landsberg *erecta* seeds, which exhibited a 'pointed pod' phenotype, and whose siliques more resembled those of the Columbia ecotype for example. Fewer 'shattered' siliques were observed on pointed pod plants compared to the wild type. This suggests that Landsberg *erecta* siliques exhibit more 'shattering' because of the blunt-ended shape of the silique. The shape of the fruit may serve to increase the tensions which develop within the carpel walls and cause the siliques to 'shatter' very readily.

The Columbia ecotype was chosen as representative of the range of ecotypes used in the comparative histological study as this ecotype has been used for much experimental work including the genetic control of flower development (Coen & Meyerowitz 1991) and mapping phenotypic and restriction fragment length polymorphism markers (Lister & Dean 1993). The pattern of dehiscence and the 'shattering' characteristics of siliques from the Landsberg *erecta* and the Columbia ecotypes were examined at a range of different relative humidities, ranging from 7% to 96%. The siliques from both ecotypes were excised from the plant for the humidity experiments and exhibited a slightly different pattern of 'yellowing'. The ripening siliques which are attached to the plant usually begin to yellow at the tip of the fruit, while those which were removed from the plant began to yellow from the base. This is most likely due to the presence of the hormone ethylene which is known to be induced following wounding (Yang & Hoffman 1984, Kende 1993).

Despite the fact that the excised siliques began to yellow from the base, the siliques from both ecotypes showed a normal pattern of dehiscence and the siliques 'shattered' on mechanical stimulation over a wide range of humidities ranging from 29.9% to 96%. Dehiscence and pod 'shattering' was only significantly affected at the lowest two humidities 7% and 12%. At these very low humidities the siliques desiccated very quickly and shrivelled up due to excessive water loss from all of the carpel wall tissue layers. The carpel walls did not detach from the siliques even under mechanical stimulation.

Dehiscence must be an active process because although cell death and desiccation are occurring in some carpel wall cell layers, it is essential that the remaining cells function normally for dehiscence to occur. Desiccation and cell death during carpel wall development are therefore temporally and spatially controlled.

4.4. Dehiscence and Pod Shatter in *Brassica napus* and *Brassica juncea*

Brassica napus and *Brassica juncea* fruits both dehisce in a similar manner to *Arabidopsis*, but exhibit different 'shattering' characteristics. The siliques from *Brassica napus* shatter, but not as readily as those from *Arabidopsis*, but the fruits from *Brassica juncea* show a reduced shattering, or non-shattering phenotype. During the early stages of post-fertilisation development the fruits from both of these species showed a similar pattern of dehiscence zone development and carpel wall differentiation to *Arabidopsis*. However during the later stages of development, although the dehiscence zone in *Brassica napus* and *Brassica juncea* showed a similar pattern of development to that observed in *Arabidopsis*, development of the endocarp layer in the carpel wall was found to be significantly different.

In *Brassica napus* the dehiscence zone showed much more extensive lignification than observed in *Arabidopsis*, and lignification was also observed in the mesocarp layer of the carpel wall, especially in those mesocarp cells which were adjacent to the lignified *Enb*. Development of the endocarp also showed a different pattern to that observed in *Arabidopsis*. The inner and outer tangential walls of *Ena* thickened in *Brassica napus*, before this cell layer collapsed to form a thick lining adjacent to the lignified *Enb*. Three of the *Brassica juncea* varieties which were examined had a reduced tendency to 'shatter', and showed a similar pattern of dehiscence zone and carpel wall development to *Brassica napus*. However, one of the varieties of *Brassica juncea*, Indian mustard, did not 'shatter' at all, and also showed a reduced tendency to dehisce. Intact fruits usually remained on the plant. The pattern of endocarp development was significantly different in Indian mustard siliques.

There was considerable thickening of the inner and outer tangential walls of *Ena* in the Indian mustard variety, as was observed in *Brassica napus*, however this cell layer did not totally collapse at stage nine, but remained mainly intact in the mature siliques. *Enb* in Indian mustard showed a significantly different pattern of development to that observed in

Arabidopsis and *Brassica napus*. Selective staining of the lignified *Enb* showed that in Indian mustard siliques lignification was limited to the secondary cell wall, whilst the primary cell walls and middle lamella remain rich in pectins. This pectin can be clearly seen in the radial cell walls between the lignified cells.

Dehiscence in *Arabidopsis*, *Brassica napus* and *Brassica juncea* is a physiological process essential to the survival of the species. The process of dehiscence can be effected over a range of climatic conditions such as temperature and humidity, ensuring the release of seed to produce the next generation of plants. The process requires that the separation layer cells within the dehiscence zone exhibit reduced cellular cohesion, and that cells within the fruit wall differentiate to produce tensions within the carpel walls, which pull these separation layer cells apart.

4.5. The Non-'Shattering' Phenotype

Pod 'shatter' occurs as a result of the tissue differentiation patterns within the silique and, although it is not essential for seed dispersal, it is beneficial to the plant as the seeds can be scattered further. The phenotype of the non-shattering variety of *Brassica juncea* results from an altered pattern of endocarp development within the carpel wall. The primary and secondary cell walls of *Enb* are lignified in *Arabidopsis* and *Brassica napus* producing a very inflexible layer, however in the non-shattering *Brassica juncea* only the secondary cell walls lignify. This results in layer of pectin which lies between the lignified cell walls. This produces a much more flexible endocarp layer which reduces the tensions which develop in the carpel wall when the mesocarp dries out. Consequently the carpel wall does not become 'sprung' along the endocarp and 'shatter' does not occur.

Although there was a slight difference in the size and number of the cells in the carpel walls among the ecotypes of *Arabidopsis*, this did not affect the 'shattering' characteristic. The siliques of *Brassica napus* and *Brassica juncea*, which are much larger than those of *Arabidopsis*, did not shatter as easily as those of *Arabidopsis*. This may be because the separation layer is thicker and contains more and larger cells, resulting in an increase in cellular cohesion in this cell layer, or that due to the increased mass of the whole silique, proportionally more tension must develop to facilitate dehiscence and to induce 'shatter'.

The strength of the forces which are produced from the tensions which develop in the siliques was not measured. However, if these forces can be accurately measured, then computer modelling may be a means of testing whether the blunt or pointed shape of the tip of the silique, or the size and number of the cells, does have an effect on the dehiscence and 'shattering' characteristics. As this approach would require in depth knowledge of stress mechanics and also adequate understanding of complex computer programmes, these may be problems more appropriate for an engineer to solve.

4.6. The Tissues of the Dehiscence Zone

The dehiscence zone was similar in structure in all of the Brassica species examined and comprises two very distinct types of tissue, the separation layer and the lignified zone. The separation layer consists of two layers of thin walled parenchymous cells, which lie adjacent to the replum. During post-fertilisation development these cells exhibit cell wall breakdown along the middle lamella, resulting in reduced cellular cohesion, however it is proposed that this loosening of cell wall components is not in itself enough to cause pod 'shatter'. Tensions must first develop within the carpel wall which are sufficient to cause the loosened separation layer cells to give way suddenly for 'shatter' to occur.

This process of cell wall breakdown has been shown to involve the enzyme cellulase in both abscission zones and in the dehiscence zones of *Brassica napus* (Meakin & Roberts 1990b, Coupe 1993), where it appears to be under the control of ethylene. In the *Arabidopsis Etr* mutant silique which is ethylene insensitive and also exhibits a non-shattering phenotype, the separation layer cells are often poorly distinguished. This suggests that the development of the separation layer cells in *Arabidopsis* is also influenced by ethylene. The separation layer cells in the *Etr* mutant silique may exhibit less cell wall degradation and may be much more tightly bound together and hence this may inhibit pod 'shatter'.

The lignified zone lies between the separation layer and the tissues of the carpel walls. It is proposed that this cell layer would be important in producing the tensions within the carpel wall, as it forms an inflexible link at the carpel margins between the exocarp and the lignified endocarp, and between the carpel walls and the separation layer. This layer may comprise only a few cells as in *Arabidopsis*, or it may comprise many cells as can be seen in *Brassica napus* and *Brassica juncea*. The lignified zone tissues show a different pattern

of development to the lignified endocarp and, although they appear to form a continuous band of cells in the mature silique, they do develop from two very distinct tissue types in the pre-fertilised silique (Spence 1992). Lignification of the dehiscence zone begins adjacent to the exocarp and gradually progresses through to the endocarp, whereas all of the endocarp cells appear to lignify evenly.

The development of the lignified dehiscence zone cells in the *Arabidopsis Etr* mutant silique appears to be delayed, as only those cells which are adjacent to the exocarp lignify, and those which are adjacent to the endocarp do not. Consequently the lignified dehiscence zone and lignified endocarp do not form a continuous band of cells and tensions within the carpel wall are reduced. This suggests that lignification in the dehiscence zone cells may be influenced by ethylene but lignification in the carpel wall is not. The development of the lignified dehiscence zone and the lignified endocarp are not affected in the *Sin 1-1* mutant silique. Although the lignin in these mutant siliques probably only comprises guaiacyl units this does not appear to affect the development or the mechanical properties of these two types of tissue.

4.7. The Tissues of the Carpel Wall

Although dehiscence is effected by the development of the carpel walls and the dehiscence zones during fruit ripening, it is proposed that it is the differentiation of the carpel wall cell layers which produce the tensions which are required for dehiscence to occur and which therefore affect dehiscence characteristics, such as 'shattering'. The differentiation of the exocarp, the mesocarp, endocarp A (*Ena*) and endocarp B (*Enb*), within the carpel wall is precisely controlled, both temporally and spatially, and will therefore involve a number of genetic and/or biochemical control factors, unique to each cell type.

Differentiation within the carpel walls during developmental stages six to ten involves diverse processes such as; thickening in specific areas of the cell wall in the exocarp, processes which resemble leaf senescence in the mesocarp, cell wall lignification in *Enb* and the specific cell wall thickening then the collapse of the cells comprising *Ena*. The similarity in the developmental pattern of the carpel wall exhibited by *Arabidopsis*, *Brassica napus* and *Brassica juncea*, suggests a group, or groups of ripening control factors which are common to all three of these species.

Parthenocarpic fruit set can be induced in *Arabidopsis* by the exogenous application of gibberellin GA₃ (Y. Vercher pres. comm.). This allows the study of developmental processes within the carpel wall which are not dependent on the concurrent development of the seeds. Parthenocarpic fruit development in *Arabidopsis* showed some similarities to those observed in the parthenocarpic fruits of pea (Vercher *et al.* 1984, 1987). Gibberellin caused the cells in the exocarp mesocarp and *Ena* to expand and the cells within *Enb* to elongate and lignify. Work by Lloyd *et al.* (1995) has shown that gibberellin changes the orientation of microtubules from the longitudinal to the transverse in elongating or differentiating cells and it is therefore most likely involved in cell expansion due to its effects on the reorientation of some cell wall polymers. The pattern of development observed in the carpel wall cells of parthenocarpic fruits of *Arabidopsis* suggests that the elongating *Enb* cells in the carpel walls of the Brassicas in this study are most likely stimulated to elongate by gibberellins during the post-fertilisation stages of development.

Many of the processes associated with the differentiation of the carpel wall indicate a major role for the hormone ethylene in the ripening of *Arabidopsis*, *Brassica napus* and *Brassica juncea* fruits. Ethylene is known to influence cell wall changes such as causing an increase in the production of the enzyme cellulase and an increase in the production of the cell wall protein extensin. Senescence has also been shown to be controlled by ethylene and it has also been implicated in the control of peroxidases enzymes during bean leaf abscission (McManus 1994). The *Arabidopsis* ethylene mutant *Etr* lacks a number of responses to ethylene, which is most likely due to a defect in one of the receptors (Bleeker *et al.* 1988) and shows an altered pattern of fruit development. Ethylene appears to influence cell elongation and expansion within the carpel wall tissues and also promote the senescence process within the mesocarp.

4.7.1. The Exocarp

The cell walls of the exocarp are the first to differentiate histologically during pre-fertilisation development. These cells secrete a cuticular layer on the outer walls to form a protective barrier to the elements and the exocarp cells are interspersed with the guard cells and stomata, which control moisture loss from the fruit. During post-fertilisation development the exocarp cells thicken throughout stages six to ten especially along the tangential walls, and produce cell walls which have a high pectin content as demonstrated by ruthenium red staining.

tangential walls, and produce cell walls which have a high pectin content as demonstrated by ruthenium red staining.

Although the exocarp layer performs essential functions throughout fruit development, it probably contributes the least in producing the tensions which develop within the carpel wall. The high pectin content of the exocarp cell walls suggests that unlike the endocarp, this layer is quite flexible. In the mature fruits of Indian mustard, the non-dehiscing variety of *Brassica juncea*, acridine orange staining revealed secondary wall lignification in the exocarp cells which is not seen in *Arabidopsis* or *Brassica napus* fruits. This indicates that although the mesocarp may have desiccated, the exocarp cells do not degrade but further differentiate and synthesise new cell wall polymers, probably as a result of the stresses on the cells caused by the shrinking mesocarp.

Immunological studies using anti-pectin antibodies showed the cell walls in mature siliques are rich in unesterified pectin recognised by the JIM5 antibody. The unesterified pectin was located in the intercellular spaces, a layer adjacent to the plasma membrane and to the middle lamella between adjacent cells. Unesterified pectin was also present in high amounts in the thicker exocarp cell walls which are adjacent to the cuticle. The precise role of pectins in the cell wall is still unknown, however unesterified pectins are able to bind calcium enabling them to cross link and form gels (Carpita & Gibeaut 1993). This has an effect on the plasticity of the wall. The orientation of the pectin molecules, the extent to which they are cross linked and the number and type of polysaccharide side chains present on the polymers were not investigated, as this was beyond the scope of this study. However, preliminary studies have shown that the monosaccharides released by the hydrolysis of exocarp tissues from *Brassica napus* are different to those from released by hydrolysis of exocarp tissues from *Arabidopsis*. The monosaccharides released from the exocarp tissues from both species were also different to those released from the endocarp.

4.7.2. The Mesocarp

The mesocarp is composed of photosynthetically active, thin-walled parenchyma cells. During post-fertilisation development these cells expand uniformly and the intercellular spaces increase in size and number. During the latter stages of ripening the mesocarp layer begins to desiccate and shrink. Because the mesocarp is attached to the inflexible endocarp, when it shrinks tensions develop within the carpel wall. Although the majority

lignification. Lignification in the mesocarp was never observed in *Arabidopsis* siliques. The position of these lignified cells suggests that the lignification in the mesocarp may be a result of cellular stress.

Cellular changes which occur within the mesocarp cell layer show many similarities to the process of cellular senescence, such as occurs in leaves for example. If, as proposed, the carpel developed from a modified leaf, then many of the biochemical processes and genetic control factors associated with mesocarp senescence may be the same, or similar, to those observed during the senescence of leaf tissues. The senescence of the rosette of leaves in *Arabidopsis* has been attributed to an age related process (Hensel *et al.* 1993), and it is most likely that senescence of the mesocarp layer is also an age related process. Mature dehiscent siliques and young developing siliques are observed on the same plant. During the senescence process cell components in many plants are often recycled for reproductive development for example, and some components from the senescence of the rosette leaves from the plants in this study are also most likely recycled, as senescence of the leaves occurs before the fruits are mature. However, senescence of the siliques occurs at the end of the plants life cycle and any recycled products are most likely only incorporated into seed production.

Senescence of the mesocarp layer is precisely controlled to temporally coincide with the development of the other carpel wall cell layers, and it is also spatially controlled as the cells which are adjacent to the exocarp begin to senesce first. Temporally controlled senescence could also imply that the mesocarp layer adjacent to the exocarp was the first to differentiate and may therefore be the first to senesce. Cellular senescence then proceeds through the mesocarp layer through to *Enb*. This suggests a signal molecule or molecules which initiate senescence and perhaps also a signal molecule or molecules which then affect adjacent cells to cause the cascade effect. Cellular breakdown products have been implicated as molecules which may influence physiological processes or induce new gene expression (Thompson and Osborne 1994) and this process of cellular signalling may be one of the controlling factors during senescence of the mesocarp in the silique.

In-situ hybridisation studies revealed the differential expression of two genes SAC51 and *ExtA*, both isolated from *Brassica napus*, in the mesocarp of young and mature post-fertilised Brassica fruit. SAC51 is a novel gene, which was isolated from silique tissues of *Brassica napus*, and which codes for a protein of unknown function (Coupe *et al.* 1994a). During developmental stages six to seven, SAC51 showed high levels of expression in

those mesocarp cells which are adjacent to the exocarp, and which are the first mesocarp cells to senesce, in the mature fruits of *Arabidopsis*, *Brassica napus* and *Brassica juncea*. Expression of this gene appeared to increase with increasing age of the mesocarp cells, as much more staining was observed during developmental stages eight and nine and more mesocarp cells showed expression of the gene. The function of the SAC51 protein and its homologues is unknown, however the results of this study would point to a role for this protein during senescence of the mesocarp.

The extensin gene *ExtA*, which is highly expressed in the phloem tissues of *Brassica napus* roots (Evans *et al.* 1990), exhibited no expression in *Brassica napus* siliques, but was detected in the mesocarp and carpel margins of *Arabidopsis* and *Brassica juncea* fruit, although staining was weaker than that observed for SAC51. There also appeared to be higher expression of *ExtA* in mesocarp cells at the carpel margins of mature fruits. Extensins are rod shaped, structural proteins which have been implicated in many physiological processes, such as strengthening the cell wall during stress. The structure of extensin varies between different plant species and between different tissue types. The hormone ethylene has been shown to regulate the expression of extensin (Showalter 1993) and previous work by Meakin and Roberts (1990b) identified a rise in the activity of ethylene in ripening *Brassica napus* fruits. The absence of any staining on sections from *Brassica napus*, and the weak staining observed on sections from *Arabidopsis* and *Brassica juncea* may be due to the amount of homology between the *ExtA* riboprobe, and the product of the extensin genes expressed in the carpel wall tissues of the three different species.

4.7.3. The Endocarp

The endocarp of the silique is composed of two histologically and physiologically different cell layers. The first endocarp layer to differentiate in the pre-fertilised fruit is the layer lining the locule *Ena*. During post-fertilisation development the cell walls of *Ena* differentially thicken mainly along the tangential walls then during the last stages of silique development, stage nine, *Ena* cells collapse to lie adjacent to *Enb*. The inner endocarp layer *Enb* gradually lignifies during post fertilisation development and this process plays a key role in developing the tensions required for dehiscence to occur. The modified pattern of development of *Enb* is associated with the non-'shattering' phenotype in Indian mustard siliques.

of development of *Enb* is associated with the non-'shattering' phenotype in Indian mustard siliques.

4.7.3.1. Endocarp α

Ena differentiates to produce cell walls with a high pectin content as demonstrated by ruthenium red staining which suggests that this layer is quite flexible. However the tensions produced in the carpel wall are eventually enough to cause the disintegration of this layer at stage nine. This process is unlike the senescence process which is observed in the mesocarp layer and appears to be caused by collapsing of the radial cell walls and or collapsing of the tangential wall which lines the locule. The reason for this phenomenon is unclear, but it is probably due to stresses on the walls of *Ena* cells caused by shrinking of the mesocarp and lignification of *Enb* and the dehiscence zone cells.

The pectic cell walls of *Ena* cells in Indian mustard were comparatively thicker than those of the other Brassicas in this study and this cell layer did not collapse in Indian mustard following lignification of *Enb*. Acridine orange staining of mature Indian mustard siliques revealed secondary wall lignification of *Ena* cells primarily along the tangential walls which line the locule. A similar process is observed in the mature exocarp cells of Indian mustard siliques and, as in the exocarp, lignification is probably induced due to stresses on this still relatively intact cell layer. The fact that *Ena* cells begin to lignify if they do not collapse supports the proposal that disintegration of this cell layer in *Arabidopsis* and *Brassica napus* is indeed due to too much stress on the radial walls and not some form of controlled cellular senescence or apoptosis.

Immunological studies using anti-pectin antibodies showed the cell walls of *Ena* in mature siliques are rich in the unesterified pectin recognised by the JIM5 antibody. The unesterified pectin showed a similar pattern of localisation to that observed in the exocarp cells, and was located in the intercellular spaces, a layer adjacent to the plasma membrane and to the middle lamella between adjacent cells. Unesterified pectin was also present in high amounts in the thicker *Ena* cell walls which are adjacent to the locule.

Immunological studies showed the same pattern of unesterified pectin distribution in the cell walls and intercellular spaces of *Ena* in Indian mustard, as that observed in *Arabidopsis*. This suggests that the cell wall structure of *Ena* cells in Indian mustard is the same as that in the other Brassicas in this study, but is thicker. This thicker highly

pectinised endocarp does not collapse under the reduced tensions within the mature carpel walls, but continues to differentiate and finally lignify. Whether the maintenance of an intact *Ena* alters the flexibility of the carpel wall and further reduces the tensions which would normally develop is unclear.

4.7.3.2. Endocarp *b*

The inner endocarp layer *Enb* is the last of the carpel wall layers to differentiate histologically and it is also the last layer to cease cell division. During developmental stages six and seven *Enb* cells continue to divide and extend predominantly along the long axis of the silique. Once cell division has ceased the cell walls then gradually lignify at stage eight and in the mature silique, *Enb* cell walls are considerably thickened prior to dehiscence. The deposition of lignin polymers in the cell wall confers a much greater rigidity to the wall reducing its flexibility.

What triggers lignification in this cell layer is unclear however it may be linked to a cessation of cell division, or it may be caused by stress on the cells from the expanding then shrinking mesocarp and the expanding then collapsing *Ena* cell layer. Two of the enzymes involved in lignin synthesis, peroxidase and phenoloxidase have been identified in lignifying *Enb* cells and the monoclonal antibody JIM13, which recognises a carbohydrate epitope of AGP's, has been localised to the cell walls and plasmalemma of *Enb* cells. Although JIM13 has also been localised to lignifying vascular tissues (Knox *et al.* 1991, Rae *et al.* 1991) its role in the lignification process is still unclear.

Comparative analysis of the phenolics released by the microwave digestion of lignin from *Arabidopsis* stem, leaf and carpel wall tissues were performed to determine if the carpel wall lignin differed in composition to lignin in other parts of the plant. Previous work (Chapple *et al.* 1992, Dharmawardhana *et al.* 1992) showed that *Arabidopsis* lignin is composed of syringyl (S) and guaiacyl (G) units and there was a predominance of G units. A predominance of G units was also found in the carpel wall and stem tissues in this study, as higher levels of vanillin were released from the digestions. Digestions from the leaf tissues also released high levels of vanillin but higher levels of syringic acid were detected. This difference in the relative amounts of oxidation products found in the leaf tissue may be due to an age related process. The leaf tissues were taken from mature plants and may therefore be undergoing senescence and have an altered lignin composition, or include the breakdown products from other phenolics.

The composition of lignin has an effect on its properties, S lignin shows less cross linking than G lignin, and is easier to pulp, and the *Sin1-1* mutant of *Arabidopsis* has a much reduced S content (Chappel *et al.* 1992). Siliques from *Sin1-1* mutant plants showed a similar pattern of dehiscence and similar shattering characteristics as the wild type siliques. The highly cross linked G lignin must therefore be important in conferring rigidity to the endocarp cell walls. It may therefore be more appropriate to replace the G lignin with the less cross linked S lignin in order to alter the tensions in the carpel wall and affect dehiscence or shattering. It may prove difficult however, to specifically target lignification in *Enb* without altering the structure of the lignin in other parts of the plant.

The changes in the pattern of differentiation of *Enb* in Indian mustard may contribute to the increased lignification in the other living carpel wall cell layers. Increased stresses are known to trigger lignification (Grand *et al.* 1982, Lewis & Yamamoto 1990) and this may account for the deposition of lignin in the exocarp, *Ena* and in the mesocarp cells adjacent to *Enb* which are the last to senesce. The deposition of lignin would serve to strengthen the cell walls. Much more lignification is seen in the mesocarp cells than in those of the exocarp or *Ena*, and in the mature non-dehisced silique the mesocarp cells in Indian mustard are labelled strongly by the JIM13 antibody whilst the exocarp and *Ena* are not. As JIM13 only labels the lignified cells of *Enb* when the walls are very thickened, this would indicate a role for the JIM13 antigen in the later stages of lignification and would also suggest that the lignification in the mesocarp cells begins well before that in the exocarp and *Ena*.

4.8. Possible Strategies to Reduce 'Pod Shatter'

The results of this study would indicate that the endocarp cell layer within the carpel wall, can be altered to reduce the shattering characteristic of Brassica siliques. The fruits of the three dehiscing Brassica species in this study appear to show the same pattern of development and pattern of dehiscence so consequently many of the control factors involved must be the same or very similar. The identification of a non-dehiscing variety of *Brassica juncea*, and the identification of the cellular basis for its phenotype, suggests that the biochemical or genetic control factors responsible for this phenotype could be isolated.

Preliminary studies on the monosaccharides released by the hydrolysis of isolated carpel wall tissues, has shown that there are significant differences in the types and amounts of

monosaccharides present in these tissue types. Further work is required to characterise and quantify the released monosaccharides, and future work should include the characterisation and quantification of monosaccharides in the non-'shattering' phenotype. Molecular biological techniques and genetic engineering also may be used to modify the developmental pattern of the siliques of the important Brassica crop plants and reduce seed loss due to 'shattering'.

Phenotypic studies of *Arabidopsis* ethylene mutants indicates that this fruit ripening hormone plays a major role in silique development and this may also be targeted for genetic manipulation. Tomatoes which do not ripen unless exposed to exogenous ethylene have been produced using antisense technology to specifically reduce ethylene biosynthesis in the fruit (Theologis 1992, Gray *et al.* 1994). This approach may also be possible in Brassicas if ethylene biosynthesis genes are differentially expressed in different tissues.

The less well studied plant hormones polyamines have been shown to be involved in fruit ripening (Malmberg 1989, Tiburcio *et al.* 1993) and, although little is known about their effects, these compounds may also prove useful for genetic manipulation experiments. These hormones may act antagonistically with ethylene and therefore alter carpel wall development by delaying senescence of the mesocarp. As polyamines are also found bound to phenolic compounds which are involved in the phenylpropanoid pathway and lignification, these compounds may also influence the development of the endocarp and lignified zone cells.

4.9. CONCLUSION

This thesis proposed that the differentiation of the endocarp layer in the carpel walls of Brassica fruits plays a key role in the pod 'shatter' characteristic. This study has examined the dehiscence characteristics and cellular differentiation of three species of Brassica and, work included in this thesis has shown that the phenotype of the non-'shattering' variety of *Brassica juncea*, Indian mustard, is associated with an altered pattern of endocarp development.

5. REFERENCES

- Aloni R. (1987)
Differentiation of Vascular Tissue
Annual Review of Plant Physiology 38: 179-204
- Alvarez J., Guli C. L., Yu X., & Smyth D. R. (1992)
Terminal Flower: A Gene Affecting Inflorescence Development in *Arabidopsis thaliana*
The Plant Journal 2 (1): 103-116
- Baldwin T. C., McCann M. C. & Roberts K. (1993)
A Novel Hydroxyproline-Deficient Arabinogalactan Protein Secreted by Suspension-Cultured Cells of *Daucus carota* Purification and Partial Characterisation
Plant Physiology 103: 115-123
- Bao W., O'Malley D. M., Whetton R. & Sederoff R. R. (1993)
A Laccase Associated with Lignification in Loblolly Pine Xylem
Science 260: 672-674
- Barbier-Brygoo H., Ephritikhine G., Klambt D., Maurel C., Palme K., Schell J. & Guern J. (1991)
Perception of the Auxin Signal at the Plasma Membrane of Tobacco Mesophyll Protoplasts
The Plant Journal 1: 83-93
- Barnett D. & Shirsat A. H. (1995)
Expression of Extensin Genes in *Arabidopsis*
Journal of Experimental Botany Supplement 46: 41
- Bell S., Coupe S. A., Webb S. J. & Roberts J. A. (1995)
Regulation of Polygalacturonase Gene Expression During Ethylene-Promoted Leaf Abscission
Journal of Experimental Botany Supplement 46: 39
- Bevan M., Shufflebottom D., Edwards K., Jefferson R. & Schuch W. (1989)
Tissue and Cell Specific Activity of a Phenylalanine Ammonia Lyase Promoter in Transgenic Plants
The Embo Journal 8 (7): 1899-1906

- Bleeker A. B., Estelle M. A., Somerville C. & Kende H. (1988)
 Insensitivity to Ethylene Conferred by a Dominant Mutation in *Arabidopsis thaliana*
 Science 241: 1086-1089
- Bowman J. L., Alvarez J., Weigel D., Meyerowitz E. M. & Smyth D. R. (1993)
 Control of Flower Development in *Arabidopsis thaliana* by APETALA1 and Interacting
 Genes
 Development 119: 721-743
- Bowman J. L., Drews G. N. & Meyerowitz E. M. (1991)
 Expression of the *Arabidopsis* Floral Homeotic Gene AGAMOUS is Restricted to Specific
 Cell Types Late in Flower Development
 The Plant Cell 3: 749-758
- Bowman J. L., Smyth D. R. & Meyerowitz E. M. (1989)
 Genes Directing Flower Development in *Arabidopsis*
 The Plant Cell 1: 37-52
- Bowman J. L., Smyth D. R. & Meyerowitz E. M. (1991)
 Genetic Interactions Among Floral Homeotic Genes of *Arabidopsis*
 Development 112: 1-20
- Brady C. J. (1987)
 Fruit Ripening
 Annual Review of Plant Physiology and Plant Molecular Biology 38: 155-177
- Bunting E. S. (1984)
 Oilseed Rape in Perspective: with Particular Reference to Crop Expansion and Distribution
 in England 1973-1983
 Aspects of Applied Biology 6: 11-22
- Carpita N. C. & Gibeaut D. M. (1993)
 Structural Models of Primary Cell Walls in Flowering Plants: Consistency of Molecular
 Structure with the Physical Properties of the Walls During Growth
 The Plant Journal 3 (1): 1-30

Cassab I. & Varner J. E. (1988)

Cell Wall Proteins

Annual Review of Plant Physiology and Plant Molecular Biology 39: 321-354

Chapple C. C. S., Vogt T., Ellis B.E. & Somerville C. R. (1992)

An *Arabidopsis* Mutant Defective in the General Phenylpropanoid Pathway

The Plant Cell 4: 1413-1424

Clark S. E., Running M. P. & Meyerowitz E. M. (1993)

CLAVATA 1, A Regulator of Meristem and Flower Development in *Arabidopsis*

Development 119: 397-418

Carpenter R. & Coen E. S. (1995)

Transposon Induced Chimeras Show That *floricaula*, a Meristem Identity Gene, Acts Non-Autonomously Between Cell Layers

Development 121: 19-26

Coen E. S. (1991)

The Role of Homeotic Genes in Flower Development and Evolution

Annual Review of Plant Physiology and Plant Molecular Biology 42: 241-279

Coen E. S. & Meyerowitz E. M. (1991)

The War of the Whorls: Genetic Interactions Controlling Flower Development

Nature 353: 31-37

Coen E. S., Romero J. M., Doyle S., Elliott R., Murphy G. & Carpenter R. (1990)

floricaula A Homeotic Gene Required for Flower Development in *Antirrhinum majus*

Cell 63: 1311-1322

Coupe S. A. (1993)

Changes in Gene Expression During Pod Development in Oilseed Rape

Ph.D. Thesis, University of Nottingham, UK

- Coupe S. A., Bell S. J. & Roberts J. A. (1995)
 Characterisation of mRNAs During Leaf Abscission and their Role in Cell Separation and Pathogenic Attack
 Journal of Experimental Botany Supplement 46: 31
- Coupe S. A., Taylor J.E., Isaac P. G. & Roberts J. A. (1994a)
 Identification and Characterisation of a Proline-Rich mRNA that Accumulates During Pod Development in Oilseed Rape (*Brassica napus* L)
 Plant Molecular Biology 23: 6, 1223-1232
- Coupe S. A., Taylor J.E., Isaac P. G. & Roberts J. A. (1994b)
 Characterisation of a mRNA that Accumulates During Development of Oilseed Rape Pods
 Plant Molecular Biology 24:1, 223-227
- Cramer C. L., Edwards K., Dron M., Liang X., Dildine S. L., Bolwell G. P., Dixon R. A., Lamb C. J. & Schuch W. (1989)
 Phenylalanine Ammonium Lyase Gene Organisation and Structure
 Plant Molecular Biology 12: 367-385
- Crone W. & Lord E. M. (1993)
 Flower Development in the Organ Number Mutant *Clavata1-1* of *Arabidopsis thaliana* (*Brassicaceae*)
 American Journal of Botany 80: (12) 1419-1426
- del Campillo E., Durbin M. L. & Lewis L. N. (1988)
 Changes in Two Forms of Membrane Associated Cellulase During Ethylene Induced Abscission
 Plant Physiology 88: 904-909
- del Campillo E., Reid P. D., Sexton R. & Lewis L. N. (1990)
 Occurrence and Localisation of 9.5 Cellulase in Abscising and Non-Abscising Tissues
 The Plant Cell 2: 245-254
- Dharmawardhana D. P., Ellis B. E. & Carlson J. E. (1992)
 Characterisation of Vascular Lignification in *Arabidopsis thaliana*
 Canadian Journal of Botany 70: 2238-2244

Drews G. N., Bowman J. L. & Meyerowitz E. M. (1991)
Negative Regulation of the *Arabidopsis* Homeotic Gene AGAMOUS by the APETALA2
Product
Cell 65: 991-1002

Drews J. E. & Gatehouse J. A. (1994)
Isolation and Characterisation of a Pea Pod cDNA Encoding a Putative Blue Copper
Protein Correlated with Lignin Deposition
Journal of Experimental Botany 45: (281), 1873-1884

Eames A. J. (1931)
The Vascular Anatomy of the Flower with Refutation of Carpel Polymorphism
American Journal of Botany 18: 147-188

Eamons A. M. C., Valster A., Valenta R. & Hepler P. K. (1995)
Probing the Plant Actin Cytoskeleton by Profilin Microinjection
Proceedings Royal Microscopical Society 30: 1, 9

Elliott K. A. & Shirsat A. H. (1995)
Promotor Analysis of a Stress Induced Rape Extensin Gene
Journal of Experimental Botany Supplement 46: 41

Estelle M. A. & Sommerville C. R. (1986)
The Mutants of *Arabidopsis*
Trends in Genetics 2: 89-93

Estruch J. J., Granell A., Hansen G., Prinsen E., Redig P., Van Onckelen H., Schwartz-
Sommer Z., Sommer H. & Spina A. (1993)
Floral Development and Expression of Floral Homeotic Genes are Influenced by Cytokinins
The Plant Journal 4: (2) 379-384

Evans I. M., Gatehouse L. N., Gatehouse J. A., Yarwood J. N., Boulter D. & Croy R. R. D. (1990)

The Extensin Gene Family in Oilseed Rape (*Brassica napus* L.): Characterisation of Sequences of Representative Members of the Family

Molecular and General Genetics 223: 273-287

Evans P. T. & Malmberg R. L. (1989)

Do Polyamines have Roles in Plant Development

Annual Review of Plant Physiology and Plant Molecular Biology 40: 235-269

Fischer R. L. & Bennett A. B. (1991)

Role of Cell Wall Hydrolases in Fruit Ripening

Annual Review of Plant Physiology and Plant Molecular Biology 42: 675-703

Fray R. G. & Grierson D. (1993)

Molecular Genetics of Tomato Fruit Ripening

Trend in Genetics 9: (12) 438-443

Gaffe J., Tieman D. M. & Handa A. K. (1994)

Pectin Methylesterase Isoforms in Tomato (*Lycopersicon esculentum*) Tissues

Effects of Expression of a Pectin Methylesterase Antisense Gene

Plant Physiology 105: 199-203

Gahan P. B. (1984)

Plant Histochemistry and Cytochemistry: An Introduction

Academic Press Inc. London

Galletti C. G., Piccaglia R., Chivari G. & Concialini V. (1989)

HPLC/Electrochemical Detection of Lignin Phenolics from Wheat Straw by Direct Injection of Nitrobenzene Hydrolysates

Journal of Agriculture Food and Chemistry 37: 985-987

Garcia-Martinez J. L. & Carbonell J. (1980)

Fruit-Set of Unpollinated Ovaries of *Pisum sativum* L. Influence of Plant-Growth Regulators

Planta 147: 451-456

- Garcia-Martinez J. L. & Carbonell J. (1985)
Induction of Fruit Set and Development in Pea Ovary Explants by Gibberellic Acid
Journal of Plant Growth Regulation 4: 19-27
- Gasser C. S. & Robinson-Beers K. (1993)
Pistil Development
The Plant Cell 5: 1231-1239
- Gillaspy G., Ben-David H. & Gruissem W. (1993)
Fruits: a Developmental Perspective
The Plant Cell 5: 1439-1451
- Goffner D., Joffroy I., Grima-Pettenati J., Halpin C., Knight M.E., Schuch W. & Boudet A. M. (1992)
Purification and Characterisation of Isoforms of Cinnamyl Alcohol Dehydrogenase from Eucalyptus Xylem
Planta 188: 48-53
- Grand C., Boudet A. M. & Ranjeva R. (1982)
Natural Variations and Controlled Changes in Lignification Process
Holz-Forschung 36: 217-223
- Gray J. E., Picton S., Giovannoni J. J. & Grierson D. (1994)
The use of Transgenic and Naturally Occurring Mutants to Understand and Manipulate Tomato Fruit Ripening
Plant Cell and Environment 17: 557-571
- Grierson D. & Schuch W. (1993)
Control of Ripening
Phil. Trans. R. Soc. Lond. B. 342: 241-250
- Gustafson-Brown C., Savidge B. & Yanofsky M. F. (1994)
Regulation of the *Arabidopsis* Floral Homeotic Gene APETELA1
Cell 76: 131-143

- Guzman P. & Ecker J. R. (1990)
Exploiting the Triple Response of *Arabidopsis* to Identify Ethylene-Related Mutants
Plant Cell 2: 513-523
- Hahlbrock K. & Scheel D. (1989)
Physiology and Molecular Biology of Phenylpropanoid Metabolism
Annual Review of Plant Physiology and Plant Molecular Biology 40: 347-369
- Hall L. N., Tucker G. A., Smith C. J. S., Watson C. F., Seymour G. B., Bundick Y., Boniwell J. M., Fletcher J. D., Ray J. A., Schuch W., Bird C. & Grierson D. (1993)
Antisense Inhibition of Pectin Esterase Gene Expression in Transgenic Tomatoes
The Plant Journal 3 (1): 121-129
- Halpin C., Knight M. E., Schuch W. & Foxon G. (1995)
Manipulation of Lignin Quality in Transgenic Tobacco
Journal of Experimental Botany Supplement 46: 39
- Hammerschmidt R. (1984)
Rapid Decomposition of Lignin in Potato Tuber Tissue as a Response to Fungi Non-Pathogenic on Potato
Physiological Plant Pathology 24: 33-42
- Hantke S. S., Carpenter R. & Coen E. S. (1995)
Expression of *floricaula* in Single Cell Layers of Periclinal Chimeras Activates Downstream Homeotic Genes in all Layers of Floral Meristems
Development 121: 27-35
- Haughn G. W., Somerville C. R. (1988)
Genetic Control of Morphogenesis in *Arabidopsis*
Developmental Genetics 9: 73-89
- Hensel L. L., Grbic V., Baumgarten D. A. & Bleeker A. B. (1993)
Developmental and Age-Related Processes that Influence the Longevity and Senescence of Photosynthetic Tissues in *Arabidopsis*
The Plant Cell 5: 553-564

- Hibino T., Shibata D., Chen J-Q. & Higuchi T. (1993)
Cinnamyl Alcohol Dehydrogenase from *Aralia cordata*: Cloning of the cDNA and
Expression of the Gene in Lignified Tissues
Plant Cell Physiology 34 (5): 659-665
- Hill J. P., Lord E. (1989)
Floral Development in *Arabidopsis thaliana*: A Comparison of the *wild type* and the
Homeotic *pistillata* Mutant
Canadian Journal of Botany 67: 2922-2936
- Holt K. A., Foxon G. A. & Halpin C. (1995)
Characterisation of a Maize Lignin Mutant
Journal of Experimental Botany Supplement 46: 31
- Huala E. & Sussex I. M. (1992)
LEAFY interacts with Floral Homeotic Genes to Regulate *Arabidopsis* Floral Development
The Plant Cell 4: 901-913
- Huala E. & Sussex I. M. (1993)
Determination and Cell Interactions in Reproductive Meristems
The Plant Cell 5: 1157-1165
- Huijser P., Klein J., Lonig W-E., Meijer H., Saedler H. & Sommer H. (1992)
Bracteomania, An Inflorescence Anomaly, is Caused by the Loss of Function of the MADS-
Box Gene *squamosa* in *Antirrhinum majus*
The EMBO Journal 11 (4): 1239-1249
- Hush J. M. (1995)
Microtubule Dynamics in Living Plant Cells
Proceedings Royal Microscopical Society 30: 1, 8
- Intapruk C., Higashimura N., Yamamoto K., Okada N., Shinmyo A. & Takano M. (1991)
Nucleotide Sequences of Two Genomic DNAs Encoding Peroxidase of *Arabidopsis*
thaliana
Gene 98: 237-241

Irish V F. & Sussex I. M. (1990)

Function of the *apetela2* Gene During *Arabidopsis* Floral Development
The Plant Cell 2: 741-753

Irish V. F. & Sussex I. M. (1992)

A Fate Map of the *Arabidopsis* Embryonic Shoot Apical Meristem
Development 115: 745-753

Jack T., Brockman L. L. & Meyerowitz E. M. (1992)

The Homeotic Gene *Apetela 3* of *Arabidopsis thaliana* Encodes a MADS Box and is
Expressed in Petals and Stamens
Cell 68: 683-697

Kakkar R. K. & Rai V. K. (1993)

Plant Polyamines in Flowering and Fruit Ripening
Phytochemistry 33: (6) 1281-1288

Karlsson B. H., Sills G. R. & Nienhuis J. (1993)

Effects of Photoperiod and Vernalisation on the Number of Leaves at Flowering in 32
Arabidopsis thaliana (Brassicaceae) Ecotypes
American Journal of Botany 80: (6), 646-648

Keller B. (1993)

Structural Cell Wall Proteins
Plant Physiology 101: 1127-1130

Kemmerer E. C. & Tucker M. L. (1994)

Comparative Study of Cellulases Associated with Adventitious Root Initiation, Apical Buds,
and Leaf, Flower, and Pod Abscission Zones in Soybean
Plant Physiology 104: 557-562

Kende H. (1993)

Ethylene Biosynthesis
Annual Review of Plant Physiology and Plant Molecular Biology 44: 283-307

- Kim S-H, Terry M. E., Hoops P., Dauwalder M. & Roux S. J. (1988)
Production and Characterisation of Monoclonal Antibodies to Wall Localised Peroxidases from Corn Seedlings
Plant Physiology 88: 1446-1453
- Klee H. J. (1993)
Ripening Physiology of Fruit from Transgenic Tomato (*Lycopersicon esculentum*) Plants with Reduced Ethylene Synthesis
Plant Physiology 102: 911-916
- Knauf V. C. (1987)
The Application of Genetic Engineering to Oilseed Crops
Trends in Biotechnology 5: 40-47
- Knox J. P., Day S. & Roberts K (1989)
A Set of Cell Surface Glycoproteins Forms an Early Marker of Cell Position, but Not Cell Type, in the Root Apical Meristem of *Daucus carota* L
Development 106: 47-56
- Knox J.P., Linstead P. J., King J., Cooper C. & Roberts K. (1990)
Pectin Esterification is Spatially Regulated both within Cell Walls and Between Developing Tissues of Root Apices
Planta 181: 512-521
- Knox J. P., Linstead P. J., Peart J., Cooper C. & Roberts K. (1991)
Developmentally Regulated Epitopes of Cell Surface Arabinogalactan Proteins and their Relation to Root Tissue Pattern Formation
The Plant Journal 1: (3): 317-326
- Komaki M. K., Okada K., Nishino E. & Shimura Y. (1988)
Isolation and Characterisation of Novel Mutants of *Arabidopsis thaliana* Defective in Flower Development
Development 104: 195-203

Labuda T. (1981)

The Oilseed Rape Crop in the U.K.

Oilseed Rape Book- a Manual for Growers, Farmers and Advisers

Cambridge Agricultural Publishing, Cambridge

Lewis G. L. & Yamamoto E. (1990)

Lignin: Occurrence Biogenesis and Biodgradation

Annual Review of Plant Physiology and Plant Molecular Biology 41: 455-496

Leyser H. M. O. & Furner I. J. (1992)

Characterisation of Three Shoot Apical Meristem Mutants of *Arabidopsis thaliana*

Development 116: 397-403

Leyser H. M. O., Edwards M., Lincoln C. A., Timpte C. S., Turner J. C., Lammer D., Pickett F. B. & Estelle M. A. (1995)

Auxin and Cell Signalling in Mutants of *Arabidopsis*

Journal of Experimental Botany 46: 72

Lincoln C., Britton J. H. & Estelle M. (1990)

Growth and Development of the *axr1* Mutants of *Arabidopsis*

The Plant Cell 2: 1071-1080

Lister C. & Dean C. (1993)

Recombinant Inbred Lines for Mapping RFLP and Phenotypic Markers in *Arabidopsis thaliana*

The Plant Journal 4:(4) 745-750

Liu C-m, Xu Z-h, & Chua N-H (1993)

Auxin Polar Transport is Essential for the Establishment of Bilateral Symmetry During Early Plant Embryogenesis

The Plant Cell 5: 621-630

Lloyd C., Yuan M., Shaw P. & Warn R. (1995)

Cytoskeletal Reorganisation in Living Plant Cells

Proceedings Royal Microscopical Society 30: 1, 11

- Lyndon R. F. (1990)
Plant Development: The Cellular Basis
London Unwin Hyman
- Ma H, Yanofski M. F. & Meyerowitz E. M. (1991)
AGL1-AGL6, an *Arabidopsis* Gene Family with Similarity to Floral Homeotic and
Transcription Factor Genes
Genes and Development 5: 484-495
- MacLeod J. (1981)
Harvesting in Oilseed Rape
Cambridge Agricultural Publishing 107-120
- Mader M., Ungemach J. & Schloss P. (1980)
The Role of Peroxidase Isoenzyme Groups of *Nicotiana tabacum* in Hydrogen Peroxide
Formation
Planta 147: 467-470
- Marcus A., Greenberg J. & Averyhart-Fullard V. (1991)
Repetitive Proline Rich Proteins in the Extracellular Matrix of the Plant Cell
Physiologia Plantarum 81: 273-279
- Markovic O. & Jornvall H. (1986)
Pectinesterase The Primary Structure of the Tomato Enzyme
European Journal of Biochemistry 158: 455-462
- Mayer U., Buttner G. & Jurgens G. (1993)
Apical-Basal Pattern Formation in the *Arabidopsis* Embryo: Studies on the Role of the
GNOM Gene
Development 117: 149-162
- McDougall G. J., Stewart D. & Morrison M. (1994)
Cell-Wall-Bound Oxidases from Tobacco (*Nicotiana tabacum*) Xylem Participate in Lignin
Formation
Planta 194: 9-14

McManus M. T. (1994)

Peroxidases in the Separation Zone During Ethylene-Induced Bean Leaf Abscission
Phytochemistry 35: 567-572

Meakin P. J. (1988)

The Physiology of Bud Abscission and Pod Shatter in Oilseed Rape (*Brassica napus* L.)
Ph.D. Thesis, University of Nottingham, UK

Meakin P. J. & Roberts J. A. (1990a)

Dehiscence of Fruit in Oilseed rape (*Brassica napus* L). 1. Anatomy of Pod Dehiscence
Journal of Experimental Botany 41 (229): 995-1002

Meakin P. J. & Roberts J. A. (1990b)

Dehiscence of Fruit in Oilseed Rape (*Brassica napus* L). 2 The Role of Cell Wall Degrading
Enzymes and Ethylene
Journal of Experimental Botany 41 (229): 1003-1011

Medford J. I. (1992)

Vegetative Apical Meristems
The Plant Cell 4: 1029-1039

Medford J. I., Behringer F. J., Callos J. D. and Feldmann K. A. (1992)

Normal and Abnormal Development in the Arabidopsis Vegetative Shoot Apex
The Plant Cell 4: 631-643

Meeks-Wagner D. R. (1993)

Gene Expression in the Early Floral Meristem
The Plant Cell 5: 1167-1174

Meyerowitz E. M. (1989)

Arabidopsis: A Useful Weed
Cell 56: 263-269

Meyerowitz E. M. & Pruitt R. E. (1985)

Arabidopsis thaliana and Plant Molecular Genetics
Science 229: 1214-1218

Miksche J. P., Brown J. A. M. (1965)

Development of Vegetative and Floral Meristems of *Arabidopsis thaliana*

American Journal of Botany 52 (6): 533-537

Mizukami Y. & Ma H (1992)

Ectopic Expression of the Floral Homeotic Gene AGAMOUS in Transgenic *Arabidopsis* Plants Alters Floral Organ Identity

Cell 71: 119-131

Montgomery J., Pollard V., Deikman J. & Fischer R. L. (1993)

Positive and Negative Regulatory Regions Control the Spatial Distribution of Polygalacturonase Transcription in Tomato Fruit Pericarp

The Plant Cell 5: 1049-1062

Morgan P. W., He C-J & Drew M. C. (1992)

Intact Leaves Exhibit a Climacteric-Like Rise in Ethylene Production Before Abscission

Plant Physiology 100: 1587-1590

Murphy D. J. (1992)

Modifying Oilseed Crops for Non-Edible Products

Trends in Biotechnology 10: 84-87

Ohl S., Hedrick S. A., Chory J. & Lamb C. J. (1990)

Functional Properties of a Phenyl Ammonia Lyase Promoter from *Arabidopsis*

The Plant Cell 2: 837-848

Okada K., Komaki M. K. & Shimura Y. (1989)

Mutational Analysis of Pistil Structure and Development of *Arabidopsis thaliana*

Cell Differentiation and Development 28: 27-38

Okada K., Ueda J., Komaki M. K., Bell C. J. & Shimura Y. (1991)

Requirement of the Auxin Polar Transport System in Early Stages of *Arabidopsis* Floral Bud Formation

The Plant Cell 3: 677-684

Okamoto J. K., den Boer B. G. W. & Jofuku K. D. (1993)

Regulation of *Arabidopsis* Flower Development

The Plant Cell 5: 1183-1193

O'Malley D. M., Whetton R., Bao W., Chen C-L. & Sederoff R. R. (1993)

The Role of Laccase in Lignification

The Plant Journal 4: 5: 751-757

Ooms J. J. J., Leon-Kloosterziel K. M., Bartels D., Koorneef M. & Karssen C. M. (1993)

Acquisition of Desiccation Tolerance and Longevity in Seeds of *Arabidopsis thaliana*

Plant Physiology 102: 1185-1191

Osborne D. J. (1989)

Abscission

Critical Reviews in Plant Science 8: 103-129

Palme K., Heisse T., Campos T., Garbers C., Yanofsky M. F. & Schell J. (1992)

Molecular Analysis of an Auxin Binding Protein Located on Chromosome 4 of *Arabidopsis*

The Plant Cell 4: 193-201

Peleman J., Boerjan W., Engler G., Seurinck J., Botterman J., Alliotte T., Van Montagu M. & Inze D. (1989)

Strong Cellular Preference in the Expression of a Housekeeping Gene of *Arabidopsis thaliana* Encoding S-Adenosylmethionine Synthase

The Plant Cell 1: 81-93

Peng J. & Harberd N. P. (1993)

Derivative Alleles of the *Arabidopsis* Gibberellin-Insensitive (*gai*) Mutation Confers a Wild Type Phenotype

The Plant Cell 5: 351-360

Pennell R. I., Knox J. P., Scofield G. N., Selvendran R. R. & Roberts K. (1989)

A Family of Abundant Plasma Membrane-Associated Glycoproteins Related to the Arabinogalactan Proteins is Unique to Flowering Plants

The Journal of Cell Biology 108: 1967-1977

Pennell R. I. & Roberts K. (1990)

Sexual Development of the Pea is Presaged by Altered Expression of Arabinogalactan Protein

Nature 344: 547-549

Pennell R. I., Janniche L., Kjellbom P., Scofield G. N., Peart J. M. & Roberts K. (1991)

Developmental Regulation of a Plasma Membrane Arabinogalactan Protein Epitope in Oilseed Rape Flowers

The Plant Cell 3: 1317-1326

Picart J. A. & Morgan D. G. (1984)

Pod Development in Relation to Pod Shattering.

Aspects of Applied Biology, 6 Agronomy, physiology, plant breeding and crop protection of oilseed rape, 101-110

Picart J. A. & Morgan D. G. (1986)

Preliminary Studies of the Effects of 4-Chlorophenoxyacetic Acid on the Senescence and Dehiscence of Pods in Oilseed Rape (*Brassica napus* L.)

Plant Growth Regulation 4: 169-175

Polowick P. L., Sawhney V. K. (1986)

A Scanning Electron Microscopic Study on the Initiation and Development of Floral Organs of *Brassica napus* (cv. westar)

American Journal of Botany 73 (2): 254-263

Prakash S. & Chopra V. L. (1988)

Introgression of Resistance to Shattering in *Brassica napus* from *Brassica juncea* Through Non-Homologous Recombination

Plant Breeding 101: 167-168

Prakash S. & Chopra V. L. (1990)

Reconstruction of Allopolyploid Brassicas Through Non-Homologous Recombination: Introgression of Resistance to Pod Shatter in *Brassica napus*

Genetic Research, Cambridge 56: 1-2

- Provan G. J., Scobbie L. & Chesson A. (1994)
Determination of Phenolic Acids in Plant Cell Walls by Microwave Digestion
Journal of Science Food and Agriculture 64: 63-65
- Pyke K. A., Marrison J. L. & Leech R. M. (1991)
Temporal and Spatial Development of the Expanding First Leaf of *Arabidopsis thaliana*
Journal of Experimental Botany 42 (244): 1407-1416
- Rae A. L., Perotto S., Knox J. P., Kannenberg E. L. & Brewin N. J. (1991)
Expression of Extracellular Glycoproteins in the Uninfected Cells of Developing Pea Nodule Tissue
Molecular Plant-Microbe Interactions 4: (6): 563-570
- Ray J., Knapp J., Grierson D., Bird C. & Schuch W. (1988)
Identification and Sequence Determination of a cDNA Clone for Tomato Pectin Esterase
European Journal of Biochemistry 174:119-124
- Raz V. & Fluhr R. (1992)
Calcium Requirement for Ethylene-Dependent Responses
The Plant Cell 4: 1123-1130
- Redei G. P. (1975)
Arabidopsis as a Genetic Tool
Annual Review of Genetics 9: 111-127
- Rinne P., Tuominen H. & Junttila O. (1992)
Arrested Leaf Abscission in the Non-Abscising Variety of Pubescent Birch: Developmental, Morphological and Hormonal Aspects
Journal of Experimental Botany 43: (252) 975-982
- Roberts K. (1990)
Structures at the Plant Cell Surface
Current Opinions in Cell Biology 2: 920-928

Roe J. L., Rivin C. J., Sessions R. A., Feldmann K. A. & Zambryski P. C. (1993)
The TOUSLED Gene in *A. Thaliana* Encodes a Protein Kinase Homolog that is Required
for Leaf and Flower Development
Cell 75: 939-950

Romano C. P., Cooper M. L., & Klee H. J. (1993)
Uncoupling Auxin and Ethylene Effects in Transgenic Tobacco and *Arabidopsis* Plants
The Plant Cell 5: 181-189

Sato Y., Sugiyama M., Gorecki R. J., Fukuda H. & Komamine A. (1993)
Interrelationship Between Lignin Deposition and the Activities of Peroxidase Isoenzymes in
Differentiating Tracheary elements of *Zinnia*
Planta 189: 584-589

Saunders E. R. (1929)
On a New View of the Nature of the Median Carpels in the Cruciferae
American Journal of Botany 16: 122-137

Schultz E. A. & Haughn G. W. (1991)
LEAFY a Homeotic Gene that Regulates Inflorescence Development in *Arabidopsis*
The Plant Cell 3: 771-781

Schultz E. A. & Haughn G. W. (1993)
Genetic Analysis of the Floral Initiation Process (FLIP) in *Arabidopsis*
Development 119: 745-765

Schwartz-Sommer Z., Huijser P., Nacken W., Saedler H. & Sommer H. (1990)
Genetic Control of Flower Development by Homeotic Genes in *Antirrhinum majus*
Science 250: 931-936

Schwartz-Sommer Z., Hue I., Huijser P., Flor P. J., Hansen R., Tetens F., Lonig W-E.,
Saedler H. & Sommer H. (1992)
Characterisation of the *Antirrhinum* Floral Homeotic MADS-Box Gene *Deficiens*: Evidence
for DNA Binding and Autoregulation of its Persistent Expression Throughout Flower
Development
The EMBO Journal 11 (1): 251-263

Sexton R. & Roberts J. A. (1982)

Cell Biology of Abscission

Annual Review of Plant Physiology 33: 133-162

Shannon S. & Meeks-Wagner D. R. (1991)

A Mutation in the *Arabidopsis* TFL1 Gene Affects Inflorescence Meristem Development

The Plant Cell 3: 877-892

Shannon S. & Meeks-Wagner D. R. (1993)

Genetic Interactions that Regulate Inflorescence Development in *Arabidopsis*

The Plant Cell 5: 639-655

Shimomura S., Liu W., Inohara N., Watanabe S. & Futai M. (1993)

Structure of a Gene for an Auxin Binding Protein and a Gene for 7SL RNA from *Arabidopsis thaliana*

Plant Cell Physiology 34 (4): 633-637

Shiraishi H., Okada k. & Shimura Y. (1993)

Nucleotide Sequences Recognised by the AGAMOUS MADS Domain of *Arabidopsis thaliana* *in Vitro*

The Plant Journal 4 (2): 385-398

Shirsat A. H., Wilford N., Evans I. M., Gatehouse L. N. & Croy R. R. D. (1991)

Expression of a *Brassica napus* Extensin Gene in the Vascular System of Transgenic Tobacco and Rape Plants

Plant Molecular Biology 17: 701-709

Showalter A. M. (1993)

Structure and Function of Plant Cell Wall Proteins

The Plant Cell 5: 9-23

Sitbon F., Edlund A., Gardestrom P., Olsson O. & Sandberg G. (1993)

Compartmentation of Indole-3-Acetic Acid Metabolism in Protoplasts Isolated from Leaves of Wild Type and IAA-Overproducing Transgenic Tobacco Plants

Planta 191: 274-279

Smith C. G., Rodgers M. W., Zimmerlin A., Ferdinando D. & Bolwell G. P. (1994)
Tissue and Subcellular Immunolocalisation of Enzymes of Lignin Synthesis in
Differentiating and Wounded Hypocotyl Tissue of French Bean (*Phaseolus vulgaris* L)
Planta 192: 155-164

Smith C. J. S., Watson C. F., Morris P. C., Bird C. R., Seymour G. B., Gray J. E., Arnold
C., Tucker G. A., Schuch W., Harding S. & Grierson D. (1990)
Inheritance and Effect on Ripening of Antisense Polygalacturonase Genes in Transgenic
Tomatoes
Plant Molecular Biology 14: 369-379

Smyth D. R., Bowman J. L., Meyerowitz E. M. (1990)
Early Flower Development in *Arabidopsis*
The Plant Cell 2: 755-767

Sommer H., Beltran J-P., Huijser P., Pape H., Lonnif W-E., Saedler H. & Schwartz-
Sommer Z. (1990)
Deficiens, A Homeotic Gene Involved in the Control of Flower Morphogenesis in
Antirrhinum majus: The Protein Shows Homology to Transcription Factors
The EMBO Journal 9 (3): 605-613

Song K. & Osborn T. C. (1992)
Polyphyletic Origins of *Brassica napus*: New Evidence Based on Organelle and Nuclear
RFLP Analyses
Genome 35: 992-1001

Spence (1992)
Development of the silique of *Arabidopsis thaliana*
MSc. Thesis, University of Durham, UK

Stacey N. J., Roberts K. & Knox J. P. (1990)
Patterns of Expression of the JIM4 Arabinogalactan Protein Epitope in Cell Cultures and
During Somatic Embryogenesis in *Daucus carota* L
Planta 180: 285-292

Steeves T. A. & Sussex I. M. (1989)
Patterns in Plant Development, 2nd ed.
New York: Cambridge University Press

Sterjiades R., Dean J. F. D. & Eriksson K-E. L. (1992)
Laccase from Sycamore Maple (*Acer pseudoplatanus*) Polymerises Monolignols
Plant Physiology 99: 1162-1168

Sterjiades R., Dean J. F. D., Gamble G., Himmelsbach D. S. & Eriksson K-E. L. (1993)
Extracellular Laccases and Peroxidases from Sycamore Maple (*Acer pseudoplatanus*) Cell
Suspension Cultures
Planta 190: 75-87

Sticher L., Penel C. & Greppin H. (1981)
Calcium Requirement for the Secretion of Peroxidase by Plant Cell Suspension
Journal of Cell Science 48: 345-355

Szymkowiak & Sussex (1992)
The Internal Meristem Layer (L3) Determines Floral Meristem size and Carpel Number in
Tomato Periclinal Chimeras
The Plant Cell 4: 1089-1100

Talon M., Koorneef M. & Zeevaart J. A. D. (1990)
Endogenous Gibberellins in *Arabidopsis thaliana* and Possible Steps Blocked in the
Biosynthetic Pathways of the Semi-Dwarf *ga4* and *ga5* Mutants
Proceedings National Academy Science USA 87: 7983-7987

Taylor J. E., Tucker G. A., Lasslett Y., Smith C. J. S., Arnold C. M., Watson C. F., Schuch
W., Grierson D. & Roberts J. A. (1990)
Polygalacturonase Expression During Leaf Abscission of Normal and Transgenic Tomato
Plants
Planta 183: 133-138

Taylor J. E., Webb S. T. J., Coupe S. A., Tucker G. A. & Roberts J. A. (1993a)
Changes in Polygalacturonase Activity and Solubility of Polyuronides During Ethylene
Stimulated Leaf Abscission in *Sambucus nigra*
Journal of Experimental Botany 44: 93-98

Taylor J. E., Webb T. J., Coupe S. A., Tucker G. A. & Roberts J. A. (1993)
Changes in Polygalacturonase Activity and Solubility of Polyuronides During Ethylene-
Stimulated Leaf Abscission in *Sambucus nigra*
Journal of Experimental Botany 44 (258): 93-98

Theologis A. (1992)
One Rotten Apple Spoils the Whole Bushel: The Role of Ethylene in Fruit Ripening
Cell 70: 181-184

Thimann K. V. (1980)
Senescence in Plants
CRC Series in Aging CRC Press Inc.

Thompson D. S. & Osborne D. J. (1994)
A Role for the Stele in Intertissue Signaling in the Initiation of Abscission in Bean Leaves
(*Phaseolus vulgaris* L.)
Plant Physiology 105: 341-347

Tieman D. M., Harriman R. W., Ramamohan G. & Handa A. K. (1992)
An Antisense Pectin Methyltransferase Gene Alters Pectin Chemistry and Soluble Solids in
Tomato Fruit
The Plant Cell 4: 667-679

Timpte C. S., Wilson A. K. & Estelle M. (1992)
Effects of the *axr2* Mutation of *Arabidopsis* on Cell Shape in Hypocotyl and Inflorescence
Planta 188: 271-278

Trobner W., Ramirez L., Motte P., Hue I., Huijser P., Lonig W-E., Saedler H., Sommer H. & Schwartz-Sommer Z. (1992)

Globosa: A Homeotic Gene which Interacts with *Deficiens* in the Control of *Antirrhinum* Floral Organogenesis

The EMBO Journal 11 (13): 4693-4704

Tsukaya H., Naito S., Redei G. P. & Komeda Y. (1993)

A New Class of Mutations in *Arabidopsis thaliana*, *acaulis* 1, Affecting the Development of both Inflorescences and Leaves

Development 118: 751-764

Tiburcio A. F., Campos J. L., Figueras X. & Besford R. T. (1993)

Recent Advances in the Understanding of Polyamine Functions During Plant Development
Plant Growth Regulation 12: 331-340

Tucker M. L., Sexton R. del Campillo E. & Lewis L. N. (1988)

Bean Abscission Cellulase, Characterisation of a cDNA Clone and Regulation of Gene Expression by Ethylene and Auxin

Plant Physiology 88: 1257-1262

Tucker M. L., Baird S. L. & Sexton R. (1991)

Bean Leaf Abscission: Tissue Specific Accumulation of a Cellulase mRNA

Planta 186: 52-57

U N. (1935)

Genomic Analysis of *Brassica* with Special Reference to the Experimental Formation of *B. napus* and its Peculiar Mode of Fertilisation

Japanese Journal of Botany 7: 389-452

Vercher Y., Molowny A., Lopez C., Garcia-Martinez J. L. & Carbonell J. (1984)

Structural Changes in the Ovary of *Pisum sativum* L. Induced by Pollination and Gibberellic Acid

Plant Science Letters 36: 87-91

- Vercher Y., Molowny A. & Carbonell J. (1987)
Gibberellic Acid Effects of the Ultrastructure of Endocarp Cells of Unpollinated Ovaries of *Pisum sativum* L
Physiologia Plantarum 71: 302-308
- van Huystee R. B. (1987)
Some Molecular Aspects of Plant Peroxidase: Biosynthetic Studies
Annual Review of Plant Physiology 38: 205-219
- Webb S. T. J., Taylor J. E., Coupe S. A., Ferrarese L. & Roberts J.A. (1993)
Purification of β -1,4-Glucanase from Ethylene-Treated Abscission Zones of *Sambucus nigra*
Plant Cell and Environment 16: 329-333
- Weberling F. (1989)
Morphology of Flowers and Inflorescences
Cambridge: Cambridge University Press
- Weigel D., Alvarez J., Smyth D. R., Yanofsky M. F. & Meyerowitz E. M. (1992)
LEAFY Controls Floral Meristem Identity in *Arabidopsis*
Cell 69: 843-859
- Wiegel D. & Meyerowitz E. M. (1994)
The ABC's of Floral Homeotic Genes
Cell 78: 203-209
- Wilkinson E. M. & Butt V.S. (1992)
Enzyme Changes During Lignogenesis in Pea Shoots Induced by Illumination
Journal of Experimental Botany 43 (254): 1259-1265
- Wilson A. K., Pickett F. B., Turner J. C. & Estelle M. (1990)
A Dominant Mutation in *Arabidopsis* Confers Resistance to Auxin, Ethylene and Abscisic Acid
Molecular and General Genetics 222: 377-383

- Wilson R. N., Heckman J. W. & Sommerville C. R. (1992)
Gibberellin is Required for Flowering in *Arabidopsis thaliana* Under Short Days
Plant Physiology 100: 403-408
- Winston P. W. & Bates D. H. (1960)
Saturated Solutions for the Control of Humidity in Biological Research
Ecology 41: (1) 232-237
- Wrathall J.E. (1978)
This Changing World. The Oilseed Revolution in England and Wales
Geography 63: 42-45
- Wrathall J. E. & Moore R. (1986)
This Changing World. Oilseed Rape in Great Britain - The End of a Revolution
Geography 71: 351-355
- Wyrambik D. & Grisbach H. (1975)
Purification and Properties of Isoenzymes of Cinnamyl Alcohol Dehydrogenase from
Soyabean Cell Suspension Cultures
European Journal of Biochemistry 59: 9-15
- Xu Y. & van Huystee R. B. (1993)
Association of Calcium and Calmodulin to Peroxidase Secretion and Activation
Journal of Plant Physiology 141: 141-146
- Yang S. F. & Hoffman N. E. (1984)
Ethylene Biosynthesis and its Regulation in Higher Plants
Annual Review of Plant Physiology 35: 155-189
- Yanofsky M. F., Ma H., Bowman J. L., Drews G. N., Feldmann K. A. & Meyerowitz E. M.
(1990)
The Protein Encoded by the *Arabidopsis* Homeotic Gene AGAMOUS Resembles
Transcription Factors
Nature 346: 35-39

Zeevaart J. A. D. & Creelman R. A. (1988)

Metabolism and Physiology of Abscisic Acid

Annual Review of Plant Physiology and Plant Molecular Biology 39: 439-473



'Pod shatter' in *Arabidopsis thaliana*, *Brassica napus* and *B. juncea*

J. SPENCE,* Y. VERCHER,† P. GATES* & N. HARRIS*

*University of Durham, Department of Biological Sciences, Durham DH1 3LE, U.K.

†Manchester Metropolitan University, Manchester M15 6BG, U.K.

Key words. *Arabidopsis thaliana*, *Brassica napus*, *B. juncea*, cytochemistry, development, pod, silique.

Summary

Wild Brassica plants release seeds by a pod shattering mechanism; in related crop plants, such as oil-seed rape, this can result in substantial loss of seed, and hence loss of revenue, and also in the distribution of seeds which can contaminate future crops and the environment. To identify strategies which may be used to reduce shatter, either by conventional breeding programmes or by genetic engineering, we have examined fruit development in oil-seed rape (*Brassica napus*), and in the related *B. juncea* and *Arabidopsis*, using a combination of cytological, cytochemical and molecular techniques. We report here on the patterns of cellular differentiation and tissue development during fruit maturation, and suggest how this results in the shattering phenotype.

Introduction

The problem

In recent years oil-seed rape (*Brassica napus*) has become an important crop plant (Wrathall, 1978; Labuda, 1981; Wrathall & Moore, 1986); although it was initially introduced as a break crop in barley production (Bunting, 1984) it is now an important source of vegetable oil for human consumption and protein meal for animal feedstuffs. Oil-seed rape belongs to the Brassica family which also includes other important crop plants such as cauliflower, turnip and mustard. The more recent introduction of oil-seed rape as a crop plant means that selection and breeding programmes have been limited in comparison with those applied, for example, to cereals and pulses. Much present research is directed at seed-oil modification using genetic engineering (Knauf, 1987; Murphy, 1992). 'Pod shatter', a means by which seed may be released, is of benefit to wild species but is an economically significant problem with Brassica crops and has still to be overcome. The fruits of the

oil-seed rape plant do not mature synchronously, but sequentially, and some pods 'shatter' before harvesting. This can cause a loss of up to 50% of the potential yield if harvesting is delayed by adverse conditions (MacLeod, 1981) and 'volunteers', which grow from the seeds of shattered pods, may remain in the soil to contaminate future crops. The seeds from shattered pods are frequently scattered outside the boundary of the field and contaminate the environment, with oil-seed rape plants now often seen, for example, in hedgerows and roadside verges.

The structure of the *B. napus* 'pod', strictly a silique/silique because of the presence of a central pseudoseptum, has been described (Picart & Morgan, 1984); the fruit wall (carpel) encloses two locules separated by the septum (see Fig. 3). The dehiscence zones develop at the carpel margins adjacent to the septum and run the length of the silique. The cells of the dehiscence zone eventually begin to degrade and this weakens the contact between the carpel walls, or valves, and the septum. The loss of cellular cohesion is confined to the cells of the dehiscence zone and results from middle lamella breakdown (Meakin & Roberts, 1990a,b).

The early differentiation of the tissues of the silique has not been described, nor have the patterns of development which result in pod shatter been clearly identified. In addition to examining these in *B. napus* we are carrying out studies of pod shatter in *Arabidopsis thaliana*. Rape is large, slow to mature and rather aromatic, whereas *Arabidopsis*, which is closely related, is small, has a rapid growth cycle, and has genetic and other characteristics which have resulted in this species being the focus of numerous international research programmes on the control of plant growth development and function (Meyerowitz, 1989, and references therein).

A 'model system'

Arabidopsis shows wide genetic diversity both in the range of ecotypes and an ever-increasing pool of mutants stocks

*Correspondence: N. Harris.

which are maintained by several international seedbanks. Many ecotypes of *Arabidopsis*, which show natural variations in their phenotype, are found in different geographical locations. The variations found among wild type plants include responses to vernalization (Karlsson *et al.*, 1993), variations in leaf morphology and number, variations in flowering time, and fruit set, but no differences in fruit dehiscence have been recorded.

Most experimental work has been carried out using the Columbia or Landsberg *erecta* phenotypes and many of the documented mutants are derived from one of these two races. The *erecta* mutation causes a short erect phenotype. These two phenotypes have also been crossed to generate recombinant inbred lines which can be used for mapping phenotypic and restriction fragment length polymorphism markers (Lister & Dean, 1993).

Changes in patterns of gene expression and metabolism within the shoot apical meristem mark the transition from vegetative to reproductive growth, with the vegetative meristem being transformed initially into an inflorescence meristem (Steeves & Sussex, 1989). This produces stem and floral meristems and may show a determinate or an indeterminate pattern of growth depending on the species (Weberling, 1989). *Arabidopsis* and *Brassica* spp. show an indeterminate pattern of growth and do not normally produce a terminal flower, but growth terminates eventually, with senescence of the shoot apical meristem after production of a few aborted flowers.

The gene *LEAFY* has been identified as one of the factors controlling the transition from an inflorescence to a floral meristem (Okamoto *et al.*, 1993). *TERMINAL FLOWER* (*TFL*) also affects the inflorescence meristem in *Arabidopsis*. In *tfl* mutants, the normally undifferentiated central zone of the inflorescence meristem produces floral meristems. This changes the pattern of growth of the inflorescence meristem from indeterminate to determinate (Shannon & Meeks-Wagner, 1991, 1993; Alvarez *et al.*, 1992).

The floral meristem produces the various floral organs, and these differ considerably among species. In *Arabidopsis* the four types of floral organs are produced in a whorled phyllotaxy, with each organ type occupying a discrete whorl. The four sepals, which develop first, occupy the outer first whorl, petals whorl two and stamens whorl three. The gynoecium, which develops into the fruit, occupies the inner fourth whorl and is the last organ to develop. The floral meristem is therefore by its nature determinate. The early development of the *Arabidopsis* flower has been described in detail (Hill & Lord, 1989; Smyth *et al.*, 1990), and is similar to that described for other crucifers including *B. napus* (Polowick & Sawhney, 1986). There are numerous floral mutants of *Arabidopsis* and analysis of these has led to the identification of floral homeotic genes; such genetic control of flower development is a topic which has been reviewed extensively (e.g. Schwartz-

Sommer *et al.*, 1990; Coen, 1991; Coen & Meyerowitz, 1991).

Fruit development and structure

The female part of the flower, the gynoecium, which develops into the fruit varies in morphology between species and although the origin and structure of the fruit is still a subject of controversy, the classical view is that the fruit developed from modified leaves or leaf-like structures (Gillaspay *et al.*, 1993). The fruit is formed from either a single or a number of units called carpels. There are conflicting hypotheses concerning the number of carpels which constitute the fruit; in keeping with recent authors (Hill & Lord, 1989; Kunst *et al.*, 1989; Okada *et al.*, 1989) we consider the gynoecium to consist simply of two carpels. The carpels form a stigma, to which the pollen adheres and germinates, a style, through which pollen tubes grow, and an ovary, which contains the ovules. The ovules are attached to the placental tissue, which lines part of the ovary wall, by a stalk called the funicle. The cavity into which the ovules protrude is called the locule, and the structure which separates two or more locules is the septum. Most gynoecia comprise two or more carpels and the carpels may be free (apocarpous) or fused (syncarpous). The fruit wall is usually termed the pericarp and generally develops from the carpel walls. The pericarp is usually differentiated into three distinct tissue layers: the outer exocarp, the middle mesocarp and the inner endocarp.

The central portion of the *Arabidopsis* flower first gives rise to a dome-shaped gynoecial primordia which consists entirely of meristematic cells. These cells differentiate to form an elliptical, open-ended cylinder with a central fissure, which is lined with meristematic cells (Hill & Lord, 1989; Okada *et al.*, 1989; Smyth *et al.*, 1990) and has two opposing, rudimentary vascular bundles. The histological development of the *Arabidopsis* silique has been studied (Spence, 1992), and the development divided into 10 stages based on distinct histological events. The first five stages are concerned with the development of the gynoecium, from inception until fertilization, and a further five stages can be identified in the post-fertilization development to senescence. Mutations which affect the gynoecium include *clavata* (*clv*); *clv1* siliques are club shaped and possess 2–5 locules, although four locules is the most common (Haughn & Sommerville, 1988; Okada *et al.*, 1989; Leyser & Furner, 1992), and some flowers also have extra organs in the other floral whorls.

Following fertilization, two of the major processes involved in fruit ripening are the development of the seeds and the fruit wall (Brady, 1987; Fisher & Bennett, 1991). Ultrastructural and biochemical changes associated with maturation of the fruit of *B. napus* have been described including the development of the dehiscence zones and

differentiation of the carpel walls (Meakin & Roberts, 1990a,b).

Fruit ripening has many features in common with both senescence, the ageing and death of organs or whole plants, and abscission, the shedding of leaves and other organs, and many plant enzymes and hormones are common to all of these processes (Thimann, 1980). *Arabidopsis* plants exhibit a monocarpic growth habit in which the entire plant senesces following reproductive growth.

Gibberellins are plant growth regulators which affect cell growth, seed germination and fruit setting (Graebe, 1987). Pea (*Pisum sativum*) has been used to study the effects of gibberellic acid on fruit set and development. Garcia-Martinez & Carbonell (1980, 1985) found that unpollinated pea ovaries treated with gibberellic acid/(GA₃) developed into mature fruits, while unpollinated untreated ovaries senesced. The cells of the pea carpel walls enlarge and differentiate as the fruit matures following pollination. One of the cell layers in the pea endocarp shows a similar pattern of differentiation to the lignified endocarp *b* cell layer in the *Arabidopsis* carpel wall, producing a single layer of elongated thick-walled cells (Vercher *et al.*, 1984). The application of GA₃ to unpollinated ovaries stimulated the enlargement of the mesocarp cells and induced the processes necessary for the elongation and cell wall thickening of the endocarp (Vercher *et al.*, 1987). The production of parthenocarpic fruit allows physiological and molecular examination of those events which are associated with fruit wall development but not dependent upon the development of the normally enclosed seeds.

There are a number of ways to approach the agricultural problem of pod shatter. The developmental pattern of the whole plant may be altered to synchronize the development of the pods, or the development of pod tissue may be modified to reduce the shattering characteristic. Modifying the pattern of development of the plant may prove difficult owing to the indeterminate nature of the inflorescence meristem. An alternative, modifying tissues within the pod to reduce the shattering characteristic, may be achieved by genetic engineering, but before appropriate molecular strategies can be designed a detailed knowledge of the developmental patterns of the tissues involved in pod shatter is required. We report here on some of the cytological and histological studies which have led us to propose a hypothesis regarding the development of the shattering characteristic, and which suggest potential routes for its reduction.

Materials and methods

Specimen preparation

Tissue samples from *A. thaliana* (*erecta* ecotype), *B. napus* (var. Westar Spring) and several lines of *B. juncea* were fixed

in 3% (para)formaldehyde and 1.25% glutaraldehyde in 0.05 M sodium phosphate buffer pH 7.0. Tissue for resin embedding was dehydrated through a graded ethanol series and infiltrated with LR White resin which was polymerized thermally. Tissue for wax embedding was dehydrated through ethanol and Histoclear prior to infiltration and embedding in Paraplast. Sections (1 µm) of resin-embedded tissue were cut and collected on TESPA-treated glass slides. Wax-embedded tissues were sectioned at 10 µm.

Cytochemistry

Toluidine blue. Sections were stained for 1 min in 0.01% (w/v) aqueous toluidine blue in 0.1% (w/v) sodium tetraborate. Sections were rinsed with water, air dried and mounted in DPX.

Acridine orange. Sections were stained with freshly made and filtered 0.01% (w/v) aqueous acridine orange for 2–3 min, rinsed and mounted in Citifluor prior to examination under UV epifluorescence (blue filter).

Ruthenium red. Sections were stained for 5 min in 0.02% aqueous ruthenium red, rinsed in distilled water, mounted in Citifluor, and examined under bright-field illumination.

Histology and histochemistry reagents were purchased from Agar Scientific (UK) or Sigma; further details of methods can be found in Harris *et al.* (1994).

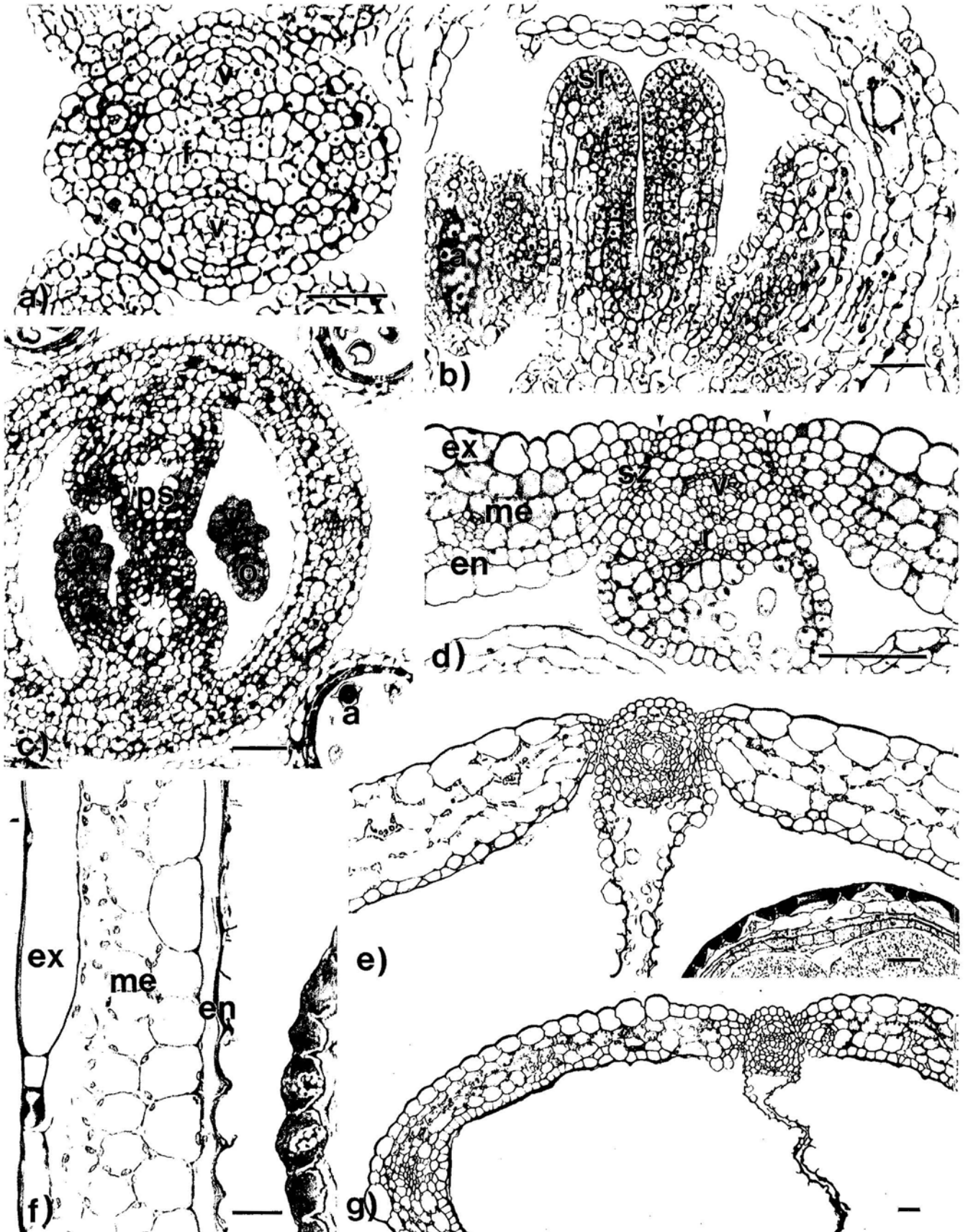
Parthenocarpic fruit set in *Arabidopsis*

Arabidopsis flower buds were carefully opened and emasculated. Gibberellic acid (GA₃; Fluka AG, Switzerland) (10 µL) was applied to the style at 100 µg mL⁻¹ in 0.1% (v/v) Tween 80. Parthenocarpic fruits developed and proceeded through to senescence, and were sampled at progressive stages of maturity.

Results

Ovary development in *A. thaliana*

Within the unopened flower bud the gynoecium of *Arabidopsis* is first evident as a small dome of meristematic cells at the centre of the floral apex; these cells divide and differentiate to form an elliptical open-ended cylinder comprising six concentric layers of cells (stage 1; Spence, 1992). The cylinder has a deep, narrow, central fissure which is lined with two layers of meristematic cells (Figs. 1a, transverse section, and 1b, longitudinal section). The layers extend around the top of the cylinder (Fig. 1b). Expansion of the cylinder occurs during stage 2, with the meristematic lining bulging to produce opposing ovule



primordia, and also the pseudosepta which develop from either side of the forming tube. Stage 3 is characterized by a restriction of the open end of the tube, and the early development of the stigma; further growth and subsequent fusion of the pseudosepta also occurs, thus forming two locules within the developing ovary (Fig. 1c). The ovules develop from the meristematic tissue on either side of the septum (Fig. 1c). Expansion and differentiation of the cells within the carpels walls occurs during stages 3–5; although there is no increase in the number of layers of cells from the six established during stage 1, three distinct tissues, the exo-, meso- and endocarp, can be identified (Fig. 1d). The exocarp (ex) contains small, isodiametric cells, mostly devoid of plastids, the mesocarp (me) contains three layers of chlorenchyma, and even at this early stage the two layers of the endocarp (en) are readily distinguishable (Figs. 1c,d). The two layers of the endocarp are quite distinct; the surface layer (ena) is composed of large, thin-walled cells which are isodiametric at the early stages, whilst the inner (enb) layer is formed from a single layer of small, tightly packed cells which arise from numerous anticlinal divisions. Two main vascular bundles run longitudinally in the repla on opposing sides of the developing gynoecium and adjacent to the meristematic tissues which give rise to the ovules and septum. Numerous minor, protovascular strands run longitudinally through the mesophyll; these aggregate to form a ring of vascular tissue towards the distal end of the ovary.

Post-fertilization development of *A. thaliana* fruit walls

Following fertilization there is a marked increase in the length of the fruit (a silique), although only a small increase in diameter. The surface develops longitudinal grooves (Fig. 1d, darts) which run either side of the repla; this leads to the formation of two regions which will later separate as the valves. The exocarp cells expand and the outer walls thicken but do not lignify. The cells of the mesocarp expand, but even with additional cell separation the three/four-cell layered structure is largely maintained (cf. Figs. 1d,e). The cells in the endocarp layers, however, undergo considerable differentiation. Cells in ena expand and remain thin walled, whereas cells in enb continue to divide anticlinally and elongate in the long axis of the silique (Fig. 1f). The enb cells develop thickened walls which subsequently lignify. The

lignified layer of cells extends into the separation layer of the dehiscence zones (sz) as a continuous single-celled band which lies around the repla and eventually joins with the exocarp (Fig. 2a). Simultaneously, the main vascular strands, which are supplying the developing seeds within the fruit, increase substantially in size and show much additional lignification (Figs. 1e and 2a). Following lignification of enb the large thin-walled cells of ena disintegrate (Figs. 1e,f).

With maturation and desiccation of the fruit, separation occurs between the layer of lignified cells running around the repla and the adjacent, non-lignified cells of the repla (Fig. 2b). It was apparent that separation occurred leaving both lignified and non-lignified cells intact, i.e. separation was between cells rather than by rupture through cells.

Development of parthenocarpic fruits of *Arabidopsis*

Application of the gibberellic acid GA₃ to unfertilized stigmas resulted in the formation of parthenocarpic fruits. These developed in a general pattern similar to that shown by fruit from fertilization, although the parthenocarpic fruit did not expand to the same size, and they did not shatter so readily. Some minor differences were observed in the relative extent of expansion of exocarp cells; a wider variation in size was observed in the parthenocarpic exocarp layer with occasional, much larger, 'balloon' cells (Fig. 1g). The cells of the mesocarp remained more closely packed in the parthenocarpic fruit. Differentiation of the endocarp, and the continuation of the lignified layer around the repla to the exocarp, was similar to that seen in fertilized fruit (cf. Figs. 1e,g).

Post-fertilization development of *B. napus* and *B. juncea* fruit walls

Structural and ultrastructural aspects of the development of *B. napus* siliques have been described previously (Meakin & Roberts, 1990a,b) with emphasis on the separation of cells in the dehiscence zone. The general pattern described is very similar to that seen in *Arabidopsis*, although there is much more lignification around the carpel valve margins prior to dehiscence in *B. napus*. The carpel walls of the pre-fertilized, and just post-fertilized, fruit also show tissue

Fig. 1. Toluidine blue stained sections of developing *A. thaliana* gynoecium. (a) Transverse section of early meristematic tissue showing central fissure (f) and opposed protovascular strands (v). (b) Longitudinal section showing meristematic tissue lining fissure and protostigmatic rim (sr); a, anther; s, sepal. (c) Transverse section showing formation of pseudoseptum (ps) from two opposed meristematic regions; c₁, developing ovules. (d) Early differentiation of separation zones (sz) on either side of the replum (r) with its main vascular bundle (v); en, endocarp; m, mesocarp; ex, exocarp. (e) Maturing fruit showing development of separation zones and disintegration of ena. (f) Longitudinal section through valve wall showing lignified enb and only residual fragments of ena; sc, seed coat. (g) Parthenocarpic fruit. Scale bars = 20 µm.

patterns similar to those described above for *Arabidopsis* but, with increasing maturation, it is apparent that the endocarp layers develop differently. In *B. napus* the inner and outer tangential walls of *ena* thicken, although the radial walls remain thin. As the fruit matures *ena* collapses but the residual thick walls line the layer of heavily thickened, sclerenchyma-like cells which have differentiated in *enb* (Fig. 2c). Some thickening of mesophyll cell walls adjacent to the endocarp is also apparent (Fig. 2c).

Examination of *B. juncea* lines, which have reduced tendencies to shatter, revealed a superficially similar development of the carpel walls (Fig. 2d). However, selective staining of cell wall components indicates that subtle but significant differences are present. Use of ruthenium red to stain pectin fractions within the cell walls showed significant staining of the intercellular junctions within the mesophyll and the inner and outer tangential walls of the *ena* layer of the endocarp in *B. napus*. The *enb* layer, however, is unstained (Fig. 2e) but, by contrast, the equivalent layer in the non-shattering *B. juncea* shows significant ruthenium red staining in the radial walls between the secondarily thickened *enb* cells (Fig. 2f). Lignification of the *enb* layer in both *Brassica* species is suggested by the metachromatic staining of toluidine blue seen in Figs. 2(c,d); acridine orange staining (Fig. 2g) confirms the specific layering of lignification (fluorescing yellow) in cells of *enb* in *B. juncea*, with the intervening regions of non-lignified wall (fluorescing orange) lying between.

Discussion

Differentiation of fruit wall tissues

On the basis of histological changes, Spence (1992) divided the development of the siliqua of *Arabidopsis* into 10 stages. The major tissue layers of the fruit wall (the exocarp, mesocarp and endocarp) are established during the first five stages of development which occur prior to fertilization. It is the differentiation of cells within these tissues during the latter five, post-fertilization stages of development which facilitates the process of dehiscence.

The differentiation of cells within the carpel walls and dehiscence zones which normally occurs after fertilization results in four cell types, the exocarp, mesocarp and two endocarp layers which are associated with the carpel wall, and two cell types, the separation layer and the lignified

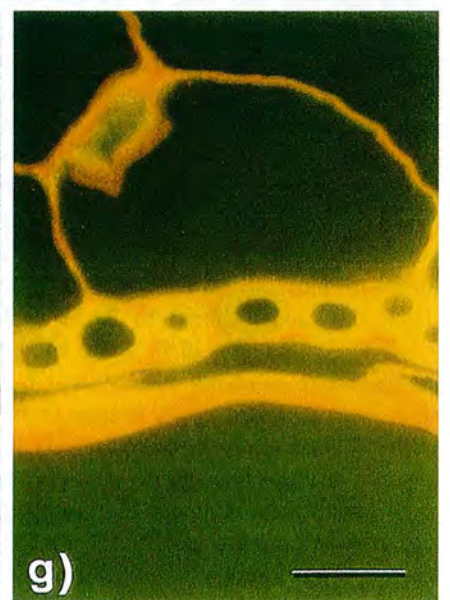
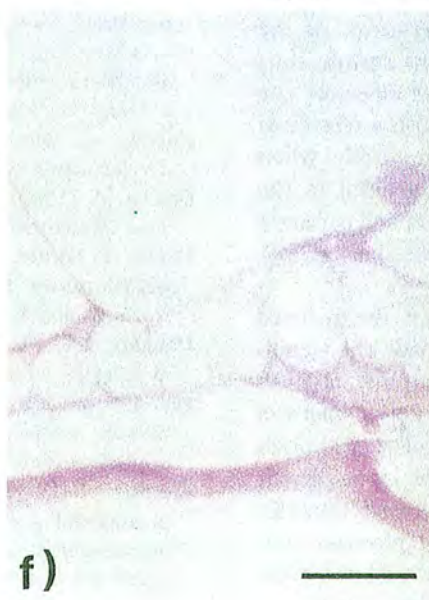
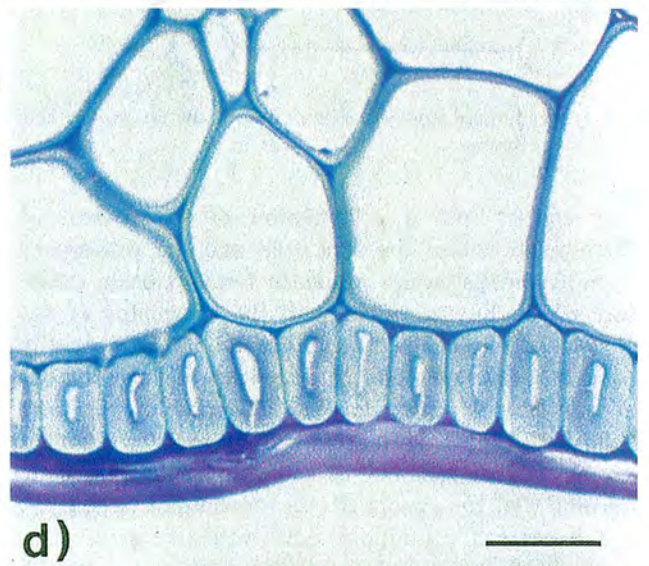
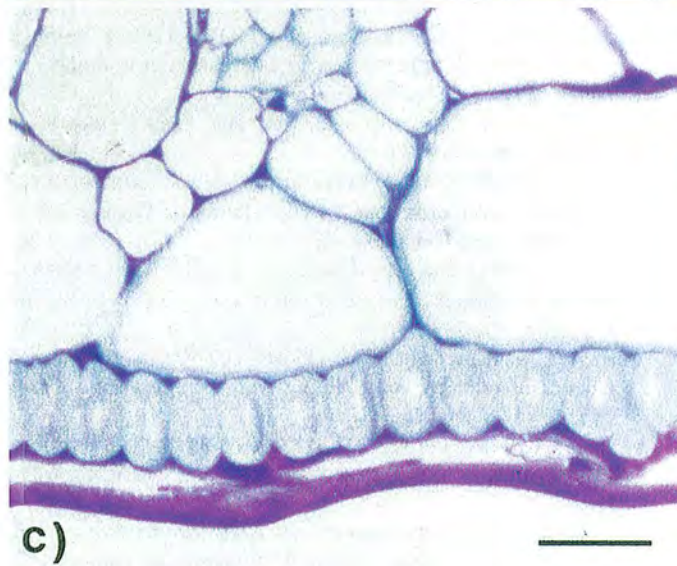
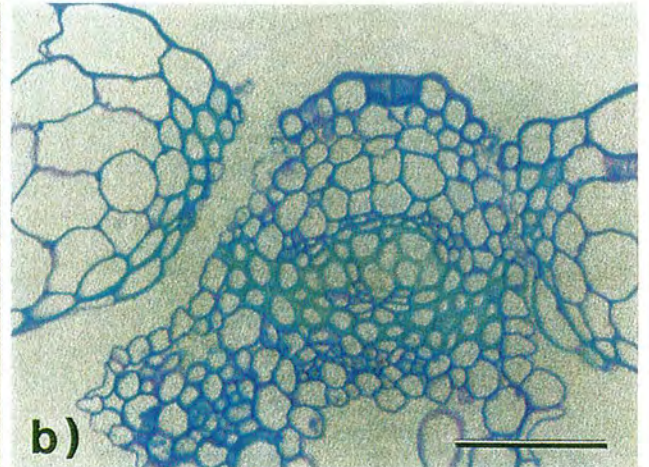
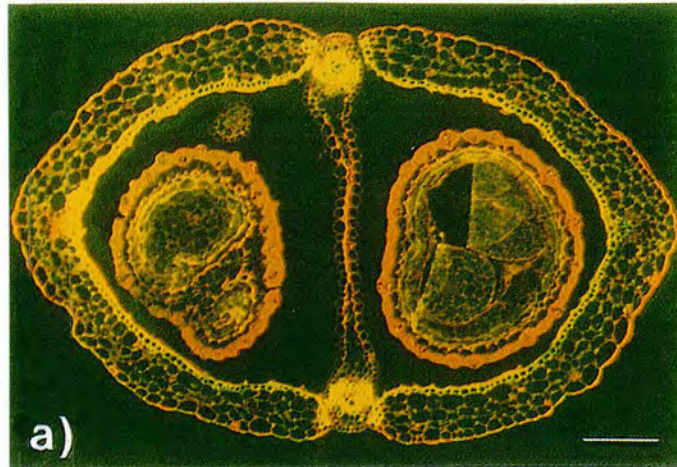
dehiscence zone cells, which are associated with the dehiscence zone. Fertilization is, however, not essential for this developmental pattern as a similar, but smaller, structure is established in parthenocarpically developed fruit. Enlargement of the fruit during post-fertilization growth is largely the result of cell expansion and, in the mesocarp, an increase in the intercellular spaces; only in the inner (*enb*) of the two endocarp layers is there any continued (anticlinal) cell division. The cells of *enb* undergo considerable elongation during fruit growth prior to the development of a substantial secondary wall which is then lignified. The single layer of lignified cells continues around the dehiscence zone to the exocarp. As a consequence of the lignification of *enb*, the outer layer (*ena*) is isolated from the rest of the carpel tissues and quickly senesces and the thin-walled cells disintegrate. In the *Brassica* spp. examined the tangential, but not radial, walls of *ena* showed thickening of the primary wall, and as the *ena* is isolated by lignification of *enb* it collapses but remains as a layer of unlignified wall lining the fruit locules. Both *B. napus*, which shatters, and the non-shattering *B. juncea* lines showed similar differentiation of *ena*, indicating that this layer may not play a significant role in the development of the shattering phenotype.

The differentiation of *enb*, however, was found to be significantly different in *Arabidopsis* and *B. napus* which shatter, and the *B. juncea* lines which show a reduced tendency to shatter.

The establishment of tensions which result in pod shatter

Pod shatter usually occurs when the dried fruits are mechanically stimulated; the pattern of dehiscence suggests that the tissues are under tension, and either naturally or under some mild mechanical stimulus the tissues separate quickly and at specific points. Examination of the cells at the margins of the separation indicates that cells separate along the middle lamella, rather than by rupture of the cells as occurs in some forms of osmotically driven abscission. Breakdown of the cell wall, and in particular the middle lamella, is a common feature of abscission and senescence and has been linked to the action of extracellular enzymes such as cellulases and pectinases. However, the action of enzymes loosening the cell wall components would not in itself lead to the more 'explosive' events sometimes observed in pod shatter.

Fig. 2. Transverse sections showing post-fertilization fruit development in *A. thaliana* (a,b), *B. napus* (c,e), and *B. juncea* (d,f,g). (a) Acridine orange staining of transverse section of fruit with two enclosed seeds, showing lignification (yellow) of *enb* and vascular bundles in wall, and cutin coating (orange) to exocarp and seed coats. (b) Toluidine blue staining of separation zone. (c) Toluidine blue staining of endocarp and mesocarp of mature *B. napus*. (d) Toluidine blue staining of endocarp and mesocarp of mature *B. juncea*. (e) Ruthenium red staining of *B. napus*. (f) Ruthenium red staining of *B. juncea*. (g) Acridine orange staining of *B. juncea* showing limited lignification of *enb*. Scale bars = (a) 150 μ m; (b)–(g) 20 μ m.



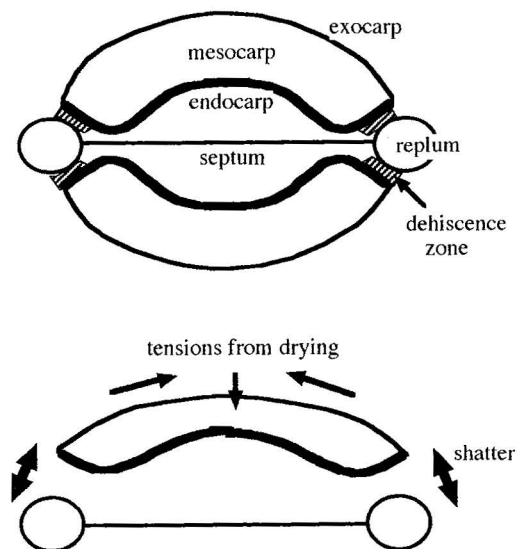


Fig. 3. Diagrammatic representation of tissues and tensions which result in pod shatter.

We suggest that a combination of the pattern of differentiation within the fruit wall and the subsequent desiccation of the tissues results in tensions being established which, in association with the weakening of the middle lamella between cells in the separation layer, results in shatter. The key features of the pattern of differentiation and desiccation which produce the tensions within the wall are illustrated in Fig. 3. Thickening of the exocarp is limited to some slight additional cuticularization to the outer tangential wall, the mesophyll cells remain thin walled, but the *enb* forms a continuous rigid wall arcing convexly around the fruit but with a reflexed concave link at the margin of the valve linking back to the exocarp. As the tissue desiccates the exocarp and mesocarp shrink, thus inevitably putting tension upon the rather inflexible *enb* layer. This effectively becomes 'sprung' and the tension is only released, and this can occur quite dramatically, when the weakened wall finally gives way, often aided in the natural environment by mechanical stimulus and certainly brought about by the vigorous mechanical shocks associated with agricultural harvesting.

Does the model shown in Fig. 3 explain the reduced tendency of some lines of *B. juncea* to shatter? The significant difference in carpel development between *Arabidopsis* and *B. napus*, and *B. juncea* is seen in the development of *enb*. In *B. juncea* *enb* is not completely lignified. Although the secondary walls do lignify this does not spread to the primary walls and middle lamella regions between the cells. These regions remain rich in pectin. The physical consequence of the intervening pectin regions would be a more flexible layer which, even with desiccation, would not develop the same types of tension within the carpel valve, and consequently there is less tendency to shatter.

The model also suggests several strategies for approaching a solution to the problem of pod shatter, including modification of the separation zone and modification of the patterns of differentiation so that tensions are not built up within the desiccating fruit.

Acknowledgments

This work has been supported by the AFRC (Plant Molecular Biology) (J.S.), and DGICT, Spain (Y.V.), and continues to be funded under the BBSRC Cell Engineering link scheme with Nickerson BIOCEM (Cambridge).

References

- Alvarez, J., Guli, C.L., Yu, X. & Smyth, D.R. (1992) Terminal flower: a gene affecting inflorescence development in *Arabidopsis thaliana*. *Plant J.* **2**, 103–116.
- Brady, C.J. (1987) Fruit ripening. *Ann. Rev. Plant Physiol. Plant Mol. Biol.* **38**, 155–177.
- Bunting, E.S. (1984) Oilseed rape in perspective: with particular reference to crop expansion and distribution in England 1973–1983. *Asp. Appl. Biol.* **6**, 11–22.
- Coen, E.S. (1991) The role of homeotic genes in flower development and evolution. *Ann. Rev. Plant Physiol. Plant Mol. Biol.* **42**, 241–279.
- Coen, E.S. & Meyerowitz, E.M. (1991) The war of the whorls: genetic interactions controlling flower development. *Nature*, **353**, 31–37.
- Fischer, R.L. & Bennett, A.B. (1991) Role of cell wall hydrolases in fruit ripening. *Ann. Rev. Plant Physiol. Plant Mol. Biol.* **42**, 675–703.
- Garcia-Martinez, J.L. & Carbonell, J. (1980) Fruit-set of unpollinated ovaries of *Pisum sativum* L. Influence of plant-growth regulators. *Planta*, **147**, 451–456.
- Garcia-Martinez, J.L. & Carbonell, J. (1985) Induction of fruit set and development in pea ovary explants by gibberellic acid. *J. Plant Growth Reg.* **4**, 19–27.
- Gillaspy, G., Ben-David, H. & Gruissem, W. (1993) Fruits: a developmental perspective. *The Plant Cell*, **5**, 1439–1451.
- Graebe, J.E. (1987) Gibberellin biosynthesis and control. *Ann. Rev. Plant Physiol.* **38**, 419–65.
- Harris, N., Spence, J. & Oparka, K.J. (1994) General and enzyme histochemistry. *Plant Cell Biology: a Practical Approach* (ed. by N. Harris and K. J. Oparka), pp. 51–68. IRL Press, Oxford.
- Haughn, G.W. & Somerville, C.R. (1988) Genetic control of morphogenesis in *Arabidopsis*. *Dev. Gen.* **9**, 73–89.
- Hill, J.P. & Lord, E. (1989) Floral development in *Arabidopsis thaliana*: a comparison of the wild type and the homeotic *pistillata* mutant. *Can. J. Bot.* **67**, 2922–2936.
- Karlsson, B.H., Sills, G.R. & Nienhuis, J. (1993) Effects of photoperiod and vernalisation on the number of leaves at flowering in 32 *Arabidopsis thaliana* (Brassicaceae) ecotypes. *Am. J. Bot.* **80**, 646–648.
- Knauf, V.C. (1987) The application of genetic engineering to oilseed crops. *Trends Biotechnol.* **5**, 40–47.
- Kunst, L., Klenz, J.E., Martinez-Zapater, J. & Haughn, G.W. (1989)

- AP2 gene determines the identity of perianth organs in flowers of *Arabidopsis thaliana*. *The Plant Cell*, **1**, 1195–1208.
- Labuda, T. (1981) *The Oilseed Rape Crop in the U.K. A Manual for Growers, Farmers and Advisers*. Cambridge Agricultural Publishing, Cambridge.
- Leyser, H.M.O. & Furner, I.J. (1992) Characterisation of three shoot apical meristem mutants of *Arabidopsis thaliana*. *Development*, **116**, 397–403.
- Lister, C. & Dean, C. (1993) Recombinant inbred lines for mapping RFLP and phenotypic markers in *Arabidopsis thaliana*. *The Plant J.* **4**, 745–750.
- MacLeod, J. (1981) *Harvesting in Oilseed Rape*. pp. 107–120. Cambridge Agricultural Publishing, Cambridge.
- Meakin, P.J. & Roberts, J.A. (1990a) Dehiscence of fruit in oilseed rape (*Brassica napus* L.). 1. Anatomy of pod dehiscence. *J. Exp. Bot.* **41**, 995–1002.
- Meakin, P.J. & Roberts, J.A. (1990b) Dehiscence of fruit in oilseed rape (*Brassica napus* L.). 2 The role of cell wall degrading enzymes and ethylene. *J. Exp. Bot.* **41**, 1003–1011.
- Meyerowitz, E.M. (1989) *Arabidopsis*: a useful weed. *Cell*, **56**, 263–269.
- Murphy, D.J. (1992) Modifying oilseed crops for non-edible products. *Trends Biotechnol.* **10**, 84–87.
- Okada, K., Komaki, M.K. & Shimura, Y. (1989) Mutational analysis of pistil structure and development of *Arabidopsis thaliana*. *Cell Different. Dev.* **28**, 27–38.
- Okamuro, J.K., den Boer, B.G.W. & Jofuku, K.D. (1993) Regulation of *Arabidopsis* flower development. *The Plant Cell*, **5**, 1183–1193.
- Picart, J.A. & Morgan, D.G. (1984) Pod development in relation to pod shattering. *Asp. Appl. Biol.* **6**, 101–110.
- Polowick, P.L. & Sawhney, V.K. (1986) A scanning electron microscopic study on the initiation and development of floral organs of *Brassica napus* (cv. westar). *Am. J. Bot.* **73**, 254–263.
- Schwartz-Sommer, Z., Huijser, P., Nacken, W., Saedler, H. & Sommer, H. (1990) Genetic control of flower development by homeotic genes in *Antirrhinum majus*. *Science*, **250**, 931–936.
- Shannon, S. & Meeks-Wagner, D.R. (1991) A mutation in the *Arabidopsis* *tfl1* gene affects inflorescence meristem development. *The Plant Cell*, **3**, 877–892.
- Shannon, S. & Meeks-Wagner, D.R. (1993) Genetic interactions that regulate inflorescence development in *Arabidopsis*. *The Plant Cell*, **5**, 639–655.
- Smyth, D.R., Bowman, J.L. & Meyerowitz, E.M. (1990) Early flower development in *Arabidopsis*. *The Plant Cell*, **2**, 755–767.
- Spence, J. (1992) *Development of the silique of Arabidopsis thaliana*. MSc thesis, University of Durham, U.K.
- Steeves, T.A. & Sussex, I.M. (1989) *Patterns in Plant Development*, 2nd edn. Cambridge University Press, New York.
- Thimann, K.V. (1980) *Senescence in Plants*. CRC Press, Boca Raton, FL.
- Vercher, Y., Molowny, A. & Carbonell, J. (1987) Gibberellic acid effects of the ultrastructure of endocarp cells of unpollinated ovaries of *Pisum sativum*. *Physiol. Plant.* **71**, 302–308.
- Vercher, Y., Molowny, A., Lopez, C., Garcia-Martinez, J.L. & Carbonell, J. (1984) Structural changes in the ovary of *Pisum sativum* L. induced by pollination and gibberellic acid. *Plant Sci. Lett.* **36**, 87–91.
- Weberling, F. (1989) *Morphology of Flowers and Inflorescences*. Cambridge University Press, Cambridge.
- Wrathall, J.E. (1978) This changing world. The oilseed revolution in England and Wales. *Geography*, **63**, 42–45.
- Wrathall, J.E. & Moore, R. (1986) This changing world. Oilseed rape in Great Britain - the end of a revolution. *Geography*, **71**, 351–355.



General and enzyme histochemistry

N. HARRIS, J. SPENCE, and K. J. OPARKA

1. Introduction

Fluorescent probes and stains have proved very valuable in identifying cell components and activities (Chapter 2). However, not all laboratories have access to fluorescence microscopes; this chapter therefore contains various protocols for both general and specific staining of plant tissues, cell types, and organelles which may be used with bright field microscopy. Generally such protocols have the added benefit of providing permanent mounts which may be viewed on numerous subsequent occasions. Only a brief selection is provided here including some of the more useful for general staining, for general light counterstaining, and for localizing some of the major cell components. Many such stains are available; used carefully the methods, though simple, can be very informative. More comprehensive lists and protocols can be found in references 1–5. Cross reference to Chapter 2 is recommended: fluorescent probes, which in many cases are not cytotoxic and may be used with living tissues, are available for many cell components.

Stains can be used with whole mounts, perhaps after ‘clearing’ to remove pigments and expose inner tissue components, or with sections of tissue cut freshly, after cryofixation (see Chapter 4, *Protocol 10*; Chapter 5, *Protocol 3*), or after embedding in wax, polyethylene glycol, or resin.

Pieces of tissue in which secondary thickening has not occurred may be rendered semi-translucent by treating with ethanol:glacial acetic acid (3:1(v/v)) at 60 °C for 15–60 min. Samples initially ‘clear’ but remain intact; longer treatment is used to macerate tissue. Cleared samples can subsequently be stained, for example with phloroglucinol/HCl (see Section 2.2.3 below), to demonstrate the distribution of lignified vascular elements and their complex inter-relationships at and between nodes. The three-dimensional inter-relationships are visible within the whole mount more readily than by reconstruction from stained sections. In many investigations, however, whole mounts are not suitable and the required details are only available following sectioning.

3. General and enzyme histochemistry

1.1 Tissue embedding and sectioning

Tissue blocks may be sectioned 'freehand' (<25 μm thick) or using various commercial tissue choppers which slice fresh tissue (to *circa* 15 μm) or microtomes which require that the tissue is first embedded in a matrix (for 0.5–10 μm thick sections). The matrix may be the frozen cell sap (for cryosectioning, see Chapter 5), wax, or a water-soluble medium such as polyethylene glycol (this chapter, *Protocol 1*), or one of various resins (this chapter, *Protocol 2*; Chapter 4, *Protocol 3*; Chapter 5, *Protocol 5*; Chapter 6, *Protocol 2*). Cryosectioning of vacuolate plant tissues containing numerous intercellular air spaces may present problems; meristematic tissues are more amenable.

Protocol 1. Tissue processing and embedding in wax or polyethylene glycol (PEG)

- crystalline paraformaldehyde
 - 25% glutaraldehyde stock solution
 - 0.5 M phosphate or cacodylate buffer pH 7.0 (stock)
 - ethanol
 - Histo-Clear or similar^a
 - wax (Paraplast or similar) or PEG 1000 or 1500
 - specimen vials and embedding moulds
 - rotator or shaker for specimen vials^b
 - oven
1. Prepare primary fixative (typical: 1.5% (w/v) formaldehyde, 2.5% (v/v) glutaraldehyde in 0.05 M phosphate buffer pH 7.0^c).
 2. Cut tissue blocks, with at least one dimension a maximum of 5 mm, in the primary fixative as soon as possible after removing from plant.
 3. Fix overnight at 4 °C (volume of fixative \gg 10 \times volume of sample).
 4. Wash in buffer (two changes with 30 min between changes).
 5. Dehydrate through a graded ethanol series (10%, 25%, 40%, 60%, 75%, and 95%) with two 15–30 min changes in each step and three 15–30 min changes in dry ethanol (ethanol kept over molecular sieve).

For polyethylene glycol embedding:

6. Infiltrate with 1:1 ethanol:PEG^d overnight at 40 °C.
7. Infiltrate with PEG for 48–72 h at 56 °C, with changes to fresh PEG each evening and morning.

8. Place in prewarmed embedding moulds with fresh PEG, orient, and cool on ice or at 4 °C.

For wax embedding:

6. Wash with 2:1 ethanol:Histo-Clear^a for 2 h at room temperature; repeat with 1:1 and 2:1 ethanol:Histo-Clear, and leave in Histo-Clear overnight.
7. Infiltrate with Histo-Clear:wax at 1:1 for 8 h at 56 °C.
8. Infiltrate with wax for 96 h at 56 °C, with changes of wax every 24 h.
9. Place in prewarmed embedding moulds with fresh wax, orient, and cool on ice or at 4 °C.

^a Xylene, toluene, or benzene are commonly replaced with Histo-Clear or a similar, less hazardous clearing reagent.

^b During fixation, washing, dehydration, and infiltration with resin, the samples should be constantly but gently moved: several manufacturers produce suitable rotators which hold 10 ml glass specimen vials.

^c Make formaldehyde freshly from crystalline paraformaldehyde; see Chapter 4, *Protocol 1*

^d PEG 1000 gives softer blocks which require cooling to 4 °C before sectioning

Protocol 2. Embedding tissue in LR White resin

- as in *Protocol 1* except LR White resin (London Resin Company) in place of wax
- sealable polypropylene embedding moulds

A. Ambient temperature embedding

1. Cut tissue blocks of (2–3 mm)³, in the primary fixative as soon as possible after removing from plant.
2. Fix for 2–6 h at 4 °C (volume of fixative >> 10 × volume of sample).
3. Wash in buffer (two changes with 15 min between changes).
4. Dehydrate through a graded alcohol series (10%, 25%, 40%, 60%, 75%, and 95%) with two 15 min changes in each step and three 15–30 min changes in dry alcohol (alcohol kept over molecular sieve).
5. Infiltrate with 2:1 ethanol:resin overnight at 4 °C, with 1:1 ethanol:resin for 4 h, and with 1:2 ethanol:resin for 4 h at room temperature.
6. Infiltrate with resin for 12–48 h with changes of fresh resin every 12 h^a.
7. Place in polypropylene or gelatin capsules, fill and seal capsules with only minimum trapped air, and allow to polymerize at 50 °C for 24 h^b.

3. General and enzyme histochemistry

Protocol 2. Continued

B. Low temperature embedding

Preliminary comments and steps 1–3 are as above.

4. Dehydrate through a graded alcohol series with 30 min changes in each step (10% and 25% ethanol at 0 °C; 40%, 60%, 75%, and 100% ethanol at –20 °C).
5. Infiltrate with 2:1 ethanol:resin overnight, with 1:1 ethanol:resin for 4 h, and h, and with 1:2 ethanol:resin for 4 h, all at –20 °C.
6. Infiltrate with resin with catalyst (0.5% (v/v) benzoin methyl ether) for 12–48 h at –20 °C with changes of fresh resin every 12 h^a.
7. Place in polypropylene or gelatin capsules, fill and seal capsules with only minimum trapped air, and polymerize by irradiating with UV light for 24 h at –20 °C and 24 h at room temperature.

^a The time taken for resin infiltration is dependent upon the type of tissue; small pieces of non-woody tissues will be infiltrated within 12 h whereas woody tissues or seed tissues packed with starch and other storage reserves require up to 48, or exceptionally, 72 h.

^b LR White may be 'cold cured' using an accelerator—the reaction is highly exothermic and not recommended for immunological work.

Sections are collected on pretreated glass slides. Pretreatments to ensure adhesion of samples include gelatin (Chapter 5, *Protocol 1*), poly-L-lysine (Chapter 10, section 3.3), or TESPA. To silanize with TESPA (3'-amino propyl triethoxysilane, Sigma A3648), wash slides with dilute detergent, rinse with distilled water, immerse in 2% TESPA in acetone for 30 sec, rinse twice in acetone and twice in distilled water, and leave to dry in a dust-free environment. For RNase-free slides water treated with diethylpyrocarbonate (DEPC) is used where appropriate (see Chapter 5).

Preparation of cryosections and sections from resin and from wax are described in Chapter 5. *Protocols 3, 7, and 8* respectively. Sections from PEG-embedded material are cut at 5–15 µm using standard microtomes with steel or disposable knives. Sections can be transferred in a ribbon to the slide which is subsequently warmed very gently so that the PEG just begins to melt. Slides with sections are then cooled and stored at 4 °C.

2. General histo- and cytochemistry

Toluidene Blue is suitable for staining structures in sections of fresh or fixed and embedded tissues; it is particularly good as a general stain of sections from resin-embedded tissues. Use at 0.01% in 0.1% aqueous sodium tetraborate: if the tissue is not overstained Toluidene Blue is metachromatic

cellulose cell walls, cytoplasm, and plastics stain blue, nuclei stain blue with the nucleolus purple, and lignified walls are green/blue.

Alternatively, two dyes may be used to contrast various components within sections, for example haematoxylin/Orange G (*Protocol 3*).

Protocol 3. Haematoxylin/Orange G for histological sections

- haematoxylin solution (Sigma)^a
 - ethanol
 - Orange G (Sigma 07252)
 - clove oil
 - 0.5% acid alcohol
 - reagents for permanent mounting^b
1. Prepare Orange G solution: dissolve 0.5 g Orange G in 100 ml ethanol and add 100 ml clove oil. Mix and allow ethanol to evaporate until 100 ml solution remains.
 2. Dewax and rehydrate sections. (see Chapter 5, *Protocol 8*, steps 1–4)
 3. Stain with haematoxylin solution for 10–15 min.
 4. Differentiate (remove excess stain) with 0.5% acid alcohol for 1 min.
 5. Wash with tap water until the haematoxylin is blue.
 6. Dehydrate through 50, 75, and 100% ethanol.
 7. Stain with Orange G for 2–5 min.
 8. Differentiate in a solution of equal parts clove oil, ethanol, and xylene (or Histo-Clear).
 9. Rinse in xylene (or Histo-Clear) and mount permanently^b. Organelles stain dark blue; cell walls and cytoplasm are orange.

^a Haematoxylin solution is available commercially or can be prepared as follows. Dissolve 1 g haematoxylin in 50 ml ethanol and then add, in this order, 50 ml glycerol, 50 ml water, 50 ml acetic acid, and 1 g potassium aluminium sulphate. The solution should be left to 'ripen' in sunlight for several weeks before use.

^b For permanent mounting, samples are air dried, or dehydrated in ethanol and xylene or Histo-Clear; mounting medium (Canada balsam, DPX, Histomount, Euparal, or similar), is then added and a clean coverslip placed on top, taking care to avoid trapping any air bubbles. The mountant may be left to set at ambient temperature or at 30 °C.

2.1 Counterstains

To contrast with the distribution of intensely stained specific tissues a variety of counterstaining methods are available to stain the general distribution of

3. General and enzyme histochemistry

tissues lightly. Light Green only, Safranin and Light Green, or Safranin and Fast Green are suitable for counterstaining.

Protocol 4. Counterstaining with Safranin and Fast green

- 1% (w/v) Safranin (Sigma S8884) in 95% aqueous ethanol
- 0.5% (w/v) Fast Green (Sigma F7258) in 95% aqueous ethanol
- ethanol
- xylene, Histo-Clear (or similar) (see *Protocol 1*, footnote *a*)
- permanent mounting reagents (see *Protocol 3*, footnote *b*)

After primary staining^a to give high contrast/high colour to specific components within the tissue section:

1. Stain with Safranin for 10–15 min.
2. Destain with water until Safranin is no longer lost from the specimen.
3. Stain with Fast Green for 5–30 sec^b.
4. Dehydrate with 50% ethanol for 1 min.
5. Rinse with xylene or equivalent.
6. Mount permanently (see *Protocol 3*, footnote *b*).

Lignified walls stain red; nuclei and plastids stain red/pale pink.

^a It is critical that the primary stain product is not alcohol-soluble.

^b If green staining masks the Safranin, dilute the Fast Green stain 5- to 10-fold with 95% ethanol.

2.2 Cell wall components

Cell wall components may be localized by 'classical' staining methods such as that in *Protocol 5*, or by techniques for individual components resulting in either bright field or fluorescence microscopy examination: fluorescent stains are listed in Chapter 2, Section 3.

Protocol 5. Chlor-zinc-iodide (Schutze's reagent) for localization of cell wall components

- zinc chloride
 - potassium iodide
 - resublimed iodine
1. Dissolve 2.5 g potassium iodide in 3 ml water and add 0.5 g resublimed iodine.

2. Add 7 ml water and 15 g ZnCl_2 and allow to dissolve.
3. Use small volumes to stain tissue sections.
4. Wash with water, cover with coverslip, and examine.

Cellulose walls stain blue/violet, lignified and suberized walls yellow/brown, starch also stains blue.

2.2.1 Cellulose

For chloride-iodide staining, dissolve 30 g zinc chloride, 5 g potassium iodide, and 1 g iodine in 15 ml distilled water, and stain fresh tissue or sections for 5–15 min; examine the sections while in staining solution; cellulose is stained blue. The stain solution should be stored in the dark. Where fluorescence microscopy is available use Calcofluor (see Chapter 2, Section 3).

2.2.2 Pectins

Pectins can be stained with 0.02% aqueous Ruthenium Red: incubate fresh tissue sections for 2–10 min, wash with distilled water, and examine by bright field microscopy. Pectins stain red (RNA may also stain). Alternatively the hydroxylamine hydrochloride-ferric chloride method may be used (*Protocol 6*).

Protocol 6. Hydroxylamine hydrochloride-ferric chloride staining for pectins

- sodium hydroxide
 - hydroxylamine hydrochloride
 - ethanol
 - ferric chloride
 - concentrated HCl
1. Prepare hydroxylamine hydrochloride stain (A) using equal volumes of 14% (w/v) sodium hydroxide in 60% aqueous ethanol and 14% (w/v) hydroxylamine hydrochloride in 60% aqueous ethanol.
 2. Prepare ferric chloride stain (B) by mixing 10% (w/v) ferric chloride in 60% aqueous ethanol with 1% 0.1 M HCl.
 3. Incubate sections of fresh tissue sections in 1 ml solution A for 5–10 min.
 4. Add 1 ml ethanolic HCl (95% ethanol:conc. HCl, 2:1 (v/v)) and leave for 30 sec.

Protocol 6. Continued

5. Remove excess liquid and stain with solution B.
6. Wash with 60% ethanol and examine by bright field microscopy. (Pectin esters stain red.)

2.2.3 Lignin

Acidic phloroglucinol is widely used as a stain for lignin. Staining involves carefully adding a solution of 10% w/v phloroglucinol in 95% ethanol to an equal volume of concentrated HCl and staining sections of fresh or fixed tissues, or cleared whole mounts, for 3–30 minutes. Wash the samples thoroughly in water and examine by bright field microscopy; lignin is stained bright red.

An alternative is aniline sulphate: stain fresh or rehydrated sections in 1% aniline sulphate in 60% aqueous ethanol with 0.005 M sulphuric acid (final concentration) for 5–10 min; mount in water and examine by bright field microscopy. Lignin is stained bright yellow.

0.01% aqueous Acridine Orange can be used as a fluorescent stain for lignin and also cutin (see Chapter 2, Section 3.8.3).

2.2.4 Callose

Callose is most conveniently stained with the fluorochrome Aniline Blue (see Chapter, Section 3.8.2). When only bright field microscopy is available, stain tissue sections or stigma squashes with Resorcinol Blue (Sigma). Make stock solution by dissolving 3 g white resorcinol in 200 ml distilled water, add 3 ml '0.88' ammonia, and heat in a water bath at 90 °C for 10 min. The red-brown solution will turn blue after storage; heat again for 30 min, filter, and store as stock. Use freshly diluted stock (1:50 in distilled water) and stain for 10–20 min. Wash with 0.1M citrate phosphate buffer at pH 3.2; callose remains blue but other wall components change from blue to red (6).

2.3 Nuclei and nucleic acids

Fluorescent staining of nuclei, chromosomal components, and RNA are covered in Chapter 2, Section 3.5.3, in Chapter 6 (*Protocol 8*), and in Chapter 5 (*Protocol 9*) respectively. For permanent mounts viewable without fluorescent optics use Methyl green/pyronin Y for DNA and RNA (*Protocol 7*), or the general staining methods described above.

Protocol 7. Methyl Green–Pyronin for localization of DNA and RNA

- Walpole's buffer pH 4.8 (60 ml 0.2 M sodium acetate and 40 ml 0.2 M acetic acid (11.54 ml glacial acetic acid in 1 litre)

- 0.2 M phosphate buffer pH 6.0
 - RNase
 - Methyl Green (Sigma M5015)
 - Pyronin Y (Sigma 6653)
 - glycerol
 - permanent mountant (see *Protocol 3*, footnote *b*)
 - coverslips
1. Dewax and rehydrate sections.
 2. Incubate control sections in 0.05 mg/ml RNase in 0.2 M phosphate buffer pH 6.0 for 1 h at 37 °C; incubate test sections in buffer only.
 3. Wash well in distilled water.
 4. Wash in Walpole's buffer pH 4.8.
 5. Stain with Methyl Green–Pyronin for 25 min (9 ml 2% (w/v) aqueous Methyl Green, 4 ml 2% (w/v) aqueous Pyronin Y or G, 14 ml glycerol and 23 ml Walpole's buffer pH 4.8).
 6. Wash in Walpole's buffer and gently blot dry.
 7. Dehydrate and mount permanently (see *Protocol 3*, footnote *b*).
 8. Examine by bright field microscopy. RNA is stained pink, DNA green/blue.

2.4 Endomembrane system

Components of the endomembrane system in living cells can be stained with the fluorochrome DiOC₆ (see Chapter 2, Protocol 8). The zinc iodide–osmium tetroxide reagent is used for contrasting the endoplasmic reticulum and Golgi apparatus in sections of resin-embedded tissue examined by optical or electron microscopy (see Chapter 4, *Protocol 5*).

2.5 Proteins

Toluidene Blue (Sigma T7029) is a valuable metachromatic stain (see page 54) which gives good general staining of protein in fresh tissues and sections from wax- and resin-embedded tissues. For protein staining make a stock of 0.1% (w/v) Toluidene Blue in 1% (w/v) aqueous sodium tetraborate; fresh and rehydrated sections from wax/embedded tissues require approximately 1 min of staining prior to distilled water washing (if staining is too intense dilute stock 1:10 or 1:100 with water). Staining of sections of resin-embedded material may be accelerated by gentle warming on a hot plate, although it is critical that the stain does not start to precipitate.

2.6 Carbohydrates and starch

Periodic acid–Schiff's reaction (*Protocol 8*) is used to localize total carbohydrates in histological sections.

Protocol 8. Periodic acid–Schiff's (PAS) stain for carbohydrates

- 0.5% (w/v) aqueous periodic acid
 - Schiff's reagent (Sigma 395-2-016)
 - 2% (w/v) aqueous sodium bisulphite
1. Rehydrate sections from wax-embedded or freeze-dried tissue.
 2. Incubate with 0.5% (w/v) aqueous periodic acid for 5 to 30 min.
 3. Wash in running water for 10 min.
 4. Stain with Schiff's reagent for 15 min.
 5. Rinse in water and incubate in 2% (w/v) aqueous sodium bisulphite for 2 min.
 6. Wash in running water.
 7. Counterstain lightly (see *Protocol 4*) if required.
 8. Dehydrate and mount permanently (see *Protocol 3*, footnote *b*) if required.

Polysaccharides, including starch, stain deep purple/red.

Iodine in potassium iodide is the classic stain for starch: made as 0.5% (w/v) iodine in 5% (w/v) aqueous potassium iodide, the stain should be stored in the dark. When used with fresh or fixed material it gives a very strong reaction within a few minutes. The deep blue/black colour indicates long chain starch, with shorter chain molecules staining red/brown. Starch may also be identified, without staining, by the 'Maltese cross' pattern given by starch grains when viewed under polarized light (see p. 13).

2.7 Lipids

Lipids may be stained with Sudan Black B (Gurr) or Sudan III (Gurr): the stains are made as saturated solutions in 70% (v/v) ethanol and sections are stained for extended periods, usually in excess of 30 min. The dye preferentially partitions from the staining solution into the specimen lipids which is stained black or blue with the former, or red with the latter. Nile Blue (Gurr) may be used to distinguish between neutral and acidic lipids: unfixed tissue is stained with 1% (w/v) aqueous Nile Blue for 30–60 sec at

37 °C, sections are rinsed briefly with 1% (v/v) acetic acid and washed with distilled water. Nile Blue is, however, a general basic stain and may give high levels of staining of non-lipid components in some tissues: it is useful where high levels of free fatty acids or phospholipids are present.

2.8 Tannins

Tannins are precipitated by 1% (w/v) aqueous osmium tetroxide to give a dense deposit which is visible by light and electron microscopy. Older, and still valuable, staining methods for tannins use ferric salts or the nitroso reaction. After incubating fresh sections in 1.0% (w/v) ferric chloride in 0.1 M HCl tannins give a blue precipitate. If a permanent mount is required, fix tissue in 2% (w/v) ferric sulphate in 10% (v/v) formalin, dehydrate, embed in wax (see *Protocol 1*), and section.

The nitroso reaction gives red deposition of tannins: use fresh sections and add equal volumes of (i) 10% (w/v) sodium nitrate, (ii) 20% (w/v) urea, (iii) 10% (v/v) acetic acid, stain for 5 min, add 2 volumes of 2 M sodium hydroxide, and observe by bright field microscopy.

3. Enzyme histochemistry

Cryosections from fresh frozen tissues are recommended for all histochemical techniques. Delicate enzymes may be damaged or lost entirely during the harsh processing procedures involved in embedding the tissue. Increasing the incubation times is usually necessary when using embedded material.

Enzyme cytochemistry for localization at the electron microscope level has recently been comprehensively and excellently reviewed by Sexton and Hall (7), and is not repeated here.

3.1 Acid and alkaline phosphatases

Phosphatases are involved in the hydrolytic cleavage of organic phosphate esters and are active under alkaline or acidic conditions. As well as indicating important physiological activities within plant tissues alkaline phosphatase is also used in immunolocalization studies where it is conjugated to a secondary antibody. Alkaline phosphatases are not as widely distributed in plant tissues as in animal ones; the conjugated calf intestinal alkaline phosphatase may be distinguished from any endogenous activity by the use of the inhibitor levamisole which, at millimolar concentrations, does not inhibit the calf enzyme. Several methods are available, based on the Gomori (8) reactions. The colour of the final precipitated reaction product may be blue (with the substrates NBT and BCIP) or red (using naphthol AS-MX phosphate and Fast Red TR).

Staining artefacts are readily produced when testing for phosphatases and a

3. General and enzyme histochemistry

comprehensive range of controls must be used, particularly with electron microscopic studies (see Chapter 4 and reference 7).

Protocol 9. Localization of acid and alkaline phosphatases

- acetate buffer pH 5 (30 ml of 0.2 M acetic acid and 70 ml of 0.2 M sodium acetate)
- naphthol AS-MX phosphate (Sigma N4875)
- Fast Red TR (Sigma F2768)
- Tris-HCl buffer pH 8
- Dimethylformamide (DMF)

A. Acid phosphatase

1. Prepare a 100× stock solution of naphthol AS-MX phosphate (A) by dissolving 20.8 mg naphthol AS/MX phosphate in 1 ml DMF (store frozen).
2. Prepare a 100× stock solution of Fast Red TR (B) by dissolving 51.4 mg Fast Red TR in 1 ml 70% (v/v) DMF (store frozen).
3. Prepare substrate solution by dissolving 10 µl solution A and 10 µl solution B in 5 ml acetate buffer.
4. Incubate test sections in substrate solution for 10–60 min at 37 °C in darkness.
5. Incubate control sections in the above solution from which the substrate has been omitted.
6. Wash in distilled water.
7. Air dry and mount permanently.

Red deposits that are absent from control sections indicate the sites of enzyme activity.

B. Alkaline phosphatase

As in *Protocol 9 A* but substitute Tris-HCl buffer pH 8 for the acetate buffer.

3.2 ATPase

Adenosine triphosphatases catalyse the hydrolysis of ATP to give inorganic phosphate: in animal and plant cells the reactions are often linked to important membrane-associated physiological processes which are energy dependent.

Protocol 10. Localization of ATPase

- 0.04 M Tris–maleate buffer pH 7
 - ATP
 - calcium nitrate
 - lead nitrate
 - H₂S water
1. Prepare substrate solution containing 2 mM ATP, 2 mM calcium nitrate, 3.6 mM lead nitrate in 0.04 M Tris–maleate buffer pH 7.
 2. Incubate test sections in substrate solution for 10–30 min at room temperature in darkness.
 3. Incubate control sections in the above solution from which the substrate has been omitted.
 4. Wash in buffer.
 5. Place sections in freshly prepared H₂S water for 2 min.
 6. Wash in distilled water.
 7. Air dry and mount permanently.

Brown/black deposits that are absent from control sections indicate the sites of enzyme activity.

3.3 Esterase

A range of esterase activities is present within plant tissues. Within this broad range, specific categories may be defined (5) by application of inhibitors: since these inhibitors include organophosphates many investigators simply refer to the localization of non-specific esterases. Esterase has been used as a marker of early developmental changes that occur during vascularization within plant tissues (9), and also as a test of cell viability (see p. 46).

Protocol 11. Localization of general esterase

- 0.2 M Tris–HCl buffer pH 6.5
 - naphthol AS-D acetate (Sigma N2875)
 - Fast Blue BB (Sigma F3378)
 - DMF
1. Prepare substrate solution as follows. Dissolve 5 mg naphthol AS-D acetate in 0.5 ml DMF. Slowly add this, while mixing, to 25 ml 0.2 M

3. General and enzyme histochemistry

Protocol 11. Continued

Tris-HCl pH 6.5 and 25 ml distilled water. Add 20 mg Fast Blue BB, shake well, and filter into a dark bottle.

2. Incubate test section in substrate solution for 10–20 min at room temperature or 37 °C in darkness.
3. Incubate control sections in the above solution from which the substrate has been omitted.
4. Wash in distilled water.
5. Air dry and mount permanently.

Blue deposits that are absent from control sections indicate the sites of enzyme activity.

3.4 Glucuronidase (GUS)

GUS is widely used as a reporter gene to examine the temporal and spatial regulatory roles of nucleic acid sequences expressed transgenically (10). GUS activity is localized using, as substrate, naphthol AS-B1- β -D-glucuronide (*Protocol 12*), or X-gluc (5-bromo-4-chloro-3-indolyl- β -D-glucuronic acid) which gives a bright blue, insoluble reaction product. This may be viewed after staining of fresh tissue (*Protocol 13*) by bright field microscopy, or may be fixed and viewed, with higher resolution, after sectioning of stained tissue which has been embedded in methacrylate (see *Protocol 13*). Where ultrastructural resolution is required GUS is localized by its antibody and electron microscopic immunocytochemistry (see Chapter 7).

Protocol 12. Localization of glucuronidase (GUS) using naphthol AS-B1- β -D-glucuronide

- 0.2 M acetate buffer pH 4.5 (51 ml 0.2 M acetate acid and 49 ml 0.2 M sodium acetate)
 - naphthol AS-B1- β -D-glucuronide (Sigma N1875)
 - DMF (Sigma D4252)
 - Fast Blue BB (Sigma F3378)
 - 0.1 M phosphate buffer pH 7.5
1. Prepare stock naphthol solution (A) as follows. Dissolve 11.4 mg naphthol AS-B1- β -D-glucuronide in 1 ml DMF. Add this to 49 ml 0.2 M acetate buffer pH 4.5.
 2. Prepare substrate solution by adding 0.8 ml solution A to 3.2 ml 0.2 M acetate buffer pH 4.5 and 4 ml distilled water.

3. Incubate test sections in substrate solution for 15–60 min at 37 °C in darkness.
4. Incubate control sections in the above solution from which the substrate has been omitted.
5. Prepare post-coupling solution. Dissolve 1 mg Fast Blue BB in 5 ml phosphate buffer pH 7.5.
6. Incubate sections in post-coupling solution for 5 min at 4 °C.
7. Wash in distilled water.
8. Air dry and mount permanently.

Blue deposits that are absent from control sections indicate the sites of enzyme activity.

Protocol 13. Localization of GUS using X-gluc

- X-gluc (5-bromo-4-chloro-3-indolyl- β -D-glucuronic acid)
- 50 mM phosphate buffer pH 7.2
- humid chamber (see Chapter 7, *Protocol 3*)

A. *For semi-permanent mounting*

- fixative (see *Protocol 1*)
 - ethanol
 - methacrylate JB4 (Polysciences)
 - catalyst for JB4
 - specimen moulds
1. Cut sections of fresh tissue into 1 mM X-gluc in 50 mM phosphate buffer pH 7.2.
 2. Incubate for 2–12 h at 37 °C.
 3. Rinse with water.
 4. Examine by bright field microscopy (GUS activity indicated by blue staining absent in controls without substrate).

B. *If a permanent mount is required*

Follow steps 1–4 above then proceed as follows.

5. Fix with buffered aldehyde for 4–12 h at 4 °C.

3. General and enzyme histochemistry

Protocol 13. Continued

6. Dehydrate through ethanol series (see *Protocol 1*, step 5).
7. Infiltrate with increasing concentrations of methacrylate JB4 in ethanol over 24 h.
8. Infiltrate with methacrylate JB4 for 24 h.
9. Embed in methacrylate JB4 with catalyst and allow to polymerize in specimen moulds at room temperature.
10. Section at 2–10 μm , mount on glass slides, and examine using bright or dark field illumination without counterstaining.

3.5 Catalase, peroxidase, and phenoloxidase

The oxidases have major roles in both primary and secondary metabolic pathways. Protocols are given here for catalase, peroxidase, and phenoloxidase; other methods available include these for localization of cytochrome oxidase (11), uricase (12), and glucolate oxidase (13). NADI reagents have been used for the localization of cytochrome oxidase; there are, however, several disadvantages to these including the migration of the stain product to adjacent lipid components within the tissues, a false positive from xylem elements, and occurrence of the reaction in the absence of enzymic activity. Catalase activity can be discriminated from peroxidase activity using the catalase inhibitor aminotriazole.

Protocol 14. Localization of catalase (after Frederick (14))

- 2-amino-2-methyl-1, 3-propanediol buffer pH 10
 - diaminobenzidine (DAB) Sigma D5637 or, with special packaging for carcinogen, D9015)
 - 30% hydrogen peroxide
1. Prepare substrate solution, as follows. Dissolve 10 mg DAB in 5 ml of 2-amino-2-methyl-1,3-propanediol buffer pH 10. Add 0.1 ml freshly prepared 3% hydrogen peroxide, adjust to pH 9, and filter into a dark bottle.
 2. Incubate a control section (i) in the catalase inhibitor 3-amino-1,2,4-triazole (20 mM) for 30 min.
 3. Incubate test and control sections in substrate solution for up to 1 h at 37 °C in darkness.
 4. Incubate control sections (ii) in the above solution from which the hydrogen peroxide has been omitted.

5. Wash in distilled water.
6. Air dry and mount permanently.

Brown/black deposits that are absent from control sections indicate the sites of enzyme activity.

Protocol 15. Localization of peroxidase (after Graham and Karnovsky (15))

- 0.05 M Tris-HCl pH 7.6
 - diaminobenzidine (DAB) (as *Protocol 14*)
 - 30% hydrogen peroxide
1. Prepare substrate solution as follows. Dissolve 5 mg DAB in 10 ml 0.05 M Tris-HCl pH 7.6. Add 0.2 ml freshly prepared 1% hydrogen peroxide.
 2. Incubate test sections in substrate solution for 5–10 min at room temperature in darkness (after optional preincubation with 1% (w/v) phenylhydrazine hydrochloride to block endogenous peroxidase).
 3. Incubate control sections (i) in the above solution from which the hydrogen peroxide has been omitted, and (ii) as in *Protocol 13*, step 2.
 4. Wash in distilled water.
 5. Air dry and mount permanently.

Brown/black deposits that are absent from control sections indicate the sites of enzyme activity

Protocol 16. Localization of phenoloxidase (after Vaughn and Duke (16))

- phosphate citrate buffer pH 4.5 (18.7 ml 0.5 M sodium phosphate, 10.65 ml 0.5 M citric acid, diluted to 100 ml)
 - naphthol (Sigma N1000)
 - 4-aminodiphenylamine (*N*-phenyl-*p*-phenylenediamine) (Sigma 5379)
 - DMF (as *Protocol 11*)
1. Prepare substrate solution as follows. Dissolve 5 mg naphthol and 5 mg 4-aminodiphenylamine in 0.5 ml DMF. Add slowly while mixing to 10 ml of phosphate citrate buffer pH 4.5.